3rd Annual Science Day
Faculty of Science - Sohag University

14 April 2018

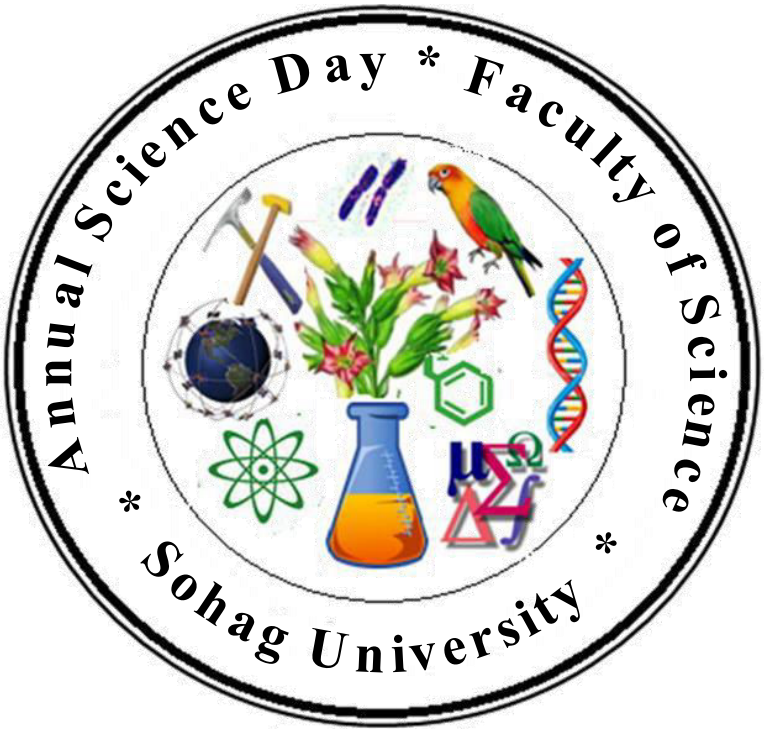

المؤتمر العلمى السنوى الثالث لكلية العلوم
جامعة سوهاج

Abstract Book for Papers Published by Staff Members of Faculty of Science during 2017

PREFACE

This abstract book is compiled of more than 280 papers published in estimated international journals by Staff members of Faculty of Science, Sohag University during 2017. The book was made on the sidelines of the 3rd Annual Science Day ceremony held on, April, 2018 at Sohag Faculty of Science under the patronage of Dr. **Ayman Abdel-Moneim**, the Governor of Sohag, Prof. Dr. **Ahmed Aziz Abdel-Monem**, President of Sohag University, and Prof. Dr. **Ahmed Mohamed Soliman**, Dean of Faculty of Science.

Besides emerging the scientific research activities of staff members, the Abstract book as a whole is an important reference of the recent advances in research. Furthermore, the Annual Science Day meeting offers an opportunity for researchers from different departments who work on similar research problems but rarely cross paths, to connect with each other. Science Day event is also a great opportunity to share the value of our research with different sectors of community services.

Congratulations to all who participated, and thanks to everyone made this event such a huge success.

Dean of Faculty of Science
Prof. Dr. Ahmed M. Soliman

Organizing Committee

Prof. Dr. Ahmed M. Soliman	Dean of Faculty of Science
Prof. Dr. Ahmed M. Ahmed Ali	Vice-Dean for Graduate Students & Research Affairs
Prof. Dr. Kamal M. S. Khalil	Vice-Dean for Education & Students Affairs
Prof. Dr. Zakaria A. Mohamed	Chairman of Botany & Microbiology Department
Prof. Dr. Hazem Elmeshneb	Physics Department
Prof. Dr. Alaa Y. Fahmey	Zoology Department
Dr. Mohamed Ismael	Chemistry Department
Dr. Omar Elhady	Chemistry Department
Dr. Mostafa G. Redwan	Geology Department
Dr. Mahmoud Abdel Aleem Ali	Chemistry Department
Dr. Naglaa Yousef	Botany & Microbiology Department
Dr. Ahmed M. Abu-Dief	Chemistry Department
Dr. Mohamed H. El-Khashab	Geology Department
Dr. Gamal Ismail	Mathematics & Computer Science Department
Dr. Hamdy Hassan	Mathematics & Computer Science Department
Dr. Mahmoud S. Bakheit	Botany & Microbiology Department
Dr. Alaa Elmeshneb	Physics Department
Dr. Mohamed Alaraby	Zoology Department

Mrs. Elham A. Abd El-Hameed	Quality Assurance Unit
Mr. Mohamed Galal	Quality Assurance Unit

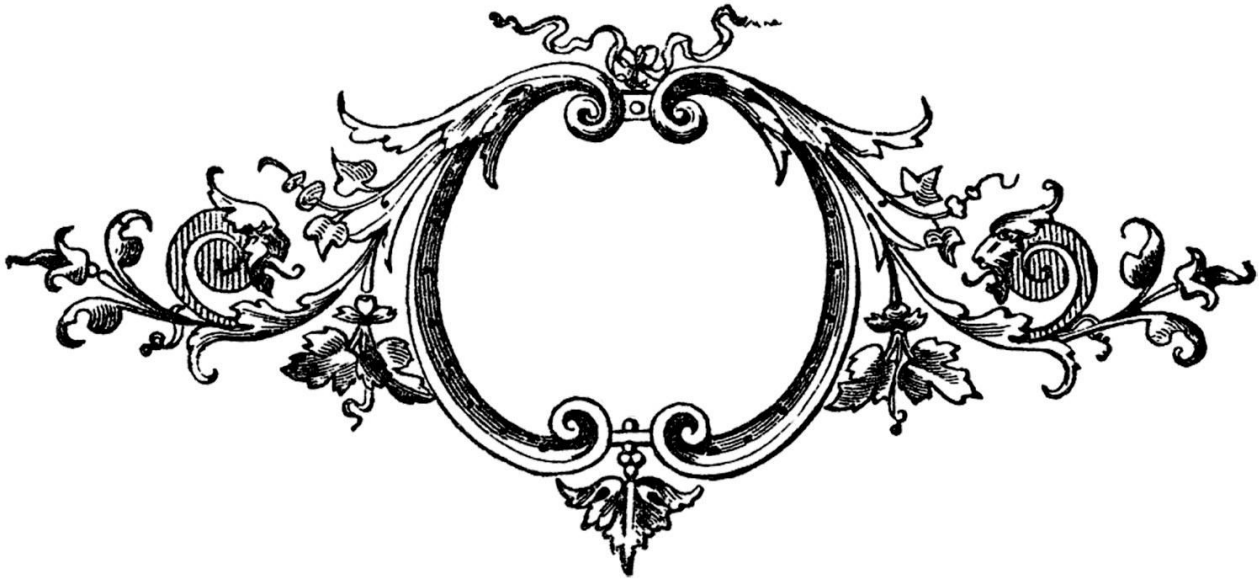

List of Publications

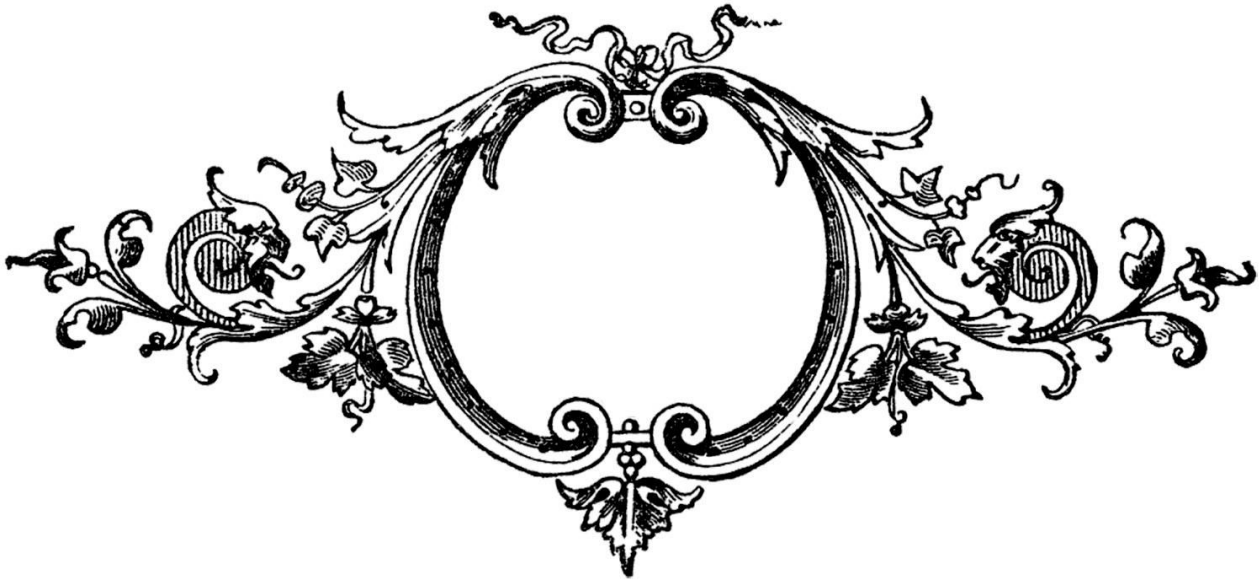

List of papers published by Staff members of Mathematics & Computer Science Department

1	**Propagation of a thermoelastic wave in a half-space of a homogeneous isotropic material subjected to the effect of gravity field** *A. M. Abd-Alla, S. M. Abo-Dahab, H. A. Alotaibi*
2	**Eigenvalue approach to two dimensional coupled magneto-thermoelasticity in a rotating isotropic medium** *F. S. Bayones, A.M. Abd-All*
3	**Rotational Effects on Magneto-Thermoelastic Stoneley, Love and Rayleigh Waves in Fibre-Reinforced Anisotropic General Viscoelastic Media of Higher Order** *A. M. Abd-Alla, S. M. Abo-Dahab, Aftab Khan*
4	**Plane Vibrations in a Transversely Isotropic Infinite Hollow Cylinder Under Effect of the Rotation and Magnetic Field** *F. S. Bayones and A. M. Abd-Alla*
5	**Peristaltic transport of a Jeffrey fluid under the effect of gravity field and rotation in an asymmetric channel with magnetic field** *A. M. Abd-Alla, S.M. Abo-Dahab and Abdullah Alsharif*
6	**Influence of magnetic field and heat and mass transfer on the peristaltic flow through a porous rotating medium with compliant walls** *A. M. Abd-Alla, S.M. Abo-Dahab and M. Elsagheer*
7	**A two-dimensional problem with rotation and magnetic field in the context of four thermoelastic theories** *S. M. Abo-Dahab, A. M. Abd-Alla and A. J. Alqarni*
8	**Rotational effect on thermoelastic Stoneley, Love and Rayleigh waves in fibre-reinforced anisotropic general viscoelastic media of higher order** *A.M. Abd-Alla, S.M. Abo-Dahab and Aftab Khan*
9	**On an influence of thermal stresses and magnetic field in thermoelastic half-space without energy dissipation** *S. M. Abo-Dahab, A. M. Abd-Alla and H. A. Alotaibi*
10	**Step-Stress Partially Accelerated Life Tests Model in Estimation of Inverse Weibull Parameters under Progressive Type-II Censoring** *G. A. A. Soliman, E. A. Ahmed, N. A. Abou-Elheggag and S. M. Ahmed*
11	**Shear horizontal waves in composite materials: Behavior under rotation and initial stress** *Abo-el-nour N Abd-alla and NF Hasbullah*
12	**The mathematical modeling for bulk acoustic wave propagation velocities in transversely isotropic piezoelectric materials** *Abo-el-nour N Abd-alla Abdelmonam M Hamdan and Adel A Almarashi*
13	**Plane waves and eigenfrequency study in a transversely isotropic magneto-thermoelastic medium under the effect of a constant angular velocity** *Abo-el-nour N. Abd-allaa,b, Fatimah Alshaikha, Dionisio Del Vescovoc and Mario Spagnuolod*
14	**New exact Bayesian prediction of the range for the exponential lifetime based on fixed and random sample sizes** *A. H. Abd Ellah*
15	**Low-cost autonomous perceptron neural network inspired by quantum computation** *Mohammed Zidan, Abdel-Haleem Abdel-Aty, Alaa El-Sadek, E. A. Zanaty, and Mahmoud Abdel-Aty*
16	**A fast and precise numerical algorithm for a class of variable–order fractional differential equations** *Ali H. Bhrawy, Mahmoud A. Zaky, Mahmoud Abdel-Aty*
17	**Incidence of HCV in duced-Esophageal varices in Egypt. Valuable knowledge using data mining analysis** *Mahmoud Abdel-aty, Mahmoud Fouad, Mohammad M. Sallam, Elsayed A. Elgohary, Ali Ismael, Abdallah Nawara, Baha Hawary, Mohammed Tag-Adeen, Salama Khaled*

18	**Photo-thermal-elastic interaction in an unbounded semiconducting medium with spherical cavity due to pulse heat flux** *Ibrahim A. Abbas and Aatef Hobiny*
19	**Analytical solutions of 2-D problem for cracked thermoelastic fiber-reinforced anisotropic material** *Ibrahim A. Abbas*
20	**Dual-Phase-Lag Model on Generalized MagnetoThermoelastic Interaction in a Functionally Graded Material** *Ibrahim A. Abbas and Elsayed A. E. Mohamed*
21	**Analytical and Computational Solution of Three-Dimensional Thermoelastic Interactions in Porous Material with Temperature-Dependent Properties** *Abbas Ibrahim A, Abd-alla, Abo-el-nour N Alshaikh, Fatimah*
22	**Free vibration of a thermoelastic hollow cylinder under two-temperature generalized thermoelastic theory** *Ibrahim A. Abbas*
23	**Analytical solution of thermoelastic interaction in a half-space by pulsed laser heating** *Ibrahim A. Abbas, Marin Marind*
24	**A Semi-Group of Contractions in Elasticity of Microstretch Materials** *M. Marin, M, I. Abbas and C. Carstea*
25	**A study on photothermal waves in an unbounded semiconductor medium with cylindrical cavity** *Aatef D. Hobiny and Ibrahim A. Abbas*
26	**Analytical solutions of thermoelastic interactions in a hollow cylinder with one relaxation time** *Ibrahim A. Abbas, Y. Abd elmaboud*
27	**Generalized thermoelastic interactions in a hollow cylinder with temperature-dependent material properties** *Ibrahim A. Abbas*
28	**On continuous dependence for the mixed problem of microstretch bodies** *M. Marin, I Abas and C. Carstea*
29	**Fractional Order Photo-Thermoelastic Interaction in a Semiconducting Media Containing a Spherical Cavity Subjected to Pulse Heat Flux** *Faris S. Alzahrani and Ibrahim A. Abbas*
30	**A Two-Temperature Photothermal Interaction in a Semiconducting Material** *Ibrahim A. Abbas, K. Aly and Faris S. Alzahrani*
31	**A Generalized Model on Plasma, Thermal and Elastic Waves in a Semiconductor Medium** *Ibrahim A. Abbas and K. A. Aly*
32	**Two-dimensional generalized thermo-elastic problem for anisotropic half-space** *Debkumar Ghosh, Abhijit Lahiri, Ibrahim A. Abbas*
33	**Eigenvalue Approach in a Generalized Thermal Shock Problem for a Transversely Isotropic Half-Space** *Ibrahim A. Abbas and Aatef Hobiny*
34	**Series Representations of the Coefficients of Quaternion Q-Type Functions** *A. A. El-Sayed and A. Fatima*
35	**Fisher information and quantum state estimation of two-coupled atoms in presence of two external magnetic fields** *Hanaa H. Abu-Zinadah, Sayed Abdel-Khalek*
36	**Effect of Time Dependent Coupling on the Dynamical Properties of the Nonlocal Correlation Between Two Three-Level Atoms** *Sayed Abdel-Khalek, S. H. A. Halawani, A-S. F. Obada*
37	**Quantum phase and nonlocal correlations for a three-level system interacting with laser light in a nonlinear kerr medium under decoherence** *K. Berrada and Sayed Abdel-Khalek*
38	**Properties of Two Two-level Atoms Interacting with Intensity-Dependent Coupling** *H. Bakry, A. S. A. Mohamed, N. Zidan*

39	**The Probe Attack on the Bennett-Brassard 1984 Protocol in the Presences of Noisy Amplitude Damping Channel** *H. F. Abdel-Hameed, N. Zidan, M. R. Wahiddin*
40	**Low-cost autonomous perceptron neural network inspired by quantum computation** *M Zidan, AH Abdel-Aty, A El-Sadek, E.A Zanaty, M Abdel-Aty*
41	**Dynamical behaviors, control and synchronization of a new chaotic model with complex variables and cubic nonlinear terms** *E. E. Mahmou, M. A. Al-Adwani*
42	**A novel sort of adaptive complex synchronizations of two indistinguishable chaotic complex nonlinear models with uncertain parameters and its applications in secure communications** *E. E. Mahmoud and F. S. Abood*
43	**An unusual kind of complex synchronizations and its applications in secure communications** *E. E. Mahmoud*
44	**Bifurcations and chaos of time delay Lorenz system with dimension 2n+1** *G. M. Mahmoud, A. A. Arafa and E. E. Mahmoud*
45	**Projective synchronization for coupled partially linear complex-variable systems with known parameters** *G. M. Mahmoud, E. E. Mahmoud and A. A. Arafa*
46	**A New Nonlinear Chaotic Complex Model and Its Complex Antilag Synchronization** *E. E. Mahmou and F. S. Abood*
47	**Complex complete synchronization of hyperchaotic complex nonlinear systems with fully uncertain parameters and its applications in secure communications** *K. M. Abualnaja, E. E. Mahmoud*
48	**A novel sort of complex synchronizations** *E. E. Mahmoud*
49	**Thermal Stresses in Thermoelastic Half-Space Without Energy Dissipation Subjected to Rotation and Magnetic Field** *S. M. Abo-Dahab, A. M. Abd-Alla and E. E. Mahmoud*
50	**(L, m)-fuzzy soft quasi- coincident neighborhood spaces** *O. R. Sayed, E. Elsanousy, Y. H. Raghp, Y.Chankim*
51	**On (L,M)-Fuzzy Soft Topological Spaces** *O. R. Sayed, E. Elsanousy, Y. H. Raghp, Y. Chankim*
52	**Fuzzy soft (α, β, θ, δ, I)-continuous functions** *S. E. Abbas, E. El-sanowsy, A. Atef*
53	**An analytical coupled homotopy-variational approach for solving strongly nonlinear differential equation** *G. M. Ismail*
54	**Common Random Fixed Point Theorems of Akram-Contraction Mappings in Cone Random Metric Spaces** *Rashwan A. Rashwan and Hasanen A. Hammad*
55	**Random Fixed Point Theorem for Weakly Compatible Mappings under Implicit Relation in Cone Random Metric Spaces** *R. A. Rashwan1 and H. A. Hammad*
56	**Convergence and Stability of Modified Random SP-Iteration for A Generalized Asymptotically Quasi-Nonexpansive Mappings** *R. A. Rashwan and H. A. Hammad*
57	**Stability and strong convergence results for random jungck-kirk-noor iterative scheme** *R. A. Rashwan and H. A. Hammad*
58	**Common random fixed point results with application to a system of nonlinear integral equations** *R. A. Rashwan, H. A. Hammad and L. Guran*
59	**A solution of nonlinear fractional random differential equation via random fixed point technique** *R. A. Rashwan and H. A. Hammad*
60	**A common random fixed point theorem of rational inequality in polish spaces with application** *R. A. Rashwan and H. A. Hammad*

61	**Data Aggregation Energy and Probability Effects on the Performance of MODLEACH Protocol in WSN** *Hamdy H El-Sayed*
62	**A Novel Image Encryption Scheme based on Different Block Sizes for Gray scale and Color Images** *Omar Reyad M. A. Mofaddel W. M. Abd-Elhafiez Mohamed Fathy*
63	**Hop by Hop Routing Problems in MANETs** *Hamdy H. El-Sayed*
64	**An Integrated Smoothing Method for Fingerprint Recognition Enhancement** *Muhammad Khfagy, Yasser AbdelSatar, Omar Reyad, and Nahla Omran*
65	**Adaptive Fingerprint Image Enhancement Based On Cascading Filtering** *Mahmoud A. Mofaddel, Samy Bakheet, Rehab Youssef*
66	**Recognition of Human Actions Based on Temporal Motion Templates** *Samy Bakheet, Ayoub Al-Hamadi and M. A. Mofaddel*
67	**Active Human Detection with a Mobile Robot** *Mohamed Heshmat&, Manuel Fernandez-Carmona, Zhi Yan and Nicola Bellotto*
68	**A novel approach for color image segmentation based on region growing** *E.A Zanaty, S.F. El-Zoghdy*

List of papers published by Staff members of Physics Department

1	**Single Folding Cluster Potential for P $^{+12}$C Elastic Scattering** *N. N. Abd Allah, M. El-Azab Farid, S. R. Mokhtar, A. A. Ebrahim and A. M. EL-Sheikh*
2	**Effect of the synthesis conditions on the structural, morphological and optical properties of $Bi_2Te_{2.7}Se_{0.3}$ nanoparticles** *H. M. Ali, E. M. M. Ibrahim, M. M. Wakkad, M. A. A. Mohamed*
3	**Optical and Photocatalytic Measurements of Co-TiO_2 Nanoparticle Thin Films** *Mai M. Khalaf & Hany M. Abd El-Lateef & H. M. Ali*
4	**Morphological and Optical Characterization of Mg-Zno Thin Films Deposited by Co-Magnetron Sputtering Technique** *S. E. Alomairy, H. M. Ali, M. M. Abd El-Raheem, A. M. Al-Baradi, F. Abdel-Wahab, S. A. Amin*
5	**Tensor target spin asymmetries in incoherent π^--photoproductionoff the deuteron including rescattering effects** *E. M. Darwish, H. M. Abou-Elsebaa, E. A. Sultan, and Kh. S. A. Hassaneen*
6	**Single and Double Spin Asymmetries in the Elastic *e-d* Scattering and Their Dependence on the Deuteron Wave Function** *E. M. Darwish, A. Abd El-Daiem, and M. M. Abd El-Wahab*
7	**Tensor target spin asymmetries in coherent π^0-photoproduction on the deuteron including intermediate ηNN interaction within a three-body approach** *E. M. Darwish, H. M. Abou-Elsebaa, and Kh. S. A. Hassaneen*
8	**Room temperature magneto-transport properties of $La_{0.7}Ba_{0.3}MnO_3$ manganite** *Abd El-Moez A. Mohamed, B. Hernando, M.E. Díaz-García*
9	**Electronic bands and optical conductivity of the Dzyaloshinsky-Moriya multiferroic $Ba_2CuGe_2O_7$** *M. Corasaniti, P. Barone, A. Nucara, M. Ortolani, L. Baldassarre, R. Fittipaldi, V. Granata, L. Rocco, A. Vecchione, W. S. Mohamed, J. Lorenzana, and P. Calvani*
10	**α-Bi_2O_3 nanorods: synthesis, characterization and UV-photocatalytic activity** *Ahmed M Abu-Dief and W. S. Mohamed*
11	**Influence of (Ar + O_2) atmosphere and $CdCl_2$ coating heattreatment on physical properties of CdS thin film for solar cell applications** *W S Mohamed, M F Hasaneen and E KhShokr*
12	**Effects of V doping on magnetic and optical properties of oxygen-deficient In_2O_3 thin films** *Mohammed S. Alqahtani, N. M. A. Hadia, S. H. Mohamed*
13	**Morphologies and optical properties of mixed tin oxysulfide produced by evaporation condensation of SnS** *S. H. Mohamed, N. M. A. Hadia, M. F. Hasaneen, Mohamed Asran Hassan*
14	**Synthesis, optical, structural, and electrical properties of singlecrystalline CdS nanobelts** *Mohammed S. Alqahtani, N. M. A. Hadia, S. H. Mohamed*
15	**Tunable properties of one-dimensional photonic crystalsthat incorporate a defect layer of a magnetized plasma** *Arafa H. Aly, Hussein A. Elsayed, Ayman A. Ameeny and S. H. Mohamed*
16	**Copper oxide nanocrystallites fabricated by thermal oxidation of pre-sputtered copper films at different temperatures and under oxygen and argon flows** *M. A. Awad, N. M. A. Hadia*
17	**Improvement of the performance of thin-film CdS/PbS solar cells using low-cost ZnO-based alloys as front electrode** *H. A. Mohamed, M. R. Ahmed*
18	**Quantitative assessment of electrical, optical and recombination losses in heterojunction CdS/CdTe solar cells** *H. A. MOHAMED, A. S. MOHAMED*
19	**Electrical, thermoelectrical and magnetic properties of approximately 20 nm Ni-Co-O nanoparticles and investigation of their conduction phenomena** *E. M. M. Ibrahim, Ahmed M. Abu-Dief, A. Elshafaie, A. M. Ahmed*

20	**Synthesis, characterization and low field magnetotransport of Nd0.6Sr0.4MnO3/CrO3 composite** *A M Ahmed, H F Mohamed, A K Diab and S A Mohamed*
21	Magnetic, magnetocaloric and thermoelectric properties of nickel doped manganites *A. E. -M. A. Mohamed, Hernando B., Ahmed, A. M.*
22	**Phase diagram, ac susceptibility and thermoelectric power properties of the $La_{0.90}Li_{0.10-x}Na_xMnO_3$ manganites** *H. F. Mohamed*
23	**Influence of sodium doping on the electrical and magnetic properties of $La_{0.90}Li_{0.10}MnO_3$ manganites** *H.F. Mohamed*
24	***Effects of annealing temperature and dopant concentration on the structure, optical, and magnetic properties of Cu-doped ZnO nanopowders*** *S. A. Ahmed*
25	**Effect of Cu- and Mn-doping on the structural, optical, and magnetic properties of $Zn_{0.98}Fe_{0.02}O$ nanopowders** *S. A. Ahmed*
26	***Structural, optical, and magnetic properties of Cu-doped TiO_2 samples*** *S. A. Ahmed*
27	**Structural, optical, and magnetic properties of Mn-doped ZnO samples** *S A Ahmed*
28	**Room-temperature ferromagnetism in Co-, Cr-, and V-doped ZnO diluted magnetic semiconductor** *S. A. Ahmed*
29	**Ferromagnetism in Cr-, Fe-, and Ni-doped TiO_2 samples** *S. A. Ahmed*
30	**Effects of Annealing Temperature and Dopant Concentration on the Structural, Optical, and Magnetic Properties of Iron-Doped ZnO Samples** *S. A. Ahmed*
31	**Effect of thermal annealing on structural, optical and electrical properties oftransparent Nb_2O_5 thin films** *A. A. Attaa, M. M. El-Nahass, A. M. Hassanienc, Khaled M. Elsabawyd, M. M. Abd El-Raheem, F. A. Alhuthali, Sultan E. Alomariy, M. S. Algamdi*
32	**Study on Transparent Oxides Thin Films Prepared using Sputtering Method** *M. M. Abd El-Raheem1و A. A. Atta, A. M. Amry ،Ateyyah M. Al-Baradi1،Sultan E. Alomairy, H. Alkhammash, and S. A. Amin*
33	**Ellipsometric study of Sb doped ZnO thin films deposited by magnetron co-sputtering method AMAL-Baradi ,M. M .Abd EL- Raheem, H .Khammash, F.Abdel-Wahab ,S .Aaomairy ,M. A .** *Alharbi, El-Naggar, A. A. Albasam*
34	**α-Cluster optical potential model ofpions scattering from ^{28}Si** *M. El-AzabFarid,A. A. Ebrahim, B. M. Elyan,S. R. Mokhtar, and M. A. El-Zohry*
35	**Sonochemically synthesized ZnOnanosheets and nanorods: Annealing temperature effects on the structure, and optical properties** *A. Othman, M. A. Osman, E. M. M. Ibrahim, Manar A. Ali*
36	**Effect of calcination temperature onmagnetic and electrical properties of $BiFeO_3$ nanoparticles prepared by sol-gel method** *E.M.M. Ibrahim, G. Farghal, Mai M. Khalaf, Hany M. Abd El-Lateef*
37	**Sonochemical synthesis, structural inspection and semiconductor behavior of three new nano sized Cu(II), Co(II) and Ni(II) chelates based on tri-dentate NOO imine ligand as precursors for metal oxides** *Laila H. Abdel Rahman, Ahmed M. Abu-Dief, Rafat M. El-Khatib, Shimaa Mahdy Abdel-Fatah, A. M. Adam, E. M. M. Ibrahim*
38	**Electrical, thermoelectrical and magnetic properties of approximately 20-nm Ni-Co-O nanoparticles and investigation of their conduction phenomena** *E. M. M. Ibrahim, Ahmed M. Abu-Dief, A. Elshafaie, A. M. Ahmed*

39	**Mn-doped ZnOnanocrystals synthesized by sonochemical method: Structural, photoluminescence, and magnetic properties** *A.Othman, M. A. Osman,E.M.M. Ibrahim, Manar A. Ali, A. G. Abd-Elrahim*
40	**Magnetic and DC electric properties of sol–gel-synthesized Ce-doped $BiFeO_3$ nanoflakes** *E. M. M. Ibrahim, G. Farghal, Mai M. Khalaf, Hany M. Abd El-Lateef*
41	**Optical And Thermoelectric Properties Of Nanocrystalline$Bi_2(Se_{1-x}Te_x)_3$ Films** *M. Adam, E. M. M. Ibrahim, L. V. Panina, P. Petkov*
42	**Electric, thermoelectric and magnetic characterization of γ-Fe_2O_3 and Co_3O_4 nanoparticles synthesized by facile thermal decomposition of metal-Schiff base complexes** *E. M. M. Ibrahim, Laila H. Abdel-Rahman, Ahmed M. Abu-Dief,A. Elshafaie, Samar Kamel, Hamdan, A. M. Ahmed*
43	**Thermoelectric materials: a crucial demand for renewable energy production** *E. M. M. Ibrahim*
44	**Surface magnetic properties and giant magnetoimpedance effect in Co-based amorphous ribbons** *A. Chizhik, V. Vega, Abd El-Moez A. Mohamed, V. M. Prida, T. Sanchez, B. Hernando, M. Ipatov, V. Zhukova, A. P. Zhukov, A. Stupakiewicz, L. Domínguez, J. Gonzalez*
45	**The effect of Cu on the properties of CdO/Cu/CdO multilayer films for transparent conductive electrode applications** *M. Raaif S. H. Mohamed*
46	**Conformity and Homogeneity Indices for Head and Neck Cancer Patients using 3DCRT** *Hanan A. Abotaleb, Ehab Maarouf, F. M. El-Hossary, M. Raaif and Mohamed Kelany*
47	**The Thermal Properties of Asymmetric Nuclear Matter within the Extended Brueckner–Hartree-Fock Approach** *Khaled Hassaneen and Hesham Mansour*
48	**Tensor target spin asymmetries in incoherent π^-photoproduction off the deuteron including rescattering effects** *E. M. Darwish, H. M. Abou-Elsebaa, E. A. Sultan and Kh. S. A. Hassaneen*
49	**Effect of Plasma Surface Treatment on AISI 316LStainless Steel for In-CoreApplications of Nuclear Reactors** *F. M. El-Hossary, S. U. El-kameesy, M. M. Eissa, Al-Zahraa A. Abd Elmula, Aly Saeed, Samah A. Al-Shelkamy*
50	**Optical and thermoelectric properties of nano-particles based $Bi_2(Te_{1-x}Se_x)_3$ thin films** *A. M. Adam, E. Lilov, P. Petkov*
51	**Impacts of thickness reduction and heat treatment on the optical properties of thin chalcogenide films** *A. M. Adama, P. Petkovc*
52	**Characterization and optical properties of bismuth chalcogenide films prepared by pulsed laser deposition technique** *A. M. Adama, E. Lilov, V. Lilova, P. Petkov*
53	**Asymmetric nuclear matter and neutron star properties withinthe extended Brueckner theory** *Khaled S.A. Hassaneen*

List of papers published by Staff members of Chemistry Department

1	**Influence of preparation conditions on the catalytic activity of high surface area silica in partial methanol oxidation** *Tarek T. Ali, Sulaiman N. Basahel, Hatem A.Mahmoud, Kamal M.S.Khalil, Katabathini Narasimharao*
2	**Hetarylcyanamides: Synthesis of Novel Thiazole, Triazole and Pyrimidine Derivatives and Prediction of their Biological Activity via PASS Inet** *Ahmed Khodairy, Amr H. Moustafa, Walaa W. Ahmed*
3	**Synthesis and characterization of binary and ternary oxovanadium complexes of *N*,*N*'-(2-pyridyl)thiourea and curcumin. Catalytic oxidation potential, antibacterial, antimicrobial, antioxidant and DNA interaction studies** *Mohamed Shaker S. Adam, Magdy M. Youssef, Maha F. Aboelghar, Usama El-Ayaan*
4	**Synthesis and characterization of binary and ternary oxovanadium complexes of *N*,*N*'-(2-pyridyl)thiourea and curcumin. Catalytic oxidation potential, antibacterial, antimicrobial, antioxidant and DNA interaction studies** *Joel T. Magu, Shaaban K. Mohamed, Mehmet Akkurt, Mohamed Shaker S. Adam, and Farouq E. Hawaiz*
5	**Three Novel Ni(II), VO(II) and Cr (III) Mononuclear Complexes Encompassing Potentially Tri -dentate imine ligand: Synthesis, Structural Characterization, DNA Interaction, Antimicrobial Evaluation and Anticancer Activity** *Laila H. Abdel-Rahman, Ahmed M. Abu-Dief, Maram Basha and Azza A. Hassan Abdel-Mawgoud*
6	**Development, Structural investigation, DNA Binding, Antimicrobial Screening and Anticancer Activities of Two Novel Quari-dentate VO(II) and Mn (II) Mononuclear Complexes** *Laila H. Abdel-Rahman, Ahmed M. Abu-Dief and Azza A. Hassan Abdel-Mawgoud*
7	**DNA Interaction, Antimicrobial, Anticancer Activities and Molecular Docking Study of Some New VO(II), Cr (III), Mn(II) and Ni(II) Mononuclear Chelates encompassing Quaridentate imine ligand** *Laila H. Abdel-Rahman, Ahmed M. Abu-Dief, Moustafa O. Aboelez and Azza A. Abdel-Mawgoud*
8	**Detailed Studies of the Alkylation Sides of Pyridin-2-yl and 4,6-Dimethylpyrimidin-2-yl-cyanamides** *Shestakov A. S., Moustafa A. H., Bushmarinov I. S., Prezent M. A., Sidorenko O.E.*
9	**Electrical, thermoelectrical and magnetic properties of approximately 20-nm Ni-Co-O nanoparticles and investigation of their conduction phenomena** *E. M. M. Ibrahim, Ahmed M. Abu-Dief, A. Elshafaie, A. M. Ahmed*
10	**Development and Functionalization of Magnetic Nanoparticles as Powerful and Green Catalysts for Organic Synthesis** *Ahmed M. Abu-Dief and Shimaa Mahdy Abdel-Fatah*
11	**DNA Binding Ability behaviour, Spectroscopic Studies, Hydrophobicity, and *In Vitro* Antibacterial Evaluation of Some New Fe(II) Complexes Bearing ONO Donors Amino acid Schiff bases** *Laila H. Abdel-Rahman, Rafat M. El-Khatib, Lobna A. E. Nassr and Ahmed M. Abu-Dief*
12	**Synthesis, characterization and UV-photocatalytic performance of α-Bi_2O_3 nanorods** *Ahmed M. Abu-Dief and W. S. Mohamed*
13	**Reactivity Trends of Hydroxide Ion Attack on High Spin Fe(II) Complexes Including Bromosalcylidene Amino Acid ligands in Some Mixed aqueous Solvents: Gibb's Free Energy of Transfer and Initial-Transition State Analysis** *Laila H. Abdel-Rahman, Rafat M. El-Khatib, Lobna A. E. Nassr and Ahmed M. Abu-Dief*
14	**Crystal structure of 1-[2-(4-nitrophenyl)-4,5-diphenyl-1H-imidazol-1-yl]propan-2-ol** *Simpson J., Mohamed S. K., Marzouk A. A., Abdelhamide A. A., Albayati M. R.*
15	**Synthesis, Characterization, Computational Calculations, Antibacterial and DNA binding activities of Cu(II), Co(II), Ni(II), Fe(II) complexes incorporating glutamine, glutaric and glutamic acid with imidazole derivatives** *Laila H. Abdel-Rahman, Ahmed M. Abu-Dief Nabawia M. Ismail and Mohamed Ismael*
16	**Corrosion inhibition of carbon steel pipelines by some novel Schiff base compounds during acidizing treatment of oil wells studied by electrochemical and quantum chemical methods** *Hany M. Abd El-Lateef, Ahmed M. Abu-Dief and Mounir A. A. Mohamed*

17	**Ni(II) and Cu(II) complexes supported by ONNO asymmetrical tetradentate Schiff base ligand: Synthesis, spectroscopic characterization, theoretical calculations, DNA interaction and antimicrobial studies** *Laila H. Abdel-Rahman, Ahmed M. Abu-Dief, H. Moustafa and Samar Kamel Hamdan*
18	**Kinetics, reactivity, initial–transition state analysis and thermodynamic parameters of base-catalyzed hydrolysis of coumalic acid in solvents with different polarities** *Ezz A. Abu-Gharib, Rafat M. EL-Khatib, Lobna A. E. Nassr and Ahmed M. Abu-Dief*
19	**Hydrophobicity, Reactivity trends of Base Catalyzed Hydrolysis of Some Novel High Spin Fe(II) Schiff Base Amino Acid Chelates in Some Binary Aqueous Solvent Mixtures: Initial-Transition State Analysis** *Laila H. Abdel-Rahman, Rafat M. El-Khatib, Lobna A. E. Nassr and Ahmed M. Abu-Dief*
20	**Sonochemical synthesis, structural inspection and semiconductor behavior of three new nano sized Cu(II), Co(II) and Ni(II) chelates based on tri-dentate NOO imine ligand as precursors for preparing of metal oxides** *Laila H. Abdel Rahman, Ahmed M. Abu-Dief, Rafat M. El-Khatib, Shimaa Mahdy Abdel-Fatah, A. M. Adam, E. M. M. Ibrahim*
21	**Effects of Nd-, Pr-, Tb- and Y-doping on the structural, textural, electrical and N2O decomposition activity of mesoporous NiO nanoparticles** *Bahaa M.Abu-Zied, Salem M. Bawaked, Samia A.Kosa, Tarek T. Ali, Wilhelm Schwiegerc Faisal M. Aqlan*
22	**Ultra-sensitive Amperometric Hydrazine Sensing via Dimethyl Glyoxomat Derived NiO Nanostructures** *Munazza Arain, Ayman Nafady, Abdullah M Al-Enizi, Tayyaba Shaikh, Zafar Hussain Ibupoto, Syed Tufail Hussain Sherazi, Syeda Sara Hassan, Muhammad Ishaque Abro, Manzoor Iqbal Khattak, Raj Kumar*
23	**Structural, Spectroscopic, and Electrochemical Characterization of Semi-Conducting, Solvated $[Pt(NH_3)_4](TCNQ)_2 \cdot (DMF)_2$ and Non-Solvated $[Pt(NH_3)_4](TCNQ)_2$**
24	**Easy, one-step synthesis of CdTe quantum dots via microwave irradiation for fingerprinting application** *Shalini Singha, Ylias M.Sabria, Deshetti Jampaiaha, P. R. Selvakannana, Ayman Nafady, Ahmad Esmaielzadeh, Kandjania Suresh, K. Bhargavaa*
25	**An amperometric sensitive dopamine biosensor based on novel copper oxide nanostructures Qurrat-ul-ain Baloach, Ayman Nafady, Aneela Tahira, Sirajuddin** *Syed Tufail Hussain Sherazi, Tayyaba Shaikh, Munazza Arain, Magnus Willander, Zafar Hussain Ibupoto*
26	**Co_3O_4@CeO_2 hybrid flower-like microspheres: a strong synergistic peroxidase-mimicking artificial enzyme with high sensitivity for glucose detection** *Deshetti Jampaiah, T. Srinivasa Reddy, Victoria E. Coyle, Ayman Nafady, Suresh K. Bhargava*
27	**Nanowire Morphology of Mono- and Bidoped α-MnO_2 Catalysts for Remarkable Enhancement in Soot Oxidation** *Deshetti Jampaiah, Vijay Kumar Velisoju, Perala Venkataswamy, Victoria E. Coyle, Ayman Nafady, Benjaram M. Reddy, and Suresh K. Bhargava*
28	**Concise synthesis of tetrazole macrocycle** *Abdelraheem E. M. M., De Haan M. P., Patil P., , Shaabani, S., Dömling A.*
29	**Fabrication of Highly Sensitive and Selective Electrochemical Sensors for Detection of Paracetamol by Using Piroxicam Stabilized Gold Nanoparticles** *Syeda Sara Hassan, Sallahuddin Panhwar, Ayman Nafady, Abdullah M. Al-Enizi, Sirajuddin, Syed Tufail Hussain Sherazi, Muhammad Siddique Kalhoro, Munazza Arain, Muhammad Raza Shah and M. Younis Talpur*
30	**Impact of porosity and thickness of nano-TiO_2 films on the corrosion protection performance of C-steel in H_2SO_4** *Mai Khalaf, Hany M. Abd El-Lateef*
31	**Sensitive determination of amlodipine besylate using bare/unmodified and DNA-modified screen-printed electrodes in tablets and biological fluids** *Mohamed Khairy, Ahmed A. Khorshed, Farouk A. Rashwan, Gamal A. Salah, Hanaa M. Abdel-Wadood, Craig E. Banks*

32	**Novel Quaternary Ammonium-Based Cationic Surfactants: Synthesis, Surface Activity and Evaluation as Corrosion Inhibitors for C1018 Carbon Steel in Acidic Chloride Solution** *Hany M. Abd El-Lateef, Ahmed H. Tantawy, Antar A. Abdelhamid*
33	**Simultaneous voltammetric determination of antihypertensive drugs nifedipine and atenolol utilizing MgO nanoplatelet modified screen-printed electrodes in pharmaceuticals and human fluids** *Mohamed Khairy, Ahmed A. Khorshed, Farouk A. Rashwan, Gamal A. Salah, Hanaa M. Abdel-Wadood, Craig E. Banks*
34	**Novel synthesized Schiff Base-based cationic gemini surfactants: Electrochemical investigation, theoretical modeling and applicability as biodegradable inhibitors for mild steel against acidic corrosion** *Hany M. Abd El-Lateef, Kamal A. Soliman, Ahmed H. Tantawy*
35	**The effects of metallic engineered nanoparticles upon plant systems: An analytic examination of scientific evidence** *Thabet Tolaymat, Ash Genaidy, Wael Abdelraheem, Dionysios Dionysiou, Christian Andersen*
36	**Magnetic and DC electric properties of sol–gel-synthesized Ce-doped $BiFeO_3$ nanoflakes** *E. M. M. Ibrahim, G. Farghal, Mai M. Khalaf, Hany M. Abd El-Lateef*
37	**Effect of Calcination Temperature on Magnetic and Electrical Properties of $BiFeO_3$ Nanoparticles Prepared By Sol-Gel Method** *E. M. M. Ibrahim, G. Farghal, Mai M. Khalaf, Hany M. Abd El-Lateef*
38	**Mechanism of Chicoric Acid Electrochemical Oxidation and Identification of Oxidation Products by Liquid Chromatography and Mass Spectrometry** *Emad F. Newair, Refat Abdel-Hamid, and Paul A. Kilmartin*
39	**Electrochemical Determination of the Antioxidant Activity in Echinacea Purpurea Roots Using Square Wave Voltammetry** *Emad F. Newair, Refat Abdel-Hamid, and Paul A. Kilmartin*
40	**Evaluation of Pt-based alloy/graphene nanohybrid electrocatalysts for triiodide reduction in photovoltaics** *Van-Duong Dao, Liudmila L. Larina, Quoc Chinh Tran, Van-Tien Bui, Van-Toan Nguyen, Thanh-Dong Pham, Ibrahim M. A. Mohamed, Nasser A.M.Barakat, Bui The Huy, Ho-Suk Choi*
41	**Electrochemical Biosensor Based on Nicotinamide Adenine Dinucleotide/Gold Nanoparticles Composite for Determination of the Antioxidant Activity of Caffeic Acid** *Emad F. Newair, Refat Abdel-Hamid, and Ayman Nafady*
42	**Synthesis and Characterization of 2-Pyridinylmethylene-2-quinolyl Hydrazone Cobalt(III) Complexes. Reactivity, Trends and Solvent Effect on the Initial and Transition States of Base Catalyzed Hydrolysis** *Ahmad Desoky M. Mohamad*
43	**Simultaneous Voltammetric Determination of Acetaminophen and Isoniazid (Hepatotoxicity-Related Drugs) Utilizing Bismuth Oxide Nanorod Modified Screen-Printed Electrochemical Sensing Platforms** *Bahaa G. Mahmoud, Mohamed Khairy, Farouk A. Rashwan, and Craig E. Banks*
44	**Synthesis and characterization of silica nanostructures for cotton leaf worm control** *Haytham A. Ayoub, Mohamed Khairy, Farouk A. Rashwan, Hanan F. Abdel-Hafez*
45	**Two selective HPTLC methods for determination of some angiotensin II receptor antagonists in tablets and biological fluids** *Gamal A. Salah, Hanaa M. Abd El-Wadood, Mohamed Khairy Ahmed A. Khorshed*
46	**Synthesis of iron oxides nanoparticles with very high saturation magnetization form TEA-Fe(III) complex via electrochemical deposition for supercapacitor applications** *Mahmoud Elrouby, A.M. Abdel-Mawgoud, Rehab AbdEl-Rahman*
47	**Electrochemical Characterization and Electrode kinetics for Antimony Electrodeposition from its Oxychloride Solution in the Presence of Tartaric Acid** *Vusala Asim Majidzade, Parvin Heydar Guliyev, Akif Shikhan Aliyev, Mahmoud Elrouby, Dilgam Babir Tagiyev*
48	**High Surface Area Nanostructured Activated Carbons Derived from Sustainable Sorghum Stalk** *Kamal M. S. Khalil, Omar A. S. Allama, Mohamed Khairy, Khaled M. H. Mohammed, Rafat M. Elkhatib and Mervat A. Hamed*

49	**The common, different and unique effects of metallic engineered nanomaterials: an analytic perspective** *Thabet Tolaymat, Ash Genaidy, Wael Abdelraheem, Dionysios Dionysiou, Amro El Badawy*
50	**Analysis of metallic and metal oxide nanomaterial environmental emissions** *Thabet Tolaymat, Amro El Badawy, Ash Genaidy, Wael Abdelraheem, Reynold Sequeira*
51	**Physicochemical and photo-electrochemical characterization of novel N-doped nanocomposite ZrO_2/TiO_2 photoanode towards technology of dye-sensitized solar cells** *Ibrahim M. A. Mohamed, Van-Duong Dao, Ahmed S.Yasin, Hamouda M. Mousa, Mohamed A. Yassin, Muhammad Yasir Khan, Ho-SukChoi, Nasser A.M. Barakat*
52	**A regioselective and convenient one-pot multicomponent synthesis of 9-amino-3,5-diaryl-4,9-dihydro-5H-[1,2,4]triazolo[5,1-c] [1,2,4] triazepine-8-thiol** *Moustafa, A. H., Amer, A. A.*
53	**Fabrication of N-doped &SnO_2-incorporated activated carbon to enhance desalination and bio-decontamination performance for capacitive deionization** *Ahmed S.Yasin, Jongku Jeong, Ibrahim M.A.Mohamed, Chan HeePark, Cheol Sang Kim*
54	**ZrO_2 nanofibers/activated carbon composite as a novel and effective electrode material for the enhancement of capacitive deionization performance** *Ahmed S.Yasin, M. Obaid, Ibrahim M.A.Mohamed, Ahmed Yousef, Nasser A M Barakat*
55	**Design of an efficient photoanode for dye-sensitized solar cells using electrospun one-dimensional GO/N-doped nanocomposite SnO_2/TiO_2** *Ibrahim M. A. Mohamed, Van-Duong Dao, Ahmed S. Yasin, Nasser A. M. Barakat, Ho-Suk Choi*
56	**Synthesis of Esters and Carbamothioates Contaminating Tramadol Moiety and Their HPLC Applications** *A. Khodiary, E.A. Ahmed, Khaled M. Mohamed and Shymaa A. Thabet*
57	**Synthesis of novel ZrO_2&GO@TiO_2 nanocomposite as an efficient photoanode in dye-sensitized solar cells** *Ibrahim M. A. Mohamed, Van-Duong Dao, Ahmed S. Yasin, Mohamed A Yassin, Nasser A. M. Barakat, Ho-Suk Choi*
58	**Hetaryl-1,5 Benzodiazepines-Part I: Synthesis of 3-pyrimidinyl- and Imidazolyl-1,5-benzodiazepines** *Ahmed Khodairy, Eman A. Ahmed, and Hossam Abdel Ghany*
59	**Assessment of the Secondary Metabolite Patulin and Lycium Barbarum Fruit on INS-1 Rat Pancreatic B-Cells** *Madeha N.Al-Seeni, Ahmed R.Shatat, Nagwa M. Elsawi and Asma S.Abdo*
60	**Evaluation of Antidiabetic Activity of *Ipomoea Aquatica* Fractions in Streptozotocin Induced Diabetic in Male Rat Model** *Nagwa El-Sawi, Mahmoud Hefny Gad, Madeha Nooh Al-Seeni, Sabry Younes, El-Mewafy El-Ghadban and Soad Shaker Ali*
61	**Identification of some Bioactive Metabolites in a Fractionated Methanol Extract from Ipomoea aquatica (Aerial Parts) through TLC, HPLC, UPLC-ESI-QTOF-MS and LC-SPE-NMR Fingerprints Analyses** *Mahmoud Hefny Gad, Emmy Tuenter, Nagwa El-Sawi, Sabry Younes, El-Mewafy El-Ghadban, Kristiaan Demeyer, Luc Pieters, Yvan Vander Heyden and Debby Mangelings*
62	**Ugi Multicomponent Reaction Based Synthesis of Medium-Sized Rings** *Abdelraheem, E. M. M., Madhavachary, R., Rossetti, A., Kurpiewska, K., Kalinowska-Tluścik, J., Shaabani, S., Dömling, A.*
63	**Utility of bis(methylthio)methylene malononitrile as a synthon in the synthesis of new poly-functionalized cyanoiminopyrimidines** *Moustafa, A. H., Amer, A. A.*
64	**Biochemical and Spectral Analysis of Roridin A Toxin and Copper (I) Nicotinate Complex as Antidote on Male Rat Liver** *Nabawia M. Ismail, Hana M.Gashlan, Ahmed M. Ali and Nagwa M. Elsawi*
65	**Microwave-Assisted, One-Pot Multicomponent Synthesis of Some New Cyanopyridines** *Amer, A. A., Abdelhamid, A. A.*

66	**Syntheses of Some New N-Linked Pyrimidine-2-amines with Pyrazinopyrimidines, Thienopyrimidines, and Benzazoles via Reactions of Various Nucleophiles with Cyanamides** *Moustafa, A. H., Ahmed, W. W., Khodairy, A.*
67	**Synthesis of Novel Chromene, Pyridine, Pyrazole, Pyrimidine, and Imidazole Derivatives via One-pot Multicomponent Reaction** *Khodairy, A., Ali, A. M., El-Wassimy, M. T.*
68	**New route for the synthesis of new cyanoimino- and cyanoaminopyrimidines** *Amer, A. A., Moustafa, A. H.*
69	**Synthesis, in vitro Antibacterial and in vivo Anti-Inflammatory Activity of Some New Pyridines** *Abd-El-Badih A. G. Ghattas, Ahmed Khodairy, Hassan M. Moustafa, Bahgat R. M. Hussein, Marwa M. Farghaly, Moustafa O. Aboelez*
70	**High Hydroxide Ion Conductivity with Enhanced Alkaline Stability of Partially Fluorinated and Quaternized Aromatic Copolymers as Anion Exchange Membranes** *Mahmoud, A. M. A., Elsaghier, A. M. M., Otsuji, K., Miyatake, K.*
71	**Ring rearrangements and reactivity of 3-((4-oxo-4H-chromen-3-yl)methylene)-4-phenyl-1H-[1,5]benzodiazepin-2(3H)-one toward some nucleophiles** *Salah, H., Ahmed, E. A., Hassan, M. M.*
72	**New Heterocyclic Compounds Derived from 4,6-Diamino-3-cyano-2-methylthiopyridine and their Biological Activity** *Ghattas, A. E.-B. A. G., Khodairy, A., Moustafa, H. M., Hussein, B. R. M.*
73	**Hetaryl-1,5 Benzodiazepines-Part I: Synthesis of 3-pyrimidinyl- and Imidazolyl-1,5-benzodiazepines** *Khodairy, A., Ahmed, E.A., Abdel Ghany, H.*
74	**Synthesis, Characterization, Antimicrobial Evaluation and DFT Calculations of Fe(III), Ni(II) and Cu(II) Complexes of Tridentate ONO Donor Ligand** *A. M. Abdel-Mawgoud, Mohamed Ismael, Aly Abdou*
75	**An Efficient One-Pot Three-Component Synthesis of Some New Polyhydroquinolines via Enaminone Intermediates** *Abdelhamid, A. A., Abd Allah, O. A., Tamam, A. H. A.*
76	**One-Pot Multicomponent Synthesis of Novel 2-Tosyloxyphenylpyrans under Green and Conventional Condition with Anti-inflammatory Activity** *Khodairy A., Ali A. M., Aboelez M. O., El-Wassimy M. T.*
77	**Facile synthesis of GO@SnO_2/TiO_2 nanofibers and their behavior in photovoltaics** *Ibrahim M. A. Mohamed, Van-Duong Dao, Ahmed S. Yasin, Ho-Suk Choi, Khalil Abdelrazek Khalil, Nasser A.M. Barakat*
78	**Synthesis and Antimicrobial Screening of Fused Heterocyclic Pyridines** *El-Remaily, M. A. A., Elhady, O. M., Abdel-Raheem, E. M. M.*
79	**Iminophosphoranes in Heterocyclic Synthesis: A Facile Synthesis of Pyrido[4,3-D]Pyrimidine and Pyrido[4,3-D][1,3]Oxazine Derivatives via Intermolecular aza-Wittig Reactions** *Omran O. A., Sayed S. M., Raslan M. A.*
80	**Utility of CyanoaceticAcid Hydrazide in Organic Synthesis: Synthesis and Characterization of Some Novel Heterocycles bearing 1,3,4-Oxadiazole Moeity** *Mounir A. A. Mohamed, Omar M. El-Hady, Ahmed M. El-Sayed*
81	**Two-Step Synthesis of Complex Artificial Macrocyclic Compounds** *Rudrakshula Madhavachary, Eman M. M. Abdelraheem, Arianna Rossetti*
82	**Morpholinium hydrogen sulfate (MHS) ionic liquid as an efficient catalyst for the synthesis of bioactive multi-substituted imidazoles (MSI) under solvent-free conditions** *Marzouk A. A., Abdelhamid A. A., Mohamed S. K., Simpson J.*
83	**Synthesis, Characterization, DFT Calculations and Biological Studies of Mn(II), Fe(II), Co(II) and Cd(II) complexes based on a tetradentate ONNO donor Schiff base ligand** *Laila H. Abdel-Rahman, Nabawia M. Ismail, Mohamed Ismael, Ahmed M. Abu-Dief and Ebtehal Abdel-Hameed Ahmed*
84	**Crystal structure of 1-[2-(4-chlorophenyl)-4,5-diphenyl-1H-imidazol-1-yl]propan-2-ol** *Mohamed S. K., Marzouk A. A., Albayati M. R., Abdelhamid A. A., Simpson J.*

85	**Design and Nonlinear Optical Properties (NLO) using DFT Approach of New Cr (III), VO(II), and Ni(II) Chelates Incorporating Tri-dentate Imine Ligand for DNA Interaction, Antimicrobial, Anticancer Activities and Molecular Docking Studies** *Laila H. Abdel-Rahman, Ahmed M. Abu-Dief, H. Moustafa and Azza A. Hassan Abdel-Mawgoud*
86	**Biochemical and Spectral Analysis of Roridin A Toxin and Copper (I) Nicotinate Complex as Antidote on Male Rat Liver** *Nabawia M. Ismail, Hana M. Gashlan, Ahmed M. Ali, Nagwa M. Elsawi*
87	**Alcohol Dehydrogenases Catalyze the Reduction of Thioesters** *Sabry H. H. Younes, Yan Ni, Sandy Schmidt, Wolfgang Kroutil, Frank Hollmann*
88	**Rapid chemoenzymatic route to glutamate transporter inhibitor L-TFB-TBOA and related amino acids** *Haigen Fu, Sabry H. H. Younes, Mohammad Saifuddin, Pieter G. Tepper, Jielin Zhang, Erik Keller, André Heeres, Wiktor Szymanski and Gerrit J. Poelarends*

List of papers published by Staff members of Botany&Microbilogy Department

1	**Extracellular biosynthesis of silver nanoparticles using Rhizopus stolonifer** *AbdelRahim K., Mahmoud S. Y. Ali, A.M. , Almaary, K. S., Mustafa, A. E.-Z. M. A, Husseiny, S. M.*
2	**Rise Potassium Content of the Medium Improved Survival, Multiplication, Growth and Scavenging System of in Vitro Grown Potato under Salt Stress** *A. M. Hassanein and Jehan M. Salem*
3	**Shoot Regeneration and Isoenzyme Expression of Moringa oleifera L. under the influence of salt stress** *A. M. Hassanein· J. M. Salem· F. A. Faheed· A. El-nagish*
4	**Response of duckweed to lead exposure: phytomining, bioindicators and bioremediation** *A. K. Hegazy, M. H. Emam, L. Lovett-Doust, E. Azab, A. A. El-Khatib*
5	**Macrophytes-cyanobacteria allelopathic interactions and their implications for water resources management-A review** *Zakaria A. Mohamed*
6	**Isolation, Optimization and Characterization of Cellulases and Hemicellulases from *Bacillus Cereus* LAZ 518 Isolated from Cow Dung Using Corn Cobs as Lignocellulosic Waste** *M. A. Abu-Gharbia, N. M. El-Sawy, A. M. Nasr and L. A. Zedan*
7	**New saprobic marine fungi and a new combination** *Abdel-Wahab M. A., Dayarathne M. C., Suetrong S., Guo S.-Y., Alias S. A., Bahkali A. H., Nagahama T., Elgorban A. M., Abdel-Aziz F. A., Hodhod M. S., Al-Hebshi M. O., Hyde K. D., Nor N. A. B. M., Ka-Lai Pang K. L. & E. B. Gareth Jones E. B. G.*
8	**Genetic analysis of *Plectranthus* L. (Lamiaceae) in Saudi Arabia based on RAPD and ISSR markers** *Kadry Abdel Khalik and Gamal Hariedy*
9	**Notes for genera: Ascomycota** *Nalin N. Wijayawardene, Kevin D. Hyde, Kunhiraman C. Rajeshkumar, David L. Hawksworth, Hugo Madrid, Paul M. Kirk, Uwe Braun, Rajshree V. Singh, Pedro W. Crous, Martin Kukwa, Robert Lu¨cking, Cletus P. Kurtzman, Andrey Yurkov, Danny Haelewaters, Andre´ Aptroot, H. Thorsten Lumbsch, Einar Timdal, Damien Ertz, Javier Etayo, Alan J. L. Phillips, Johannes Z. Groenewald, Moslem Papizadeh, Laura Selbmann, Monika C. Dayarathne, Gothamie Weerakoon, E. B. Gareth Jones, Satinee Suetrong, Qing Tian, Rafael F. Castan˜eda-Ruiz, Ali H. Bahkali, Ka-Lai Pang, Kazuaki Tanaka, Dong Qin Dai, Jariya Sakayaroj. Martina Hujslova´, Lorenzo Lombard, Belle D. Shenoy, Ave Suija, Sajeewa S. N. Maharachchikumbura, Kasun M. Thambugala, Dhanushka N. Wanasinghe, Bharati O. Sharma, Subhash Gaikwad, Gargee Pandit, Laura Zucconi, Silvano Onofri, Eleonora Egidi, Huzefa A. Raja, Rampai Kodsueb, Marcela E. S. Ca´ceres, Sergio Pe´rez-Ortega, Patrı´cia O. Fiuza, Josiane Santana Monteiro, Larissa N. Vasilyeva, Roger G. Shivas, Maria Prieto, Mats Wedin, Ibai Olariaga, Adebola Azeez Lateef, Yamini Agrawal, Seyed Abolhassan Shahzadeh Fazeli, Mohammad Ali Amoozegar, Guo Zhu Zhao, Walter P. Pfliegler, Gunjan Sharma, Magdalena Oset, Mohamed A. Abdel-Wahab, Susumu Takamatsu, Konstanze Bensch, Nimali Indeewari de Silva, Andre´ De Kesel, Anuruddha Karunarathna, Saranyaphat Boonmee, Donald H. Pfister, Yong-Zhong Lu, Zong-Long Luo, Nattawut Boonyuen, Dinushani A. Daranagama, Indunil C. Senanayake, Subashini C. Jayasiri, Milan C. Samarakoon, Xiang-Yu Zeng, Mingkwan Doilom, Luis Quijada, Sillma Rampadarath, Gabriela Heredia, Asha J. Dissanayake, Ruvishika S. Jayawardana, Rekhani H. Perera, Li Zhou Tang, Chayanard Phukhamsakda, Margarita Herna´ndez-Restrepo, Xiaoya Ma, Saowaluck Tibpromma, Luis F. P. Gusmao, Darshani Weerahewa, Samantha C. Karunarathna*
10	**Micromorphological studies on the genus *Lotus* L. (Fabaceae: Loteae) from Egypt** *Momen Zareh, Ahmed Faried, Nashwa Farghaly*
11	**Natural products of *Nothophoma multilocularis* sp. nov. an endophyte of the medicinal plant *Rhazya stricta*** *Mohamed A. Abdel-Wahab, Ali H. A. Bahkali, Abdallah M. El-Gorban and Mohamed S. Hodhod*
12	**Floristic composition and vegetation: Environmental relationships of Wadi Fatimah, Mecca, Saudi Arabia** *Kadry Abdel Khalik, Iman H. Al-Gohary, Yassin Al-Sodany*

13	**HPLC Profile of Phenolic Constituents, Essential Oil Analysis and Antioxidant Activity of Six *Plectranthus* Species Growing in Saudi Arabia** *Usama Shaheen, Kadry Abdel Khalik, Mohamed I. S. Abdelhady, Mohamed Aborehab*
14	**Action of cadmium toxicity on growth, physiological activities and subcellular components of watercress (Eruca sativa L.) plant: The protective role of salicylic acid** *Khalaf Ali Fayez*
15	**Impact of Glyphosate Herbicide and Salicylic Acid on Seed Germination, Cell Structure and Physiological Activities of Faba Bean (*Vicia faba* L.) Plant** *Khalaf Ali Fayez and Esmat F. Ali*
16	**Toxicity of biosynthetic silver nanoparticles on the growth, cell ultrastructure and physiological activities of barley plant** *K. A. Fayez, B. A. El-Deeb, N. Y. Mostafa*
17	**Exhalation Air Fungal Culture of Mechanically Ventilated Aspergillosis Suspected Patients in Concordance with Other Conventional Diagnostic Techniques** *M Bassam Aboul-Nasr, Abdel-Nasser Zohri, Mohamed Adam and Enas Mahmoud Amer*
18	**Impact of Enzymes and Toxins Potentiality of Four Aspergillus Species to Cause Aspergillosis** *Abdel-Nasser Zohri, M Bassam Aboul-Nasr, Mohamed Adam, Mohamed A Mustafa and Enas Mahmoud Amer*
19	**Physico-chemical changes in karkade (Hibiscus sabdariffa L.) seedlings responding to salt stress** *Galal A.*
20	**Synthesis, *in vitro* antibacterial and *in vivo* anti-inflammatory activity of some new pyridines** *Abd-El-Badih A. G. Ghattas, Ahmed Khodairy, Hassan M. Moustafa, Bahgat R. M. Hussein, Marwa M. Farghaly, and Moustafa O. Aboelez*
21	**Antioxidant and antimicrobial activities of the methanolic extracts of some edible seed spices** *Deya Eldeen Mohammed Radwan, Ashraf Mohammed Mohammed Essa and Dia Mohammed Soltan*
22	***In vitro* propagation, microtuberization, and molecular characterization of three potato cultivars** *J. Salem and A. M. Hassanein*
23	**Differential responses of esterase isoenzyme of peanut to salinity and drought as influenced by salicylic acid** *Dia M. Soltan and Jehan M. Salem*
24	**Chemical Structure of Natural roducts and haracterization of Secretory issue of Sweet Basil (*Ocimumbasilicum L.*) Under Lead Stress** *Naglaa Y. Abdallah, Amany M. Aboel kassem and Omer M. Elsheikh*
25	**Identification and in vitro Susceptibility Pattern of Fungal Infection Isolated from Patients with Otomycosis** *Abeer Sheneef, Hameda Hassan, Khaled A. Ali, Mahmoud Saad-Eldin, Amira Esmail*
26	**Pollen morphology and numerical analysis of *Tamarix* L. (Tamaricaceae) in Egypt and its systematic implication** *Ahmed Elkordy and Ahmed Faried*
27	**Impact of some essential oils on the growth of toxigenic fungi and their toxin production** *Zohri A. A., Saber S. M., Youssef M. S. and Marwa Abdel-Kareem, M*
28	**Impact of some essential oils on the growth of toxigenic fungi and their toxin production** *Zohri A. A., Saber S.M., Youssef, M.S. and Marwa Abdel-Kareem M.*
29	**Inhibition of three toxigenic fungal strains and their toxins production using selenium nanoparticles** *Marwa Mahmoud Abdel-Kareem[1], Abdel-Naser Ahmed Zohri*
30	**Responses of maize crop (Zea mays L.) to foilar spraying with humic acid at different nitrogen levels** *E. I. Mohamed, Fayza A. Faheed and Huda M. Mahmoud*

31	**Fungal diversity notes 603–708: taxonomic and phylogenetic notes on genera and species** *Kevin D. Hyde, Chada Norphanphoun, Vanessa P. Abreu, Anna Bazzicalupo, K. W. Thilini Chethana, Marco Clericuzio, Monika C. Dayarathne, Asha J. Dissanayake, Anusha H. Ekanayaka, Mao-Qiang He, Sinang Hongsanan, Shi-Ke Huang, Subashini C. Jayasiri, Ruvishika S. Jayawardena, Anuruddha Karunarathna, Sirinapa Konta, Ivana Kusˇan, Hyun Lee, Junfu Li, Chuan-Gen Lin, Ning-Guo Liu, Yong-Zhong Lu, Zong-Long Luo, Ishara S. Manawasinghe, Ausana Mapook, Rekhani H. Perera, Rungtiwa Phookamsak, Chayanard Phukhamsakda, Igor Siedlecki, Adriene Mayra Soares, Danushka S. Tennakoon, Qing Tian, Saowaluck Tibpromma, Dhanushka N. Wanasinghe, Yuan-Pin Xiao, Jing Yang, Xiang-Yu Zeng, Faten A. Abdel-Aziz, Wen-Jing Li, Indunil C. Senanayake, Qiu-Ju Shang, Dinushani A. Daranagama, Nimali I. de Silva, Kasun M. Thambugala, Mohamed A. Abdel-Wahab, Ali H. Bahkali, Mary L. Berbee, Saranyaphat Boonmee, D. Jayarama Bhat, Timur S. Bulgakov, Bart Buyck, Erio Camporesi, Rafael F. Castan˜eda-Ruiz, Putarak Chomnunti, Minkwan Doilom, Francesco Dovana,Tatiana B. Gibertoni, Margita Jadan, Rajesh Jeewon, E. B. Gareth Jones, Ji-Chuan Kang, Samantha C. Karunarathna, Young Woon Lim, Jian-Kui Liu, Zuo-Yi Liu, Helio Longoni Plautz Jr., Saisamorn Lumyong, Sajeewa S. N. Maharachchikumbura, Neven Matocˇec, Eric H. C. McKenzie, Armin Mesˇic´, Daniel Miller, Julia Pawłowska, Olinto L. Pereira, Itthayakorn Promputtha, Andrea I. Romero, Leif Ryvarden, Hong-Yan Su, Satinee Suetrong, Zdenko Tkalcˇec, Alfredo Vizzini, Ting-Chi Wen, Komsit Wisitrassameewong, Marta Wrzosek, Jian-Chu Xu, Qi Zhao, Rui-Lin Zhao, Peter E. Mortimer***

List of papers published by Staff members of Zoology Department

1	**3-Glucocorticoid and cytokine crosstalk: Feedback, feedforward, and co-regulatory interactions determine repression or resistance** *Newton R , Shah S., Altonsy M. O., Gerber A. N.*
2	**4-Long-acting β -agonists promote glucocorticoid-mediated repression of NF-κB by enhancing expression of the feedback regulator TNFAIP3** *Altonsy MO , Mostafa MM , Gerber AN, Newton R*
3	**Distribution and Morphology of Defensive Acid-Secreting Glands in Nudipleura (Gastropoda: Heterobranchia), With an Emphasis on Pleurobranchomorpha** *Heike Wägele , Kristina Knezevic and Alaa Y. Moustafa*
4	**Effects of seasonal acclimatization on thermal tolerance of inward currents in roach (Rutilus rutilus) cardiac myocytes** *Ahmed Badr, Minna Hassinen, Mohamed F. El-Sayed, Matti Vornanen*
5	**Assessment of Biochemical and Histopathological Effects of Crude Venom of Cone Snail *Conus flavidus* on *albino* Mice** *Mona F. Abou-Elezz , Alaa Y. Moustafa , Mohamed S. El-Naggar*
6	**Pathogenic bacteria carried by synanthropic filthy flies (*Musca* species) at farmed animals in Sohag Governorat, Egypt: 2-Percentage of bacterial infection in Musca species** *Azza M. Khedre, Tarek G. Ismail, Amany A. Yousif , Gehad A. Hashem*
7	**Do the environment or the carcass affect the sarcosaprophagous community?** *María Pérez-Marcos, María-Dolores García, María-Isabel Arnaldos, Elena López Gallego, Azza Khedre, Aurelio Luna*
8	**Insulin-like 3 expression and fibrosis induction after intra-testicular injection of magnetic nanoparticles in rat testis and the ameliorative role of Echinacea purpurea extract** *Aziz Awaad, Mohamed A. Adly & Doaa Hosny*
9	**Scanning electron morphological studies of *Tribolium confusum* Jacquelin du Val (Coleopteran: Tenebrionidae)** *Nasra M. H. Zohry*
10	**Evaluation of Two Novel Feeding Protocols Utilizing Alive and Dried Chlorella *vulgaris* to Grow *Heterocypris salina* (Ostracoda: Crustacea)** *Ebtesam A Yousef and Mahmoud H.Hegab*
11	**Histological and histopathological studies on the protective role of Echinacea purpurea extract after intra-testicular injection of magnetic nanoparticles in male albino rats** *Aziz Awaad, Mohamed A. Adly & Doaa Hosny*
12	**Some biological aspects and population dynamics of the five-lined snapper, *Lutjanus quinquelineatus* (Family:Lutjanidae) from Red Sea off Hurghada, Egypt** *Sahar F Mehanna, Taha S Baker, Faiza M Soliman and Hamdy A Soliman*
13	**Protein, Electrophoresis Analysis and Heavy Metals in Muscles of Wild and Farmed *Oreochromis Niloticus*** *Hamdy A. M. Soliman*
14	**Effects of seasonal acclimatization on action potentials and sarcolemmal K+ currents in roach (Rutilus rutilus) cardiac myocytes** *Ahmed Badr, Minna Hassinen, Mohamed F. El-Sayed, Matti Vornanen*
15	**A New Aquatic Oribatid Mite, *Trimalaconothrus Crassipes* SP. N. (Family: Malaconothridae), Sohag, Egypt** *Ramadan S. A., Ismail T. G. and Mustafa, A. N.*
16	**Immunohisto Chemical Expression Patterns of Glial Cell Line-Derived Neurotrophic Factor and its Cognate Receptor GFRα-1 in Lichen Planus** *Mohamed A. Adly, Hanan A. Assaf, Mohammed Abu El-Hamd, Nagwa Sayed, Hemat Mostafa and Mahmoud Rezk A. Hussein*
17	**Copper Oxide Nanoparticles and Copper Sulphate Act as Antigenotoxic Agents in Drosophila melanogaster** *Mohamed Alaraby, Alba Hernandez and Ricard Marcos*
18	**The Ontogeny of Appendages and Carapace of *Neonesidea Schulzi* (Ostracoda: Bairdiidae) from the Red Sea Coast, Egypt** *Ebtesam A. Yousef & Alaa Y. Moustafa*

List of papers published by Staff members of Geology Department

1	**Coupling of field investigations and remote sensing data for karst hazards in Egypt: case study around the Sohag City** *Ahmed M. Youssef, Abdel-Hamid El-Shater, Mohamed H. El-Khashab, Bosy A. El-Haddad*
2	**Rainfall-induced landslide susceptibility assessment at the Chongren area (China) using frequency ratio, certainty factor, and index of entropy** *Haoyuan Hong, Wei Chen, Chong Xu, Ahmed M. Youssef, Biswajeet Pradhan and Dieu Tien Bui*
3	**Karst induced geo-hazards in Egypt: Case study slope stability problems along some selected desert highways** *Ahmed M. Youssef, Abdel-Hamid El-Shater, Mohamed H. El-Khashab, Bosy A. El-Haddad*
4	**Suitability estimation for urban development using multi-hazard assessment map** *George D.Bathrellos, Hariklia D. Skilodimou, Konstantinos Chousianitis, Ahmed M.Youssef, Biswajeet Pradhan*
5	**Site investigation using engineering geology mapping and geological hazard evaluation: Case study of the New Hail Economic City, Hail Region, KSA** *T. E. Al-Sehly, A. M. Youssef, A. A. Al-Otaibi, H. M. Al-Harbi*
6	**Slope stability hazard assessment using 3D remote sensing and field sketching techniques along Sohag-Red Sea-Cairo highway, Egypt** *Bosy A. El-Haddad, Ahmed M. Youssef, Abdel-Hamid El-Shater, Mohamed H. El-Khashab*
7	**Dynamic geotechnical properties evaluation of a candidate nuclear power plant site (NPP): P- and S-waves seismic refraction technique, North Western Coast, Egypt** *A. M. Abudeif, A. E. Raef, A. A. Abdel Moneim, M. A. Mohammed, A. F. Farrag*
8	**Geology, structure, geochemistry and ASTER-based mapping of Neoproterozoic Gebel El-Delihimmi granites, Central Eastern Desert of Egypt** *Asran Mohamed Asran, Ashraf Emam, Abdelhamid El-Fakharani*
9	**Historical Bricks Deterioration and Restoration from the Red Monastery, Sohag, Egypt: A Geochemical, Petrological and Statistical Approaches** *Abd-Elkareem, E., Ali, M. & El-Sheikh, A.*
10	**The Bivalve Fauna of the Eocene Succession of the Maghagha Area, East and West of the Nile Valley, Egypt** *Elattaar, A. A. and Seddik, A. A.*
11	**Study of Sea urchin Jacksonaster depressum (L. Agassiz, 1841) (Echinodermata, Echinoidea) from the Northern Bay of Safaga, Red Sea coast, Egypt, as an indicator of the change in the Red Sea Environment** *Atef Abdelhamied Elattaar*
12	**Heavy metals seasonal variability and distribution in Lake Qaroun sediments, El-Fayoum, Egypt** *Mostafa Redwan, Engy Elhaddad*
13	**Application of quantitative mineralogy on the neutralization–acid potential calculations within µm-scale stratified mine tailings** *Mostafa Redwan, Dieter Rammlmair, Wilhelm Nikonow*
14	**Influence of Organo-Metal Interactions on Regeneration of Exhausted Clay Mineral Sorbents in Soil Columns Loaded with Heavy Metals** *Yasser Refaey, Boris Jansen, Pim DE Voogt, John Rparsons, Abdel-Hamid EL-Shater, Abdel-Aziz EL-Haddad, Karsten KALBITZ*
15	**Effects of clay minerals, hydroxides, and timing of dissolved organic matter addition on the competitive sorption of copper, nickel, and zinc: A column experiment** *Yasser Refaey, Boris Jansen, John R. Parsons, Pimde Voogt, Simone Bagnis, Adriaan Markus, Abdel-Hamid El-Shater, Abdel-Aziz El-Haddad, Karsten Kalbitz*
16	**Geomorphic and lithologic characteristics of wadi feiran basin, southern Sinai, Egypt, using remote sensing and field investigations** *Ayman A Ahmed, Mohamed Abdelkareem, Asran M Asran, Tawfig M Mahran*
17	**The impact of eustasy, tectonics, and paleoclimate on the dolomitization of the syn-rift neogene carbonate platforms in the red sea coastal area, Egypt** *Abdallah M. Hassan*

18	**Miocene echinoids from the Sadat area, south Gebel Ataqa, NW Gulf of Suez, Egypt: systematics, palaeobiogeography** *Atef A. Elattaar*
19	**Mineral composition and geochemistry of the Upper Cretaceous siliciclastics (Nubia Group), Aswan District, south Egypt: Implications for provenance and weathering** *Abdallah M. Hassan*
20	**Engineering properties of concrete made with crushed aggregates of diorite, Jeddah, Saudi Arabia** *El-Sayed Sedek Abu Seif and Abdullah R. Sonbul*
21	**Geotechnical hazardous effects of municipal wastewater on plasticity and swelling potentiality of clayey soils in Upper Egypt** *El-Sayed Sedek Abu Seif*
22	**Palynofacies analysis and palaeoenvironmental reconstruction of the Upper Cretaceous sequence drilled by the Salam-60 well, Shushan Basin: Implications on the regional depositional environments and hydrocarbon exploration potential of north-western Egypt** *Magdy S. Mahmoud, Amr S. Deaf, Mohamed A. Tamam, Miran M. Khalaf*
23	**Comparison of four kernel functions used in support vector machines for landslide susceptibility mapping: A case study at Suichuan area (China)** *Haoyuan Hong, Biswajeet Pradhan, Dieu Tien Bui, Chong Xu, Ahmed M. Youssef and Wei Chen*
24	**Damage Blocks Granite of Philip Arrhidaeus Compartment and its Source and Treatment, Karnak, Egypt** *Abd-Elkareem, E., Asran, M. & El Shater, A.*
25	**GIS-based multi-criteria earthquake hazards evaluation using analytic hierarchy process for a nuclear power plant site, west Alexandria, Egypt** *A. M. Abudeif, A. A. Abdelmoneim, A. F. Farrag*

Number of published papers by staff members of Faculty of Science during 2016

Department	Number
Mathematics	68
Physics	53
Chemistry	88
Botany & Microbiology	31
Zoology	18
Geology	25
Total	283

- **Collaborative research publications include:**
  Departments of Physics and Chemistry collaborate and success to publish four articles within 2017
  Chemistry department also collaborate with Botany Department and publishes one article within 2017.

Mathematics

Propagation of a thermoelastic wave in a half-space of a homogeneous isotropic material subjected to the effect of gravity field

A. M. Abd-Alla[a], S. M. Abo-Dahab[b,c], H. A. Alotaibi[c]

[a]*Department of Mathematics, Faculty of Science, Sohag University, Egypt*

[b]*Department of Mathematics, Faculty of Science, SVU, Qena 83523, Egypt*

[c]*Department of Mathematics, Faculty of Science, Taif University, 888, Saudi Arabia*

The propagation of thermoelastic waves in a homogeneous, isotropic elastic semi-infinite space is subjected to a gravitational field, which is at temperature T0 initially, and whose boundary surface is subjected to heat source and load moving with finite velocity. Temperature and stress distribution occurring due to heating or cooling and have been determined using certain boundary conditions. Numerical results have been given and illustratedgraphically in each case considered. The results indicate that the effect of gravity field is very pronounced. Comparison is made with the results predicted by the theory of thermoelasticity in the absence of gravity. The results indicate that the effect of the gravity is very pronounced.

Archives of Civil and Mechanical Engineering 17 (2017) 564-573

Eigenvalue approach to two dimensional coupled magneto-thermoelasticity in a rotating isotropic medium

F.S. Bayones[a], A.M. Abd-All[a,b]

[a]*Mathematics Department, Faculty of Science, Taif University, Saudi Arabia*

[b]*Mathematics Department, Faculty of Science, Sohag University, Sohag, Egypt*

This paper is devoted to two-dimensional problem of thermoelasticity dealing with thermoelastic wave propagation in a rotating medium with magnetic field effects and a time-dependent heat source effect due to thermomechanical source. The normal mode analysis and eigenvalue approach techniques are applied to solve the problem. The expressions of displacement, mean value of normal stress, dilatation and temperature are obtained in the domain. Numerical simulated results are depicted graphically to show the effect of magnetic field and rotation on resulting quantities. The results indicate that the effect of magnetic field, rotation, frequency, wave number and time are very pronounced.

Results in Physics 7 (2017) 2941-2949

Rotational Effects on Magneto-Thermoelastic Stoneley, Love and Rayleigh Waves in Fibre-Reinforced Anisotropic General Viscoelastic Media of Higher Order

A. M. Abd-Alla[1,2], S. M. Abo-Dahab[1,3], Aftab Khan[4]

[1]Math. Dept., Faculty of Science, Taif University 888, Saudi Arabia.
[2]Math. Dept., Faculty of Science, Sohag University, Egypt.
[3]Math. Dept., Faculty of Science, SVU, Qena 83523, Egypt
[4]Department of Mathematics, COMSATS, Institute of Information, Park Road, Chakshahzad, Islamabad, Pakistan

In this paper, we investigated the propagation of magneto-thermoelastic surface waves in fibre-reinforced anisotropic general viscoelastic media of higher order ofnth order, including time rate of strain under the influence of rotation and magnetic field.The general surface wave speed is derived to study the effects of rotation, magnetic field and thermal on surface waves. Particular cases for Stoneley, Love and Rayleigh waves are discussed. The results obtained in this investigation are more general in the sense that some earlier published results are obtained from our result as special cases. Our results for viscoelastic of order zero are well agreed to fibre-reinforced materials. Comparison was made with the results obtained in the presence and absence of rotation, magnetic field and parameters for fibre-reinforced of the material medium. It is also observed that, surface waves cannot propagate in a fast rotating medium. Numerical results for particular materials are given and illustrated graphically. The results indicate that the effect of rotation, magnetic field on fibre-reinforced anisotropic general viscoelastic media are very pronounced.
CMC, Computers, Materials & Continua 53(1), 2017, pp.49-72.

Plane Vibrations in a Transversely Isotropic Infinite Hollow Cylinder Under Effect of the Rotation and Magnetic Field

F. S. Bayones[1] and A. M. Abd-Alla[2]

[1]Math. Dept., Faculty of Science, Taif University, Saudi Arabia.
[2]Mathematics Department, Faculty of Science, Sohag, Egypt.

The aim of this paper is to study the effects of rotation and magnetic field on the plane vibrations in a transversely isotropic material of an infinite hollow cylinder. The natural frequency of the plane vibrations in the case of harmonic vibrations has been obtained. The natural frequencies are calculated numerically and the effects of rotation and magnetic field are discussed. The numerical results obtained have been illustrated graphically to understand the behavior of frequency equation with different values of frequencyω under effects the rotation and magnetic field. Comparison was made with the results obtained in the presence and absence of the rotation and magnetic field. The results indicate that the effect of rotation and magnetic field are very pronounced.
CMES, Computers, Materials & Continua 113(2) 2017, pp.155-175

Peristaltic transport of a Jeffrey fluid under the effect of gravity field and rotation in an asymmetric channel with magnetic field

A. M. Abd-Alla[1], S.M. Abo-Dahab[2,3] and Abdullah Alsharif[3]

[1]Department of Mathematics, Faculty of Science, Sohag University, Sohag, Egypt
[2]Department of Mathematics, Faculty of Science, South Valley University, Qena, Egypt
[3]Department of Mathematics, Faculty of Science, Taif University, Taif, Saudi Arabia,

Purpose-The Purpose-The purpose of this paper is to study the peristaltic flow of a Jeffrey fluid in an asymmetric channel, subjected to gravity field and rotation in the presence of a magnetic field. The channel asymmetry is produced by choosing the peristaltic wave train on the walls to have different amplitude and phase. The flow is investigated in a wave frame of reference moving with the velocity of the wave. Involved problems are analyzed through long wavelength and low Reynolds number.
Design/methodology/approach-The analytical expressions for the pressure gradient, pressure rise, stream function, axial velocity and shear stress have been obtained. The effects of Hartmann number, the ratio of relaxation to retardation times, time-mean flow, rotation, the phase angle and the gravity field on the pressure gradient, pressure rise, streamline, axial velocity and shear stress are very pronounced and physically interpreted through graphical illustrations. Comparison was made with the results obtained in the asymmetric and symmetric channels. Findings-The results indicate that the effect of the Hartmann number, the ratio of relaxation to retardation times, time-mean flow, rotation, the phase angle and the gravitational field are very pronounced in the phenomena.
Originality/value–In the present work, the authors investigate gravity field, and rotation through an asymmetric channel in the presence of a magnetic field has been analyzed. It also deals with the effect of the magnetic field and gravity field of peristaltic transport of a Jeffrey fluid in an asymmetric rotating channel.
Multidiscipline Modeling in Materials and Structures, 13(4) (2017), pp.522-538

Influence of magnetic field and heat and mass transfer on the peristaltic flow through a porous rotating medium with compliant walls

A. M. Abd-Alla[1], S.M. Abo-Dahab[2,3] and M. Elsagheer[1]

[1]Department of Mathematics, Faculty of Science, Sohag University, Sohag, Egypt
[2]Department of Mathematics, Faculty of Science, South Valley University, Qena, Egypt
[3]Department of Mathematics, Faculty of Science, Taif University, Taif, Saudi Arabia,

Purpose – The purpose of this paper is to predict the effects of magnetic field, heat and mass transfer and rotation on the peristaltic flow of an incompressible Newtonian fluid in a channel with compliant walls. The whole system is in a rotating frame of reference. Design/methodology/approach - The governing equations of two-dimensional fluid have been simplified under long wavelength and low Reynolds number approximation. The solutions are carried out for the stream function, temperature, concentration field, velocity and heat transfer coefficient. Findings-The results indicate that the effects of permeability, magnetic field and rotation are very pronounced in the phenomena. Impacts of various involved parameters appearing in the solutions are carefully analyzed.
Originality/value – The effect of the concentration distribution, heat and mass transfer and rotation on the wave frame is analyzed theoretically and computed numerically. Numerical results are given and illustrated graphically in each case considered. A comparison was made with the results obtained in the presence and absence of rotation, magnetic field and heat and mass transfer.
Multidiscipline Modeling in Materials and Structures, 3(4) (2017), pp. 648-663.

A two-dimensional problem with rotation and magnetic field in the context of four thermoelastic theories

S.M. Abo-Dahab[a,b], A. M. Abd-Alla[c] and A. J. Alqarni[b]

[a]*Mathematics Department, Faculty of Science, SVU, Qena 83523, Egypt*

[b]*Mathematics Department, Faculty of Science, Taif University, 888, Saudi Arabia*

[c]*Mathematics Department, Faculty of Science, Sohag University, Egypt*

The aim of the present paper is to study the effect of rotation and magnetic field on the general model of the equations of generalized thermoelasticity for a homogeneous isotropic elastic half-space. The formulation is applied under four theories of generalized thermoelasticity: the coupled theory (CT), LordSchulman (LS) theory, Green-Lindsay (GL) theory as well as Green-Naghdi (GN) theory. By employing normal mode analysis, the analytical expressions for the temperature, displacement components and the (Mechanical and Maxwell's) stresses distribution are obtained in the physical domain. These expressions are also calculated numerically and corresponding graphs are plotted to illustrate and compare theoretical results. The effect of rotation and magnetic field are also studied.

Results in Physics 7 (2017) 2742-2751

Rotational effect on thermoelastic Stoneley, Love and Rayleigh waves in fibre-reinforced anisotropic general viscoelastic media of higher order

A.M. Abd-Alla[1], S.M. Abo-Dahab[2,3] and Aftab Khan[4]

[1]Mathematics Department, Faculty of Science, Sohag University, Egypt

[2]Mathematics Department, Faculty of Science, SVU, Qena 83523, Egypt

[3]Mathematics Department, Faculty of Science, Taif University 888, Saudi Arabia

[4]Department of Mathematics, COMSATS, Institute of Information, Park Road, Chakshahzad, Pakistan

In this paper, we investigated the propagation of thermoelastic surface waves in fibre-reinforced anisotropic general viscoelastic media of higher order of nth order including time rate of strain under the influence of rotation. The general surface wave speed is derived to study the effectsof rotation andthermal onsurface waves. Particular cases for Stoneley, Love and Rayleighwaves are discussed.The results obtained in this investigation are more general in the sense that some earlier published results are obtained from our result as special cases. Our results for viscoelastic of order zero are well agreed to fibre-reinforced materials. Comparison was made with the results obtained in the presence and absence of rotation and parameters for fibre-reinforced of the material medium. It is also observed that, surface waves cannot propagate in a fast rotating medium.Numerical results for particular materials are given and illustrated graphically. The results indicate that the effect of rotation on fibre-reinforced anisotropic general viscoelastic media are very pronounced.

Structural Engineering and Mechanics, 61(2) (2017) 221-230

On an influence of thermal stresses and magnetic field in thermoelastic half-space without energy dissipation

S. M. Abo-Dahab[a,b], A. M. Abd-Alla[c] and H. A. Alotaibi[b]

[a]*Department of Mathematics, Faculty of Science, South Valley University, Qena, Egypt;*
[b]*Department of Mathematics, Faculty of Science, Taif University, Taif, Saudi Arabia;*
[c]*Department of Mathematics, Faculty of Science, Sohag University, Sohag, Egypt*

In this article, a two-dimensional problem for a homogeneous, isotropic, and thermoelastic half-space subjected to magnetic field and time-dependent heat source is investigated. The boundary conditions at the surface have been considered in the context of Green-Naghdi's second model (GN-II) of thermoelasticity. The normal mode analysis and eigenvalue pproach techniques are used to solve the nondimensional coupled equations. The eect of magnetic field, frequency, wave number, and time is analyzed theoretically and computed numerically. Comparison was made with the results obtained in the presence and absence of the magnetic field. Numerical results for the displacement components, mean value of normal stresses, dilatation, and temperature have been represented graphically to show the physical meaning of the external parameters. The results indicate that the eect of magnetic field, frequency, wave number, and time is very pronounced and eective on the phenomena.

Journal of hermal Stresses, 40(3), 2017 pp. 267-280.

Step-Stress Partially Accelerated Life Tests Model in Estimation of Inverse Weibull Parameters under Progressive Type-II Censoring

G. A. A. Soliman[1,2], E. A. Ahmed[2], N. A. Abou-Elheggag[2] and S. M. Ahmed[2]

[1]*Faculty of Science, Islamic University, Madinah, KSA*
[2]*Mathematics Department, Sohag University, Sohag 82524, Egypt*

In this paper, inverse Weibull (IW) distribution with the step-stress model and progressive type-II censoring data are considered. The maximum likelihood and Bayesian estimation are discussed for the distribution parameters and the acceleration factor. The outline criteria in Bayesian approach are settled under utilized non-informative and gamma informative priors under balancedsquared error and balanced linear-exponential loss functions with the help of MCMC method. Finally, the numerical example and simulation study are constructed to assess the obtaining results.

Appl. Math. Inf. Sci. 11, No. 5, 1369-1381 (2017)

Shear horizontal waves in composite materials: Behavior under rotation and initial stress

Abo-el-nour N Abd-alla[a,b] and NF Hasbullah[c]

[a]*Department of Mathematics, Faculty of Science, Jazan University, Jazan, Saudi Arabia*

[b]*Department of Mathematics, Faculty of Science, Sohag University, Sohag, Egypt*

[c]*Department of Electrical and Computer Engineering, International Islamic University Malaysia, Kuala Lumpur, 53100, Malaysia*

The main scope of this paper is to present in a simple and concise way a mathematical model of composite materials able to describe the propagation of shear horizontal waves in the case where composite is rotating and subjected to an initial stress. This work is aimed at the relevant possibility to apply the obtained results for the establishment of highachievement applications of piezoelectric and semiconductor composites and surface acoustic waves devices. We conclude by analyzing numerical computations in which the influence of the rotation, initial stress and electromagnetic boundary conditions are graphically observed.

Mathematics and Mechanics of Solids, (2017), 1-13

The mathematical modeling for bulk acoustic wave propagation velocities in transversely isotropic piezoelectric materials

Abo-el-nour N Abd-alla[a,b] Abdelmonam M Hamdan[a] and Adel A Almarashi[c]

[a]*Department of Mathematics, Faculty of Science, Jazan University, Jazan, Saudi Arabia*

[b]*Department of Mathematics, Faculty of Science, Sohag University, Sohag, Egypt*

[c]*Dipartimento di Ingegneria Meccanica e Aerospaziale, Sapienza Universita` di Roma, Italy.*

The objective of this paper is to study the bulk acoustic wave (BAW) propagation velocities in transversely isotropic piezoelectric materials, aluminum nitride , zinc oxide , cadmium sulfide and cadmium selenide. The bulk acoustic wave velocities are computed for each direction by solving the Christoffel's equation based on the theor y of acoustic waves in anisotropic solids exhibiting piezoelectricity. These values are calculated numerically and implemented on a computer by Bisection Method Iterations Technique (BMIT). The modification of the bulk acoustic wave velocities caused by the piezoelectric effect are graphically compared with the velocities in the corresponding non-piezoelectric materials. The results obtained in this study can be applied to signal processing, sound systems and wireless communication in addition to the improvement of surface acoustic wave (SAW) devices and militar y defense equipment.

Mathematics and Mechanics of Solids, 22(4), 2017, 823-836.

Plane waves and eigenfrequency study in a transversely isotropic magneto-thermoelastic medium under the effect of a constant angular velocity

Abo-el-nour N. Abd-alla[a,b], Fatimah Alshaikh[a], Dionisio Del Vescovo[c] and Mario Spagnuolo[d]

[a]Department of Mathematics, Faculty of Science, Jazan University, Jazan, Saudi Arabia; [b]Department of Mathematics, Faculty of Science, Sohag University, Sohag, Egypt

[c]Dipartimento di Ingegneria Meccanica e Aerospaziale, Universitá degli Studi di Roma La Sapienza, Roma, Italy; International Research Center on Mathematics and Mechanics of Complex Systems (M&MOCS), Universitá degli Studi dell'Aquila, L'Aquila, Italy

[d]International Research Center on Mathematics and Mechanics of Complex Systems (M&MOCS), Universitá degli Studi dell'Aquila, L'Aquila, Italy; Laboratorie des Sciences des Procédés et des Matériaux (LSPM), Universitè Paris 13, Paris, France

In this article, we investigate the influence of (i) relaxation times according to the theory of Green–Lindsay, (ii) rotation, and (iii) magnetic field on incident and reflected plane waves in a transversely isotropic magneto-thermoelastic medium. We moreover make a numerical study to analyze the amplitude ratios for incident plane waves and a numerical eigenfrequency study presenting some shape modes for the displacement and temperature fields of a physical suitable cylindrical system. The medium rotates with a constant angular velocity, in the presence of a magnetic field orthogonal to the stress-free and thermally insulated plane. We solve the equations of this system and show the arising of three quasi-plane waves in the medium. The theoretical aspects of this article are focused on the reflection of these qp-waves from one of the surfaces of the medium, which we impose to be stress-free and thermally insulated: We obtain the reflection coefficients by numerical simulations considering a cylinder of cobalt.

Journal of Thermal Stresses 40 (9), (2017) 1079-1092

New exact Bayesian prediction of the range for the exponential lifetime based on fixed and random sample sizes

A. H. Abd Ellah

Department of Mathematics, Faculty of Science, Sohag University 82524, Egypt

Mathematics Department, Faculty of Science, Al-Baha University, P.O. Box 1988, Saudi Arabia.

We consider the problem of predictive interval for the range of the future observations from an exponential distribution. Two cases are considered, (1) Fixed sample size (FSS). (2) Random sample size (RSS). Further, I derive the predictive function for both FSS and RSS in closely forms. Random sample size is appeared in many application of life testing. Fixed sample size is a special case from the case of random sample size. Illustrative examples are given. Factors of the predictive distribution are given. A comparison in savings is made with the above method. To show the applications of our results, we present some simulation experiments. Finally, we apply our results to some real data sets in life testing.

International Journal of Algebra and Statistics 6 (1-2) 2017, 169-184

Low-cost autonomous perceptron neural network inspired by quantum computation

Mohammed Zidan[1,4], Abdel-Haleem Abdel-Aty[2], Alaa El-Sadek[1,3], E. A. Zanaty[4], and Mahmoud Abdel-Aty[1,3,4,5,*]

[1]University of Science and Technology, Zewail City, Sheikh Zayed District, 12588, 6th of October City, Giza, Egypt

[2]Physics Department, Faculty of Science, Al-Azhar University, 71524 Assiut, Egypt

[3]Water, Energy and Food Center, University of Science and Technology, Zewail City, Egypt

[4]Mathematics Department, Faculty of Sciences, Sohag University, Sohag, Egypt

[5]Applied Sciences University, Kingdom of Bahrain

Achieving low cost learning with reliable accuracy is one of the important goals to achieve intelligent machines to save time, energy and perform learning process over limited computational resources machines. In this paper, we propose an efficient algorithm for a perceptron neural network inspired by quantum computing composite from a single neuron to classify inspirable linear applications after a single training iteration O(1). The algorithm is applied over a real world data set and the results are outer performs the other state-of-the art algorithms.

AIP Conference Proceedings 1905, 020005 (2017)

A fast and precise numerical algorithm for a class of variable–order fractional differential equations

Ali H. Bhrawy[1], Mahmoud A. Zaky[2,3], Mahmoud Abdel-Aty[3,*]

[1]Beni-Suef University, Faculty of Science, Department of Mathematics, Beni-Suef, Egypt

[2]National Research Centre, Department of Applied Mathematics, Dokki, Giza 12622, Egypt

[3]University of Science and Technology, Zewail City of Science and Technology, Zayed City, 12588 Giza, Egypt

The variable-order fractional differential equations appear in modeling diverse physical problems. The main issue we address in this paper concerns an accurate numerical solution of a class of variable-order differential equations. The given problem is transformed into a system of algebraic equations using the so-called operational matrix of variable-order differentiation and the shifted LegendeGauss-Radau collocation approach. Accordingly, the effort performed in calculations can be reduced. Numerical simulation for a specific problem is presented to demonstrate the computational efficiency and accuracy of the proposed algorithm.

Proceedings of the Romanian Academy, Series A 18(1), 2017, pp. 17-24

Incidence of HCV in duced-Esophageal varices in Egypt. Valuable knowledge using data mining analysis

Mahmoud Abdel-aty[a,*], Mahmoud Fouad[b], Mohammad M. Sallam[c], Elsayed A. Elgohary[c], Ali Ismael[c], Abdallah Nawara[c], Baha Hawary[d], Mohammed Tag-Adeen[e,f], Salama Khaled[g]

[a]Department of Mathematics and Information Technology, Zewail City for Biosciences and Technology, Giza,

[b]Department of Gynecology and Obstetrics, Al Azhar Asuit Faculty of Medicine, Al Azhar University,

cDepartment of Internal Medicine, Zagazig Faculty of Medicine, Zagazig University,

[d]Department of Pediatrics and Neonatology, Aswan School of Medicine, Aswan University,

[d]Department of Internal Medicine, Qena Faculty of Meidicne, South Valley University,

[f]Department of Gastroenetrology, Nagazaki School of medicine, Nagazaki University, Japan,

[g]Department of Gastroenterology and Hepatology, Nasser Institute Hospital for Research and Therapy, Cairo, Egypt.

Esophageal varices is one of the most important comorbidity related liver cirrhosis, patients usually presented with hematemesis, melena, or both, ultimately 20% is the mortality during the first attack, hence we aimed to investigate the incidence of such esophageal varices related chronic Hepatitis C virus (HCV) in randomized Egyptian population. One thousand eighteen Egyptian patients, aged between 17 and 58 years, positive for Hepatitis C virus genotype 4 (HCV-4) by enzyme linked immunosorbent assay Ab and HCV RNA-polymerase chain reaction were screened for the presence of esophageal varices. Incidence of esophageal varices was 62.3%; 635 patients, those with large Esophageal varices (LEVs) was 47.4%; 301 patients. Model for end-stage liver disease (MELD) score has not been significantly improved post variceal band ligation (VBL). Using 2D U/S was useful for EVs prediction. Incidence of esophageal varices in HCV Egyptian patients still high, valuable knowledge would be helpful in clinical field have been discovered by data mining computational intelligent analysis using in practical medicine to improve overall health care.
Medicine (2017) 96:4(e5647)

Photo-thermal-elastic interaction in an unbounded semiconducting medium with spherical cavity due to pulse heat flux

Ibrahim A. Abbas[1] and Aatef Hobiny[2]

[1]Department of Mathematics, Faculty of Science, Sohag University, Sohag, 82524, Egypt

[2]Department of Mathematics, King Abdulaziz University, Jeddah, Saudi Arabia

In this work, the photothermal waves in an unbounded semiconducting medium with spherical cavity are studied. This problem is solved using the theory of coupled plasma, thermal, and elastic wave. An unbounded material, elastic semiconductor containing a spherical cavity with isotropic and homogeneous thermal and elastic properties has been considered. The inner surface of the cavity is taken traction-free and subjected to an exponentially decaying pulse boundary heat flux. Laplace transform techniques and eigenvalue approach were used to obtain the analytical solutions. Numerical computations have been done for silicon-like semiconductor material, and the results are presented graphically to estimate the effect of time and the coupling between the plasma, thermal, and elastic waves.
Waves in Random and Complex Media 1-13, (2017)

Analytical solutions of 2-D problem for cracked thermoelastic fiber-reinforced anisotropic material

Ibrahim A. Abbas

Department of Mathematics, Faculty of Science, Sohag University, Sohag, Egypt

Department of Mathematics, King Abdulaziz University, Jeddah, Saudi Arabia

In this article, the analytical solution of the 2D problem for cracked thermoelastic fiber-reinforced anisotropic material is investigated. The boundary of the crack is due to a prescribed temperature and stress distribution. In the case of one relaxation time, the generalized thermoelastic theory has been employed. In the transformed domain using exponential Fourier and Laplace transformations, the eigenvalues approach are used to obtain the analytical solutions. The inverse of Fourier transform has been obtained analytically. Comparisons with expected results by the absence and presence of reinforcement have been presented. Results were verified numerically and are represented graphically.

Theoretical and Applied Fracture Mechanics 91, 2017, 31-36

Dual-Phase-Lag Model on Generalized MagnetoThermoelastic Interaction in a Functionally Graded Material

Ibrahim A. Abbas[1,2,3] and Elsayed A. E. Mohamed[1,4]

[1]*Department of Mathematics, Faculty of Science and Arts - Khulais, University Of Jeddah, Saudi Arabia*

[2]*Department of Mathematics, King Abdulaziz University, Jeddah, Saudi Arabia*

[3]*Department of mathematics, Faculty of Science, Sohag University, Sohag, Egypt*

[4]*Department of mathematics, Faculty of Education, Alzaeim Alazhari University, Khartoum, Sudan*

In this work, we consider the problem of magneto-thermoelastic interactions in a functionally graded material (FGM) under dual-phase-lag model in the presence of thermal shock. The generalized thermoelasticity theory with one relaxation time has been employed. The material is assumed to be elastic and functionally graded (FGM) (i.e. material with spatially varying properties). The basic equations have been written in the form of a vectormatrix differential equation in the Laplace transform domain, which is then solved by an eigenvalue approach. Numerical inversion of the transforms is carried out using the Stehfest method. Further, graphs have been drawn to show the effect of the nonhomogeneity parameter, magnetic field, and dual-phase-lag parameters on displacement, temperature, stress, and strain.

International Journal of Acoustics and Vibration, 22(3) 2017, 369-376

Analytical and Computational Solution of Three-Dimensional Thermoelastic Interactions in Porous Material with Temperature-Dependent Properties

Abbas, Ibrahim A[1,2]; Abd-alla, Abo-el-nour N[2,3]; Alshaikh, Fatimah[3]

[1]*Department of Mathematics, Faculty of Science and Arts—Khulais, University of Jeddah, Saudi*

[2]*Department of Mathematics, Faculty of Science, Sohag University, Sohag, Egypt*

[3]*Department of Mathematics, Faculty of Science, Jazan University, Jazan, Saudi Arabia*

The present work deals with a new problem of generalized thermoelastic interaction on a porous material with temperature-dependent mechanical properties in the context of Green and Naghdi type II. The surface of the half-space is taken to be traction free and heated by subjected to a time-dependent heat source. The eigenvalue approach techniques under normal mode analysis are used to solve the resulting non-dimensional coupled equations. The effect of the dependence of modulus of elasticity on the displacement components, the stress components, changes in volume fraction field and temperature distribution have been computed and illustrated graphically.

Journal of Computational and Theoretical Nanoscience, 14(8), 2017, 4021-4033

Free vibration of a thermoelastic hollow cylinder under two-temperature generalized thermoelastic theory

Ibrahim A. Abbas[1,2,3]

[1]*Department of mathematics, Faculty of Science, Sohag University, Sohag, Egypt.*

[2]*Department of Mathematics, Faculty of Science and Arts - Khulais, University Of Jeddah, Saudi Arabia*

[3]*Nonlinear Analysis and Applied Mathematics Research Group (NAAM), Department of Mathematics, King Abdulaziz University, Jeddah, Saudi Arabia*

The aim of this article is to study the exact solution for a free vibration in a thermoelastic hollow cylinder, which is initially undeformed and at uniform temperature. The formulation is applied in the context of two-temperature Green and Naghdi (2TGNIII) theory. Both the inner and outer curved surfaces of the cylinder are considered stress free and isothermal surfaces. The exact analytic solutions are obtained with the use of eigenvalue approach. The dispersion relations for the existence of various types of possible modes of vibrations in the considered hollow cylinder are derived in a compact form. The validation of the roots for the dispersion relation are presented. The numerical results of natural frequency, thermoelastic damping and frequency shift of vibrations have been presented graphically.

Mechanics Based Design of Structures and Machines, 45(3), 2017, 395-405

Analytical solution of thermoelastic interaction in a half-space by pulsed laser heating

Ibrahim A. Abbas[a,b,c], Marin Marind[d]

[a]*Department of Mathematics, Faculty of Science and Arts - Khulais, University Of Jeddah, Saudi Arabia*
[b]*Nonlinear Analysis and Applied Mathematics Research Group (NAAM), Department of Mathematics, King Abdulaziz University, Jeddah, Saudi Arabia*
[c]*Department of mathematics, Faculty of Science, Sohag University, Sohag, Egypt*
[d]*Department of Mathematics and Computer Sciences, Transilvania University of Brasov, Romania*

In this article, we consider the problem of a two-dimensional thermoelastic half-space in the context of generalized thermoelastic theory with one relaxation time. The surface of the half-space is taken to be traction free and thermally insulated. The solution of the considered physical quantity can be broken down in terms of normal modes. The nonhomogeneous basic equations have been written in the form of a vector-matrix differential equation, which is then solved by an eigenvalue approach. The exact analytical solution is adopted for the temperature, the components of displacement and stresses. The results obtained are presented graphically for the effect of laser pulse to display the phenomena physical meaning. The graphical results indicate that the thermal relaxation time has a great effect on the temperature, the components of displacement and the components of stress.

Physica E 87 (2017) 254-260

A Semi-Group of Contractions in Elasticity of Microstretch Materials

M. Marin, M[1], I. Abbas[2,3] and C. Carstea[1]

[1]*Department of Mathematics and Computer Science, Transilvania University of Brasov, Brasov, Romania*
[2]*Department of Mathematics, Faculty of Sciences and Art-Khulais, King Abdulaziz University, Jeddah, Saudi Arabia*
[3]*Department of Mathematics, Faculty of Sciences, University of Sohag, Sohag, Egypt*

Our study is dedicated to mixed initial-boundary value problem in elastodynamic theory of microstretch bodies. This problem is transformed in an abstract temporally evolutionary equation in a Hilbert space. Then, using some results from the theory of semigroups of linear operators we deduce the existence and uniqueness of solution. In the same manner, the continuous dependence of the solutions upon initial data and supply therms is also proved.

Journal of Computational and Theoretical Nanoscience, 14(3), 2017, 1634-1639

A study on photothermal waves in an unbounded semiconductor medium with cylindrical cavity

Aatef D. Hobiny[1,3] and Ibrahim A. Abbas[2,3,4]

[1]Department of Mathematics, Faculty of Science, King Abdulaziz University, Jeddah, Saudi Arabia
[2]Department of Mathematics, Faculty of Science and Arts-KhulaisUniversity of JeddahJeddahSaudi Arabia
[3]Nonlinear Analysis and Applied Mathematics Research Group (NAAM), Department of MathematicsKing Abdulaziz UniversityJeddahSaudi Arabia
[4]Department of mathematics, Faculty of Science Sohag University, Sohag, Egypt

In this article, the theory of coupled plasma, thermal, and elastic waves was used to investigate the wave propagation on semiconductor material with cylindrical cavity during photo-thermoelastic process. An unbounded material, elastic semiconductor containing a cylindrical cavity with isotropic and homogeneous thermal and elastic properties has been considered. The inner surface of cavity is constrained, and the carrier density is photogenerated by an exponentially decaying pulse boundary heat flux. The eigenvalue approach, together with Laplace transform techniques, was used to obtain the analytical solutions. Numerical computations have been done for a silicon-like semiconductor material, and the results are presented graphically to estimate the effect of the coupling between the plasma, thermal, and elastic waves. The graphical results indicate that the thermal activation coupling parameter is an important phenomenon and has a great effect on the distribution of field quantities.

Mechanics of Time-Dependent Materials, 2017, 21(1), 61-72

Analytical solutions of thermoelastic interactions in a hollow cylinder with one relaxation time

Ibrahim A. Abbas[1,2], Y. Abd elmaboud[3,4]

[1]Department of Mathematics Faculty of Science and Arts - Khulais, University of Jeddah, Saudi Arabia,
[2]Department of Mathematics, King Abdulaziz University, Jeddah, Saudi Arabia,
[1]Department of mathematics, Faculty of Science, Sohag University, Sohag, Egypt
[3]Department of Mathematics, Faculty of Science and Arts - Khulais, University of Jeddah, Saudi ArabiaMathematics
[4]Department, Faculty of Science, Al-Azhar University (Assiut Branch), Assiut, Egypt

In this study, we aim to compare the optimal homotopy analysis solution with the exact solution of the thermoelastic interactions problem in an isotropic hollow cylinder. The thermoelastic interactions in a hollow cylinder in the context of the theory of generalized thermoelasticity with one relaxation time (Lord and Shulman's theory) are considered. An application of a hollow cylinder is investigated where the inner surface is traction-free and subjected to a decaying-with-time thermal field, while the outer surface is traction-free and thermally isolated. The mathematical model is solved by analytical method and optimal homotopy analysis method (OHAM). In addition, the convergence of the obtained homotopy analysis method solution is discussed explicitly. Numerical results for the temperature distribution, displacement and radial stress are represented graphically. The accuracy of the optimal homotopy analysis method is validated by comparing the analytical and exact solutions for the field quantities

Mathematics and Mechanics of Solids, 22(2), (2017), 210-223

Generalized thermoelastic interactions in a hollow cylinder with temperature-dependent material properties

Ibrahim A. Abbas

Department of Mathematics, Faculty of Science and Arts - Khulais, University Of Jeddah, Nonlinear Analysis and Applied Mathematics Research Group (NAAM), Department of MathematicsKing Abdulaziz University, Jeddah, Saudi Arabia

Department of mathematics, Faculty of Science, Sohag University

In this study, in the present work, the generalized thermoelastic interactions in a hollow cylinder with one relaxation time are considered. The modulus of elasticity are taking as function of temperature. Due to the nonlinearity of the governing equations, finite element method is adopted to solve such problem. The exact solution in the case of temperature-independent is discussed explicitly. Numerical results for the temperature distribution, displacement and radial and hoop stresses represented graphically. The accuracy of the finite element method validated by comparing between the finite element and exact solutions for temperature-independent.

Journal of Thermal Science and Technology, 12(1), 2012

On continuous dependence for the mixed problem of microstretch bodies

M. Marin[1], I Abas[2,3] and C. Carstea[3]

[1]Department of Mathematics, Faculty of Science and Arts - Khulais, University of Jeddah, [2]Department of Mathematics, King Abdulaziz University,

[3]Department of mathematics, Faculty of Science, Sohag University

We do a qualitative study on the mixed initial-boundary value problem in the elastodynamic theory of microstretch bodies. After we trans- form this problem in a temporally evolutionary equation on a Hilbert space, we will use some results from the theory of semigroups of linear operators in order to prove the continuous dependence of the solutions upon initial data and supply terms.

Seria Matematica, 21(1), (2017), 9-21

Fractional Order Photo-Thermoelastic Interaction in a Semiconducting Media Containing a Spherical Cavity Subjected to Pulse Heat Flux

Faris S. Alzahrani[1], and Ibrahim A. Abbas[1,2]

[1]*Nonlinear Analysis and Applied Mathematics Research Group (NAAM), Department of Mathematics, King Abdulaziz University, Jeddah, Saudi Arabia*

[2]*Department of mathematics, Faculty of Science Sohag University, Sohag, Egypt*

In the present study, the theory of generalized photo-thermoelasticity under fractional order derivative was used to investigate the coupled of thermal, plasma, and elastic waves on unbounded semiconductor medium with spherical hole during the photothermoelastic process. Without neglecting the coupling between the thermoelastic and plasma waves that photo-generated through intensity modulated laser beam and tightly focused, a semiconducting isotropic elastic medium has homogeneity in thermal and elastic properties was considered. The analytical solutions in the transformed domain by the eigenvalue approach were observed through the transform techniques of Laplace. For silicon-like semiconductor material, the numerical computations have been done and the results are displayed graphically to estimate the effects of the thermal relaxation time and the fractional order parameters on the plasma, thermal, and elastic waves.

Journal of Advanced Physics 6.4 (2017): 470-476.

A Two-Temperature Photothermal Interaction in a Semiconducting Material

Ibrahim A. Abbas[1,2,3] , K. Aly[4,5] and Faris S. Alzahrani[3]

[1]*Department of Mathematics, Faculty of Science and Arts - Khulais, University of Jeddah, Saudi Arabia*

[2]*Nonlinear Analysis and Applied Mathematics Research Group (NAAM), Department of Mathematics, King Abdulaziz University, Jeddah, Saudi Arabia*

[3]*Department of Mathematics, Faculty of Science, Sohag University, Sohag, Egypt*

[4]*Department of Physics, Faculty of Science and Arts - Khulais, University of Jeddah, Saudi Arabia*

[5]*Department of Physics, Faculty of Science, Al-Azhar University, Assuit Branch, Assuit, Egypt*

This work is concerned with the study of the carrier density, thermodynamic temperature, conductive tempera- ture, displacement and stress in a semi-infinite semiconducting medium during the photo-thermal process. The medium is considered to be a semiconductor medium with homogeneous, isotropic. In addition, the thermal and elastic properties have been considered without neglecting the coupling between the thermoelastic and the plasma waves. Laplace transform techniques are used to obtain the exact solution of the problem in the transformed domain by the eigenvalue approach and the inversion of Laplace transforms have been carried numerically. A semiconducting material like as silicon was considered. The results were graphically represented to show the effect of the two-temperature parameter.

Journal of Advanced Physics6.3 (2017): 402-407

A Generalized Model on Plasma, Thermal and Elastic Waves in a Semiconductor Medium

Ibrahim A. Abbas[1,2,3] and K. A. Aly[4,5]

[1] *Department of Mathematics, Faculty of Science and Arts - Khulais, University of Jeddah, Saudi Arabia*

[2] *Nonlinear Analysis and Applied Mathematics Research Group (NAAM), Department of Mathematics, King Abdulaziz University, Jeddah, Saudi Arabia*

[3] *Department of Mathematics, Faculty of Science, Sohag University, Sohag, Egypt*

[4] *Department of Physics, Faculty of Science and Arts - Khulais, University of Jeddah, Saudi Arabia*

[5] *Department of Physics, Faculty of Science, Al-Azhar University, Assuit Branch, Assuit, Egypt*

In this work, a generalized model on plasma, thermal and elastic waves was used to study the wave propagation of semiconducting material during the photo-thermal process. The thermal relaxation time, the coupling between the plasma, thermal, and elastic waves has been considered. The analytical solutions in the trans- formed domain by the eigenvalue approach have been obtained based on the techniques of Laplace's transform. A semiconducting material like as silicon was considered. The results were graphically represented to show the effect of the thermal relaxation time, the thermal activation coupling parameter, the lifetime on the physical quantities.

Journal of Advanced Physics6.3 (2017): 317-325

Two-dimensional generalized thermo-elastic problem for anisotropic half-space

Debkumar Ghosh[1], Abhijit Lahiri[2], Ibrahim A. Abbas[3]

[1, 2]Department of Mathematics, Jadavpur University, Kolkata, 700032, India

[3]Department of Mathematics, Sohag University, Sohag, Egypt

[1]Corresponding author

E-mail: ibrabbas7@science.sohag.edu.eg

This paper concerns with the study of wave propagation in fiber-reinforced anisotropic half space under the influence of temperature and hydrostatic initial stress. Lord-Shulman theory is applied to the heat conduction equation. The resulting equations are written in the form of vector matrix differential equation by using Normal Mode technique, finally which is solved by Eigen value approach.

Journal of Mathematical Models in Engineering (MME) 2017, 3 (1), 27-41

Eigenvalue Approach in a Generalized Thermal Shock Problem for a Transversely Isotropic Half-Space

Ibrahim A. Abbas[1] and Aatef Hobiny[2]

[1]*Department of Mathematics, Faculty of Science, Sohag University, Sohag, 82524, Egypt*

[2]*Department of Mathematics, King Abdulaziz University, Jeddah, Saudi Arabia*

In the present work, the investigating of the disturbances in a homogeneous, transversely isotropic elastic medium with generalized thermoelastic theory has been concerned. The formulation is applied to generalized thermoelasticity based on three different theories. Laplace and Fourier transforms are used to solve the problem analytically. The essential equations have been written as a vector-matrix differential equation in the Laplace transform domain, then solved by an eigenvalue approach. The inverses of Fourier transforms are obtained analytically. The result is used to solve a specific two-dimensional problem. The technique is illustrated by means of several numerical experiments performed. The results were verified numerically and are plotted.

Journal of Molecular and Engineering Materials 5 (01), 1750002

Series Representations of the Coefficients of Quaternion Q-Type Functions

A. A. El-Sayed and A. Fatima

Department of Mathematics, Faculty of Science, Sohag University, Sohag, 82524, Egypt

In this paper, we give a scale of weighted spaces of quaternion-valued functions of three real variables. This scale gives a representation of the coefficients of quaternion Qp, ω -type functions. Necessary and sufficient conditions for a hyperholomorphic function f on the unit ball with Hadamard gaps, to belong to the weighted Q-type functions are obtained. Moreover, we prove that the inclusions of spaces from the scale are strict inclusions.

Journal of Computational and Theoretical Nanoscience, 14(6), 2017, 2759-2765

Fisher information and quantum state estimation of two-coupled atoms in presence of two external magnetic fields

Hanaa H. Abu-Zinadah[a], Sayed Abdel-Khalek[b,c,d]

[a]*Department of Statistics, Faculty of Science-AL Faisaliah, King Abdulaziz University, P.O. Box 32691, Jeddah 21438, Saudi Arabia*

[b]*Mathematics Department, Faculty of Science, Taif University, Taif, Saudi Arabia*

[c]*Mathematics Department, Faculty of Science, Sohag University, Sohag, Egypt*

[d]*The Abdus Salam International Centre for Theoretical Physics, Strada Costiera 11, Miramare-Trieste, Italy*

We consider a quantum system of an atom-atom interaction in the presence of two external magnetic and classical fields inx, and zdirections. The dynamical behavior of single atom quantum quantifiers such as the atomic Wehrl entropy, atomic Fisher information and quantum entropy are investigated. The quantum entanglement degradation in regard to the atomic state estimation are discussed through the evolution of the atomic Fisher information flow, and the effects of the external classical fields and types of time dependent coupling between the two atoms are examined. We explore the relationship between different statistical quantities in the absence and presence of classical field during the time evolution. The results show that the creation and manipulation of entanglement by external fields greatly benefit within the suitable choice of the kind of time dependent coupling among the two atoms and external.

Results in Physics 7 (2017) 4318-4323

Effect of Time Dependent Coupling on the Dynamical Properties of the Nonlocal Correlation Between Two Three-Level Atoms

Sayed Abdel-Khalek[a,b], S. H. A. Halawani[b], A-S. F. Obada[c]

[a]*Mathematics Department, Faculty of Science, Sohag University, Sohag, Egypt*

[b]*Mathematics Department, Faculty of Science, Taif University, Taif, Saudi Arabia*

[c]*Mathematics Department, Faculty of Science, Azhar University, Cairo, Egypt*

In this article, we present the analytical solution for the pair of entangled two three-level atoms in the cascade configuration with and without the atomic motion effect. The effects of time dependent coupling and photon multiplicity on the evolution of the nonlocal correlation between the two atoms are examined. It is shown that the amount of atom-atom entanglement increases for one photon transition when the atomic motion effect is considered. Also, the entanglement between the two atoms decreases by increasing the photons multiplicity when the time dependent coupling effect is ignored. Finally, the results explored very important phenomena such as entanglement sudden death and entanglement sudden birth.

Int J Theor Phys (2017) 56:2898-2910.

Quantum phase and nonlocal correlations for a three-level system interacting with laser light in a nonlinear kerr medium under decoherence

K. Berrada[a] and Sayed Abdel-Khalek[b]

[a]Department of Physics, College of Science Al Imam Mohammad Ibn Saud Islamic University (IMSIU) Riyadh, Saudi Arabia

[b]Department of Mathematics, Faculty of Science Taif University, Saudi Arabia

In this paper, we study the time evolution of the geometric phase and nonlocal correlations for a three-level atom interacting with the quantum field emerged in a nonlinear Kerr medium. We discuss the dependence of the physical quantifiers on the phase damping effect. We examine the effects of the initial state and different system parameters on the evolution of the nonlocal correlation and geometric phase with and without the phase damping effect. Furthermore, we explore the link between the geometric phase and the nonlocal correlation during the time evolution. Finally, we show that the model proposed will be very useful to avoid the phase damping effect by a proper choice of the physical parameters in the field for both cases of the initial pure and mixed states of the three-level atom.

Journal of Russian Laser Research, 38(2), 2017

Properties of Two Two-level Atoms Interacting with Intensity-Dependent Coupling

H. Bakry[1], A. S. A. Mohamed[2,3], N. Zidan[1]

[1]Mathematics Department, Faculty of Science, Sohag University, Sohag, Egypt

[2]Engineering Math and Physics Department, Faculty of Engineering, Cairo University, Giza, Egypt

[3]Zewail City of Science and Technology, University of Science and Technology, Giza, Egypt

We discuss some new features of the model of two two-level atoms interacting with two single-mode thermal cavity field via multi-photon transitions under intensity-dependent coupling. We examine the dynamics of quantum and classical correlations of the system initially exists in Werner states. The results show that the sudden death and sud-den birth of quantum entanglement occur but the geometric measure of quantum discord remains non-zero. It is observed that, by increasing the number of photons, the periods become shorter and the quantum discord and entanglement become irregular.

International Journal of Theoretical Physics

The Probe Attack on the Bennett-Brassard 1984 Protocol in the Presences of Noisy Amplitude Damping Channel

H. F. Abdel-Hameed[1,2], N. Zidan[1], M. R. Wahiddin[3]

[1]Department of Mathematics, Faculty of Science, Sohag University, Sohag, Egypt

[2]Department of Mathematics, Faculty of Science and Education, Al-Khurma Branch, Taif University, Al-Khurma 29372, Kingdom of Saudi Arabia

[3]Department of Computer Science, Faculty of ICT, International Islamic University Malaysia (IIUM), P.O. Box 10, 50728 Kuala Lumpur, Malaysia

In this contribution, we investigate the effect of the generalized amplitude damp-ing as Eve's strategy to cause an error on the received signal during generating a quantum key distribution between Alice and Bob using Bennett-Brassard 1984 (BB84) protocol. For small values of the channel strength and larger values of the decay parameter, the entangle-ment decays gradually. The phenomena of the sudden changes of entanglement are observed for smaller and larger values of the willing initial error. These changes of entanglement decay gradually when Alice prepares her qubit in horizontal-vertical basis. While the sud-den changes are depicted if the initial state is prepared in the diagonal-anti-diagonal basis. Bob will get his measurement with an error, where the probability of this error depends on the initial polarized angle, the initial desired error and the channel parameters.

International Journal of Theoretical Physics

Low-cost autonomous perceptron neural network inspired by quantum computation

M Zidan, AH Abdel-Aty, A El-Sadek, E.A Zanaty, M Abdel-Aty

Achieving low cost learning with reliable accuracy is one of the important goals to achieve intelligent machines to save time, energy and perform learning process over limited computational resources machines. In this paper, we propose an efficient algorithm for a perceptron neural network inspired by quantum computing composite from a single neuron to classify inspirable linear applications after a single training iteration O(1). The algorithm is applied over a real world data set and the results are outer performs the other state-of-the art algorithms.

International Journal of Computers and Applications, 39 (3), 2017

Dynamical behaviors, control and synchronization of a new chaotic model with complex variables and cubic nonlinear terms

E. E. Mahmoud[a,b], M. A. Al-Adwani[b]

[a]Department of Mathematics, Faculty of Science, Sohag University, Sohag 82524, Egypt

[b]Department of Mathematics, Faculty of Science, Taif University, Taif, Saudi ArabiaEgypt

A novel chaotic model with complex variables and cubic non-linear terms was proposed. The new system is a six dimensional continuous real autonomous chaotic system. The characteristics of this system containing invariance, dissipation, equilibria and their stability, Lyapunov exponents, Lyapunov dimension, bifurcation diagrams and chaotic achievement are studied. Converting and turning the system chaotic behavior to its unstable trivial fixed point via the Lyapunov stability theorem. An approach proposed to analyze the system chaos synchronization. Analytical expressions are derived for control functions. The chaos synchronization results were employed to develop a simple application in secure communication. Numerical effects computed to experiment the control forces scientific expressions gravity and to show the chaos synchronization of a chaotic system.

Results in Physics 7 (2017) 1346-1356

A novel sort of adaptive complex synchronizations of two indistinguishable chaotic complex nonlinear models with uncertain parameters and its applications in secure communications

E. E. Mahmoud[a,b] and F. S. Abood[c]

[a]Department of Mathematics, Faculty of Science, Sohag University, Sohag 82524, Egypt

[b]Department of Mathematics, Faculty of Science, Taif University, Saudi Arabia

[c]Department of Mathematics, Faculty of Science, King Khalid University, Abha, Saudi Arabia

In this paper, we will demonstrate the adaptive complex anti-lag synchronization (CALS) of two indistinguishable complex chaotic nonlinear systems with the parameters which are uncertain. The significance of CALS is not advised well in the literature yet. The CALS contains or consolidate two sorts of synchronizations (anti-lag synchronization ALS and lag synchronization LS). The state variable of the master system synchronizes with an alternate state variable of the slave system. Depending on the function of Lyapunov, a plan is orchestrated to achieve CALS of chaotic attractors of complex systems with unverifiable parameters. CALS of two indistinguishable complexes of Lü systems is viewed as, for example, an occasion for affirming the likelihood of the plan exhibited. In physics, we can see complex chaotic systems in numerous different applications, for example, applied sciences or engineering. With a specific end goal to affirm the proposed synchronization plan viability and demonstrate the hypothetical outcomes, we can compute the numerical simulation. The above outcomes will give the hypothetical establishment to the secure communication applications. CALS of complex chaotic systems in which a state variable of the master system synchronizes with an alternate state variable of the slave system is an encouraging sort of synchronization as it contributes excellent security in secure communication. Amid this secure communication, the synchronization between transmitter and collector is shut and message signals are recouped. The encryption and restoration of the signals are simulated numerically.

Results in Physics 7 (2017) 4174-4182.

An unusual kind of complex synchronizations and its applications in secure communications

E. E. Mahmoud

Department of Mathematics, Faculty of Science, Sohag University, Sohag 82524, Egypt
Department of Mathematics, Faculty of Science, Taif University, Saudi Arabia

In this paper, we talk about the meaning of complex anti-syncrhonization (CAS) of hyperchaotic nonlinear frameworks comprehensive complex variables and indeterminate parameters. This sort of synchronization can break down just for complex nonlinear frameworks. The CAS contains or fuses two sorts of synchronizations (complete synchronization and anti-synchronization). In the CAS the attractors of the master and slave frameworks are moving opposite or orthogonal to each other with a similar form; this phenomenon does not exist in the literature. Upon confirmation of the Lyapunov function and a versatile control strategy, a plan is made to play out the CAS of two indistinguishable hyperchaotic attractors of these frameworks. The adequacy of the obtained results is shown by a simulation case. Numerical issues are plotted to decide state variables, synchronization errors, modules errors, and phases errors of those hyperchaotic attractors after synchronization to determine that the CAS is accomplished. The above outcomes will present the possible establishment to the secure communication applications. The CAS of hyperchaotic complex frameworks in which a state variable of the master framework synchronizes with an alternate state variable of the slave framework is an encouraging kind of synchronization as it contributes fantastic security in secure communications. Amid this secure communications, the synchronization between transmitter and collector is shut and message signs are recouped. The encryption and reclamation of the signs are reproduced numerically.

Eur. Phys. J. Plus (2017) 132: 466

Bifurcations and chaos of time delay Lorenz system with dimension 2n+1

G. M. Mahmoud[a], A. A. Arafa[b] and E. E. Mahmoud[b,c]

[a]Department of Mathematics, Faculty of Science, Assiut University, Assiut 71516, Egypt
[b]Department of Mathematics, Faculty of Science, Sohag University, Sohag 82524, Egypt
[c]Department of Mathematics, Faculty of Science, Taif University, Taif, Saudi Arabia

In this paper, The aim of this paper is to introduce a generalized form of the Lorenz system with time delay. Instead of considering each state variable of the Lorenz system belonging to R, the paper considers two of them belonging to Rn. Hence the Lorenz system has (2n + 1) dimension. This system appears in several applied sciences such as engineering, physics and networks. The stability of the trivial and nontrivial fixed points and the existence of Hopf bifurcations are studied analytically. Using the normal form theory and center manifold argument, the direction and the stability of the bifurcating periodic solutions are determined. Finally, numerical simulations are calculated to confirm our theoretical results. The paper concludes that the dynamics of this system are rich. Additionally, the values of the delay parameter at which chaotic and hyperchaotic solutions exist for different values of n using Lyapunov exponents and Kolmogorov-Sinai entropy are calculated numerically.

Eur. Phys. J. Plus (2017) 132: 461

Projective synchronization for coupled partially linear complex-variable systems with known parameters

G. M. Mahmoud[a], E. E. Mahmoud[b,c] and A. A. Arafa[b]

[a]*Department of Mathematics, Faculty of Science, Assiut University, Asyut 71516, Egypt*
[b]*Department of Mathematics, Faculty of Science, Sohag University, Sohag 82524, Egypt*
[c]*Department of Mathematics, Faculty of Science, Taif University, Taif, KSA*

The passivity theory is used to achieve projective synchronization in coupled partially linear complex-variable systems with known parameters. By using this theory, the control law is thus adopted to make state vectors asymptotically synchronized up to a desired scaling factor. This paper deals with sending different large messages which include image and voice signals. The theoretical foundation of the projective synchronization based on the passivity theory is exploited for application to secure communications. The numerical simulations of secure communication are used to send large message, an image and sound (voice) signal. The errors are controlled to zero that show the agreement between theoretical and numerical simulations results.

Mathematical Methods in the Applied Sciences 40 (2017), 1214-1222

A New Nonlinear Chaotic Complex Model and Its Complex Antilag Synchronization

E. E. Mahmoud[a,b] and F. S. Abood[c]

[a]*Department of Mathematics, College of Science, Sohag University, Sohag 82524, Egypt*
[b]*Department of Mathematics, College of Science, Taif University, Taif, Saudi Arabia*
[c]*Department of Mathematics, College of Science, King Khalid University, Abha, Saudi Arabia*

Another chaotic nonlinear Lu model with complex factors is covered here. We can build this riotous complex system when we add a complex nonlinear term to the third condition of the complex Lu system and think of it as if every one of the factors is mind boggling or complex. Ths system in real adaptation is a 6-dimensional continuous autonomous chaotic system. Diffrent types of chaotic complex Lu system are developed. Also, another sort of synchronization is presented by us which is simple for anybody to ponder for the chaotic complex nonlinear system. Ths sort might be called a complex antilag synchronization (CALS). Thre are irregular properties for CALS and they do not exist in the literature; for example, (i) the CALS contains or fused two sorts of synchronizations (antilag synchronization ALS and lag synchronization LS); (ii) in CALS the attractors of the main and slave systems are moving opposite or similar to each other with time lag; (iii) the state variable of the main system synchronizes with a diffrent state variable of the slave system. A scheme is intended to accomplish CALS of chaotic complex systems in light of Lyapunov function. Th acquired outcomes and effctiveness can be represented by a simulation case for our new model.

Complexity 2017, Article ID 3848953, 13 pages

Complex complete synchronization of hyperchaotic complex nonlinear systems with fully uncertain parameters and its applications in secure communications

K. M. Abualnaja[a], E. E. Mahmoud[b,c]

[a]Department of Mathematics, Umm Al-Qura University, P.O. Box 14949, Makah, KSA

[b]Department of Mathematics, Faculty of Science, Sohag University, Sohag 82524, Egypt

Department of Mathematics, Faculty of Science, Taif University, Taif, Kingdom of Saudi Arabia.Arabia

In this manuscript, we discuss the definition of complex complete synchronization (CCS) of hyperchaotic nonlinear systems inclusive complex variables and uncertain parameters. This type of synchronization can analyze only for complex nonlinear systems. The CCS contains or incorporates two kinds of synchronizations (complete synchronization and anti-synchronization). In CCS the attractors of the master and slave systems are moving perpendicular or orthogonal to each other with the same shape, this phenomenon does not exist in the literature. On the evidence of Lyapunov function and adaptive control technique, a scheme is created to perform the CCS of two identical hyperchaotic attractors of these systems. The effectiveness of the acquired results is shown by a simulation example. Numerical issues are plotted to determine state variables, synchronization errors, modules errors, and phases errors of those hyperchaotic attractors after synchronization to ascertain that CCS is achieved. The above results will provide the theoretical foundation for the secure communication applications. CCS of hyperchaotic complex systems in which a state variable of the master system synchronizes with a different state variable of the slave system is an encouraging type of synchronization as it contributes excellent security in secure communication. During this secure communication, synchronization among transmitter and receiver is closed and message signals are recovered. The encryption and restoration of the signals are simulated numerically.

Journal of Scientific and Engineering Research, 2017, 4(9):331-341

A novel sort of complex synchronizations

E. E. Mahmoud

Department of Mathematics, Faculty of Science, Sohag University, Sohag 82524, Egypt.

Department of Mathematics, Faculty of Science, Taif University, Taif, Kingdom of Saudi Arabia.Arabia

In this Our primary goal of this work is to exhibit and examine a novel kind of complex synchronization. We may call it a complex phase synchronization (CPHS). There are bizarre properties of the CPHS and do not exist in the writing, for example, (i) this sort of synchronization can be investigated just for complex nonlinear systems; (ii) the CPHS contains or includes two sorts of synchronizations (anti-phase synchronization APS and phase synchronization PHS); (iii) the state variable of the main system synchronizes with a different state variable of the slave system. A description of the CPHS is presented for two identical chaotic or hyperchaotic complex nonlinear models. In view of the stability theorem, a scheme is intended to fulfill CPHS of chaotic or hyperchaotic attractors of these systems. The effectiveness of the acquired outcomes is shown by a reproduction illustration on the hyperchaotic complex Chen system. Numerical outcomes are plotted to show state variables, modulus errors, phase errors and the development of the attractors of these hyperchaotic models after synchronization to demonstrate that CPHS is achieved.

ACTA PHYSICA POLONICA B, 8, 2017, 1441-1454.

Thermal Stresses in Thermoelastic Half-Space Without Energy Dissipation Subjected to Rotation and Magnetic Field

S. M. Abo-Dahab[a,b], A. M. Abd-Alla[a,c] and E. E. Mahmoud[a,c]

[a]*Department of Mathematics, Faculty of Science, Taif University, Taif 888, Saudi Arabia*

[b]*Department of Mathematics, Faculty of Science, South Valley University, Qena 83523, Egypt*

[c]*Department of Mathematics, Faculty of Science, Sohag University, Sohag 82524, Egypt*

The present paper is concerned with the investigation of disturbances in a homogeneous, isotropic and thermoelastic rotating medium withmagnetic fieldand a time-dependent heat source effect due to thermomechanical source. The formulation is without energy dissipation subjected to thermomechanical source. The normal mode analysisand eigenvalue approach techniques are applied to solve the problem. The expressions of displacement, mean value of normal stress, dilatation and temperature are obtained in the domain. Numerical simulated results are depicted graphically to show the effect of magnetic field and rotation on resulting quantities. The results indicate that the effect of magnetic field, rotation, frequency, wave number and time are very pronounced.

Appl. Math. Inf. Sci. 11(6), (2017) 1-11

(L, m)-fuzzy soft quasi- coincident neighborhood spaces

O. R. Sayed[1], E. Elsanousy[2], Y. H. Raghp[2], Y.Chankim[3]

[1]*Department of Mathematics, Faculty of Science, Assiut University, Assiut 71516, Eygpt*

[2]*Department of Mathematics, Faculty of Science, Sohag University, Sohag, 82524, Eygpt*

[3]*Department of Mathematics, Gangneung-Wonju National University, Gangneung, 25457, Korea*

In this paper, we introduce the concepts of (L, M)-fuzzy soft quasi-coincident neighborhood spaces and study their properties, where L be a completely distributive lattice with 0 and 1 elements and M be a strictly two-sided, commutative quantale lattice. Also, the relationships between these concepts were investigated. Furthermore, a characterization of LFS-continuous and LSN-mappings were given.

J. Math. Comput. Sci. 7 (2017), No. 2, 321-334

ON (L,M)-FUZZY SOFT TOPOLOGICAL SPACES

O. R. Sayed[1], E. Elsanousy[2], Y. H. Raghp[2], Y.Chankim[3]

[1]*Department of Mathematics, Faculty of Science, Assiut University, Assiut 71516, Eygpt*
[2]*Department of Mathematics, Faculty of Science, Sohag University, Sohag, 82524, Eygpt*
[3]*Department of Mathematics, Gangneung-Wonju National University, Gangneung, 25457, Korea*

In this paper, the concepts of (L, M)-fuzzy soft topological spaces, (L, M)-fuzzy soft base and (L, M)-fuzzy soft filter spaces were introduced and their properties were studied, where L be a completely distributive lattice with 0 and 1 elements and M be a strictly two-sided, commutative quantale lattice. Also, the relationships between these concepts were investigated.

J. Math. Comput. Sci. 7(2) (2017), 280-291

Fuzzy soft (α, β, θ, δ, I)-continuous functions

S. E. Abbas[a], E. El-sanowsy[b], A. Atef[c]

[a]Department of Mathematics, Faculty of Science, Jazan University, Saudi-Arabia
[b]Department of Mathematics, Faculty of Science, Sohag 82524, Egypt
[c]Preparatory Year Deanship, King Saud University, Saudi-Arabia

In this paper, we introduce the concept of fuzzy soft (α, β, θ, δ, I)-continuous functions. In order to unify several characterizations and properties of some kinds of modifications of fuzzy soft continuous functions and fuzzy soft open functions, we introduce and explore a generalized form of fuzzy soft continuous and fuzzy soft open functions, namely fuzzy soft ηη-continuous functions and fuzzy soft ηη-open functions.

Journal of the Egyptian Mathematical Society 25 (2017) 59-64

An analytical coupled homotopy-variational approach for solving strongly nonlinear differential equation

G. M. Ismail

Department of Mathematics, Faculty of Science, Sohag University, Sohag, 82524, Egypt

In the present paper, a novel technique combining the homotopy concept with variational formula has been presented to find accurate analytical solution for nonlinear differential equation with inertia and static non-linearity. The obtained results are compared with other analytical and exact solutions to confirm the excellent accuracy and correctness of the approximate analytical technique. The results of the present paper are valid for large amplitudes of oscillation; also the approximate solutions give excellent result than other methods. We concluded that the first order approximation obtained in current work are almost the same with exact solutions, also works very well for the whole range of initial amplitudes.

Journal of the Egyptian Mathematical Society 25 (2017) 434-437.

Common Random Fixed Point Theorems of Akram-Contraction Mappings in Cone Random Metric Spaces

Rashwan A. Rashwan[1] and Hasanen A. Hammad[2]

[1]*Department of Mathematics, Faculty of Science, Assuit University, Assuit 71516, Egypt*

[2]*Department of Mathematics, Faculty of Science, Sohag University, Sohag 82524, Egypt*

In this paper, we prove a unique common random fixed point theorems in the framework of cone random metric spaces for generalized MJ -contraction and generalized MJψ-contraction condition. An example to justify our theorems is given. Our results extends some previous work related to cone random metric spaces from the current existing literature.

Journal of Analysis & Number Theory 5(1), 2017, 1-7

Random Fixed Point Theorem for Weakly Compatible Mappings under Implicit Relation in Cone Random Metric Spaces

R. A. Rashwan[1] and H. A. Hammad[2]

[1]*Department of Mathematics, Faculty of Science, Assuit University, Assuit 71516, Egypt*

[2]*Department of Mathematics, Faculty of Science, Sohag University, Sohag 82524, Egypt*

In this paper, we establish a unique common random fixed p oint t heorem i n c one r andom m etric spaces for four weakly compatible mappings by using an implicit relation. Some corollaries of this theorem for two and three random weakly compatible mappings are obtained. Some examples are given to support our generalization. Our results presented in this paper extend and improve several recent results in the setting of cone random metric spaces.

Universal Journal of Computational Mathematics 5(1): 2017, 8-16.

Convergence and Stability of Modified Random SP-Iteration for A Generalized Asymptotically Quasi-Nonexpansive Mappings

R. A. Rashwan[1] and H. A. Hammad[2]

[1]*Department of Mathematics, Faculty of Science, Assuit University, Assuit 71516, Egypt*

[2]*Department of Mathematics, Faculty of Science, Sohag University, Sohag 82524, Egypt*

The purpose of this paper is to study the convergence and the almost sure T-stability of the modified SP-type random iterative algorithm in a separable Banach spaces. The Bochner integrability of random fixed points of this kind of random operators, the convergence and the almost sure T-stability for this kind of generalized asymptotically quasi-nonexpansive random mappings are obtained. Our results are stochastic generalizations of the many deterministic results.

Mathematics Interdisciplinary Research 2 (2017), 9-21

Stability and strong convergence results for random jungck-kirk-noor iterative scheme

R. A. Rashwan[1] and H. A. Hammad[2]

[1]*Department of Mathematics, Faculty of Science, Assuit University, Assuit 71516, Egypt*

[2]*Department of Mathematics, Faculty of Science, Sohag University, Sohag 82524, Egypt*

The purpose of this study is to introduce a JungckKirk-Noor type random iterative scheme and prove stability and strong convergence of this to establish a general theorem to approximate the unique common random coincidence point for two or more nonself random commuting mappings under general contractive condition in various spaces. Also we give the stability and convergence for random Jungck-Kirk-Ishikawa and random Jungck-Kirk-Mann as a corollaries. The results obtained in this paper improve the corresponding results announced recently.

Fasciculi Mathematici, 2017

Common random fixed point results with application to a system of nonlinear integral equations

R. A. Rashwan[1], H. A. Hammad[2] and L. Guran[3]

[1]*Department of Mathematics, Faculty of Science, Assuit University, Assuit 71516, Egypt*

[2]*Department of Mathematics, Faculty of Science, Sohag University, Sohag 82524, Egypt*

[3]*Department of Pharmaceutical Sciences, "Vasile Goldis¸" Western University of Arad, Revolut¸iei Avenue, no. 94-96, 310025, Arad, Roumania.*

The purpose In this paper, we prove a common random fixed point theorem for two pair of weakly compatible mappings in separable Banach spaces. A corollary of the theorem is obtained and an example is given to verify this corollary. An application is given to obtain the existence and unique solution of system of random nonlinear integral equations.

Malaya Journal of Matematik, 5(4), 2017, 667-674

A solution of nonlinear fractional random differential equation via random fixed point technique

R. A. Rashwan[1] and H. A. Hammad[2]

[1]*Department of Mathematics, Faculty of Science, Assuit University, Assuit 71516, Egypt*

[2]*Department of Mathematics, Faculty of Science, Sohag University, Sohag 82524, Egypt*

In this paper, we investigate a new type of random F-contraction and obtain a common random fixed point theorem for a pair of self stochastic mappings in a separable Banach space. The existence of a unique solution for nonlinear fractional random differential equation is proved under suitable conditions.

Journal of Linear and Topological Algebra Vol. 06, No. 04, 2017, 277-287.

A common random fixed point theorem of rational inequality in polish spaces with application

R. A. Rashwan[1] and H. A. Hammad[2]

[1]*Department of Mathematics, Faculty of Science, Assuit University, Assuit 71516, Egypt*

[2]*Department of Mathematics, Faculty of Science, Sohag University, Sohag 82524, Egypt*

In In this paper, we prove a new common random fixed point theorem for a pair of random operators satisfying random F-contraction of rational inequality in polish spaces. An application to a system of random nonlinear integral equations is discussed. Finally, we give some examples to verify our results.

FACTA UNIVERSITATIS (NIS)˘ Ser. Math. Inform. 32(5), (2017), 703-714

Data Aggregation Energy and Probability Effects on the Performance of MODLEACH Protocol in WSN

Hamdy H El-Sayed
Mathematics Department, Faculty of Science, Sohag University, Egypt

WSNs are quickly gaining popularity due to they are potentially low cost solutions to a variety of real world challenges. They continue to grow day after day, so it needs the effective protocol mechanisms. There are various areas where research activities are going on in Wireless sensor networks. Data-centric technologies are needed that perform in network aggregation of data to yield energy-efficient dissemination. We examine changes of data aggregation energy and probability effects on the performance of MODLEACH protocol. Our study uses Dead Nodes, Alive Nodes, Packet sends to BS Nodes and Count of Cluster Heads as a parameters. These parameters have been affected and changed with different data aggregation energy and probability. In this research work the results and observations made from the analyses of results about this protocol is presented.

Appl. Math. Inf. Sci. Lett. 5 (2), 57-61 (2017)
6th International Conference on Mathematics and Information Sciences Feb. 09-11, 2017, Egypt

A Novel Image Encryption Scheme based on Different Block Sizes for Gray scale and Color Images

Omar Reyad M. A. Mofaddel W. M. Abd-Elhafiez Mohamed Fathy
Sohag University, Egypt Sohag University, Sohag University, Sohag University, Egypt

In this paper, two image encryption schemes are proposed for grayscale and color images. The two encryption schemes are based on dividing each image into blocks of different sizes. In the first scheme, the two dimension (2D) input image is divided into various blocks of size *N X N*. Each plainimage block is transformed into a one dimensional (1D) array using the Zigzag pattern mode. Then, the exclusive or (XOR) logical operation is used to encrypt each block with the analogous secret key. In the second scheme, after the transformation process, the first block of each image is encrypted by the corresponding secret key. Then, before the next block is encrypted, it is XORed with the first encrypted block to become the next input to the encrypting routine and so on. This feedback mechanism depends on the cipher block chaining (CBC) mode of operation which considers the heart of some ciphers because it is highly nonlinear. In the case of color images, the color component is separated into blocks with the same size and different secret keys. The used secret key sequences are generated from elliptic curves (EC) over a *binary* finite field $\mathbf{F}_{2^m}$. Finally, the experimental results are carried out and security analysis of the ciphered images are demonstrated that the two proposed schemes had a better performance in terms of security, sensitivity and robustness.

Springer International Publishing AG 2017
A.E. Hassanien et al. (eds.), ***Proceedings of the International Conference on Advanced Intelligent Systems and Informatics 2016*****, Advances in Intelligent Systems and Computing 533,**

Hop by Hop Routing Problems in MANETs

Hamdy H. El-Sayed
Mathematics Department, Faculty of Science, Sohag University, Egypt

Mobile networks have attracted huge interest in recent years because of their improved flexibility and reduced costs. Sending and receiving data packets between nodes is the main function of routing protocols. Because of the limited resource of mobile ad hoc network routing protocols is needed. Hop-by-hop routing means that routing decisions are made at each node independently and locally, based only on packets destination addresses and their route computation using corresponding topology knowledge. This paper introduced the difference between source routing and hop-by-hop routing and presented a lot of protocols that has been presented by different researchers. Also this paper presented the weakness of the paper that has been presented.

IEEE, 978-1-5386-1191-3/17

An Integrated Smoothing Method for Fingerprint Recognition Enhancement

Muhammad Khfagy[1,2], Yasser AbdelSatar[1], Omar Reyad[2,3], and Nahla Omran[1]
[1]Faculty of Science, South Valley University, Qena, Egypt
[2]Faculty of Science, Sohag University, Sohag, Egypt
[3]Faculty of Electronics and Information Technology, Warsaw University of Technology, Warsaw, Poland

Fingerprint identification systems are one of the most well known and publicized biometrics because of the inherent ease in acquisition, the numerous sources (ten fingers) available for collection, and their established use by law enforcement and immigration. These systems rely on the unique biological characteristics of individuals to accurately verify their identities. To get reliable and accurate verification results, these systems need high quality images. The quality of the fingerprint image is obtained by using noise-free images during the pre-processing and filtering stages. In this paper, we proposed an integrated smoothing method (ISM) for fingerprint image recognition enhancement based on a linear combination of three different filtering techniques named median filter (MF), Wiener filter (WF) and anisotropic diffusion filter (ADF). This combination is made by using two coefficient parameters (α, β) with different values to enhance the quality of images and remove the unwanted distortion or noise that affect a fingerprint recognition system. The ISM is applied in the pre-processing stage to get a noise-free fingerprint image with high accuracy factor. We used the benchmarking FVC2004 and FVC2006 databases to test our method and the Wilcoxon signed-rank test (**W**) and the peak signal-to-noise ratio (PSNR) for results evaluation. The experimental results indicate that the proposed ISM improves the performance of the fingerprint identification significantly.

International Journal of Engineering and Information Systems (IJEAIS), 1 (6), 157-161

Adaptive Fingerprint Image Enhancement Based On Cascading Filtering

Mahmoud A. Mofaddel, Samy Bakheet, Rehab Youssef
Department of Computer Science Faculty of Science, Sohag University Sohag, Egypt

Automated Fingerprint Identification Systems (AFIS) have recently become one of the best-known and most widely used biometric technologies, which consists of various stages such as Image acquisition, enhancement, feature extraction and matching. The enhancement process is conducted to improve the quality of the fingerprint image and make it more legible and convenient for the further feature extraction process. In this paper, we propose an adaptive methodology for fingerprint image enhancement, where multiple techniques are adopted in conjunction, namely, Histogram Equalization, Fast Fourier Transformation and Image Binarization. The experiments are all performed using OpenCV library and the obtained results reveal the potential of the proposed methods.
British Journal of Applied Science & Technology, 20(5), 1-11, 2017

Recognition of Human Actions Based on Temporal Motion Templates

Samy Bakheet[1;2]*, Ayoub Al-Hamadi[2] and M. A. Mofaddel[1]
[1]*Department of Mathematics and Computer Science, Faculty of Science, Sohag University, P.O.Box 82524 Sohag, Egypt*
[2]*Institute for Information Technology and Communications, Otto-von-Guericke-University Magdeburg, P.O.Box 4120, 39016 Magdeburg, Germany.*

Despite their attractive properties of invariance, robustness and reliability, statistical motion descriptions from temporal templates have not apparently received the amount of attention they might deserve in the human action recognition literature. In this paper, we propose an innovative approach for action recognition, where a novel fuzzy representation based on temporal motion templates is developed to model human actions as time series of low-dimensional descriptors. An NB (Na¨ıve Bayes) classifier is trained on these features for action classification. When tested on a realistic action dataset incorporating a large collection of video data, the results demonstrate that the approach is able to achieve a recognition rate of as high as 93.7%, while remaining tractable for real-time operation.
UK-RAS 2017

Active Human Detection with a Mobile Robot

Mohamed Heshmat*&, Manuel Fernandez-Carmona*, Zhi Yan* and Nicola Bellotto*
**L-CAS, School of Computer Science, University of Lincoln (UK)*
& Faculty of Science, Sohag University (Egypt)
mabdelwahab, mfernandezcarmona, zyan, nbellotto @lincoln.ac.uk

The problem of active human detection with a mobile robot equipped with an RGB-D camera is onsidered in this work. Traditional human detection algorithms for indoor mobile robots face several challenges, including occlusions due to cluttered dynamic environments, changing backgrounds, and large variety of human movements. Active human detection aims to improve classic detection systems by actively selecting new and potentially better observation points of the person. In this preliminary work, we present a system that actively guides a mobile robot towards high-confidence human detections, including initial simulation tests that highlight pros and cons of the proposed approach.
Conference: Proceedings Of The 13th Imt-Gt International Conference on Mathematics, Statistics and their Applications (Icmsa2017)

A novel approach for color image segmentation based on region growing

E. A Zanaty[1], S. F. El-Zoghdy[2]
[1]Department of Mathematics and Computer Science, Faculty of Science, Sohag University, P.O.Box 82524 Sohag, Egypt
[2]Department of Mathematics and Computer Science, Faculty of Science, Mounovia University, shebin El-Kom, Egypt

In this paper, a novel approach for obtaining all possible uniform regions in the color image is proposed. The proposed approach integrates a color edge detection method; image partitioning; the initial seeds and thresholding region growing; the average overlap metric (AOM) and voting algorithms. It starts by decomposing the color image into less complicated component images. The edges of the color image are detected to extract the non-edge pixels during the region growing processes. Then, a source image is partitioned into cells while seeds are obtained by applying the local search algorithm in the image histogram. The growing processes are improved by color image thresholding algorithm which is necessary for finding the homogeneity criterion to merge similar pixels. The seeds and the homogeneity criterion values are the input to the region growing method to segment an image into regions; some of them are overlapped or been redundant. The AOM algorithm is applied to classify the redundant regions based on pixel similarity. These regions are fed to voting technique in order to produce region of points whose have similar values to utilize the compactness of the clusters forming these uniform regions. Experimental results are conducted using different color images with different sizes. Moreover, the proposed method is experimented by different noisy images and is compared with the well-known existing methods to prove its efficiency. The obtained results reveal the accuracy and stability of proposed technique and its superiority over other three well-known existing methods.


قسم الفيزياء
Physics Department

Physics


قسم الفيزياء
Physics Department

Single Folding Cluster Potential for P $^{+12}$C Elastic Scattering

N. N. Abd Allah[1], M. El-Azab Farid[2], S. R. Mokhtar[2], A. A. Ebrahim[2] and A. M. EL-Sheikh[1]
[1]*Physics Department, Sohag University, Sohag 82524, Egypt*
[2]*Physics Department, Assiut University, Assuit 71516, Egypt*

The proton scattering from carbon has been analyzed within the framework, using the single folding optical model with a Gaussian shape of the effective alpha-nucleon interaction. In addition, the angular distributions of the differential cross-sections of the proton elastic scattering from l2C were analyzed, using the alpha-cluster structure of ^{12}C, where carbon has three atoms of helium and oxygen has four atoms of helium. Furthermore, we analyzed the P $^{+12}$C elastic scattering at twenty energies, ranging from 7 to 494 MeV. The Gaussian shape of the effective alpha-nucleon interaction was used at two values for the depth at 36.4 MeV with the range of 0.265 f m^{-2} and 47.3 MeV with the range of 0.189 f m^{-2} . Thus, each of the two values for the depth succeeded to describe the proton scattering from carbon. Keywords: Single Folding Model, Elastic Scattering, Nuclear Reactions, Proton Carbon Reactions.
J. Rad. Nucl. Appl. 2, No. 3, 115-120 (2017)

Effect of the synthesis conditions on the structural, morphological and optical properties of $Bi_2Te_{2.7}Se_{0.3}$ nanoparticles

H. M. Ali, E. M. M. Ibrahim, M. M. Wakkad, M. A. A. Mohamed
Physics Department, Faculty of Science, Sohag University, Sohag 82524, Egypt

Beside their promising utility as thermoelectric generators, Bi_2Te_3 and related compounds have several applications in electronic and optoelectronic devices. In this work, $Bi_2Te_{2.7}Se_{0.3}$ nanoparticles (NPs) were successfully prepared via physical vapor deposition technique at different conditions of flow rate and temperature. The x-ray diffraction patterns show that, the NPs crystallize in a rhombohedral crystal structure with preferable growth along the (015) plane. Field-emission scanning electron microscope (FE-SEM) investigation shows that the NPs size depends significantly on the synthesis conditions of flow rate and temperature where it decreases with the decrease in the former or with the increase in the later. The effect of deposition conditions on the final morphology can be interpreted through the accompanied variation in the concentration of the gaseous precursors in the hot zone. The optical properties were studied using Kubelka-Munk theory. Optical band gaps of 0.52, 0.58, 0.53 eV were determined for the samples synthesized under different conditions.
Optik - International Journal for Light and Electron Optics

Optical and Photocatalytic Measurements of Co-TiO_2 Nanoparticle Thin Films

Mai M. Khalaf[1,2] & Hany M. Abd El-Lateef[1,2] & H. M. Ali[3]

[1]Department of Chemistry, College of Science, King Faisal University, Al Hufuf, Al Hassa 31982, KSA
[2]Chemistry Department, Faculty of Science, Sohag University, Sohag 82524, Egypt
[3]Physics Department, Faculty of Science, Sohag University, Sohag 82524, Egypt

Co-TiO_2 nanoparticle thin films were synthesized by sol-gel method. The structural properties of the synthesized sample were studied using FTIR, XRD, and TEM. XRD confirmed the presence of double-phase anatase/rutile for the TiO2 nanoparticles. Effect of annealing temperature and exposure to microwave energy on the optical properties were studied for transparent conductive oxide (TCO) application. The optical energy gap and refractive index were determined. It was found that microwave treatment is an effective method for reinforcing optical properties of films. The photocatalytic properties were studied by determining the absorbance of methylene blue (MB) using UV source as a function of illumination time.
Plasmonics

Morphological and Optical Characterization of Mg-Zno Thin Films Deposited by Co-Magnetron Sputtering Technique

S. E. ALOMAIRY[a], H. M. ALI[b], M. M. ABD EL-RAHEEM[a,b], A. M. AL-BARADI[a], F. ABDEL-WAHAB[a,c], S. A. AMIN[d]

[a]Department of physics, Faculty of Science, Taif University, Taif 888, KSA
[b]Department of physics, Faculty of Science, Sohag University, Sohag 82524, Egypt [c]Department of physics, Faculty of Science, Aswan University, Aswan. Egypt
[d]Department of physics, Faculty of Science, Assiut University, Assiut 71516. Egypt

This paper reports the structural and optoelectronic properties of prepared pure and Mg doped ZnO nanoparticles using co-magnetron sputtering technique. The phase purity and crystallites size of synthesized ZnO and Mg doped nanoparticles were characterized and examined using X-ray diffractometar XRD and scanning electron microscopy SEM . The elemental analysis was examined by using energy-dispersive X-ray spectroscopy EDX. The optical properties Eop were carried out by using U-V-VIS double beam spectroscopy to study the optoelectronic properties of the thin films under test. The power on Mg target (ratio of Mg) affected the structural parameters such as lattice constant, grain size, strain e as well as the optical parameters such as Urbach tail, optical energy gap, refractive index and carrier concentration.
Keywords: sputtering; thin film; Mg-ZnO; optical gap; refractive index.
Digest Journal of Nanomaterials and Biostructures, 12, No. 2, April - June 2017, p. 533 – 547

Tensor target spin asymmetries in incoherent π^--photoproductionoff the deuteron including rescattering effects

E. M. Darwish[1,2,*], H. M. Abou-Elsebaa[1,2], E. A. Sultan[2], and Kh. S. A. Hassaneen[2]
[1]*Physics Department, Faculty of Science, Taibah University, Medinah 41477, Saudi Arabia*
[2]*Physics Department, Faculty of Science, Sohag University, Sohag 82524, Egypt*

Tensor target spin asymmetries $T_{2M}(M=0,1,2)$ in the reaction $\gamma d \rightarrow \pi^- pp$are studied for photon energies from π-threshold up to 1.5 GeV with inclusion of rescattering effects. It is shown that the influence of rescattering effects on the tensor target spin asymmetries is sizable in the energy region near π-threshold. At higher energies, much smaller influence of rescattering effects is seen. The sensitivity of the obtained results to the elementary pion photoproduction operator is investigated and a considerable dependence is found, in particular at forward pion angles. In addition, a comparison with results of other theoretical models is also given. The extracted spin asymmetries are compared with available experimental data and a qualitative agreement is obtained. The predictions presented here may be useful to interpret the recent measurements from the VEPP-3 electron storage ring.
International Journal of Modern Physics E, Vol. 26, No. 10 (2017) 1750059

Single and Double Spin Asymmetries in the Elastic *e-d* Scattering and Their Dependence on the Deuteron Wave Function

E. M. Darwish[1,2,*], A. Abd El-Daiem[2], and M. M. Abd El-Wahab[3]
[1]*Physics Department, Faculty of Science, Taibah University, Medinah 41477, Saudi Arabia*
[2]*Physics Department, Faculty of Science, Sohag University, Sohag 82524,Egypt*
[3]*Physics Department, Faculty of Science, AswanUniversity,Aswan 81528, Egypt*
[*]*E-Mail: darwish@science.sohag.edu.eg*

Single and double spin asymmetries in the elastic electron-deuteron (*e-d*) scattering were investigated.The tensor-deuteron asymmetries $T_{2i}(i = 0, 1, 2)$ and the beam-vector-deuteron asymmetries$T_{1i}(i = 0, 1)$were calculated and compared with the available experimental data. The sensitivity of the results forthese spin asymmetries to the deuteron wave function has been investigated. The predicted asymmetries werefound to be agree with one another and with experiment. It was found that, the double spin asymmetry T_{10}ismuch smaller than the T_{11}-asymmetry. Therefore, in addition to the single tensor-deuteron asymmetry T_{20},the doubly beam-vector-deuteron asymmetry T_{11} can be used as an another tool for extracting the deuteronelectromagnetic form factors.
Physics of Particles and Nuclei Letters, Vol. 14, No. 6 (2017) 822-835

Tensor target spin asymmetries in coherent π^0-photoproduction on the deuteron including intermediate ηNN interaction within a three-body approach

E. M. Darwish[1,2,*], H. M. Abou-Elsebaa[1,2], and Kh. S. A. Hassaneen[2]

[1]*Physics Department, Faculty of Science, Taibah University, Medinah 41477, Saudi Arabia*

[2]*Physics Department, Faculty of Science, Sohag University, Sohag 82524,Egypt*

[*]*E-Mail: darwish@science.sohag.edu.eg*

Motivated by the recent measurements from the VEPP-3 electron storage ring, we investigate thetensor target polarization asymmetries $T_{2M}(M=0,1,2)$ in the reaction $\gamma d \rightarrow \pi^0 d$ with a particularinterest in the effect of the intermediate ηNN three-body approach. This approach is based onrealistic separable representations of the driving two-body interaction in the πN, ηN, and NNsubsystems. It is shown that the influence of rescattering effects in the intermediate state on thetensor target spin asymmetries is sizable at extreme backward pion angles. At forward angles,the contribution from the pure impulse approximation is dominated and the spin asymmetriesshow very little influence of rescattering effects. The sensitivity of results to the elementary pion photoproduction operator and to the NN potential model adopted for the deuteron wave functionis investigated and considerable dependences are found. The predicted spin asymmetries are alsocompared with available experimental data and a satisfactory agreement with the recent data fromVEPP-3 is obtained at photon energies below 400 MeV. At higher energies, the calculated spinasymmetries are slightly underestimate the data.

Brazilian Journal of Physics, accepted for publication (2017)

Room temperature magneto-transport properties of $La_{0.7}Ba_{0.3}MnO_3$ manganite

Abd El-Moez A. Mohamed[a,b,*], B. Hernando[b], M.E. Díaz-García[c]

[a]*Physics Department, Faculty of Science, Sohag University, Sohag 82524, Egypt*

[b]*Physics Department, Faculty of Science, Oviedo University, Oviedo 33007, Spain*

[c]*Department of Physical and Analytical Chemistry, Faculty of Chemistry, Oviedo University, Oviedo 33006, Spain*

Polycrystalline $La_{0.7}Ba_{0.3}MnO_3$ manganite compound with high homogeneity was prepared by the sol-gel method. This compound shows a metal-semiconductor dc resistivity transition at Tms temperature of 300 K. The resistivity shows a dc electric field dependence relation, where, it increases monotonically with the applied dc electric current. In contrast, the Tms is insensitive to the applied electric field, where, it is kept unchanged. The dramatic increase in the dc resistivity with the applied electric current leads to a positive electroresistance that also increases monotonically with the applied electric current. The ac resistivity and the effect of low frequencies are also studied, the results show the monotonic increase in the ac resistivity with increasing the frequency due to the skin effect. The zero frequency (dc) magnetoresistance is enhanced with the frequency increase, where, the magnetoresistance peak shows the values 2.05, 2.9, 4.5 and 4.8% for dc, 3, 70 and 128 Hz, respectively. The dc magnetization measurement shows the ferromagnetic-paramagnetic transition at 300 K revealing the room temperature magnetocaloric properties for the La0.7Ba0.3MnO3 compound. For example, it shows a magnetic entropy change (DS) of 1.3 J kg^{-1} K^{-1} with a relative cooling power of 41 J kg^{-1} at 2 T applied magnetic field. In addition, the experimental data of DS were modeled by Landau theory that proves the absence of elastic, magnetoelastic and magnetoelectronic coupling effects in the magnetocaloric properties.

Journal of Alloys and Compounds 695 (2017) 2645e2651

Electronic bands and optical conductivity of the Dzyaloshinsky-Moriya multiferroic $Ba_2CuGe_2O_7$

M. Corasaniti,[1] P. Barone,[2] A. Nucara,[3] M. Ortolani,[1] L. Baldassarre,[3] R. Fittipaldi,[4] V. Granata,[4] L. Rocco,[4] A. Vecchione,[4] W. S. Mohamed,[5] J. Lorenzana,[6] and P. Calvani[3]

[1]*Dipartimento di Fisica, Sapienza Università di Roma, P.le A. Moro 5, 00185 Roma, Italy*
[2]*CNR-SPIN c/o Università dell'Aquila, L'Aquila, Italy*
[3]*CNR-SPIN and Dipartimento di Fisica, Sapienza Università di Roma, P.le A. Moro 5, 00185 Roma, Italy*
[4]*CNR-SPIN and Dipartimento di Fisica "E. R. Caianiello", Via Ponte don Mellillo, I-84084 Fisciano, Salerno, Italy*
[5]*Physics Department, Faculty of Science, Sohag University, 82524 Sohag, Egypt*
[6]*CNR-ISC c/o Dipartimento di Fisica, Sapienza Università di Roma, P.le A. Moro 5, 00185 Roma, Italy*

We have measured the reflectivity in the *ab* plane and along the *c* axis of a single crystal of the Dzyaloshinsky- Moriya multiferroic $Ba_2CuGe_2O_7$, from 20 to 300 K and from 700 to 24 000 cm^{-1}. The resulting optical conductivity $\sigma(\omega)$ has been compared with the results of calculations of its electronic band structure based on density functional theory (DFT). A broad midinfrared band, which in the *ab* plane strongly hardens for decreasing temperature, is consistent with d-d transitions of the Cu atom. A further electronic absorption, whose edge falls in the near infrared and has a strong O-*p* character, unusually softens with decreasing temperature by more than 0.15 eV, in both polarizations. Calculations show that the behavior with temperature of those electronic bands can be related to distortions of the CuO4 tetrahedra.
PHYSICAL REVIEW B 96, 085115 (2017)

α-Bi_2O_3 nanorods: synthesis, characterization and UV-photocatalytic activity

Ahmed M Abu-Dief[1] and W. S. Mohamed[2]
[1]*Faculty of Science, Chemistry Department, Sohag University, 82524 Sohag, Egypt*
[2]*Faculty of Science, Physics Department, Sohag University, 82524 Sohag, Egypt*

In this study, Monoclinic bismuth oxide nanorods (α-Bi_2O_3 NRs) were successfully synthesized by a simple one-step hydrothermal route using (water: ethanol) (1:1) as a mixed solvents at optimum conditions. The Bi_2O_3nano-powder was characterized in detail by different techniques in terms of their structural, morphological, compositional, optical and photocatalytic properties. X-ray diffraction (XRD) analysis indicated that the as-synthesized Bi_2O_3 NRs exhibited high purity with monoclinic structure (α-Bi_2O_3) and good crystallinity. The Transmission electron microscope (TEM), Energy dispersive x-ray spectroscopy (EDXS) and Field Emission scanning electron microscope (FE-SEM) analysis clearly confirmed the high purity and the nanorod morphology of the as-synthesized Bi_2O_3 sample. The optical band gap of α-Bi_2O_3 NRs was estimated using the UV–Vis diffuse reflectance spectroscopy (UV–Vis DRS) analysis according to the Kubelka–Munk theory. The optical band gap of α-Bi_2O_3 NRs was found to be 3.55 eV for an indirect allowed transition and 3.63 eV for a direct allowed transition. The Fourier transfer infrared spectroscopy (FTIR) was employed to check the structure as well as to evaluate the phonon vibration modes corresponding to Bi_2O_3. Photocatalytic activity of α-Bi_2O_3 NRs was investigated using UV source lamp. The as-synthesized α-Bi_2O_3 NRs photocatalyst exhibited better performance for degradation and decolorization of Methylene blue (MB) under ultraviolet (UV) irradiation. MB was completely photodegraded after 210 min under UV irradiation using α-Bi_2O_3 NRs as photocatalyst.
Mater. Res. Express 4 (2017) 035039

Influence of (Ar + O_2) atmosphere and $CdCl_2$ coating heattreatment on physical properties of CdS thin film for solar cell applications

W S Mohamed, M F Hasaneen and E KhShokr
Physics Department, Faculty of Science, Sohag University, 82524 Sohag, Egypt

Cadmium sulphide (CdS) thin films have been grown on corning glass substrate by thermalevaporation technique under base pressure 2×10^{-5} mbar. In this study we investigate the influenceof Cadmium chloride ($CdCl_2$) heat treatment and argon and oxygen (Ar+ O_2) annealing on thestructural, morphological optical and electrical properties of CdS thin films to achieve high qualitythin films for solar cells applications. X-ray diffraction (XRD), Field Emission scanning electronmicroscope (FE-SEM) and UV–Vis-NIR spectrophotometer were used to confirm and investigatethe different physical properties of CdS films. The quality of CdS thin films crystallinity including theaverage grain size (D_{avg}), the average lattice strain (ε_{ls}) and the dislocation density (ρ_D) were extractedvia XRD line broadening analysis. XRD analysis revealed that the samples are polycrystalline innature with a mixed (hexagonal + cubic) structure and the crystallinity of the films increases withboth (Ar+ O_2) annealing and $CdCl_2$ heat treatment. After (Ar+ O_2) annealing and $CdCl_2$ heattreatment processes the mean values of the grain size indicating the grain growth of CdS films.The surface morphology of the CdS films was examined by (FE-SEM) analysis; which confirmedthe nano-crystalline nature of the CdS films with uniform coverage of the substrate surface; Theoptical properties of as-deposited, (Ar+ O_2) annealed and CdCl2 treated CdS films were discussedin detail. The optical energy gap was calculated using Tauc plot extrapolation. It was found to beincreased from 2.43 eV for as-deposited film to 2.45 for $CdCl_2$ treated CdS film. Swanepoel method was employed to estimate the thicknesses and extract the refractive index of the CdS films. The Roomtemperature resistivity decreased from 13.4 Ω cm for as-deposited CdS film to 2 and 0.8 Ω cm for(Ar+ O_2) annealed and $CdCl_2$treated CdS films respectively. The $CdCl_2$ treated CdS film has thehighest figure of merit value of $29 \times 10{-}4\ \Omega^{-1}$. The obtained results confirm that the $CdCl_2$ heattreatment process in (Ar+ O_2) atmosphere can enhance the physical properties of CdS thin films asa promising window layer or buffer layer material for CdS/CdTe and Cu(In,Ga)Se_2 solar cells.
Mater. Res. Express 4 (2017) 046406

Effects of V doping on magnetic and optical properties of oxygen-deficient In_2O_3 thin films

Mohammed S. Alqahtani[a], N.M.A. Hadia[b], S.H. Mohamed[b]
[a]Department of Physics and Astronomy, King Saud University, Riyadh 11451, Saudi Arabia
[b]Physics Department, Faculty of Science, Sohag University, 82524 Sohag, Egypt

The scope of the work was to study structural, optical and magnetic behaviors of vanadium (V) doped indium oxide thin films prepared by thermal evaporation. Thin films of vanadium doped oxygen deficient In2O3 were deposited on sapphire, corning glass and Si(100) sub-strates. EDAX analysis revealed a great reduction in oxygen was happen during evaporation and oxygen deficient undoped and V doped In2O3 thin films were formed. XRD charac-terization suggested that the present In2O3 portion was in the amorphous state and the observed crystalline peaks were indexed as tetragonal metallic indium. The undoped In2O3 had the lowest transmittance and the transmittance increased with increasing V doping. The optical band gap and refractive index values decreased with increasing V doping. The dependence of magnetization on magnetic field for V doped In2O3 thin films were studied at 300 K and 5 K. All the samples exhibited soft ferromagnetic behaviour. The parameters of the hysteresis loop were extracted. The achieved results may find usage in magneto-optical applications.
Optik 145 (2017) 377–386

Morphologies and optical properties of mixed tin oxysulfide produced by evaporation condensation of SnS

S.H. Mohamed, N.M.A. Hadia, M.F. Hasaneen, Mohamed Asran Hassan
Physics Department, Faculty of Science, Sohag University, 82524 Sohag, Egypt

The goal of the present study was to use the evaporation-condensation method of SnS to synthesize mixed novel tin oxysulfide nanostructures. Structural, morphological and optical properties of these nanomaterials were investigated. Synthesis was carried out in horizontal tube furnace using Au coated quartz and Si(100) substrates. The substrates were set along 1–25 cm from the centered alumina boat. The deposition was observed mainly in two regions. Region A was close to the boat and extended approximately 6 cm from it and region B started approximately 15 cm from the center of the boat and extended over 10 cm towards the end of the tube. EDAX and XRD analysis revealed formation of mixed tetragonal SnO2 and tetragonal tin oxide sulfate, SnO2SO4, in region A whereas mixed orthorhombic SnS and tetragonal tin oxide sulfate in region B. SEM investigations showed randomly oriented nanowires and cotton candy morphologies for samples prepared in regions A and B, respectively. Moderate transmittance, high refractive index (2.218 at 550 nm) and two optical band gaps of 1.87 eV and 3.35 eV were obtained for samples prepared in region A whereas high transmittance, moderate refractive index and optical band gap of 1.82 eV were obtained for the samples prepared in region B. The obtained results, especially the new oxysulfide samples, may have find applications in various fields.
Materials Science in Semiconductor Processing 72 (2017) 72–77

Synthesis, optical, structural, and electrical properties of singlecrystalline CdS nanobelts

Mohammed S. Alqahtani[1], N. M. A. Hadia[2] · S. H. Mohamed[2]
[1]Department of Physics and Astronomy, King Saud University, Riyadh 11451, Saudi Arabia
[2]Physics Department, Faculty of Science, Sohag University, 82524 Sohag, Egypt

CdS nanobelts (NBs) were synthesized by vapor transport of CdS powders. The growth was carried out without any catalyst on quartz and Si (100) substrates. The synthesized CdS NBs were examined by transmission electron microscopy (TEM), field emission scanning electron microscopy (FE-SEM) and selected area electron diffraction (SAED), high-resolution transmission electron microscopy (HR-TEM), X-ray powder diffraction (XRD), energy dispersion analysis of X-ray (EDAX), spectrophotometer, and photoluminescence spectroscopy. CdS NBs were indexed as hexagonal wurtzite structure. The growth was via vapor–solid growth mechanism and along the [100] direction. The refractive index was evaluated in the transparent region, as suggested by Swanepoel, using the envelope method. The refractive index values and the extinction coefficient were decreased by increasing the wavelength. The calculated optical band gap was 2.50 eV. The photoluminescence (PL) spectrum of the synthesized CdS NBs exhibited a green emission peak at 510 nm and a broad red emission peak at 696 nm. The conductivity measurements were achieved, in the temperature range from 300 to 600 K, using the conventional two-probe technique. Two different slopes with different activation energies of 0.618 and 0.215 eV were obtained. The CdS NBs are likely being novel functional materials. Thus, they can be used in the manufacture of innovative optoelectronic nanodevices.
Appl. Phys. A (2017) 123:298

Tunable properties of one-dimensional photonic crystalsthat incorporate a defect layer of a magnetized plasma

Arafa H. Aly[1], Hussein A. Elsayed[1], Ayman A. Ameeny[2] and S. H. Mohamed[2]

[1]*Physics Department, Faculty of Science, Beni-Suef University, Egypt*

[2]*Physics Department, Faculty of Science, Sohag University, Egypt*

In this paper, we theoretically investigate the transmittance characteristics of one-dimensional defective photonic crystal in microwave radiations based on the fundamentals of the characteristic matrix method. Here, the defect layer is magnetized plasma.The numerical results show the appearance of defect peaks inside the Photonic BandGap. The external magnetic field has a significanteffect on the permittivity of the defect layer. Therefore, the position and intensity of the defect peak are strongly affectedby the external magnetic _eld. Moreover, we have investigated the different parameterson the defect peaks as the plasma density, the thickness of the plasma layer and theangle of incidence. Wherefore, the proposed structure could be the cornerstone for manyapplications in microwave regions such as narrowband filters**.**

International Journal of Modern Physics B31 (2017) 1750239 (9 pages)

Copper oxide nanocrystallites fabricated by thermal oxidation of pre-sputtered copper films at different temperatures and under oxygen and argon flows

M. A. Awad, N. M. A. Hadia

Physics Department, Faculty of Science, Sohag University, 82524 Sohag, Egypt

Copper oxide nanocrystallites were synthesized from Cu thin films via controlled thermal treatment under O_2 and Ar flows. The nanocrystallites were synthesized at 350, 400 and 500°C. XRD revealed that substoichiometric copper oxides such as Cu_4O_3 and $Cu_{64}O$ were emerged with Cu and CuO for samples treated at 350°C and 450°C, respectively, whereas single monoclinic CuO was emerged for the samples treated at 500°C. EDAX quantitative analysis confirmed the presence of both Cu and oxygen in the films with slightly excess oxygen for films treated at 400 and 500°C. SEM examinations confirmed the nanocrystallite morphologies for the examined samples and that more coalescent nanocrystallites, with diameters in the range 42-75 nm, were obtained for the samples treated at 500°C. With increasing treatment temperature from 350 to 500°C, the films vary from highly reflecting reddish brown color to highly transparent. The estimated band gap values for the mixed copper oxide phases, samples treated at 450°C, and pure CuO phase were 1.27 eV and 2.00 eV, respectively. High refractive index and moderate extinction coefficient values were calculated for the samples containing mixed phases which may find new application in optoelectronics. The refractive index values for pure CuO were matched with the previously reported values. The samples treated at 350°C had very low resistivity and metallic behavior, whereas a semiconducting behavior was observed for the samples treated at 400 and 500°C.

Optik 142 (2017) 334–342

Improvement of the performance of thin-film CdS/PbS solar cells using low-cost ZnO-based alloys as front electrode

H. A. Mohamed, M. R. Ahmed

Physics Department, Faculty of Science, Sohag University, 82524 Sohag, Egypt

All thin film solar cells require the use of transparent conductive electrodes such as indium tin oxide (ITO) due to its unique combination of transparency, high conductivity, durability, and favourable surface properties. Indium, however, is a rare and expensive metal; proposed large-area installations of photovoltaic (PV) cells will add further strain to global indium supply. Transparent conductive materials that are abundant, inexpensive, and enable efficient thin film solar cells must therefore be developed. Zinc oxide (ZnO), tin doped zinc oxide (ZnO:Sn), aluminum doped zinc (ZnO:Al) and indium doped zinc oxide (ZnO:In) were theoretically investigated as alternatives transparent conductive oxides (TCO) to indium tin oxide that used as front electrode in CdS/PbS thin-film solar cells. The effect of optical and recombination losses as well as the reflectivity from metallic back contact were investigated in this work. It was found that the spectral quantum efficiency depends on the width of space-charge region (*W*) and the thickness of absorber layer (*d*PbS). The maximum short-circuit current density of about 20.9 mA/cm2 was achieved at *W*= 3μm and *d*PbS=2μm for ZnO:Al. The average optical losses due to reflection from all interfaces and due to absorption in CdS and TCO layers were about 32%. The total reflected back contact lead to increase the short-circuit current density by 20% and hence the efficiency of CdS/PbS cell recorded a value of 7.89 % for ZnO:Al.

Journal of Optoelectronics and Advanced Materials 19 (2017) 359:367

Quantitative assessment of electrical, optical and recombination losses in heterojunction CdS/CdTe solar cells

H. A. MOHAMED, A. S. MOHAMED

Physics Department, Faculty of Science, Sohag University, 82524 Sohag, Egypt

In this paper, electrical, optical and recombination losses in thin-film solar cells passed on CdS/CdTe have been evaluated. Electrical losses due to series and shunt resistances are quantitatively estimated from *J-V* curves. *J-V* characteristics are described in terms of the Sah– Noyce–Shockley theory of generation–recombination in the space-charge region of the CdS/CdTe heterostructure. Optical losses due to multiple reflections from the cell interfaces as well as absorption in the ITO and CdS layers are found using the refractive index and the extinction coefficient of the used materials. Losses arise from the recombination of the generated carriers at the front and rare surface of CdTe layer are carried out on the basis of the width of the space-charge region and other parameters of the absorber layer. It is found that the fill factor, output power density and the cell efficiency decreases with increasing the series resistance and decreasing the shunt resistance. The electrical losses due to series and shunt resistance are about 6%. Decreasing the thickness of window layer from 100 nm to 50 nm leads to increase the short-circuit current density from 23.6 mA/cm^2 to 24.8 mA/cm^2 and then reducing the optical losses from 24% to 20%. The recombination losses record a minimum value of 5% at width 1 μm of the space-charge region and record a maximum value of 27% at width=7μm.

Optoelectronics and advanced materials - rapid communications 11 (2017) 171:179

Electrical, thermoelectrical and magnetic properties of approximately 20 nm Ni-Co-O nanoparticles and investigation of their conduction phenomena

E. M. M. Ibrahim[a], Ahmed M. Abu-Dief[b,c], A. Elshafaie[a], A. M. Ahmed[a]

[a]*Physics Department, Faculty of Science, Sohag University, Sohag, 82524, Egypt*

[b]*Chemistry Department, Faculty of Science, Sohag University, Sohag, 82524, Egypt*

[c]*Departamento de Quimica Organicae Inorganica, Faculad de Quimica, Universdad de Oviedo, 33006, Oviedo, Spain*

Understanding the properties of semiconductor nanostructures is important for developing their practical applications in the nanodevices. Although the electrical properties of spinel oxides containing Ni and Co have been studied extensively over the last decades, there is still a significant disagreement on their electrical conduction mechanisms and the distribution of the various charge states of Co and Ni in the octahedral and tetrahedral sites of the spinel crystal lattice. In this study, Co3O4, NiO, and mixed Ni-Co oxide nanoparticles (NPs) of ~20 nm are synthesized by co-precipitation method. The mechanism of the electrical conduction in the Co3O4and Ni-Co oxides NPs is due to the hopping process in the octa-hedral site or between the octahedral and tetrahedral sites while in the NiO NPs, the large polarons conduction mechanism dominates. The thermoelectric power measurements confirm that the Ni-Co oxides NPs are non-degenerate semiconductors and the diffusion mechanism is the dominant compo-nent of the Seebeck coefficient. In contrast, the Co3O4NPs show degenerate features with Fermi energy 0.45 eV. The NiO NPs exhibit a transition from non-degenerate to degenerate state. The magnetic measurements reveal an antiferromagnetic-paramagnetic transition at N eel transition temperature. The results are helpful to understanding the fundamental characteristics of the NPs under study.

Materials Chemistry and Physics 192 (2017) 41e47

Synthesis, characterization and low field magnetotransport of Nd0.6Sr0.4MnO3/CrO3 composite

A M Ahmed, H F Mohamed, A K Diab and S A Mohamed

Physics Department, Faculty of Science, Sohag University, Soha˜g 82524, Egypt

$(Nd_{0.6}Sr_{0.4}MnO_3)_{1-x}/(CrO_3)_x$ with x=0.0–0.030 step 0.005 weight% composites have been prepared by the solid state reaction process. The X-ray and scanning electron microscopic manifest that all composites are a single orthorhombic phase and there are no CrO_3 grains separated from NdSrMnO matrix. The electrical measurements have revealed an increase of resistivity and a decrease of metal semiconductor transition with increasing CrO_3. The composite x=0.025 has largest magnetoresistance nearly one hundred percent at room temperature.

Indian J Phys (February 2017) 91(2):169–181

Magnetic, magnetocaloric and thermoelectric properties of nickel doped manganites

A.E.-M.A. Mohamed[ab], Hernando, B.[b], Ahmed, A.M.[a]
[a]*Physics Department, Faculty of Science, Sohag University, Sohag, Egypt*
[b]*Physics Department, Faculty of Science, Oviedo University, Oviedo, Spain*

In this study, we investigate structural, magnetic, magnetocaloric and thermoelectric properties of $La_{0.7}Sr_{0.3}Mn_{1-x}Ni_xO_3$compounds with $0.025 \leq x \leq 0.125$. X-ray diffraction analysis shows the structure transformation from the R-3c rhombohedral to the Pbnm orthorhombic structure with Ni^{2+}doping at $x \geq 0.075$ composites. The dc thermal magnetization measurements reveal the monotonic decrease in both Curie temperature and magnetization values with Ni^{2+}addition. The change in magnetic properties of the studied system is correlated to the ferromagnetism suppression and the antiferromagnetism promotion according to some cooperative intrinsic and extrinsic factors. Results show that Ni^{2+}addition affects the magnetocaloric properties, where it shifts the maximum value of the magnetic entropy change towards lower temperatures with relative cooling power of 88, 105, 47 J/kg for $x = 0.025$, 0.075 and 0.125 composites, respectively. Moreover, it is observed that Ni^{2+}doping increases the absolute value of Seebeck coefficient and decreases hole conduction interval.
Journal of Alloys and Compounds 692, 2017, Pages 381-387

Phase diagram, ac susceptibility and thermoelectric power properties of the $La_{0.90}Li_{0.10-x}Na_xMnO_3$ manganites

H.F. Mohamed
Physics Department, Faculty of Science, Sohag University, Sohag, Egypt

Ac susceptibility and thermoelectric power properties of bulk $La_{0.90}Li_{0.10-x}Na_xMnO_3$ ($0 \leq x \leq 0.10$ at. %, step 0.02 at. %) compounds have been studied. The temperature dependence of the ac susceptibility measurements showed a cusp and shoulder below Curie temperature (T_C) related to a frequency-independent and dependent peak in χ'' (T) curves respectively. Slower spin dynamics and the cluster sizes augment with increases the Na content. In terms of magneto-transport a properties, a peak is observed in vicinity of T_{ms} transition, which it has industrial applications. The thermoelectric power data analyzed at low temperature by the magnon and phonon drag concept, while at high temperature by small polaron conduction mechanism. We found an unexpected correlation of structures in MR (T) and S(T) curves.
Journal of Alloys and Compounds 712 (2017)

Influence of sodium doping on the electrical and magnetic properties of $La_{0.90}Li_{0.10}MnO_3$ manganites

H.F. Mohamed

Physics Department, Faculty of Science, Sohag University, Sohag, Egypt

Monovalent perovskite manganites $La_{0.90}Li_{0.10-x}Na_xMnO_3$ were synthesized by using the solid-state reaction method. The crystal structure analysis presented that the samples are a single-phase rhombohedral ($R3^-c$) structure with no detectable impurity phases. Magnetic measurement showed a cusp at a certain temperature $T_{C/F}$ that gradually disappeared with adding the Na content. The samples undergo ferromagnetic-paramagnetic transition, accompanying the metal-semiconductor transition at T_{ms}. There is irreversible on low field $M(T)_{ZFC}$ and $M(T)_{FC}$ curves which gradual decrease with increasing the Na doping. The resistivity values decreased and the Tms increased as doping of sodium increased. In addition, two-transition temperature Tms appeared just by adding the sodium. In short, the influence of partial substitution of lithium by sodium at A-site cation of lanthanum manganite on its physical properties was studied.

Journal of Magnetism and Magnetic Materials , 424 (2017)44

Effects of annealing temperature and dopant concentration on the structure, optical, and magnetic properties of Cu-doped ZnO nanopowders

S. A. Ahmed[1,2]

[1]Physics Department, Faculty of Science, Sohag University, Sohag 82524, Egypt

[2]Physics Department, College of Arts and Science, Qassim University, P.O. 3137, Unayzah 51911, KSA

This study analyzed the effects of annealing temperature and dopant concentration on the structural, optical, and magnetic properties of Cu-doped ZnO nanopowders. Cu-doped ZnO nanopowders were prepared using a solid-state reaction method. The X-ray diffraction (XRD) results demonstrated that the Cu ions successfully substituted the Zn ions in the hexagonal wurtzite structure of the ZnO nanoparticles. Ultraviolet-visible spectroscopy (UV–vis) measurements revealed that the band gap decreased due to the incorporation of Cu. The photoluminescence (PL) results showed that the intensity of the emissions increased with doping and decreased as the annealing temperature (T_A) increased, which can be attributed to the increase and decrease of the oxygen vacancies (V_O), respectively. The magnetic properties of the ZnO nanopowders were also found to be affected by Cu doping and T_A. The ferromagnetic behavior of the ZnO nanopowders decreased as both the doping concentration and T_A increased. This behavior can be explained by the increase in the antiferromagnetic superexchange interaction along with Cu doping due to the decrease in the distance between the Cu ions and the decrease in V_O, respectively. Thus, the results indicate oxygen stoichiometry and V_O both play a dominate role in the room temperature ferromagnetic response of ZnO nanopowders.

Journal of Materials Science: Materials in Electronics (2017) 28:3733-3739

Effect of Cu- and Mn-doping on the structural, optical, and magnetic properties of $Zn_{0.98}Fe_{0.02}O$ nanopowders

S. A. Ahmed[1,2,*]
[1]*Physics Department, Faculty of Science, Sohag University, Sohag 82524, Egypt*
[2]*Physics Department, College of Arts and Science, Qassim University, P.O. 3137, Unayzah 51911, KSA*

This paper reports on the structural and magnetic properties of $Zn_{0.98-x}Fe_{0.02}(Cu/Mn)_xO$(x=0.0 and 0.02) nanopowders synthesized using a solid-state reaction method. Ultraviolet-visible spectroscopy (UV-vis) measurements demonstrated that the band gap increased in Fe-doped ZnO and decreased in both Cu- and Mn-doped $Zn_{0.98}Fe_{0.02}O$. Photoluminescence (PL) studies confirmed the formation of oxygen vacancies (V_O) in all the samples. The magnetization measurements revealed that the doping of Cu or Mn ions in $Zn_{0.98}Fe_{0.02}O$ increased the saturation magnetization (M_s). The M_s value of the Cu-doped $Zn_{0.98}Fe_{0.02}O$ is about five times larger than that of the undoped ZnO. The M_s value of the Mn-doped $Zn_{0.98}Fe_{0.02}O$ is of a magnitude larger than that obtained for the Cu-doped $Zn_{0.98}Fe_{0.02}O$, and it is about one and a half times larger than the magnitude of the $Zn_{0.98}Fe_{0.02}O$ and seven times larger than the magnitude of the undoped ZnO. We believe that the ferromagnetism (FM) is intrinsic, and it results from the interactions induced by the V_O incorporated into the ZnO lattice.
Journal of Materials Science (2017) 52:4977-4987

Structural, optical, and magnetic properties of Cu-doped TiO_2 samples

S. A. Ahmed[1,2]
[1]*Physics Department, Faculty of Science, Sohag University, Sohag 82524, Egypt*
[2]*Physics Department, College of Arts and Science, Qassim University, P.O. 3137, Unayzah 51911, KSA*

We report here the microstructure, optical, and magnetic properties of Cu-doped TiO_2 ($Ti_{1-x}Cu_xO_2$) nanopowder samples with x=0.02, 0.04, and 0.06 prepared by a solid-state reaction method. XRD studies indicated the incorporation of Cu into the TiO_2 lattice. Ultraviolet-visible spectroscopy (UV–vis) measurements revealed that the band gap decreased due to the incorporation of Cu. Photoluminescence (PL) results showed an enhanced photoluminescence property associated with oxygen vacancies from TiO_2 due to the incorporation of Cu. Magnetic investigations demonstrated that all of the samples had room temperature ferromagnetism (RTFM). RTFM was observed in the $Ti_{0.98}Cu_{0.02}O_2$ samples annealed at 500°C and reduced RTFM was clearly observed in the samples annealed at high temperatures of 600 and 700 ºC. Furthermore, the saturation magnetic moment decreased with increasing Cu content for the samples annealed at 500 ºC with different doping Cu contents, due to the increased Cu atoms occupying neighbouring cation lattice sites, which resulted in an antiferromagnetic configuration. The results demonstrated that defects and/or oxygen vacancies, and the distances between nearest-neighbour Cu atoms, have a significant influence on ferromagnetism in Cu-doped TiO_2 powder samples.
Crystal Research & Technology 52 (2017) 1600335 (8 pages)

Structural, optical, and magnetic properties of Mn-doped ZnO samples

S A Ahmed[a,b,*]

[a]*Physics Department, Faculty of Science, Sohag University, Sohag 82524, Egypt*

[b]*Physics Department, College of Arts and Science, Qassim University, P.O. 3137, Unayzah 51911, KSA*

This study investigated the microstructure, optical and magnetic properties of $Zn_{1-x}Mn_xO$ powder samples with x=0.02–0.08 synthesized by a solid-state reaction route. X-ray diffraction revealed that the cell parameters, a and c, increased with the increase in Mn content, which indicated that Mn ions substitute into the lattice of ZnO. UV–vis measurements revealed that the band gap decreased due to the incorporation of Mn. Photoluminescence studies confirmed the formation of oxygen vacancies (V_O) in all samples. Magnetic measurements revealed that all samples exhibited room temperature ferromagnetism (RTFM), and the average magnetic moment per Mn atom decreased as the Mn content, and annealing temperature (T_A) increased. However, our results indicate that the ferromagnetic property is an intrinsic property of the ZnO:Mn samples due to V_O and/or defects, and it does not originate from any secondary magnetic phase.

Results in Physics 7 (2017) 604–610

Room-temperature ferromagnetism in Co-, Cr-, and V-doped ZnO diluted magnetic semiconductor

S. A. Ahmed [1,2]

[1]*Physics Department, Faculty of Science, Sohag University, Sohag 82524, Egypt*

[2]*Physics Department, College of Arts and Science, Qassim University, P.O. 3137, Unayzah 51911, KSA*

In this study, diluted magnetic semiconductors $Zn_{0.998}TM_{0.002}O$ (TM=Co, Cr, or V) samples were synthesized using the solid-state reaction method. X-ray diffraction measurements indicated that all the samples had a single crystalline wurtzite structure; moreover, no metallic transition metal (TM) or other secondary phases were found. The magnetization measurements showed that all the samples exhibited room temperature ferromagnetism (RTFM) with a saturation magnetization and a coercive field of 2.310 μ_B/Co and ~350Oe, 2.479 μ_B/Cr and ~325Oe, and 2.198 μ_B/V and ~170Oe for Co-, Cr-, and V-doped ZnO, respectively. The structural and magnetic investigations demonstrate that RTFM is an intrinsic property of the samples. Thus, ferromagnetism does not originate from clusters or secondary phases; it is due to the Co/Cr/V:ZnO matrices. This study has shown that very light doping of Co, Cr, or V in ZnO results in appreciable RT ferromagnetic ordering that is useful for spintronic applications.

Appl. Phys. A 123 (2017) 440 (9 pages)

Ferromagnetism in Cr-, Fe-, and Ni-doped TiO_2 samples

S. A. Ahmed[1,2]

[1]*Physics Department, Faculty of Science, Sohag University, Sohag 82524, Egypt*

[2]*Physics Department, College of Arts and Science, Qassim University, P.O. 3137, Unayzah 51911, KSA*

Ferromagnetic Cr-, Fe-, and Ni-doped TiO_2 nanopowder samples (with 0.2% Cr, Fe, or Ni) were synthesized using the solid-state reaction method. The X-ray diffraction pattern showed that all the samples possessed typical anatase structure, and no other impurity phases were observed. Ultraviolet-visible spectroscopy (UV–vis) measurements revealed that the band gap decreased due to the incorporation of Cr, Fe, or Ni. The photoluminescence results showed the presence of oxygen defect related emission peaks in Cr-, Fe-, and Ni-doped TiO_2. Room temperature ferromagnetism is observed in all the Cr-, Fe-, and Ni-doped TiO_2 samples. Saturation magnetic moment is the highest for Fe-doped TiO_2. The Fe:TiO_2 samples were found to have a magnetic moment of 4.58 μ_B/Fe, and they seem to have greater ferromagnetism than the Cr/Ni-doped TiO_2 samples. The structural and magnetic investigations demonstrate that ferromagnetism at room temperature is an intrinsic property of the samples. Thus, ferromagnetism does not originate from clusters or secondary phases; it is due to the Cr/Fe/Ni:TiO_2 matrices. This study has shown that substituting a very light percentage of Cr, Fe, or Ni for Ti in TiO_2 gives rise to appreciable room temperature ferromagnetic ordering useful for spintronic applications.

Journal of Magnetism and Magnetic Materials 442 (2017) 152–157

Effects of Annealing Temperature and Dopant Concentration on the Structural, Optical, and Magnetic Properties of Iron-Doped ZnO Samples

S.A. Ahmed[1,2,*]

[1]*Physics Department, Faculty of Science, Sohag University, Sohag 82524, Egypt*

[2]*Physics Department, College of Arts and Science, Qassim University, P.O. 3137, Unayzah 51911, KSA*

This paper reports on the structural, optical, and magnetic properties of as-prepared and annealed $Zn_{1-x}Fe_xO$ ($0.02 \leq x \leq 0.08$) powders synthesized using the solid-state reaction method. X-ray diffraction (XRD) studies showed that Fe was incorporated into the ZnO lattice. Ultraviolet-Visible (UV-vis) spectrophotometry measurements revealed that the bandgap initially increased and then decreased with Fe doping. Photoluminescence (PL) studies confirmed the formation of oxygen vacancies (V_O) in all of the samples. All of the samples exhibited ferromagnetic behavior at room temperature (RT). Ferromagnetic behavior decreased with increased Fe concentrations, due to the increase in the number of Fe atoms occupying the neighboring cation lattice sites, which resulted in an antiferromagnetic configuration. Ferromagnetic behavior also decreased with the increase in the annealing temperature (T_A) due to the reduction of defects and/or V_O. However, our results indicate that the ferromagnetic property is intrinsic to the ZnO system due to defects and/or V_O, and the extrinsic impurity origin was excluded.

4th Int'l Conference on Chemical, Materials, Mining and Manufacturing Engineering (CM3E-17) Aug. 3-4, 2017 Pattaya (Thailand) pp. 64-70.

Effect of thermal annealing on structural, optical and electrical properties oftransparent Nb_2O_5 thin films

A. A. Attaa, M. M. El-Nahass, A. M. Hassanienc, Khaled M. Elsabawyd, M. M. Abd El-Raheem, F. A. Alhuthali, Sultan E. Alomariy, M. S. Algamdi

We report on the structural, optical and electrical properties of RF sputtered Niobium pentoxide (Nb_2O_5) thinfilms. The structural studies have been carried out using XRD, and AFM techniques. Optical constants such asoptical band gap energy, absorption coefficient, refractive index, complex dielectric constant and optical conductivityhave been estimated for as-deposited and annealed Nb_2O_5 thin films. The estimated direct optical bandgap energy values were found to be E_g^d3.62 eV for the as deposited which = decreases to E_g^d3.07 eV for theannealed films at 973 K. The dispersion curves of the refractive index of Nb2O5 thin films in the optical transparencyregion are explained by using single oscillator and Drude models. The correlations between opticalparameters and the annealing temperature of the Nb_2O_5 thin films are discussed. The DC activation energy hasbeen estimated by using two probe technique.Mott's variable range hopping conduction process (VRH) andsmall-polaron hopping have been used to understand DC electrical conductivity.

Materials Today Communications 13 (2017) 112–118

Study on Transparent Oxides Thin Films Prepared using Sputtering Method

M. M. Abd El-Raheem1و A. A. Atta,A. M. Amry ,Ateyyah M. Al-Baradi1,Sultan E. Alomairy, H. Alkhammash, and S. A. Amin

This work presents the structural and optical features of magnetron Co-sputtered Al–ZnO thin films.The structure of the films have been carried out using by X-ray diffraction (XRD), scan electronmicroscope (SEM) and X-ray fluorescence (XRF). The optical constants of the thin films have beendepicted in the wavelength range 300–2500 nm using spectrophotometric measurements. The opticalband gap of the as-prepared films increases with increasing the content of aluminum. Therefractive index as well as the optical conductivity varies with content of aluminum too.

Journal of Computational and Theoretical Nanoscience, Vol. 14 (2017) 2501–2507

Ellipsometric study of Sb doped ZnO thin films deposited by magnetron co-sputtering method

AMAL-Baradi ,M. M .Abd EL- Raheem, H .Khammash, F.Abdel-Wahab ,S .Aaomairy ,M. A . Alharbi, El-Naggar, A. A. Albasam

In this study, thin films of antimony zinc oxide were prepared at room temperature usingthemagnetronco-sputtering technique. The power on Sb target was varied from zero wattto 20 watt, whereas the power on ZnO target was fixedat100watt. The contents of theconstituents of Sb-ZnO was determined using energy dispersive X-ray (EDX)spectrometry. The structural quality andsurfacemorphology of the films were studiedusing X-ray diffraction (XRD) and scanning electron microscopy (SEM),respectively .Spectroscopic ellipsometery was used to determine the structural and optical properties of polycrystalline Sb-ZnO thin films under test. To evaluate ellipsometric measurements theTauc-Lorenz model was used. The ellipsometric investigation showed, that the opticalband gap decreased with increasing the ratio of Sb. The refractive index showedadecrease withincreasing the content of Sbin addition to its behavior as a normaldispersion.

Digest Journal of Nanomaterials and Biostructure, Vol. 12 (2017) 697-705.

α-Cluster optical potential model ofpions scattering from ^{28}Si

M. El-AzabFarid,A. A. Ebrahim, B. M. Elyan,S. R. Mokhtar, and M. A. El-Zohry

Analysis of $\pi^{\pm}$+ ^{28}Si elastic scattering at energies 21.69, 48.9, 130, 180and 226 MeV and inelastic scattering at energies 130, 180 and 226 MeV leading to the lowest $2^{+}$and 3^{-}states of^{28}Sihas been carried out in the framework of the alpha-clustering single folding model. In the elastic scattering analysis, the real part of the considered potential is taken also in the phenomenological Woods-Saxon form besides the alpha-clustering SF model. Our results are compared with the experimental data and gavea good fit. The values of the extracted reaction cross sections in the two cases are similar to each other. The calculated deformations lengths are similar to those estimated from other studies.

International Journal of New Horizons in Physics Vol. 4, No. 2, 35-41 (2017)

Sonochemically synthesized ZnOnanosheets and nanorods: Annealing temperature effects on the structure, and optical properties

A. Othman, M. A. Osman, E. M. M. Ibrahim, Manar A. Ali

ZnOnanopowders were successfully synthesized by the ice-bath assisted sonochemical method. The nanopowders were annealed in air for 3 h at different annealing temperatures (T_a) ranging from 300 to 700 °C. The effect of T_a on the structural and morphological properties was investigated by the x-ray diffraction (XRD) and the transmission electron microscopy (TEM). The optical properties were studied by recording the optical absorption and photoluminescence (PL) spectra. The XRD analysis showed that the thermal annealing leads to an improvement in the crystallinity associated with an increase in the crystallite size as well as an increase in both the Zn-O bond length and unit cell volume. Also, it was found that the increase of T_a results in a shift in the diffraction angle toward lower values associated with a decrease in the micro-strain. The morphological study confirms that the samples are mixtures of nanosheets and nanorods. In addition, the length and diameter of the nanorods increase as the annealing temperature increases. The optical absorption spectra show that the exciton peak of the as-prepared sample is red shifted from 370 to 378 nm by thermal annealing, and the optical band gap decreases from 3.45 to 3.36 eV. The photoluminescence spectra were reordered at an excitation wavelength of 325 nm, and the deconvolution of the spectra reveals four emission bands where the main UV band (at λ=397 nm) can be attributed to exciton recombination related to near-band-edge. Furthermore, the thermal annealing results in a reduction of the PL intensity of the annealed samples.

Ceramics International, 43, 2017, 527-533

Effect of calcination temperature onmagnetic and electrical properties of $BiFeO_3$ nanoparticles prepared by sol-gel method

E.M.M. Ibrahim, G. Farghal, Mai M. Khalaf, Hany M. Abd El-Lateef

In this work, a BiFeO3 nanoparticle was synthesized by sol–gel method followed by calcination at different temperature 300, 400 and 500 ˚C. Effect of calcination temperature on the structure, morphology, electrical and magnetic properties was studied by using x-ray diffraction, scanning electron microscopy, electrical conductivity measurements and vibrating sample magnetometer, respectively. Structural analysis revealed a typical rhombohedral phase of the prepared BiFeO3 nanoparticles. Scanning electron microscope investigations show that the materials are mesoporous nature with average particle size ~ (52) nm. The magnetic measurement shows significant enhancement of the ferromagnetism with the increasing of the calcination temperature which may be mainly attributed to the crystallinity improvement and the change of the oxygen vacancies content. The DC electrical resistivity measurement was carried out by the two-probe method. The temperature dependence of resistivity behavior shows typical semiconductor features for the synthesized nanoparticles.

J. Nano. Adv. Mat 5, 2017, 1

Sonochemical synthesis, structural inspection and semiconductor behavior of three new nano sized Cu(II), Co(II) and Ni(II) chelates based on tri-dentate NOO imine ligand as precursors for metal oxides

Laila H. Abdel Rahman, Ahmed M. Abu-Dief, Rafat M. El-Khatib, Shimaa Mahdy Abdel-Fatah, A. M. Adam, E. M. M. Ibrahim

Three novel nanosized Cu(II), Co(II) and Ni(II) complexes of imine ligand attained from the condensation of 2-amino-3-hydroxypyridine and 3-methoxysalicylaldehyde have been prepared and investigated using diverse chemical methods such as NMR, CHN analysis, conductance, IR, Spectral studies, TGA and magnetic moment measurements. The obtained data confirmed that the synthesized complexes have metal: ligand ratio of 1:1 and octahedral geometry for Co(II) and Ni(II) complexes. Interestingly, The complexes are used as precursors for producing CuO, Co_2O_3 and NiO nanoparticles by calcination at 500 °C and their structures were described by powder x-ray and transmittance electron microscopy. Furthermore, to investigate the feasibility of using the synthesized materials for semiconductor based nanodevices, the electrical properties of the prepared imine complexes and their corresponding metal oxides were investigated by measuring the electrical conductivity over a temperature range 373-593 K. The data confirm that the materials are semiconductor. The electrical conduction process in the complexes is governed by intermolecular and intramolecular transfer of the charge carriers. But, the conduction mechanism arises from the contribution of the phonon-assisted small polaron hopping in NiO nanoparticles and charge carrier hopping in CuO and Co_2O_3nanoparticles. The results indicate that the complexes under study are promising candidates for wide scale of organic based semiconducting devices.

Applied Organometallic Chemistry

Electrical, thermoelectrical and magnetic properties of approximately 20-nm Ni-Co-O nanoparticles and investigation of their conduction phenomena

E. M. M. Ibrahim, Ahmed M. Abu-Dief, A. Elshafaie, A. M. Ahmed

Understanding the properties of semiconductor nanostructures is important for developing their practical applications in the nanodevices. Although the electrical properties of spinel oxides containing Ni and Co have been studied extensively over the last decades, there is still a significant disagreement on their electrical conduction mechanisms and the distribution of the various charge states of Co and Ni in the octahedral and tetrahedral sites of the spinel crystal lattice. In this study, Co_3O_4, NiO, and mixed Ni-Co oxide nanoparticles (NPs) of ~20 nm are synthesized by co-precipitation method. The mechanism of the electrical conduction in the Co_3O_4 and Ni-Co oxides NPs is due to the hopping process in the octahedral site or between the octahedral and tetrahedral sites while in the NiO NPs, the large polarons conduction mechanism dominates. The thermoelectric power measurements confirm that the Ni-Co oxides NPs are non-degenerate semiconductors and the diffusion mechanism is the dominant component of the Seebeck coefficient. In contrast, the Co_3O_4 NPs show degenerate features with Fermi energy 0.054 eV. The NiO NPs exhibit a transition from non-degenerate to degenerate state. The magnetic measurements reveal an antiferromagnetic-paramagnetic transition at Néel transition temperature. The results are helpful to understanding the fundamental characteristics of the NPs under study.

Materials Chemistry and Physics, 192, 2017, 41-47

Mn-doped ZnOnanocrystals synthesized by sonochemical method: Structural, photoluminescence, and magnetic properties

A.Othman, M. A. Osman,E.M.M. Ibrahim, Manar A. Ali, A. G. Abd-Elrahim

This work reports the synthesis of Mn-doped ZnO nanostructures using ice-bath assisted sonochemical technique. The impact of Mn-doping on structural, morphological, optical, and magnetic properties of ZnO nanostructures is studied. The morphological study shows that the lower doped samples possess mixtures of nanosheets and nanorods while the increase in Mn content leads to improvement of an anisotropic growth in a preferable orientation to form well-defined edge rods at Mn content of 0.04. UV–vis absorption spectra show that the exciton peak in the UV region is blue shifted due to Mn incorporation into the ZnO lattice. Doping ZnO with Mn ions leads to a reduction in the PL intensity due to a creation of more non-radiative recombination centers. The magnetic measurements show that the Mn-doped ZnO nanostructures exhibit ferromagnetic ordering at room temperature, as well as variation of the Mn content can significantly affect the ferromagnetic behavior of the samples.

Materials Science and Engineering: B, 219, 2017, 1-9

Magnetic and DC electric properties of sol–gel-synthesized Ce-doped $BiFeO_3$ nanoflakes

E. M. M. Ibrahim, G. Farghal, Mai M. Khalaf, Hany M. Abd El-Lateef

In this work, $Bi_{1-x}Ce_xFeO_3$ (x = 0.0, 0.04, 0.06, 0.08, 0.1) mesoporousnanoflakes with average thickness 36–122 nm have been synthesized using the sol–gel method. The effect of Ce doping on the structural, morphological, magnetic, and electrical properties was investigated. The samples were characterized by the X-ray diffraction, Fourier transform infrared spectroscopy, transmission electron microscopy, and scanning electron microscopy. The magnetic measurements show that the $Bi_{1-x}Ce_xFeO_3$ nanoflakes have weak ferromagnetic ordering which can be attributed to the oxygen vacancies and Ce^{4+} substitution in the Bi sites. The DC electric transport properties were studied in the temperature range (300–700) K by the two-probe method. The materials show typical semiconductor features and the conduction mechanisms are governed by the hopping process. The Ce doping results in a significant enhancement in the electrical conductivity and the magnetic features of the BFOnanoflakes

Applied Physics A 123, 2017, 533

Optical And Thermoelectric Properties Of Nanocrystalline$Bi_2(Se_{1-x}Te_x)_3$ Films

M.Adam, E.M.M. Ibrahim, L.V. Panina, P.Petkov

Granular nanocrystalline$Bi_2(Se_{1-x}Te_x)_3$ films were prepared from highly crystalline bulk alloys used as source materials by means of thermal evaporation under vacuum (2×10^{-6} mbar). The nanofilms were deposited onto highly cleaned glass substrates of BK7 type. The structural characteristics, including surface morphology, roughness, and crystallite size, were studied by X-ray diffraction (XRD), atomic force microscopy (AFM), and transmission electron microscopy (TEM) analysis. Perfect crystallinity and nanoscalability of the prepared samples were asserted. Transmittance and reflectance spectra of the prepared nanofilms were investigated over the wavelength range of 400–2,700 nm. In the visible light region, all of the films showed an opaque behavior; however, as the wavelength increased into the infrared region, a growing transparency was observed. Based on the measured transmission and reflection spectra, the coefficients of absorbance and extinction as well as the optical band gap were determined. The refractive index was deduced from the reflectance measurements using the determined extinction coefficient. Direct allowed band transitions were confirmed in all films with a band gap energy of 0.85–1.05 eV, depending on the Te content. The possibility of an indirect band gap in the lower photon energy region was discussed. The Seebeck coefficient and electrical conductivity were measured in the temperature range of 300–500 K. Very large values of the power factor of 80 and 131x10^2□W/m.K^2 were obtained for Be_2Se_3 films at room temperature and 473 K, respectively; the latter is three times larger than best previously reported values for similar film systems.

doi.org/10.1080/15567265.2017.1363835

Electric, thermoelectric and magnetic characterization of γ-Fe_2O_3 and Co_3O_4 nanoparticles synthesized by facile thermal decomposition of metal-Schiff base complexes

E. M. M. Ibrahim, Laila H. Abdel-Rahman, Ahmed M. Abu-Dief,A. Elshafaie, Samar Kamel, Hamdan, A. M. Ahmed

Using novel compounds for synthesis of metal oxide nanomaterials can tune their physical properties due to the associated variation in the shape, size and crystallinity. In this work, γ-Fe_2O_3 and Co_3O_4 nanoparticles were successfully prepared by a facile thermal decomposition route, employing $[Fe(C_{32}H_{22}N_4O_2)]\cdot 2H_2O$ and $[Co(C_{16}H_{11}N_3O_4)].12H_2O$ complexes, respectively as new precursors. The x-ray diffraction and high resolution transmission electron microscopy investigation confirmed that the materials consist of highly pure spinel γ-Fe_2O_3 and Co_3O_4 nanoparticles with average size of ~ 9 and 30 nm, respectively. The electrical conduction is governed by the hopping mechanism. The thermoelectric power measurements confirmed that Co_3O_4 nanoparticles are non-degenerate semiconductor with Fermi energy ~1.21 eV while γ-Fe_2O_3 nanoparticles showed a degenerate to non-degenerate transition. The Co_3O_4 nanoparticles showed a weak ferromagnetic ordering that could be attributed to uncompensated surface spins due to finite-size effects. But γ- Fe_2O_3 NPs show superparamagnetic behavior at room temperature.

doi.org/10.1016/j.materresbull.2017.11.002

Thermoelectric materials: a crucial demand for renewable energy production

E. M. M. Ibrahim

Humankind is facing a serious increasing demand for energy. With the decrease in fossil fuels, renewable energy sourceswill be essential for resolving the power crisis in the future. In this respect, thermoelectric materials are crucial in renewable energy conversion technologies to solvethe global energy crisis. Thermoelectric devices are used for the direct conversion of heat to electricity. In principle, these devices can use any thermal source including solar and waste heat.Furthermore, these thermoelectric devices do not have anymoving parts and are thus free of vibration and noise. Current thermoelectric materials exhibit a conversion efficiencyof 5–20%, which can be further enhanced with appropriate strategies such as doping, alloying, and nanostructuring. In thecase of thermoelectric materials, the thermoelectric figure of merit (*ZT*) can be defined by $ZT=\square^2\square/k$where□□ is the electrical conductivity, □ is the Seebeck coefficient, and *k* is the thermal conductivity of the material. For idealthermoelectric materials, *ZT* should be ≥1 to obtain a conversion efficiency of >10%.

The development of superiorthermoelectric materials requires an in-depth understanding of the electron and phonon transport phenomena in suchmaterials. Inorganic materials are classic materials used in thermoelectric research. Some examples include skutterudites,telluride-based materials (e.g., PbTe, Bi_2Te_3, etc.), rare earth chalcogenides (e.g., $La_{3-x}Te_4$), copper ion liquid-like materials(e.g., Cu_2Se), Si–Ge alloys, half-Heusler (HH) alloys, and clathrates. Recently, new classes of materials such as carbon nanomaterials,electronically conducting polymers, and carbon nanomaterial/polymer nanocomposites have been proposed. In the talk, the synthesis, properties, and characterization of various thermoelectric materials includinginorganic materials, organic materials, and nanocomposites will be presented. The physics underlying the thermoelectric responses such as material transport and semiconductor physics will be discussed. The talk will focuseon the dependence of thermoelectric properties of various materials on the synthesis process, crystal structure, grain sizeand grain orientation, morphology, etc. Furthermore, the **The** potential methods of enhancing thermoelectric properties will be presented.

2nd international conference on applied chemistry ICAC2, 25-28 Nov. 2017, Hurghada, Egypt

Surface magnetic properties and giant magnetoimpedance effect in Co-based amorphous ribbons

A. Chizhik [a,*] , V. Vega [b] , Abd El-Moez A. Mohamed [b,c] , V.M. Prida [b] , T. Sanchez [b] , B. Hernando [b] , M. Ipatov [a] , V. Zhukova [a] , A.P. Zhukov [a,d] , A. Stupakiewicz [e] , L. Domínguez [f] , J. Gonzalez [a]

[a]*Department of Materials Physics, Faculty of Chemistry, University of the Basque Country, Manuel de Lardizabal 3, 20018 San Sebastian, Spain*

[b]*Department of Physics, Faculty of Sciences, University of Oviedo, Calvo Sotelo s/n, 33007 Oviedo, Spain*

[c]*Department of Physics, Faculty of Science, Sohag University, 82524 Sohag, Egypt*

[d]*IKERBASQUE Foundation, Bilbao, Spain*

[e]*Laboratory of Magnetism, University of Bialystok, 15-245 Bialystok, Poland*

[f]*Department of Applied Physics I, University of the Basque Country, Plaza Europa s/n, 20018 San Sebastian, Spain*

Correlationship between surface magnetic properties studied using the MOKE technique and giant magnetoimpedance effect (GMI) of nearly-zero magnetostrictive $Co_{66.5}Fe_{3.5}Si_{12.0}B_{18.0}$amorphous ribbons in as-cast state has been investigated in the frequency range of 10 MHz–1.5 GHz. It was found that the surface anisotropy is different in the sides of the ribbon: it is transversal to the ribbon axis with multiple domain walls in one side and axial with a single domain wall in the other. The effect of permanent bias current on surface domain structure was investigated and it was found that the multidomain transversal is very sensitive to the bias current while the axial anisotropy is practically not affected by the applied bias current. This finding can be applied in design of highly sensitive material for magnetic sensors.

Intermetallics, 86, July 2017, Pages 15-19

The effect of Cu on the properties of CdO/Cu/CdO multilayer films for transparent conductive electrode applications

M. Raaif S. H. Mohamed
Physics Department, Faculty of Science, Sohag University, 82524-Sohag, Egypt

Transparent conductive CdO/Cu/CdO multilayerfilms were prepared using rf plasma magnetron sputteringand electron beam evaporation techniques. The CdO layerswere prepared using rf plasma magnetron sputtering, whilethe Cu interlayer was prepared by electron beam evaporationtechnique. The Cu layer thickness was variedbetween 1 and 10 nm. The structural and optical propertiesas well as the sheet resistance of the multilayer films werestudied. X-ray diffraction measurements revealed thepresence of cubic CdO structure and the Cu peak was onlyobserved for the multilayers prepared with 10 nm of Cu. Ithas been observed that the Cu interlayer thickness has agreat influence on the optical and electrical properties ofthe multilayers. The transmittance of the multilayer filmsdecreased while the reflectance increased with increasingCu interlayer thickness. The refractive index and theextinction coefficient of the multilayer films were calculated.The estimated optical band gap values were found tobe decreased from 2.75 ± 0.02 to 2.40 ± 0.02 eV as theCu interlayer thickness increased from 1 to 10 nm. Thesheet resistance was sensitive to the Cu interlayer thicknessand it decreased with increasing Cu interlayer thickness. Asheet resistance of 21.7 Ω/sq, an average transmittance(between 700 and 1000 nm) of 77%, and an optical band gap of 2.5 ± 0.02 eV were estimated for the multilayerfilm with 2 nm Cu layer. The multilayer film with 2 nm Culayer has the highest figure of merit value of3.2 9 $10^{-3}\Omega^{-1}$. This indicates that the properties of thismultilayer film are suitable for transparent conductiveelectrode applications.
Appl. Phys. A (2017) 123:441

Conformity and Homogeneity Indices for Head and Neck Cancer Patients using 3DCRT

Hanan A. Abotaleb[1], Ehab Maarouf[2], F. M. El-Hossary[1], M. Raaif[1]and Mohamed Kelany[4]
[1]*Sohag Armed Forced oncology Center, Sohag, Egypt*
[2]*Department of Radiotherapy and Nuclear Medicine, NationalCancer Institute, Cairo University, Cairo, Egypt*
[3]*Department of Physics, Faculty of Science, Sohag Universityy, Sohag, Egypt*
[4]*Department of Radiotherapy and Nuclear Medicine, El-Demerdash Hospital, Faculty of Medicine, Ain Shams University, Cairo,Egypt*

This study aims to demonstrate the conformity and homogeneity level achieved by 3D conformal radiation therapy for head and neck malignant tumors patients. Conformity and homogeneity indices are good quantitative tools for assessing and comparing the dose conformity and homogeneity of various treatment plans of one patient. In this study fifteen patients with advanced head and neck tumors have been selected. For each patient, five plans were promoted by using four planning techniques which were, Field-in-Field(FIF), Bellinzona, Conpas, Forward-Planned Multi-segments (FPMS) with multiple energies denoted as FPMS (M) and another identical plan of FPMS but with using single energy denoted as FPMS (S).The*CIRT OG*recorded values of 1.46±0.16, 1.47±0.16, 1.52±0.18,1.564±0.20, 1.58±0.21 for FPMS (M), FPMS (S), FIF,Conpas,and Bellinzona respectively. The *HI* recorded values of 0.187±0.014, 0.193±0.011, 0.196±0.031, 0.202±0.017, 0.219±0.02 for FPMS (S), FPMS (M), FIF, Bellinzona, and Conpas, respectively. It has been observed from the results that FPMS technique either using multiple energies or single has the highest conformity andhomogeneity followed by FIF technique. For conformity, Conpas has the thirdrank followed by Bellinzona technique. Forhomogeneity,Bellinzona has the third rank followed by Conpas technique
Sohag J. Sci. 2. No. 2, 19-25 (2017)

The Thermal Properties of Asymmetric Nuclear Matter within the Extended Brueckner–Hartree-Fock Approach

Khaled Hassaneen[1,2] and Hesham Mansour[3]
1Physics Department, Faculty of Science, Sohag University, Sohag, Egypt
2Physics Department, Faculty of Science, Taif University, Taif, KSA
3Department of Physics, Faculty of Science, Cairo University, Giza, Egypt

The single-particle potentials and other properties at absolute zero temperature in isospin asymmetric nuclear matterare investigated in the frame of an extended Brueckner theory. Also thermal quantities are calculated in asymmetricnuclear matter using CD-Bonn potential and the Urbana three-body forces (3BF). Also, the effects of the hole–holecontributions are investigated within the self-consistent Greens function approach. The inclusion of 3BF or the hole–hole contributions improves the predicted saturation property of symmetric nuclear matter within the Brueckner–Hartree–Fock approach and it leads to a significant stiffening of the density dependence of symmetry energy at highdensities but the exact saturation point is not reproduced. This is of great importance in astrophysical calculation. Aphenomenological term simulating the three-body interaction is introduced to assure the empirical saturation property.The hot properties of asymmetric nuclear matter such as the internal energy and the pressure are analyzed using T2-approximation method at low temperatures.
Journal of the Physical Society of Japan 86, 024201 (2017)

Tensor target spin asymmetries in incoherent π^-photoproduction off the deuteron including rescattering effects

E. M. Darwish, H. M. Abou-Elsebaa, E. A. Sultan† and Kh. S. A. Hassaneen†
Physics Department, Faculty of Science, Taibah University, P.O. Box 30002, Al-Madinah Al-Munawarah 41411, Saudi Arabia
Physics Department, Faculty of Science, Sohag University, Sohag 82524, Egypt

Tensor target spin asymmetries $T2M$ (M=0,1,2) in the reaction $\gamma\mathbf{d}\rightarrow\pi^- pp$are studiedfor photon energies from π-threshold up to 1.5 GeV with inclusion of rescatteringeffects. It is shown that the influence of rescattering effects on the tensor target spinasymmetries is sizable in the energy region near π-threshold. At higher energies, muchsmaller influence of rescattering effects is seen. The sensitivity of the obtained results tothe elementary pion photoproduction operator is investigated and a considerable dependenceis found, in particular at forward pion angles. In addition, a comparison withresults of other theoretical models is also given. The extracted spin symmetries arecompared with available experimental data and a qualitative agreement is obtained.The predictions presented here may be useful to interpret the recent measurements fromthe VEPP-3 electron storage ring.
International Journal of Modern Physics E, Vol. 26, No. 10 (2017) 1750059 (17 pages)

Effect of Plasma Surface Treatment on AISI 316LStainless Steel for In-CoreApplications of Nuclear Reactors

F. M. El-Hossary1, S. U. El-kameesy3, M. M. Eissa2, Al-Zahraa A. Abd Elmula1, Aly Saeed4*, Samah A. Al-Shelkamy5

The effect of nitrogen plasma surface treatment on the structural, mechanical, and neutron attenuation properties of AISI316L stainless steel was carried out. The mechanical and rate of plasma treatment results show that the treated N316L stainless steel has superior wear and micro-hardness values than that of the untreated one AISI316L.The experimental measurements of total slow neutron removal cross section Σ*T* were carried out using 241Am-Be neutron source. The results showed that the treated N316L sample has a higher removal cross-section than the untreated AISI316L. The obtained results indicated that the rf plasma surface treatment is an effective method for developing the properties of stainless steel alloys for in-core applications of nuclear reactors.

Proceedings of 4th International Conference on Energy Engineering, Faculty of Energy Engineering - Aswan University -Aswan - Egypt

Optical and thermoelectric properties of nano-particles based $Bi_2(Te_{1-x}Se_x)_3$ thin films

A.M. Adam [a, b], * , E. Lilov [a] , P. Petkov [a]

[a] *Physics Department, University of Chemical Technology and Metallurgy, Sofia, Bulgaria*

[b] *Physics Department, Faculty of Science, Sohag University, Egypt*

Nano-particles of Bi_2Te_3 and $Bi2(Te_{1-x}Se_x)_3$ films were deposited using vacuum thermal evaporation technique from previously prepared bulk alloys synthesized by melting method. Optical and thermoelectric properties were studied in the temperature range of 300-473K. The formation of none- and Se-doped Bi_2Te_3 nano-particles was verified by EDX and XRD analysis. TEM, SEM and AFM analysis showed the prepared films are polycrystalline in nature. The measurements of electrical conductivity and Seebeck coefficient, alongside with thermal conductivity calculations, resulted in the highest values of thermoelectric power at high temperature to be reported. The maximum value of power factor was calculated at 62.82917 mWK^{-2} cm^{-1} for ($Bi_2Se_{0.3}Te_{1.7}$) sample at 463 K. On the addition of Se to Bi_2Te_3 film, a significant decrease of the electronic thermal conductivity (Kel) from 2.181 $x10^{-2}$ to 0.598 $x10^{-2}$ (mW/cm.K) could be achieved. Figure of merit (ZT) calculations showed a maximum value of 0.85 at room temperature, for Bi_2Te_3. Besides the increase of ZT value for all samples at higher temperature, surprisingly, a value of 2.75 for ($Bi_2Se_{1.2}Te_{1.8}$) was obtained. We believe our results could open avenues for new applications.

Superlattices and Microstructures 101 (2017) 609e624

Impacts of thickness reduction and heat treatment on the optical properties of thin chalcogenide films

A.M. Adama,[b,c] , P. Petkovc [a]

[a]*National University of Science and Technology MISiS, Leninsky Prospekt, 4, 119049 Moscow, Russia*

[b]*Physics Department, Faculty of Science, Sohag University, Sohag, Egypt*

[c]*Physics Department, University of Chemical Technology and Metallurgy, Sofia, Bulgaria*

Bi-based chalcogenides, in the form of thin crystalline films, were deposited at different thicknesses onto highly cleaned glass slides with the aid of vacuum thermal evaporation technique. The influence of thermal annealing on the optical properties of Bi_2Te_3-Bi_2Se_3 films at different thicknesses is investigated in this work. Wavelength dependence of the optical transmittance and reflectance was recorded, for the as-prepared and the annealed films, in the wavelength range from 350 to 2700 nm using a double beam spectrophotometer. Fundamental optical properties such as absorption coefficient and energy band gap were derived based on the measured spectra and film's thickness. We demonstrate in the present work that the synergy of annealing and thickness reduction can be exploited for light transmittance enhancements, and consequently for optoelectronic applications including transparent conductive electrodes.

Ceramics International 43 (2017) 11015–11022

Characterization and optical properties of bismuth chalcogenide films prepared by pulsed laser deposition technique

A.M. Adama,[b,c,*] , E. Lilov[a] , V. Lilova[a] , P. Petkov[a]

[a]Physics Department, University of Chemical Technology and Metallurgy, Sofia, Bulgaria

[b]Physics Department, Faculty of Science, Sohag University, Egypt

[c] College of novel materials and nanotechnology, National University of Science and Technology MISiS, 119049, Moscow, Leninsky Prospekt, 4, Russia

Thin films of Bi-based chalcogenides were prepared by pulsed laser deposition (PLD) technique according to the stoichiometric formula: $Bi2(Se_{1-x}Te_x)_3$. Their optical properties were studied aiming to find the suitable area of application and the optimum composition amongst the samples under study. X-ray diffraction analysis proved the crystallinity of the deposited samples; in addition, surface roughness and films homogeneity were studied by atomic force microscopy (AFM) confirming the suitability of PLD technique to prepare homogenous and smooth films of the concerned alloys. Absorption coefficient calculations showed higher absorption values of 5×10^5 and 6×10^5 cm^{-1} for Te contents of 90% and 100% in the $Bi_2(Se_{1-x}Tex)_3$ system respectively. Optical band gap of the concerned films were calculated and found to be in the range of 0.76–1.11 eV, exhibiting comparable values with the previously reported by other authors. Optical studies conformed direct and allowed transitions in all films. Refractive index (n) and dielectric constants (Ɛr) and (Ɛi) were calculated and studied as a function of the wavelength. Values and behavior of (n), (Ɛr) and (Ɛi) indicated strong dependence on the composition and the wavelength range.

Materials Science in Semiconductor Processing 57 (2017) 210–219

Asymmetric nuclear matter and neutron star properties withinthe extended Brueckner theory

Khaled S.A. Hassaneen

Physics Department, Faculty of Science, Sohag University, Sohag, Egypt

Abstract:

Microscopically, the equation of state (EOS) and other properties of asymmetric nuclear matterat zero temperature have been investigated extensively by adopting the non-relativistic Brueckner-Hartree-Fock (BHF) and the extended BHF approaches by using the self-consistent Green's function approach orby including a phenomenological three-body force. Once three-body forces are introduced, the phenomenologicalsaturation point is reproduced and the theory is applied to the study of neutron star properties.We can calculate the total mass and radius for neutron stars using various equations of state at highdensities in β-equilibrium without hyperons. A comparison with other microscopic predictions based onnon-relativistic and density-dependent relativistic mean-field calculations has been done. It is found thatrelativistic EOS yields however larger mass and radius for neutron star than predictions based on nonrelativisticapproaches. Also the three-body force plays a crucial role to deduce the theoretical value of themaximum mass of neutron stars in agreement with recent measurements of the neutron star mass.

Eur. Phys. J. A (2017) 53: 9

Chemistry

Influence of preparation conditions on the catalytic activity of high surface area silica in partial methanol oxidation

Tarek T.Ali[ab], Sulaiman N.Basahel[a], Hatem A.Mahmoud[bc], Kamal M.S.Khalil[b], Katabathini Narasimharao[a]

[a]Chemistry Department, Faculty of Science, King Abdulaziz University, P. O. Box 80203, Jeddah 21589, Saudi Arabia

[b]Chemistry Department, Faculty of Science, Sohag University, Sohag, P.O. Box 82524, Egypt

[c]Chemistry Department, College of Science, University of Hail, Hail 81451, Saudi Arabia

High surface area SiO_2 samples were synthesized by one-step hydrolysis and co-condensation at different pH (between 3.0 and 6.0) using tetraethyl orthosilicate as the Si source and formamide as the drying additive. The effects of the presence of H_2O, formamide and NH_3 solution on the hydrophobic nature, textural properties and catalytic functionality of SiO_2 were investigated. The physico-chemical properties of the samples were measured by XRD, FTIR, SEM, TEM, N_2-physisorption and NH_3-TPD techniques. It was observed that the use of formamide led to the formation of strong Si-O-Si bonds and the samples possessed a high surface area (325–853 $m^2\ g^{-1}$), large pore size (42.5 Å) and large pore volume (0.875 $cm^3\ g^{-1}$). The characterization results also indicated that SiO_2 sample prepared in the absence of water at pH = 3 possessed fewer surface hydroxyl groups, leading the sample to have predominantly hydrophobic nature. An increase in water content in the SiO_2 precursor solutions resulted in an increase in the average particle size with a more hydrophilic nature. All synthesized SiO_2 samples were tested for partial oxidation of methanol at a temperature range of 200–400 °C. The sample synthesized at pH = 3 without water offer 90% conversion at 400 °C; however the SiO_2 sample synthesized with low water content (100 mmol) at pH = 4 offered the best selectivity (83%) to methyl formate and formaldehyde with moderate methanol conversion (72%). The SiO_2 sample prepared at pH = 6 with more water content offered less methanol conversion (60%) and low selectivity toward oxygenated products. It is evident that SiO_2 samples that possessed better textural properties and moderate hydrophobicity performed better in partial methanol oxidation.

Chemical Engineering Journal, 330, 15, 2017, 852-862

Hetarylcyanamides: Synthesis of Novel Thiazole, Triazole and Pyrimidine Derivatives and Prediction of their Biological Activity via PASS Inet

Ahmed Khodairy, Amr H. Moustafa, Walaa W. Ahmed

Department of Chemistry, Faculty of Science, Sohag University, Sohag 82524, Egypt

Some new N-thiazolylaminopyrimidine derivatives 3a,b have been synthesized via the reaction of 1-(4,6- dimethylpyrimidin-2-yl)thiourea 2, obtained via sulfidation of cyanamide 1a with phenacyl bromides. Acid hydrolysis of N-(pyrimidin-2-yl)cyanamides 1b,c gave the corresponding pyrimidinylurea derivatives 4a,b. Reaction of cyanamide 1b with thieno[2,3-b]thiophene derivative 5, at molar ratios (1:1 or 2:1), gave the unexpected thienopyrimidine derivative 6, not the expected bis-thienopyrimidine derivative 7. Triazolylaminopyrimidine derivative 8 has been obtained via the heterocyclization reaction of cyanamide 1b with benzhydrazide. Prediction the activity spectra of synthesized compounds using PASS Inet at Pa > 70%, showing high probability of Mucomembranous protector, Transcription factor STAT inhibitor and Gluconate 2-dehydrogenase (acceptor) inhibitor.

Journal of Pharmaceutical and Applied Chemistry, 3(3), (2017), 267-273

Synthesis and characterization of binary and ternary oxovanadium complexes of *N*,*N*'-(2-pyridyl)thiourea and curcumin. Catalytic oxidation potential, antibacterial, antimicrobial, antioxidant and DNA interaction studies

Mohamed Shaker S. Adam[1,2*], Magdy M. Youssef[1,3], Maha F. Aboelghar[1,4], Usama El-Ayaan[1,3]

[1]Department of Chemistry, College of Science, King Faisal University, P.O. Box 380 Al Hufuf 31982 Al Hassa, Saudi Arabia.

[2]Department of Chemistry, Faculty of Science, Sohag University, Sohag-82534, Egypt.

[3]Chemistry Department, Faculty of Science, Mansoura University, Mansoura 35516, Egypt.

[4]Chemistry Department, Faculty of Science, Cairo University, Giza, Egypt.

Two binary and two ternary mono-oxovanadium (IV) complexes of acetylacetonate, curcumin and N,N'-bis(2-pyridyl)thiourea are synthesized. They are characterized by elemental analysis, IR and UV-Vis. spectra, magnetic and conductivity measurements. The formation constants K_f were determined from the spectrophotometric measurements. The catalytic potential of VO-complexes has been tested by the oxidation of 1-octene by an aqueous H_2O_2 in acetonitrile. They display high catalytic potential for the conversion of 1-octene with low chemoselecticvity to the epoxy product. VO-complexes exhibit good antibacterial and antimicrobial activities. The antioxidant activity of VO-complexes and their ligands has been investigated. VO-complexes exercise high DNA affinity and DNA cleavage ability.

Applied Organometallic Chemistry, 31(7) (2017) aoc.3650.

Synthesis and characterization of binary and ternary oxovanadium complexes of *N*,*N*'-(2-pyridyl)thiourea and curcumin. Catalytic oxidation potential, antibacterial, antimicrobial, antioxidant and DNA interaction studies

Joel T. Magu,[e,a] Shaaban K. Mohamed,[b,c] Mehmet Akkurt,[d] Mohamed Shaker S. Adam,[e] and Farouq E. Hawaiz[f]*

[a]Department of Chemistry, Tulane University, New Orleans, LA 70118, USA, [b]Chemistry and Environmental Division, Manchester Metropolitan University, Manchester M1 5GD, England, [c]Chemistry Department, Faculty of Science, Minia University, 61519 El-Minia, Egypt, [d]Department of Physics, Faculty of Sciences, Erciyes University, 38039 Kayseri, Turkey, [e]Chemistry Department, Faculty of Science, Sohag University, Sohag-82534, Egypt, and [f]Chemistry Department, College of Education, Salahaddin University-Hawler, Erbil, Kurdistan Region, Iraq

The conformation of the title molecule, $C_{16}H_{12}N_2O_3$, is partly determined by an intramolecular C=O···π interaction between one carbonyl group and the five membered ring of the other indolinone moiety. The crystal packing consists of layers parallel to (001) formed by a combination of N—H···O and O—H···O hydrogen bonds and π–π stacking interactions. Both the N—H···O and O—H···O hydrogen bonds generate inversion dimers.

IUCrData, 2 (2017) x170139- x170741

Three Novel Ni(II), VO(II) and Cr (III) Mononuclear Complexes Encompassing Potentially Tri -dentate imine ligand: Synthesis, Structural Characterization, DNA Interaction, Antimicrobial Evaluation and Anticancer Activity

Laila H. Abdel-Rahman[a], Ahmed M. Abu-Dief[a], Maram Basha[b] and Azza A. Hassan Abdel-Mawgoud[a]

[a]*Chemistry Department, Faculty of Science, Sohag University, 82524 Sohag, Egypt*

[b]*Department of Chemistry, Faculty of Science Alfaisaliah Campus, King Abdulaziz University, Jeddah*

Three novel Cr(III),VO(II) and Ni(II) imine complexes derived from the condensation of 2-aminophenol (AP) with 2-hydroxynapthaldehyde (HN) were synthesized. The prepared HNAP imine ligand and its complexes were investigated *via* different physicochemical tools. The results suggest that the parent ligand behaves as dibasic tridentate ONO ligand when coordinated to Cr(III) in octahedral and to Ni(II) in tetrahedral geometry. Where in case of VO(II), it coordinates in distorted square pyramidal geometry. Also, the prepared compounds were screened for their antimicrobial activities on different pathogenic bacteria against some types of bacteria such as *Escherichiacoli(-ve), Bacillus subtilis (+ve)* and *Staphylococcus aureus (+ve)* and some types of fungi such as *Asperagillus niger, Candida glabrata* and *Trichophyton rubrum*. The results indicate that the complexes show a stronger antimicrobial efficiency compared to its pro- ligand. Moreover, the interaction of the prepared complexes with CT-DNA was detected using spectral studies, viscosity and gel electrophoreses measurements. The obtained results clearly demonstrate that, the binding affinity with CT-DNA followed the order HNAPCr > HNAPV > HNAPNi complex. Furthermore, the cytotoxic activity of the prepared compounds on human colon carcinoma cells, (HCT-116 cell line), hepatic cellular carcinoma cells, (HepG-2cell line) and breast carcinoma cells (MCF-7cell line has been examined. From these results it was found that the investigated complexes have potent cytotoxicity against growth of carcinoma cells compared to the corresponding imine pro-ligand.

Appl. Organometal. Chem. 31 (11) e3750 (2017)

Development, Structural investigation, DNA Binding, Antimicrobial Screening and Anticancer Activities of Two Novel Quari-dentate VO(II) and Mn (II) Mononuclear Complexes

Laila H. Abdel-Rahman, Ahmed M. Abu-Dief* and Azza A. Hassan Abdel-Mawgoud

Chemistry Department, Faculty of Science, Sohag University, 82524 Sohag, Egypt

Two novel VO(II) and Mn(II) imine chelates derived from the condensation of o-phenylenediamine (PN) with 3-ethoxysalicylaldehyde(ES) were synthesized. The prepared ESPN imine ligand and its chelates were investigated *via* different analytical and physicochemical tools. Correlation between all the obtained results, the parent ligand behaves as tetra-dentate ONNO ligand and coordinates to Mn(II) and VO(II), in octahedral and square pyramidal geometry, respectively. Also, the prepared compounds were screened for their antimicrobial activities on different pathogenic bacteria and fungi. The results show that the complexes have a stronger antimicrobial activity in comparison with its ligand. Moreover, the interaction of the prepared metal chelates with CT-DNA was detected utilizing spectral studies, viscosity and gel electrophoreses measurements. The obtained results clearly demonstrate that, the binding affinity with CT-DNA for ESPN> ESPNV complex. Furthermore, the cytotoxic activity of the tested compounds on human colon carcinoma cells, hepatic cellular carcinoma cells and breast carcinoma cells has been examined. From these results it was found that the investigated complexes have effective cytotoxicity against growth of carcinoma cells with respect of its imine ligand.

Journal of King Saud University - Science (2017)

DNA Interaction, Antimicrobial, Anticancer Activities and Molecular Docking Study of Some New VO(II), Cr (III), Mn(II) and Ni(II) Mononuclear Chelates encompassing Quaridentate imine ligand

Laila H. Abdel-Rahman[a], Ahmed M. Abu-Dief[a], Moustafa O. Aboelez[b] and Azza A. Abdel-Mawgoud[a]

[a]*Chemistry Department, Faculty of Science, Sohag University-82524, Egypt*

[b]*Department of Pharmaceutical Chemistry, Faculty of Pharmacy, Sohag University, Egypt*

The present study was conducted to synthesis of some new imine Cr(III), VO(II), Mn(II) and Ni(II) complexes derived from the condensation of 2-amino phenol with 2-hydroxynapthaldehyde were synthesized. The prepared HNPN imine ligand was analyzed by its melting point, IR, ^{1}H NMR and ^{13}C NMR spectroscopies. The investigated HNPN imine complexes were characterized by elemental analysis, FT IR, Uv-vis and thermal analysis (TGA) under nitrogen atmosphere from ambient temperature to 750^{o} C. The experimental results revealed that the investigated complexes contain hydrated water molecules. The molar conductance values of complexes are relatively low, indicating the non-electrolytic nature of these complexes. Magnetic susceptibility measurements show that the investigated complexes are paramagnetic. Moreover, the stability constants of the preparing complexes were determined spectrophotometrically. All the complexes were found to be monomeric 1: 1 (M: L) stoichiometry in nature with octahedral geometry for Cr(III), tetrahedral for Mn(II), square planner for Ni(II) and square pyramidal for VO(II). Moreover, the prepared imine ligand and their complexes were evaluated for antimicrobial effect against some types of bacteria such as *Bacillus subtilis (+ve)*, *Escherichia coli (-ve)* and *Staphylococcus aureus (+ve)* and some types of fungi such as *Asperagillus niger, Candida glabrata* and *Trichophyton rubrum*. The results of these studies indicate that the metal complexes exhibit a stronger antibacterial and antifungal efficiency compared to their corresponding imine ligand. Moreover, the interaction of the investigated complexes with CT-DNA was checked using spectral studies, viscosity measurements and gel electrophoreses. The absorption titration studies revealed that each of these complexes is an avid binder to calf thymus-DNA. Also, there was appreciable changes in the relative viscosity of DNA, which is consistent with enhanced hydrophobic interaction of the aromatic rings and intercalation mode of binding. In addition to, the cytotoxic activity of the prepared imine complexes on human colon carcinoma cells, (HCT-116 cell line), hepatic cellular carcinoma cells, (HepG-2 cell line) and breast carcinoma cells (MCF-7 cell line) has cytotoxicity effect against growth of carcinoma cells compared to the clinically used Vinblastine standard. Furthermore, the molecular docking into TRK (PDB: 1t46) was done for the optimization of the investigated compounds as potential TRK inhibitors.

Journal of Photochemistry & Photobiology, B: Biology 170 (2017) 271–285

Detailed Studies of the Alkylation Sides of Pyridin-2-yl and 4,6-Dimethylpyrimidin-2-yl-cyanamides

Shestakov A. S., Moustafa A. H., Bushmarinov I. S., Prezent M. A., Sidorenko O.E.

Chemistry Department, Faculty of Science, Sohag University, Sohag, Egypt

Pyridin-2-yl- and 4,6-dimethylpyrimidin-2-yl-cyanamides entered into an alkylation reaction in the form of sodium salts. Pyridin-2-yl cyanamide 2 was alkylated at endo-nitrogen atom of pyridine ring, while 4,6-dimethylpyrimidin-2-yl cyanamide 1 was effectively alkylated at exo-nitrogen atom of amino cyanamide group. The alkylation of cyanamides 1 and 2 with phenacylbromide gave the corresponding acetophenone derivatives. As a result of their intramolecular cyclization reactions 3-(4,6-dimethylpyrimidin-2-yl)-5-phenyloxazol-2(3H)-imine in the case of cyanamide 1 and 2-amino-3-benzoylimidazo[1,2-a]pyridine in the case of cyanamide 2 were formed. The alkylated derivatives of pyridin-2-ylcyanamide 2 possess visible blue fluorescence with the main peak at 421 – 427 nm.

Journal of Heterocyclic Chemistr, 54(1), 551-560, 2017

Electrical, thermoelectrical and magnetic properties of approximately 20-nm Ni-Co-O nanoparticles and investigation of their conduction phenomena

E. M. M. Ibrahim[1], Ahmed M. Abu-Dief[2],[3] A. Elshafaie[1], A. M. Ahmed[1]

[1]*Physics Department, Faculty of Science, Sohag University, Sohag 82524, Egypt*

[2]*Chemistry Department, Faculty of Science, Sohag University, Sohag 82524, Egypt*

[3]*Departamento de Quimica Organica e Inorganica, Faculad de Quimica, Universdad de Oviedo 33006, Oviedo, Spain*

Understanding the magnetic and electrical transport properties of semiconductor nanostructures is important to developing their practical applications in high-performance nano devices. Although the electrical transport properties of spinel oxides containing Ni and Co have been studied extensively over the last decades, there is still significant disagreement on their electrical conduction mechanism and the distribution of the various charge states of Co and Ni in the octahedral and tetrahedral sites of the spinel crystal lattice. In this study, Co_3O_4, NiO and mixed Ni-Co oxides are synthesized in nanosized scale by co-precipitation method. Variation of the Co/Ni ratios shows no changes in the overall morphology of the nanoparticles. However, the nanoparticles size decreases with increase of the Ni content in the Co_3O_4(24 nm) in direction of the synthesis of pure NiO (18 nm) nanoparticles. The mechanism of the electrical conduction in the Co_3O_4 and Ni-Co oxides nanoparticles is due to hopping process whether between the Ni^{2+} and/or Co^{2+} and the Co^{3+} in the octahedral site or between the octahedral and tetrahedral sites. For NiO nanoparticles, the results indicate that the large polarons conduction mechanism dominates. The thermoelectric power measurements confirm that all the samples are P-type semiconductor. However, the Ni-Co oxides nanoparticles are non degenerate semiconductors and the diffusion mechanism is dominant component of the See beck coefficient. In contrast, the Co_3O_4 nanoparticles show degenerate features with Fermi energy 0.054 eV. The NiO nanoparticles exhibit transition from non-degenerate to degenerate state at 213 K. The plots of the temperature dependence of the magnetic susceptibility reveal a typical antiferromagnetic-paramagnetic transition at Néel transition temperature. The results are helpful to understanding the fundamental characteristics of these nanoparticles and to designing functional nano devices from Co_3O_4, NiO and Ni-Co mixed oxides nanoparticles.

Materials Chemistry and Physics 192 (2017) 41-47

Development and Functionalization of Magnetic Nanoparticles as Powerful and Green Catalysts for Organic Synthesis

Ahmed M. Abu-Dief and Shimaa Mahdy Abdel-Fatah

Chemistry Department, Faculty of Science, Sohag University, 82534Sohag, Egypt

Magnetic nanoparticles are a highly worthy reactant for the correlation of homogeneous inorganic and organic containing catalysts. This review deals with the very recent main advances in the development of various nano catalytic systems by the immobilization of homogeneous catalysts onto magnetic nanoparticles. Catalytic fields include the use of mainly cobalt, nickel, copper, and zinc ferrites, as well as their mixed-metal combinations with Cr, Cd, Mn and sometimes some lanthanides. The ferrite nanomaterials are obtained mainly by co-precipitation and hydrothermal methods, sometimes by the sonochemical technique, micro emulsion and flame spray synthesis route. Catalytic processes with application of ferrite nanoparticles include degradation (in particular photocatalytic), reactions of dehydrogenation, oxidation, alkylation, C–C coupling, among other processes. Ferrite nano catalysts can be easily recovered from reaction systems and reused up to several runs almost without loss of catalytic activity. Finally, we draw conclusions and present a futurity outlook for the further development of new catalytic systems which are immobilised onto magnetic nanoparticles.

Beni-Suef University Journal of Basic and Applied Sciences xxx (2017) xxx–xxx

DNA Binding Ability behaviour, Spectroscopic Studies, Hydrophobicity, and *In Vitro* Antibacterial Evaluation of Some New Fe(II) Complexes Bearing ONO Donors Amino acid Schiff bases

Laila H. Abdel-Rahman, Rafat M. El-Khatib, Lobna A. E. Nassr and Ahmed M. Abu-Dief*
Chemistry Deptartment, Faculty of Science, Sohag University, 82534, Sohag, Egypt

New series of Fe(II) complexes and schiff bases amino acids have been designed and synthesized from the bioactive ligands by condensation of 5-bromo-2-hydroxybenzaldehyde and α-amino acids (L-alanine (ala), L-phenylalanine (phala), L-aspartic acid (aspa), L-histidine (his) and L-arginine (arg)). Elemental analyses, infrared, ultraviolet-visible spectra, as well as conductivity and magnetic susceptibility measurements are used to elucidate the structure of the newly prepared iron(II) complexes. Moreover, the stoichiometry and the stability constants of the prepared complexes have been determined spectrophotometrically. The results suggest that the prepared Schiff base amino acid ligands behave as dibasic tridentate ONO ligands and bind to Fe(II) in octahedral geometry according to the general formula $[Fe(bs:aa)_2].nH_2O$. The DNA interaction of these complexes with was tested at pH = 7.2, by using electronic absorption spectra and viscosity measurements. The experimental results indicated that the investigated complexes could bind to DNA via intercalative mode and showed a different DNA binding according to the sequence: bsari > bshi > bsali > bsasi > bsphali. Moreover, the prepared compounds are tested for their *in-vitro* antibacterial activity against three types of bacteria, *Escherichia coli*, *Pseudomonas aeruginosa* and *Bacillus cereus*. The results show that the metal complexes are more reactive with respect to their corresponding Schiff base ligands.

Arabian Journal of Chemistry, 10, 2, 2017, S1835-S1846

Synthesis, characterization and UV-photocatalytic performance of α-Bi_2O_3 nanorods

Ahmed M. Abu-Dief[a] and W.S.Mohamed[b,*]
[a]*Chemistry Department, Faculty of Science, Sohag University, 82524 Sohag, Egypt*
[b]*Physics Department, Faculty of Science, Sohag University, 82524 Sohag, Egypt*

In this study, Monoclinic bismuth oxide nanorods (α-Bi_2O_3 NRs) were successfully synthesized by a simple one-step hydrothermal route using (water: ethanol) (1:1) as a mixed solvents at optimum conditions. The Bi_2O_3 nano-powder was characterized in detail by different techniques in terms of their structural, morphological, compositional, optical and photocatalytic properties. X-ray diffraction (XRD) analysis indicated that the as-synthesized Bi_2O_3 NRs exhibited high purity with monoclinic structure (α-Bi_2O_3) and good crystallinity. The Transmission electron microscope (TEM) and Energy dispersive X-ray spectroscopy (EDXS) analysis clearly confirmed the high purity and the nanorod morphology of the as-synthesized Bi_2O_3 sample, respectively. The optical band gap of α-Bi_2O_3 NRs was estimated using the UV–Vis Diffuse Reflectance Spectroscopy (UV–Vis DRS) analysis according to the Kubelka-Munk theory. The optical band gap of α-Bi_2O_3 NRs was found to be 3.55 eV for an indirect allowed transition and 3.63 eV for a direct allowed transition. The Fourier transfer infrared spectroscopy (FTIR) was employed to check the structure as well as to evaluate the phonon vibration modes corresponding to Bi_2O_3. Photocatalytic activity of α-Bi_2O_3NRs was investigated using UV source lamp. The as-synthesized α-Bi_2O_3 NRs photocatalyst exhibited better performance for degradation and decolorization of Methylene blue (MB) under ultraviolet (UV) irradiation. MB was completely photodegraded after 210 min under UV irradiation using α-Bi_2O_3 NRs as photocatalyst.

Materials Research Express, 2017, 4 (3), 035039

Reactivity Trends of Hydroxide Ion Attack on High Spin Fe(II) Complexes Including Bromosalcylidene Amino Acid ligands in Some Mixed aqueous Solvents: Gibb's Free Energy of Transfer and Initial-Transition State Analysis

Laila H. Abdel-Rahman, Rafat M. El-Khatib, Lobna A. E. Nassr and Ahmed M. Abu-Dief*

Chemistry Department, Faculty of Science, Sohag University, 82534, Sohag, Egypt

The kinetics of hydroxide ion attack on bis(bromosalicylidene alanate)iron (II) (bsali), bis(bromosalicylidene phenylalanate)iron(II) (bsphali), bis(bromosalicylidene aspartate)iron(II) (bsasi), (bromosalicylidene histidinate)iron(II) (bshi), bis(bromosalicylidene arginate)iron(II) (bsari) have been reported in different binary aqueous solvent mixtures at 298 K. The observed reactivity trends are discussed in terms of the hydrophilic and hydrophobic forms of the complexes investigated, as well as the transfer chemical potentials of hydroxide ion and the complex. Both the solvent–solute and solvent–solvent interactions have been considered. The hydrophobic character of the complexes studied was manifested by decreasing in reactivity. Solvent effect on reactivity trends of the investigated complexes have been analyzed into initial and transition state components by using the transfer chemical potentials of the reactants and the kinetic data of the studied compounds. The decrease in the observed rate constant values (k_{obs}) of the base hydrolysis of the investigated complexes with increasing of solvent % is dominated by the initial state (IS).

Arabian Journal of Chemistry, 10, 2017, S3338-S3346

Crystal structure of 1-[2-(4-nitrophenyl)-4,5-diphenyl-1H-imidazol-1-yl]propan-2-ol

Simpson J., Mohamed S. K., Marzouk A. A., Abdelhamide A. A., Albayati M. R.

Chemistry Department, Faculty of Science, Sohag University, Sohag, Egypt

The title compound, C24H21N3O3, crystallizes with two unique but closely r.m.s. overlay fit = 0.215Å) comparable molecules (1 and 2) in the asymmetric unit of the triclinic unit cell. In molecule 1, the dihedral angles between the central imidazlole ring and the benzene-ring substituents are 42.51(9), 45.41(9) and 56.92(8)°, respectively. Comparable data for molecule 2 are 39.36(10), 34.45(11) and 60.34(8)°, respectively. The rings at the 2-positions carry p-nitro substituents that subtend dihedral angles of 12.9(4)° in molecule 1 and 11.7(4)° in molecule 2 to their respective benzene ring planes. The imidazole rings also have propan-2-ol substituents on the 1-N atoms, which adopt extended conformations for the N-C-C-C chains. In the crystal, classical O-H···N hydrogen bonds combine with C-H···O, C-H···N and C-H···π(ring) hydrogen bonds and stack the molecules along the a-axis direction.

Acta Crystallographica Section E: Crystallographic Communications , 73, 1398-1401, 2017

Synthesis, Characterization, Computational Calculations, Antibacterial and DNA binding activities of Cu(II), Co(II), Ni(II), Fe(II) complexes incorporating glutamine, glutaric and glutamic acid with imidazole derivatives

Laila H. Abdel-Rahman, Ahmed M. Abu-Dief*, Nabawia M. Ismail and Mohamed Ismael
Chemistry Department, Faculty of Science, Sohag University, 82534, Sohag, Egypt

A new series of ternary complexes of Cu(II), Co(II), Ni(II), Fe(II) complexes of glutamine, glutaric and glutamic acid with imidazole derivatives have been synthesized. The nature of bonding and the stereochemistry of the complexes have been deduced from elemental analyses, infrared, electronic spectra, conductivity measurements and thermogravimetric analysis. The structure of $[Co(glu)(imi)_2]$ and $[Fe(glu)(imi)_2(H_2O)_2]$ complexes was validated using quantum mechanics calculations based on accurate DFT methods. Calculations revealed that both complexes had distorted tetrahedral geometry. In case of $[Co(glu)(imi)_2]$, glu ligand was coordinated through the terminal part which consists of carboxylate and amine groups. The formation constants of mixed ligand complexes of copper (II) and nickel (II) with (glutamic- glutamine- glutaric as primary ligands and imidazole or its derivatives as secondary ligands have been determined by pH metric technique at (T = 298 K and c = 1M $NaNO_3$) in aqueous medium. The data obtained were used to evaluate the values of metal- ligand stability constants using Irving-Rossotti titration technique. Mixed ligand complexes studies of these metal ions have been carried pH-metrically at the same conditions. In addition, the interaction of these complexes with (CT-DNA) was investigated at pH = 7.2, by using UV–vis absorption, and viscosity measurements. Results indicated that the investigated complexes strongly bind to calf thymus DNA via intercalative mode. Moreover, the prepared compounds are screened for their in vitro antibacterial activity against two types of bacteria, *Pseudomonas aeruginosa and Bacillus cereus*. In general, based on the data obtained in this study, the synthesized metal complexes might be taken into consideration as promising antibacterial compounds.

Synthesis and Reactivity in Inorganic, Metal-Organic, and Nano-Metal Chemistry, 2017, 47,467-480 .

Corrosion inhibition of carbon steel pipelines by some novel Schiff base compounds during acidizing treatment of oil wells studied by electrochemical and quantum chemical methods

Hany M. Abd El-Lateef*, Ahmed M. Abu-Dief and Mounir A. A. Mohamed
Chemistry Department, Faculty of Science, Sohag University, 82524 Sohag, Egypt

Three novel Schiff bases were prepared and their structures were characterized by X-ray, ^{13}C-NMR, ^{1}H-NMR, mass, UV-Vis, FT-IR, spectral data and elemental analyses. The corrosion inhibition of the investigated inhibitors towards carbon steel in 15% HCl was investigated by using electrochemical measurements (EIS, LPR corrosion rate and Tafel plots), SEM, EDX and quantum chemical methods. The results showed that, the inhibitors are efficient mixed type corrosion inhibitors, and their inhibition performance increased with the rise of inhibitor concentration and temperature. The adsorption of the inhibitors on steel surface was found to obey Langmuir's adsorption isotherm and chemisorption. Quantum chemical calculations provide good support to empirical results.

Journal of Molecular Structure, 2017, 1130, 522-542

Ni(II) and Cu(II) complexes supported by ONNO asymmetrical tetradentate Schiff base ligand: Synthesis, spectroscopic characterization, theoretical calculations, DNA interaction and antimicrobial studies

Laila H. Abdel-Rahman[a], Ahmed M. Abu-Dief*[a], H. Moustafa[b] and Samar Kamel Hamdan[a]

[a]Chemistry Department, Faculty of Science, Sohag University, 82534 Sohag, Egypt

[b]Chemistry Department, Faculty of Science, Cairo University, 12613 Giza, Egypt

A novel Schiff base Z-3-((2-((E)-(2-Hydroxynaphthyl)methylene)-amino)-5-nitro-phenylimino)-1,3-dihydro-indin-2-one (HL) was synthesized from the condensation of 2-hydroxy-1-npathaldehyde and isatin with 4-nitro-o-phenylenediamine. It was structurally characterized on the basis of ^{1}H and ^{13}C NMR, elemental analyses and infrared spectra. In addition to, Ni(II) and Cu(II) complexes of the titled Schiff base ligand (HL) were prepared. The nature of bonding and the stereochemistry of the investigated complexes were elucidated by several techniques using elemental analysis (C, H, N), FT-IR, electronic spectra and molar conductivity. Moreover, thermal behaviors (TGA/DTA) of the complexes were studied and kinetic-thermodynamic parameters were determined by Coats-Redfern method. Density Functional Theory (DFT) calculations at the B3LYP/6-311G++ (d, p) level of theory have been carried out to explain the equilibrium geometry of the ligand. The optimized geometry parameters of the complexes were evaluated using LANL2DZ basis set. The total energy of HOMO and LUMO, Mullikan atomic charges, dipole moment and orientation have been performed and discussed. Moreover, the interaction of metal complexes with calf thymus (CT-DNA) has been explored by electronic spectra, viscosity measurements and gel electrophoresis. The experimental evidences indicated that the two complexes could strongly bind to CT-DNA via an intercalation mechanism. The intrinsic binding constants of the investigated complexes Ni(II) and Cu(II) with CT-DNA were 1.02×10^{6} and 2.15×10^{6} M^{-1}, respectively, which is higher than the standard ethidium bromide. Furthermore, the bio-efficacy of the ligand and its complexes has been examined *in vitro* against the growth of bacteria and fungi to evaluate their antimicrobial potential. Based on the obtained results, the prepared complexes could promise to be used as a drug.

Appl. Organomet. Chem., 2017, 31, e3555

Kinetics, reactivity, initial–transition state analysis and thermodynamic parameters of base-catalyzed hydrolysis of coumalic acid in solvents with different polarities

Ezz A. Abu-Gharib, Rafat M. EL-Khatib, Lobna A. E. Nassr and Ahmed M. Abu-Dief

Chemistry Department, Faculty of Science Sohag University, 82534, Sohag, Egypt

Base-catalyzed hydrolysis of coumalic acid (COU) in binary aqueous-methanol and aqueous-acetone mixtures has been studied kinetically at temperature range from 283 to 313 K. Moreover, the change in the activation energy barrier of COU from water to water–methanol and water–acetone mixtures is estimated from the kinetic data. Solvent effects on reactivity trends have been analyzed into initial and transition state components by using transfer chemical potentials of the reactants and kinetic data. The transfer chemical potentials ($\delta_m\mu^{\theta}$) for COU^{-} anion are derived from solubility data from its calcium, cerium and lanthanum salts. The decrease in rate constant of the base hydrolysis reaction COU as the percentage of methanol or acetone increases is dominated by transition state (TS). The base hydrolysis reaction of COU follows a rate law with $k_{obs}= k_2[OH^{-}]$ and the reaction mechanism was suggested. The high negative values of entropy of activation supports the proposal mechanism, i.e. the investigated reaction takes place via the formation of an intermediate complex. Thus, the ring opening of the intermediate complex would be the rate controlling step.

Arabian journal of Chemistry, 2017, 10, S988–S995

Hydrophobicity, Reactivity trends of Base Catalyzed Hydrolysis of Some Novel High Spin Fe(II) Schiff Base Amino Acid Chelates in Some Binary Aqueous Solvent Mixtures: Initial-Transition State Analysis

Laila H. Abdel-Rahman, Rafat M. El-Khatib, Lobna A. E. Nassr and Ahmed M. Abu-Dief*

Chemistry Department, Faculty of Science, Sohag University, 82534, Sohag, Egypt

Rate constants for the base hydrolysis of bis(naphthylidene alanate)iron (II) (nali), bis(naphthylidene phenylalanate)iron(II) (nphali), bis(naphthylidene aspartate)iron(II) (nasi), (naphthylidene histidinate)iron(II) (nhi), bis(naphthylidene arginate)iron(II) (nari) have been reported in different binary aqueous solvent mixtures at 298 K. The observed reactivity trends are discussed in terms of the hydrophilic and hydrophobic forms of the complexes investigated, as well as the transfer chemical potentials of hydroxide ion and the complex. Both the solvent–solute and solvent–solvent interactions have been considered. The hydrophobic character of the complexes studied was manifested by decreasing in reactivity. Solvent effect on reactivity trends of the investigated complexes have been analyzed into initial and transition state components by using the transfer chemical potentials of the reactants and the kinetic data of the studied compounds. The decrease in the observed rate constant values (k_{obs}) of the base hydrolysis of the investigated complexes with increasing of solvent % is dominated by the initial state (IS).

Journal of Saudi Chemical Society, 2017, 21, S128-S135

Sonochemical synthesis, structural inspection and semiconductor behavior of three new nano sized Cu(II), Co(II) and Ni(II) chelates based on tri-dentate NOO imine ligand as precursors for preparing of metal oxides

Laila H. Abdel Rahman[a], Ahmed M. Abu-Dief [*a], Rafat M. El-Khatib [a], Shimaa Mahdy Abdel-Fatah [a], A. M. Adam[b], E.M.M. Ibrahim[b]

[a]Chemistry Department, Faculty of Science, Sohag University, 82534Sohag, Egypt

[b]Physics Department, Faculty of Science, Sohag University, 82534Sohag, Egypt

Three novel nanosized Cu(II), Co(II) and Ni(II) complexes of imine ligand attained from the condensation of 2-amino-3-hydroxypyridine and 3-methoxysalicylaldehyde have been prepared and investigated using diverse chemical methods such as NMR, CHN analysis, conductance, IR, Spectral studies, TGA and magnetic moment measurements. The obtained data confirmed that the synthesized complexes have metal: ligand ratio of 1:1 and octahedral geometry for Co(II) and Ni(II) complexes. Interestingly, The complexes are used as precursors for producing CuO, Co_2O_3 and NiO nanoparticles by calcination at 500 °C and their structures were described by powder x-ray and transmittance electron microscopy. Furthermore, to investigate the feasibility of using the synthesized materials for semiconductor based nanodevices, the electrical properties of the prepared imine complexes and their corresponding metal oxides were investigated by measuring the electrical conductivity over a temperature range 373-593K. The data confirm that the materials are semiconductor. The electrical conduction process in the complexes is governed by intermolecular and intramolecular transfer of the charge carriers. But, the conduction mechanism arises from the contribution of the phonon-assisted small polaron hopping in NiO nanoparticles and charge carrier hopping in CuO and Co_2O_3 nanoparticles. The results indicate that the complexes under study are promising candidates for wide scale of organic based semiconducting devices.

Applied organometalic chemistry (2017)

Effects of Nd-, Pr-, Tb- and Y-doping on the structural, textural, electrical and N_2O decomposition activity of mesoporous NiO nanoparticles

Bahaa M.Abu-Zied[a] Salem M.Bawaked[b] Samia A.Kosa[b] Tarek T.Ali[b] WilhelmSchwieger[c]Faisal M.Aqlan[b]

[a]Center of Excellence for Advanced Materials Research (CEAMR), King Abdulaziz University, P.O. Box 80203, Jeddah 21589, Saudi Arabia

[b]Chemistry Department, Faculty of Science, King Abdulaziz University, P.O. Box 80203, Jeddah 21589, Saudi Arabia

[c]Institut Für Chemische Reaktionstechnik, Friedrich-Alexander-Universität Erlangen-Nürnberg, Egerlandstraße 3, 91058 Erlangen, Germany

Recently, nickel oxide, NiO, promoted with various dopants showed an interesting activity behavior in N_2O direct decomposition. In this paper, the activity of a series of rare earth (Nd, Pr, Tb and Y) doped NiO catalysts was investigated for this reaction. These catalysts have been prepared by the calcination of their corresponding oxalate mixtures, which have been synthesized via the microwave-assisted precipitation route using oxalic acid as precipitant. Characterization of the obtained catalysts was carried out by using various physico-chemical techniques including TGA, FT-IR, XRD, FE-SEM, TEM, TPR, XPS and electrical conductivity. The results obtained revealed the nanocrystalline nature of the prepared catalysts. Moreover, the presence of the various dopants has led to a noticeable decrease of the NiO crystallites size, mesoporosity development and an increase of its surface area and pore volume. There is a substantial activity increase upon doping NiO with the various rare earth oxides. Such activity increase is associated with the structural modifications as well as the electrical conductivity increase of these catalysts.

Applied Surface Science, 419, 2017, 399-408

Ultra-sensitive Amperometric Hydrazine Sensing via Dimethyl Glyoxomat Derived NiO Nanostructures

Munazza Arain[1], Ayman Nafady[2,3], Abdullah M Al-Enizi[3], Tayyaba Shaikh, Zafar Hussain Ibupoto[1], Syed Tufail Hussain Sherazi, Syeda Sara Hassan, Muhammad Ishaque Abro, Manzoor Iqbal Khattak, Raj Kumar[4]

[1]M.A. Kazi Institute of Chemistry, University of Sindh, Jamshoro, Pakistan

[2]Chemistry Department, Faculty of Science, King Saud University, Riyadh, Saudi Arabia

[3]Chemistry Department, Faculty of Science, Sohag University, Sohag, Egypt

[4]National Centre of Excellence in Analytical Chemistry, University of Sindh, Jamshoro, Pakistan

Here we report the synthesis of NiO nanostructures via glyoxomat assisted precipitation protocol using hydrothermal route under the influence of ammonia followed by annealing at 450 ^{o}C. These nanostructures were characterized via Scanning Electron Microscopy (SEM) and X-ray Diffraction (XRD) method. The morphological investigation of the finally prepared NiO revealed foam-like porous nanostructures. These NiO nanostructures were immobilized onto glassy carbon electrode (GCE) with nafion as binding material and used as highly sensitive and selective sensor for determining hydrazine in the range of 100–500 nM and 600–1600 nM with a calculated limit of detection (LOD) equal to 5 nM. The as prepared sensor was tested for the presence of various interfering species such as Na^{+}, Cu^{2+}, uric acid, hydrogen peroxide and glucose in the presence of equimolar concentration of hydrazine and negligible interference was noticed. The sensor was further tested for hydrazine detection using square wave voltammetry (SWV) however it only worked in the range of 50–1200 μM. Finally the sensor was successfully implemented for hydrazine determination in real water samples using amperometric protocol.

Electroanalysis, 29 (12), 2017, 2803-2809

Structural, Spectroscopic, and Electrochemical Characterization of Semi-Conducting, Solvated $[Pt(NH_3)_4](TCNQ)_2 \cdot (DMF)_2$ and Non-Solvated $[Pt(NH_3)_4](TCNQ)_2$

[a]School of Chemistry, Monash University, Clayton, Vic. 3800, Australia, [b]Chemistry Department, College of Science, King Saud University, Riyadh 11451, KSA, [c]School of Chemistry, University of Melbourne, Melbourne, Vic. 3010, Australia, [d]Current address: Department of Applied Physics, Chalmers University of Technology, Göteborg SE-412 96, Sweden, [e]Materials Engineering, Monash University, Clayton, Vic. 3800, Australia, [f]Current address: Department of Advanced Science and Engineering, Waseda University, Tokyo 169-8555, Japan

The demand for catalysts that are highly active and stable for electron-transfer reactions has been boosted by the discovery that $[Pt(NH_3)_4](TCNQF_4)_2$ ($TCNQF_4$ = 2,3,5,6-tetrafluoro-7,7,8,8-tetracyanoquinodimethane) is an efficient catalyst. In this work, we prepare and characterize the two related $[Pt(NH_3)_4]^{2+}$ complexes, $[Pt(NH_3)_4](TCNQ)_2 \cdot (DMF)_2$ (**1**) and $[Pt(NH_3)_4](TCNQ)_2$ (**2**). Reaction of $[Pt(NH_3)_4](NO_3)_2$ with LiTCNQ in a mixed solvent (methanol/dimethylformamide, 4 : 1 v/v) gives $[Pt(NH_3)_4](TCNQ)_2 \cdot (DMF)_2$ (**1**), whereas the same reaction in water affords $[Pt(NH_3)_4](TCNQ)_2$ (**2**). **2** has been previously reported. Both **1** and **2** have now been characterized by single-crystal X-ray crystallography, Fourier-transform (FT)IR, Raman and UV-vis spectroscopy, and electrochemistry. Structurally, in **1**, the $TCNQ^{1-}$ anions form infinite stacks with a separation between adjacent anions within the stack alternating between 3.12 and 3.42 Å. The solvated structure **1** differs from the non-solvated form **2** in that pairs of $TCNQ^{1-}$ anions are clearly displaced from each other. The conductivities of pressed pellets of **1** and **2** are both in the semi-conducting range at room temperature. **2** can be electrochemically synthesized by reduction of a TCNQ-modified electrode in contact with an aqueous solution of $[Pt(NH_3)_4](NO_3)_2$ via a nucleation growth mechanism. Interestingly, we discovered that **1** and **2** are not catalysts for the ferricyanide and thiosulfate reaction. Li^+ and tetraalkylammonium salts of $TCNQ^{1-/2-}$ and $TCNQF_4^{1-/2-}$ were tested for potential catalytic activity towards ferricyanide and thiosulfate. Only $TCNQF_4^{1-/2-}$ salts were active, suggesting that the dianion redox level needs to be accessible for efficient catalytic activity and explaining why **1** and **2** are not good catalysts. Importantly, the origin of the catalytic activity of the highly active $[Pt(NH_3)_4](TCNQF_4)_2$ catalyst is now understood, enabling other families of catalysts to be developed for important electron-transfer reactions.

Australian Journal of Chemistry 70(9) 997-1005

Easy, one-step synthesis of CdTe quantum dots via microwave irradiation for fingerprinting application

Shalini Singh[a] Ylias M.Sabri[a] Deshetti Jampaiah[a] P.R. Selvakannan[a] Ayman Nafady[b] Ahmad Esmaielzadeh Kandjani[a] Suresh K. Bhargava[a]

[a]Centre for Advanced Materials & Industrial Chemistry (CAMIC), School of Applied Sciences, RMIT University, GPO BOX 2476, Melbourne 3001, Australia

[b]Department of Chemistry, College of Science, King Saud University, Riyadh, Saudi Arabia

A novel one-step microwave irradiation method has been introduced to synthesize 3-mercaptopropionic acid capped CdTe QDs (Quantum dots). The synthesis process required no special conditions such as an inert nitrogen atmosphere but was carried out using TeO_2 (Tellurium oxide) as opposed to the Te powder, Na_2TeO_3 or Al_2TeO_3 usually used for the tellurium source. The characterization of the QDs revealed that they were 2–3 nm in size. The application of aqueous synthesis of capped CdTe QDs for latent fingerprinting was explored and fast turnaround times were achieved.

Materials Research Bulletin, 90, 2017, 260-265

An amperometric sensitive dopamine biosensor based on novel copper oxide nanostructures

Qurrat-ul-ain Baloach[1], Ayman Nafady[2,3], Aneela Tahira[1], Sirajuddin[4], Syed Tufail Hussain Sherazi[4], Tayyaba Shaikh[4], Munazza Arain[4], Magnus Willander[5], Zafar Hussain Ibupoto[1]

[1]Dr. M.A.Kazi Institute of Chemistry, University of Sindh, Jamshoro, Pakistan, [2]Department of Chemistry, College of Science, King Saud University, Riyadh, Saudi Arabia, [3]Chemistry Department, Faculty of Science Sohag University, Sohag, Egypt, [4]National Center of Excellence in Analytical Chemistry University of Sindh Jamshoro, Pakistan, [5]Department of Science and Technology Linkoping University Norrkoping, Sweden

It is highly important to explore the influence of counter anions on the morphology in order to have a desired nanostructure with unique properties. Therefore, in this research work the influence of counter anions on the morphology of copper oxide (CuO) nanostructures is presented using copper chloride and copper acetate salts. A significant role of counter anions on the morphology of CuO nanostructures is observed. The hydrothermal method is used to carry out the synthesis of CuO nanomaterial. The prepared CuO nanostructures are characterized by scanning electron microscopy and X-ray diffraction techniques. The prepared CuO nanomaterial exhibits porous nature with thin nanowires and sponge like morphologies. The dopamine sensing application was carried for exploring the electrocatalytic properties of CuO nanostructures. The presented dopamine biosensor exhibited wide linear range for detection of dopamine from 5 to 40 µM with sensitivity of 12.8 µA mM^{-1} cm^{-2}. The limit of detection and limit of quantification were estimated in order 0.11 and 0.38 µM respectively. The developed dopamine biosensor is highly sensitive, selective, stable and reproducible. The common interfering species such as glucose, ascorbic acid and uric acid showed negligible change in the current when same concentration of dopamine and these interfering species was used. The fabricated biosensor could be used for the determination of dopamine from real blood samples.

Microsystem Technologies, 2017, 23, 5, 1229 - 1235

Co_3O_4@CeO_2 hybrid flower-like microspheres: a strong synergistic peroxidase-mimicking artificial enzyme with high sensitivity for glucose detection

Deshetti Jampaiah[a], T. Srinivasa Reddy[a], Victoria E. Coyle[a], Ayman Nafady[bc], Suresh K. Bhargava*[a]

[a]Centre for Advanced Materials & Industrial Chemistry (CAMIC), School of Applied Sciences, RMIT University, GPO BOX 2476, Melbourne-3001, Australia

[b]Chemistry Department, College of Science, King Saud University, Riyadh, Saudi Arabia

[c]Chemistry Department, Faculty of Science, Sohag University, Sohag 82524, Egypt

In recent years, the development of artificial nanostructured enzymes has received enormous interest in nanobiotechnology due to their advantages over natural enzymes. In the present work, different amounts (5, 10, and 20 wt%) of Co_3O_4 nanoparticle decorated CeO_2 hybrid flower-like microspheres (Co_3O_4@CeO_2) have been investigated for peroxidase-like activity and it was found that 10 wt% of Co_3O_4@CeO_2 exhibited excellent peroxidase-like activity for the catalytic oxidation of the 3,3′,5,5′-tetramethylbenzidine (TMB) substrate in the presence of H_2O_2. The formation of more Ce^{3+} ions associated with the oxygen vacancies and a strong synergistic interaction between CeO_2 and Co_3O_4 may be responsible for the enhanced peroxidase-like activity. Based on their peroxidase activity, Co_3O_4@CeO_2 hybrid microspheres were used for the colourimetric detection of glucose. It was found that Co_3O_4@CeO_2 hybrid microspheres showed a substantial enhancement in the detection selectivity. The limit of detection (LOD) was also improved with a limit as low as 1.9 µM. Thus, we believe that Co_3O_4@CeO_2 hybrid flower-like microspheres with high peroxidase-like activity can be exploited for biosensing applications.

J. Mater. Chem. B, 2017, 5, 720-730

Nanowire Morphology of Mono- and Bidoped α-MnO_2 Catalysts for Remarkable Enhancement in Soot Oxidation

Deshetti Jampaiah[*†], Vijay Kumar Velisoju[†‡], Perala Venkataswamy[§], Victoria E. Coyle[†], Ayman Nafady[ǁ], Benjaram M. Reddy[‡], and Suresh K. Bhargava[*†]

[†]Centre for Advanced Materials & Industrial Chemistry (CAMIC), School of Science, RMIT University, GPO BOX 2476, Melbourne, Victoria 3001, Australia, [‡]Inorganic and Physical Chemistry Division, CSIR-Indian Institute of Chemical Technology, Uppal Road, Hyderabad 500 007, India, [§]Department of Chemistry, Osmania University, Hyderabad 500 007, India, [ǁ]Department of Chemistry, College of Science, King Saud University, Riyadh 11451, Saudi Arabia

In the present work, nanowire morphologies of α-MnO_2, cobalt monodoped α-MnO_2, Cu and Co bidoped α-MnO_2, and Ni and Co bidoped α-MnO_2 samples were prepared by a facile hydrothermal synthesis. The structural, morphological, surface, and redox properties of all the as-prepared samples were investigated by various characterization techniques, namely, scanning electron microscopy (SEM), transmission and high resolution electron microscopy (TEM and HR-TEM), powder X-ray diffraction (XRD), N_2 sorption surface area measurements, X-ray photoelectron spectroscopy (XPS), hydrogen-temperature-programmed reduction (H_2-TPR), and oxygen-temperature-programmed desorption (O_2-TPD). The soot oxidation performance was found to be significantly improved via metal mono- and bidoping. In particular, Cu and Co bidoped α-MnO_2 nanowires showed a remarkable improvement in soot oxidation performance, with its T_{50} (50% soot conversion) values of 279 and 431 °C under tight and loose contact conditions, respectively. The soot combustion activation energy for the Cu and Co bidoped MnO_2 nanowires is 121 kJ/mol. The increased oxygen vacancies, greater number of active sites, facile redox behavior, and strong synergistic interaction were the key factors for the excellent catalytic activity. The longevity of Cu and Co bidoped α-MnO_2 nanowires was analyzed, and it was found that the Cu/Co bidoped α-MnO_2 nanowires were highly stable after five successive cycles and showed an insignificant decrease in soot oxidation activity. Furthermore, the HR-TEM analysis of a spent catalyst after five cycles indicated that the (310) crystal plane of α-MnO_2 interacts with the soot particles; therefore, we can assume that more-reactive exposed surfaces positively affect the reaction of soot oxidation. Thus, the Cu and Co bidoped α-MnO_2 nanowires provide promise as a highly effective alternative to precious metal based automotive catalysts.

ACS Appl. Mater. Interfaces, 2017, 9 (38), pp 32652–32666

Concise synthesis of tetrazole macrocycle

Abdelraheem E. M. M., De Haan M. P., Patil P., , Shaabani, S., Dömling A.

Chemistry Department, Faculty of Science, Sohag University, Sohag, Egypt

A concise two step synthesis of tetrazole containing macrocycles from readily accessible starting materials is presented. The first step comprises a chemoselective amidation of amino acid derived isocyanocarboxylicacid esters with unprotected symmetrical diamines to afford diverse α-isocyano-ω-amines. In the second step, the α- isocyano-ω-amines undergo an Ugi tetrazole reaction to close the macrocycle. Advantageously, this strategy allows short access to 11-19-membered macrocycles in which substituents can be independently varied at three different positions.

Organic Letters, 19(19), 5078-5081, 2017

Fabrication of Highly Sensitive and Selective Electrochemical Sensors for Detection of Paracetamol by Using Piroxicam Stabilized Gold Nanoparticles

Syeda Sara Hassan[a,z], Sallahuddin Panhwar[a], Ayman Nafady[b,c],Abdullah M. Al-Enizi[b], Sirajuddin[d,z], Syed Tufail Hussain Sherazi[d], Muhammad Siddique Kalhoro[e], Munazza Arain[f], Muhammad Raza Shah[g] and M. Younis Talpur[h]

[a]*US.-Pakistan Centers for Advanced Studies in Water (USPCAS-W), Mehran University of Engineering and Technology (MUET), Jamshoro 76062, Sindh, Pakistan*

[b]*Department of Chemistry, College of Science, King Saud University, Riyadh, Saudi Arabia*

[c]*Chemistry Department, Faculty of Science, Suhag University, Suhag, Egypt*

[d]*National Center of Excellence in Analytical Chemistry, University of Sindh, Jamshoro 76080, Pakistan*

[e]*Institute of Physics, University of Sindh, Jamshoro 76080, Pakistan*

[f]*Dr. M. A. Kazi Institute of Chemistry, University of Sindh, Jamshoro 76080, Sindh, Pakistan*

[g]*International Center for Chemical and Biological Sciences, HEJ Research Institute of Chemistry, University of Karachi, Karachi 75270, Sindh, Pakistan*

[h]*Government Muslim Science Degree College, Hyderabad 71000, Sindh, Pakistan*

In this study, a simple, faster and eco-friendly method was used for the synthesis of piroxicam drug derived gold nanoparticles (PX-AuNPs) in aqueous solution. The electrochemical behavior of paracetamol (PAR) was investigated at a PX-AuNPs modified glassy carbon electrode (GCE) by using differential pulse voltrammetry (DPV) in Britton Robinson Buffer solution in strong acidic medium. It showed excellent electrocatalytic activity towards the anodic oxidation of PAR at the peak potential value of 0.66 V and considerable improvement in the peak currents as compared to that observed at the bare GCE. The advantages are related to the unique properties of modified nanosensor such as large surface area, catalytic behavior and hence increased electron transfer abilities compared to GC electrode. The calibration of peak current vs. concentration of PAR was linear in the range of 0.05–12 μM with correlation coefficient R^2 = 0.996 and limit of detection (LOD) of 5 nM. We successfully applied this sensor for determination of PAR in drug samples with a mean recovery of 99.7%. The proposed sensor is simple, novel, rapid, reproducible and sensitive. It can be used as an alternative for chromatography and other voltammetric methods involving mercury electrode. The proposed method could be used for water analysis from pharmaceutical industrial effluents and so on.

***J. Electrochem. Soc.* 2017 volume 164, issue 9, B427-B434**

Impact of porosity and thickness of nano-TiO_2 films on the corrosion protection performance of C-steel in H_2SO_4

Mai Khalaf, Hany M. Abd El-Lateef

Faculty of Science, Chemistry Department, Sohag University, Sohag, Egypt

The current study investigates the improvement in the corrosion protection performance of C-steel after being dip-coated with nano-films from both pure TiO_2 and poly ethylene glycol (PEG) modified TiO_2. Characterization of the deposited TiO_2 films was performed by different techniques. Effect of morphology, porosity, and thickness of the deposited TiO_2 layers were also studied. Results revealed an increased corrosion protection of both coated TiO_2 films as compared to uncoated samples, with pure TiO_2 (without PEG) samples showing higher protection. More- over, increasing the layer thickness of both types of TiO_2 coated films improved the protective properties.

Int J Appl Ceram Technol. 2017; 14: 145–161

Sensitive determination of amlodipine besylate using bare/unmodified and DNA-modified screen-printed electrodes in tablets and biological fluids

Mohamed Khairy,[a*] Ahmed A. Khorshed,[b] Farouk A. Rashwan,[a] Gamal A. Salah,[c] Hanaa M. Abdel-Wadood,[c] Craig E. Banks[d]

[a]*Chemistry Department, Faculty of Science, Sohag University, Sohag 82524, Egypt*

[b]*Department of Pharmaceutical Analytical Chemistry, Faculty of pharmacy, Sohag University, Sohag 82524, Egypt*

[c]*Department of Pharmaceutical Analytical Chemistry, Faculty of Pharmacy, Assiut University, Assiut 71526, Egypt*

[d]*Faculty of Science and Engineering, Manchester Metropolitan University, Chester Street, Manchester M1 5GD, UK*

The screen-printed technique is widely used as an efficient tool for electrochemical analysis in environment, clinical and agri-food areas. Significantly, it has the ability to transfer electrochemical laboratory experiments into the field. In the present work, we report a highly sensitive, simple, low-cost protocol for determination of amlodipine (AML) using bare/unmodified and DNA-modified screen-printed electrodes (SPEs). The immobilization of DNA molecules onto SPE offers promising robust and chemically stable molecular wires, which provides a unique opportunity for charge transfer processes. Consequently, the electroanalytical sensing of AML was explored at bare/unmodified and DNA-modified SPEs in a linear range between 0.066–1.0 μM and 0.066–2.0 μM with the detection limit (3σ) found to be 20.70 nM and 14.94 nM, whilst corresponding sensitivities of: 0.43 A L mol $^{-1}$ and 4.23 A L mol^{-1} respectively. Although, the superior electrochemical signature of bare SPEs is evident, the immobilization of DNA onto SPEs enhances the sensitivity 10-times more than the bare SPEs. Furthermore, the optimized electroanalytical protocol using the unmodified SPEs, which requires no pre-treatment and electrode modification step, was then further applied to the determination of AML in real samples.

Sens. Actuators B 239 (2017) 768–775

Novel Quaternary Ammonium-Based Cationic Surfactants: Synthesis, Surface Activity and Evaluation as Corrosion Inhibitors for C1018 Carbon Steel in Acidic Chloride Solution

Hany M. Abd El-Lateef [1]• Ahmed H. Tantawy[2]• Antar A. Abdelhamid[1]

[1]Chemistry Department, Faculty of Science, Sohag University, Sohag 82524, Egypt [2]Chemistry Department, Faculty of Science, Benha University, Benha, Egypt

A novel class of quaternary ammonium-based cationic surfactants is synthesized and characterized via spectroscopic methods (FTIR, 1 HN M Ra n d 13 C NMR). The surface properties, foaming power and biodegradability of the synthesized cationic surfactants are deter- mined using the surface tension technique. The protection performance with their adsorption mechanisms for carbon steel is evaluated in a 15% HCl solution by a series of techniques including electrochemical impedance spectroscopy, potentiodynamic polarization curves, scanning electron microscopy (SEM), X-ray spectroscopy, and UV–visible spectroscopy. The surfactants are found to be excellent corrosion inhibitors for carbon steel. The results show that the inhibition efficiencies are increased by increasing the concentration and the hydrophobic chain length of the tested com- pounds reaching the maximum at 250 ppm. The potentiodynamic polarization curves suggested that the inhibitors behave as a mixed type with predominant cathodic inhibition and the corrosion behaviour can be explained by the adsorption film mechanism. Moreover, the mode of adsorption obeys the Langmuir adsorption isotherm; also, the adsorbed layer on the surface of the metal is approved by using SEM.

J Surfact Deterg (2017) 20:735–753

Simultaneous voltammetric determination of antihypertensive drugs nifedipine and atenolol utilizing MgO nanoplatelet modified screen-printed electrodes in pharmaceuticals and human fluids

Mohamed Khairy,[a*] Ahmed A. Khorshed,[b] Farouk A. Rashwan,[a] Gamal A. Salah,[c] Hanaa M. Abdel-Wadood,[c] Craig E. Banks[d]

[a]*Chemistry Department, Faculty of Science, Sohag University, Sohag 82524, Egypt*
[b]*Department of Pharmaceutical Analytical Chemistry, Faculty of pharmacy, Sohag University, Sohag, Egypt*
[c]*Department of Pharmaceutical Analytical Chemistry, Faculty of Pharmacy, Assiut University, Assiut, Egypt*
[d]*Faculty of Science and Engineering, Manchester Metropolitan University, Chester Street, Manchester M1 5GD, UK*

Nifedipine and atenolol dugs are conjugated in several anti-hypertensive pharmaceutical formulations. Herein, a reproducible and sensitive voltammetric procedure has been developed for the simultaneous analysis of nifedipine and atenolol for the first time using MgO − nanoplatelets modified screen-printed electrodes (MgO − SPEs) via differential pulse voltammetry (DPV). Two very well-resolved and reproducible signals/oxidation peaks with a voltammetric separation of 0.35 V were obtained in Britton–Robinson (BR) buffer (pH 9). The MgO NPLs are found to exhibit a high electrocatalytic activity and improved voltammetric response compared to unmodified (bare) SPEs. Under optimum pH conditions (pH 9), the DPV curves exhibit linear responses to nifedipine and atenolol over the concentration ranges of 0.2–104.41 μM and 6.66–909.09 μM with detection limits of 0.032 μM and 1.76 μM, respectively. The applicability of the MgO-SPEs is successfully utilized for simultaneous determination of nifedipine and atenolol in pharmaceutical tablets and human urine samples with good accuracy and precision, these results agreeing with independent high-performance liquid chromatography (HPLC).

Sens. Actuators B 252 (2017) 1045–1054

Novel synthesized Schiff Base-based cationic gemini surfactants: Electrochemical investigation, theoretical modeling and applicability as biodegradable inhibitors for mild steel against acidic corrosion

Hany M. Abd El-Lateef[a], Kamal A. Soliman[b], Ahmed H. Tantawy[b]

[a]*Chemistry Department, Faculty of Science, Sohag University, 82524 Sohag, Egypt*
[b]*Chemistry Department, Faculty of science, Benha University, 13518 Benha, Egypt*

Three novel Schiff base compounds were synthesized and characterized using spectroscopic methods (FT-IR, ^{1}H NMR and ^{13}C NMR). Their critical micelle concentrations were determined by conductimetric and surface tension measurements. The inhibition potentials of the prepared surfactants on mild steel corrosion in H_2SO_4 have been investigated using electrochemical and scanning electron microscopy techniques. The results showed that all surfactants are good inhibitors for mild steel corrosion with the percentage inhibition efficiency of up to 99.21% at 1.0 mM. The data showed that the studied surfactants are mixed-type inhibitors. Adsorption of the inhibitors obeyed the Langmuir isotherm. The results obtained from theoretical calculations support our experimental studies

Journal of Molecular Liquids 232 (2017) 478–498

The effects of metallic engineered nanoparticles upon plant systems: An analytic examination of scientific evidence

Thabet Tolaymat[a], Ash Genaidy[b], Wael Abdelraheem[b,c], Dionysios Dionysiou[d], Christian Andersen[e]
[a]U.S. Environmental Protection Agency, Office of Research and Development, Cincinnati, OH 45221, USA
[b]WorldTek Inc., Cincinnati, OH 45249, USA
[c]Chemistry Department, Faculty of Science, Sohag University, Sohag 82524, Egypt
[d]Environmental Engineering Program, University of Cincinnati, Cincinnati, OH 45221, USA
[e]U.S. Environmental Protection Agency, National Health and Environmental Effects Research Laboratory, Corvalis, OR 97333, USA

Recent evidence for the effects of metallic engineered nanoparticles (ENPs) on plants and plant systems was examined together with its implications for other constituents of the Society-Environment-Economy (SEE) system. In this study, we were particularly interested to determine whether or not metallic ENPs have both stimulatory and inhibitory effects upon plant performance. An emphasis was made to analyze the scientific evidence on investigations examining both types of effects in the same studies. Analysis of evidence demonstrated that metallic ENPs have both stimulatory and inhibitory effects mostly in well-controlled environments and soilless media. Nano zero-valent iron (nZVI) and Cu ENPs have potential for use as micronutrients for plant systems, keeping in mind the proper formulation at the right dose for each type of ENP. The concentration levels for the stimulatory effects of Cu ENPs are lower than for those for nZVI. Newer findings showed that extremely smaller concentrations of Au ENPs (smaller than those for nZVI and Cu ENPs) induce positive effects for plant growth, which is attributed to effects on secondary metabolites. Ag ENPs have demonstrated their usage as antimicrobial/pesticidal agents for plant protection; however, precautions should be taken to avoid higher concentrations not only for plant systems, but also, other constituents in the SEE. Further research is warranted to investigate the stimulatory and inhibitory effects of metallic ENPs in soil media in order to broaden the horizon of sustainable agriculture production in terms of higher and safer yields so as to meet the food requirements of human population.
Science of The Total Environment, 579 (2017) 93–106

Magnetic and DC electric properties of sol–gel-synthesized Ce-doped $BiFeO_3$ nanoflakes

E. M. M. Ibrahim[1]•G. Farghal[1]•Mai M. Khalaf[2]•Hany M. Abd El-Lateef[2]
[1]Physics Department, Faculty of Science, Sohag University, Sohag 82524, Egypt
[2]Chemistry Department, Faculty of Science, Sohag University, Sohag 82524, Egypt

In this work, Bi 1-xCe x FeO_3 (x = 0.0, 0.04, 0.06, 0.08, 0.1) mesoporous nanoflakes with average thickness 36–122 nm have been synthesized using the sol–gel method. The effect of Ce doping on the structural, morphological, magnetic, and electrical properties was investigated. The samples were characterized by the X-ray diffraction, Fourier transform infrared spectroscopy, transmission electron microscopy, and scanning electron microscopy. The magnetic measurements show that the Bi1–xCex FeO_3 nanoflakes have weak ferromagnetic order- ing which can be attributed to the oxygen vacancies and Ce^{+4} substitutions in the Bi sites. The DC electric transport properties were studied in the temperature range (300–700) K by the two-probe method. The materials show typical semiconductor features and the conduction mechanisms are governed by the hopping process. The Ce doping results in a significant enhancement in the electrical conductivity and the magnetic features of the BFO nanoflakes.
Appl. Phys. A (2017) 123:533

Effect of Calcination Temperature on Magnetic and Electrical Properties of $BiFeO_3$ Nanoparticles Prepared By Sol-Gel Method

E. M. M. Ibrahim[1] • G. Farghal [1] • Mai M. Khalaf [2] • Hany M. Abd El-Lateef[2]

[1]*Physics Department, Faculty of Science, Sohag University, Sohag 82524, Egypt*

[2]*Chemistry Department, Faculty of Science, Sohag University, Sohag 82524, Egypt*

In this work, a $BiFeO_3$ nanoparticle was synthesized by sol– gel method followed by calcination at different temperature 300, 400 and 500 ˚C. Effect of calcination temperature on the structure, morphology, electrical and magnetic properties was studied by using x-ray diffraction, scanning electron microscopy, electrical conductivity measurements and vibrating sample magnetometer, respectively. Structural analysis revealed a typical rhombohedral phase of the prepared $BiFeO_3$ nanoparticles. Scanning electron microscope investigations show that the materials are mesoporous nature with average particle size ~ (52) nm. The magnetic measurement shows significant enhancement of the ferromagnetism with the increasing of the calcination temperature which may be mainly attributed to the crystallinity improvement and the change of the oxygen vacancies content. The DC electrical resistivity measurement was carried out by the two -probe method. The temperature dependence of resistivity behaviour shows typical semiconductor features for the synthesized nanoparticles.

J. Nano. Adv. Mat. 5, No. 1, 33-39 (2017)

Mechanism of Chicoric Acid Electrochemical Oxidation and Identification of Oxidation Products by Liquid Chromatography and Mass Spectrometry

Emad F. Newair[a], Refat Abdel-Hamid[a], and Paul A. Kilmartin[b]

[a]*Unit of Electrochemistry Applications (UEA), Department of Chemistry, Faculty of Science, University of Sohag, Sohag 82524, Egypt*

[b]*School of Chemical Sciences, University of Auckland Private Bag 92019, Auckland, New Zealand*

Electrochemical oxidation of chicoric acid (ChA) was investigated using cyclic voltammetry and chronoamperometry at a glassy carbon electrode. Chicoric acid generates single quasi-reversible redox wave in cyclic voltammetry over a wide pH range, and an ECEC dimerization mechanism is proposed. Effect of glutathione (GSH) on the electrochemical oxidation of chicoric acid (ChA) was investigated in Britton-Robinson buffer solution. Ultra-high-performance liquid chromatography (UPLC) coupled with mass spectrometry (MS) was used to show that the naturally occurring chicoric acid (ChA) underwent an electrochemical oxidation in the presence of glutathione (GSH) to form mono-, bi-, tri-, and four-glutathione conjugates of chicoric acid and a mono-glutathione conjugate of a chicoric acid dimer. The obtained results are useful for understanding and predicting the oxidative degradation pathway of chicoric acid.

Electroanalysis 2017, 29, 850 - 860

Electrochemical Determination of the Antioxidant Activity in Echinacea Purpurea Roots Using Square Wave Voltammetry

Emad F. Newair[a], Refat Abdel-Hamid[a], and Paul A. Kilmartin[b]

[a]*Unit of Electrochemistry Applications (UEA), Department of Chemistry, Faculty of Science, University of Sohag, Sohag 82524, Egypt*

[b]*School of Chemical Sciences, University of Auckland Private Bag 92019, Auckland, New Zealand*

A simple and rapid electrochemical method was established to quantify the total polyphenol (TP) content and assess their antioxidant activity (AA) in roots of three Echinacea purpurea (E. purpurea) species using square wave voltammetry (SWV). Individual polyphenol components were identified, and then quantified by ultra-high performance liquid chromatography coupled with mass spectrometery (UPLC-MS). Two major polyphenols, chicoric (ChA) and caftaric (CFT) acids, were identified by mass spectroscopy in the extract of E. purpurea samples. The Accuracy of the proposed SWV electrochemical method for TP content and AA analysis was validated by the highly sensitive UPLC-MS technique and standard ABTS method, respectively. A high correlation was noticed between the results, indicating the high sensitivity and reliability of the proposed SWV method for polyphenols analysis and AA evaluation in natural herbal samples.

Electroanalysis 2017, 29, 1131 - 1140

Evaluation of Pt-based alloy/graphene nanohybrid electrocatalysts for triiodide reduction in photovoltaics

Van-Duong Dao[a], Liudmila L. Larina [a,b], Quoc Chinh Tran[a], Van-Tien Bui[ac], Van-Toan Nguyen[a], Thanh-Dong Pham[d], Ibrahim M. A. Mohamed[e,f], Nasser A.M.Barakat[e], Bui The Huy[c,g], Ho-Suk Choi[a]

[a]*Department of Chemical Engineering and Applied Chemistry, Chungnam National University, 220 Gung-Dong, Yuseong-Gu, Daejeon, 305-764, Republic of Korea*

[b]*Department of Solar Photovoltaics, Institute of Biochemical Physics, Russian Academy of Sciences, Kosygin St. 4, 119334, Moscow, Russia*

[c]*Institute of Research and Development, Duy Tan University, Da Nang, Viet Nam*

[d]*Department of Civil and Environmental Engineering, University of Ulsan, Daehakro 93, Namgu, Ulsan, 680-749, Republic of Korea*

[e]*Bionanosystem Engineering Department, Chonbuk National University, Jeonju, 561-756, Republic of Korea*

[f]*Department of Chemistry, Faculty of Science, Sohag University, Sohag, 82524, Egypt*

[g]*Department of Chemistry, Changwon National University, Changwon, 641-773, South Korea*

This work focuses on systematic studies of dissolution engineering for $Pt_{0.9}M_{0.1}$/graphene (M = Au, Co, Cu, Fe, Mo, Ni, Pd, Ru, and Sn) counter electrodes (CEs). The developed nanohybrid materials exhibit higher catalytic activity and electrical conductivity compared with those of Pt/graphene CEs. The results also indicate the improved stability of the developed CEs in iodide electrolyte. Furthermore, the trend in the variation of the reactivity of the PtM alloys agrees well with the concept of density functional theory (one-electron description). An enhancement in the catalytic activity of the developed nanohybrids results from the electronic effect that originates from an upward shift of the platinum *d*-band to the Fermi energy level upon alloying. Thus, the $Pt_{0.9}M_{0.1}$/graphene nanohybrids are cost-effective alternative CE materials to the expensive Pt. The obtained results provide a foundation for enhancing the catalytic activities of CEs for dye-sensitized solar cells (DSCs). The implementation of the $Pt_{0.9}M_{0.1}$/graphene nanohybrids offers significant potential for increasing the efficiency of DSCs.

Carbon 116 (2017), 294-302.

Electrochemical Biosensor Based on Nicotinamide Adenine Dinucleotide/Gold Nanoparticles Composite for Determination of the Antioxidant Activity of Caffeic Acid

Emad F. Newair[a], Refat Abdel-Hamid[a], and Ayman Nafady[a,b]

[a]*Unit of Electrochemistry Applications (UEA), Department of Chemistry, Faculty of Science, University of Sohag, Sohag 82524, Egypt*

[b]*Department of Chemistry, College of Science, King Saud University, Riyadh, Saudi Arabia*

A simple and rapid electrochemical method was established to quantify the total polyphenol (TP) content and assess their antioxidant activity (AA) in roots of three Echinacea purpurea (E. purpurea) species using square wave voltammetry (SWV). Individual polyphenol components were identified, and then quantified by ultra-high-performance liquid chromatography coupled with mass spectrometery (UPLC-MS). Two major polyphenols, chicoric (ChA) and caftaric (CFT) acids, were identified by mass spectroscopy in the extract of E. purpurea samples. The Accuracy of the proposed SWV electrochemical method for TP content and AA analysis was validated by the highly sensitive UPLC-MS technique and standard ABTS method, respectively. A high correlation was noticed between the results, indicating the high sensitivity and reliability of the proposed SWV method for polyphenols analysis and AA evaluation in natural herbal samples.

International Journal of Nanomaterials and Chemistry 2017, 3, 51-58.

Synthesis and Characterization of 2-Pyridinylmethylene-2-quinolyl Hydrazone Cobalt(III) Complexes. Reactivity, Trends and Solvent Effect on the Initial and Transition States of Base Catalyzed Hydrolysis

Ahmad Desoky M. Mohamad

Department of Chemistry, Faculty of Science, Sohag University, Sohag 82534, Egypt

The complexes of pyridine-2-aldehyde-2-quinolylhydrazone Co(III) nitrate $[Co(paqh)_2](NO_3)_2$, methyl-2-pyridylketone-2-quinolinhyrazone Co(III) nitrate $[Co(mpkqh)_2](NO_3)_2$, and phenyl-2-pyridylketon-2-quinolinhyrazone Co(III) nitrate $[Co(ppkqh)_2](NO_3)_2$ were prepared and characterized. Solubilities of Co(III)–hydrazine complexes were measured. Transfer chemical potentials were calculated from the measured solubilities of the Co(III) complexes in aqueous methanol mixtures at 25 ^{O}C. The reactivity trends in the transfer chemical potentials are discussed in terms of the nature of the bonded ligands. Kinetics of the base hydrolysis of Co(III)–hydrazone complexes in the aqueous methanol mixtures have been studied at 25 ^{O}C, and follow the rate law $k_{obs} = k_2[OH^-]$. The solvent effects on the reactivity trends of Co(III) complexes are analyzed into initial state (is) and transition states (ts) components. The reaction rates are reduced by the increase of methanol content. The destabilization of the transition state is remarkable compared to the initial state in the aqueous methanol mixtures. The initial state is more hydrophobic in nature than the transition state for Co(III) complex reactions.

J. Solution Chem. V. 46 (2017) 1575–1595

Simultaneous Voltammetric Determination of Acetaminophen and Isoniazid (Hepatotoxicity-Related Drugs) Utilizing Bismuth Oxide Nanorod Modified Screen-Printed Electrochemical Sensing Platforms

Bahaa G. Mahmoud,[†] Mohamed Khairy,[*,†] Farouk A. Rashwan,[†] and Craig E. Banks[*,‡]

†Chemistry Department, Faculty of Science, Sohag University, 82524 Sohag, Egypt

‡Faculty of Science and Engineering, Manchester Metropolitan University, Chester Street, Manchester M1 5GD, United Kingdom

To overcome the recent outbreaks of hepatotoxicity-related drugs, a new analytical tool for the continuously determination of these drugs in human fluids is required. Electrochemical-based analytical methods offer an effective, rapid, and simple tool for on-site determination of various organic and inorganic species. However, the design of a sensitive, selective, stable, and reproducible sensor is still a major challenge. In the present manuscript, a facile, one-pot hydrothermal synthesis of bismuth oxide ($Bi_2O_{2.33}$) nanostructures (nanorods) was developed. These BiO nanorods were cast onto mass disposable graphite screen-printed electrodes (BiO-SPEs), allowing the ultrasensitive determination of acetaminophen (APAP) in the presence of its common interference isoniazid (INH), which are both found in drug samples. The simultaneous electroanalytical sensing using BiO-SPEs exhibited strong electrocatalytic activity toward the sensing of APAP and INH with an enhanced analytical signal (voltammetric peak) over that achievable at unmodified (bare) SPEs. The electroanalytical sensing of APAP and INH are possible with accessible linear ranges from 0.5 to 1250 μM and 5 to 1760 μM with limits of detection (3σ) of 30 nM and 1.85 μM, respectively. The stability, reproducibility, and repeatability of BiO-SPE were also investigated. The BiO-SPEs were evaluated toward the sensing of APAP and INH in human serum, urine, saliva, and tablet samples. The results presented in this paper demonstrate that BiO-SPEs sensing platforms provide a potential candidate for the accurate determination of APAP and INH within human fluids and pharmaceutical formulations.

Anal. Chem., 89 (2017) 2170–2178

Synthesis and characterization of silica nanostructures for cotton leaf worm control

Haytham A. Ayoub,[1,2] Mohamed Khairy,[1] Farouk A. Rashwan,[1] Hanan F. Abdel-Hafez[2]

[1]Chemistry Department, Faculty of Science, Sohag University, Sohag 82524, Egypt

[2] Plant Protection Research Institute, ARC, Dokki, Giza, Egypt

Herein, silica nanostructures with various physicochemical characteristics were synthesized via surfactant-assisted methods. Potent entomotoxic effects of silica nanostructures were explored against cotton leaf worm (Spodoptera littoralis) for the first time by utilizing surface contact and feeding bioassay protocols. The mortality of the treated larvaes by surface contact was faster than feeding bioassay method. The results showed that the surface characteristics and particle size of silica nanostructures could effectively control their entomotoxic effects compared to commercial silica or even organic pesticides. It was also observed that the dead bodies of the insects became extremely dehydrated due to the damage of insect cuticular water barrier as a result of abrasion. Furthermore, the physical mode of action of silica nanostructures makes insects is unlikely to become physiologically resistant; hence, silica nanostructures can be efficiently used as a valuable tool in S. littoralis management programs.

J Nanostruct Chem 7 (2017) 91–100

Two selective HPTLC methods for determination of some angiotensin II receptor antagonists in tablets and biological fluids

Gamal A. Salah,[1] Hanaa M. Abd El-Wadood,[1] Mohamed Khairy,[2] Ahmed A. Khorshed[1,3]

[1]*Department of Pharmaceutical Analytical Chemistry, Faculty of Pharmacy, Assiut University, Assiut, Egypt*

[2]*Department of Chemistry, Faculty of Science Sohag University, Sohag, Egypt*

[3]*Department of Pharmaceutical Analytical Chemistry, Faculty of Pharmacy, Sohag University, Sohag, Egypt*

Two simple, selective, precise and highly sensitive high-performance thin-layer chromatography (HPTLC) methods have been developed and validated for analysis of five angiotensin II receptor antagonists, namely losartan, irbesartan valsartan, candesartan and olmesartan, which are widely used in clinical practice. HPTLC of the drugs was performed on pre-coated silica gel HPTLC plates 60 F254 by development using a mobile phase composed of chloroform–acetone–glacial acetic acid (7.8:1.5:0.7m v/v/v), which was suitable for all of the studied drugs. The first method depended on utilizing reflectance/fluorescence mode for detection while the second method depended on using 2,3,5,6-tetrachloro-1,4-benzoquinone as spraying reagent for the first time to form orange spots scanned at 460 nm. A good linear relationship was obtained over the concentration ranges of 1.2–60 and 360–3000 ng/band while detection and quantification limits were in the ranges of 0.07–0.43, 45.2–140.49 and 0.21–1.29, 137.05–425.74 ng/band for reflectance/fluorescence and reflectance/absorbance methods respectively. The developed methods were applied successfully for their determination in tablets and spiked human plasma for reflectance/fluorescence method with good accuracy and precision, and so can be applied in the pharmacokinetic and bioavailability studies.

Biomedical Chromatography, 2017; e3916

Synthesis of iron oxides nanoparticles with very high saturation magnetization form TEA-Fe(III) complex via electrochemical deposition for supercapacitor applications

Mahmoud Elrouby, A.M. Abdel-Mawgoud, Rehab AbdEl-Rahman

Sohag University, Faculty of Science, Chemistry Department, Sohag, 82524, Egypt

This work is devoted to the synthesis of magnetic iron oxides nanoparticles with very high saturation magnetization to be qualified for supercapacitor applications using, a simple electrodeposition technique. It is found that the electrochemical reduction process depends on concentration, temperature, deposition potential and the scan rate of potential. The nature of electrodeposition process has been characterized via voltammetric and chronoamperometric techniques. The morphology of the electrodeposits has been investigated using scanning electron microscopy (SEM) and transmission electron microscopy (TEM). The structure and phase content of these investigated electrodeposits have been examined and calculated. The obtained iron oxides show a high saturation magnetization (Ms) of about 229 emu g^{-1}. The data exhibited a relation between Ms of electrodeposited iron oxide and specific capacitance. This relation exhibits that the highest Ms value of electrodeposited iron oxides gives also highest specific capacitance of about 725 Fg^{-1}. Moreover, the electrodeposited iron oxides exhibit a very good stability. The new characteristics of the electro synthesized iron oxides at our optimized conditions, strongly qualify them as a valuable material for high-performance supercapacitor applications.

Journal of Molecular Structure, 1147 (2017) 84-95.

Electrochemical Characterization and Electrode kinetics for Antimony Electrodeposition from its Oxychloride Solution in the Presence of Tartaric Acid

Vusala Asim Majidzade[a], Parvin Heydar Guliyev[b], Akif Shikhan Aliyev[a], Mahmoud Elrouby[c]*, Dilgam BabirTagiyev[a]

[a]*Institute of Catalysis and Inorganic Chemistry, Azerbaijan National Academy of Sciences, AZ1143 Baku, Azerbaijan*

[b]*Nakhchivan State University, AZ7012 Nakhchivan, Azerbaijan*

[c]*Chemistry Department, Faculty of Science, Sohag University, 82524 Sohag, Egypt*

This work is devoted to investigate the process of the electrochemical deposition of antimony from antimony oxychloride solution in the presence of tartaric acid in aqueous media. The kinetics and the mechanism of the electrodeposition process at the electrode surface are studied and proposed by the aid of cyclic, linear sweep voltammetric and chronoamperometric characterization methods. It is found that, the process is affected by the presence of tartaric acid and some factors during the electro-reduction process. The results also show that, the temperature, the potential sweep rate and the concentration of antimony have a great influence on the achievement of the electrodeposition process. Some important parameters are calculated such as, the activation energy of the electrochemical reaction, the diffusion coefficient and the number of saturated nucleation sites. The electrodeposited film is examined using X-ray diffraction, scanning electron microscopy and Energy Dispersive Spectroscopy.

Journal of Molecular Structure, 1136 (2017) 7-13

High Surface Area Nanostructured Activated Carbons Derived from Sustainable Sorghum Stalk

Kamal M.S.Khalil,[a] Omar A. S. Allama,[b] Mohamed Khairy,[a] Khaled M. H. Mohammed,[a] Rafat M. Elkhatib[a] and Mervat A. Hamed[b]

[a]*Chemistry Department, Faculty of Science, Sohag University, Sohag 82524, Egypt*

[b]*Agricultural Research Center, ARC, Ministry of Agriculture, Giza, Egypt*

The Durra (Sorghum) stalk was employed as a novel precursor for the formation of high surface area activated carbons (ACs) by utilizing $ZnCl_2$ as activating agent followed by pyrolysis in a flow of N_2 gas. The formation of ACs has been investigated at different pyrolysis temperatures (400, 500 and 600 °C) and different $ZnCl_2$ impregnation concentrations. The results indicated that, the AC could be formed with high carbon contents, good thermal stability, large specific surface areas in the range of 1200–1817 m^2/g and nanostructured in graphene-like layers of 5–6 nm in thickness. In addition, textural flexibility (in terms of supermicro/meso porosity) of the produced ACs can be fine-tuned by pyrolysis conditions. The potential application of ACs was tested towards the removal of hazardous cationic dye, methylene blue (MB), in aqueous media. The adsorption isotherms and kinetics of MB on ACs were examined at 25 °C. The ACs showed a high adsorption capacity, as high as 386 mg^2/g. The adsorption of MB was better described by the Langmuir isotherm model and followed the pseudo-second-order equation. In light of the vast availability of durra stalks, as a sustainable residual, non-food/non-feed biomass material and quality of the produced AC materials. The presented ACs are very promising materials for application in many adsorption and purification processes.

Journal of Molecular Liquids, 247 (2017) 386-396.

The common, different and unique effects of metallic engineered nanomaterials: an analytic perspective

Thabet Tolaymat[1], Ash Genaidy[2], Wael Abdelraheem[2,3,4], Dionysios Dionysiou[4], Amro El Badawy[2]

[1]Office of Research and Development, U.S. Environmental Protection Agency, Cincinnati, OH, USA

[2]WorldTek Inc, Cincinnati, OH, USA

[3]Chemistry Department, Faculty of Science, Sohag University, Sohaˆg 82524, Egypt

[4]Environmental Engineering Program, University of Cincinnati, Cincinnati, OH 45221, USA

From regulatory perspectives, there has been a debate in the scientific literature as to whether or not metallic engineered nanomaterials (ENMs) should be treated as new chemicals in terms of their toxic effects upon biological species. This debate has prompted us to examine the scientific evidence to validate those paradoxical claims. Investigations covering the effects of metallic ENMs and metal-based ions in the same study were included in this research. The findings reported herein suggest that the different arguments are valid if a wider perspective takes into account the common, different and unique effects of metallic nanoparticles versus metal-based ions. This perspective has been evident from investigations of aquatic (lower organisms such as Daphnia magna and higher organisms like zebra fish) and other organisms (e.g., microbes, nematodes, animal and human cells). It is suggested that the regulation of metallic nanomaterial-based products be transformed to a tier-based approach as a function of the common, different and unique effects to manage the complexity brought into light due to the infinite combinations of the particle physical–chemical properties.

Clean Techn Environ Policy, 19 (2017) 1487-1507

Analysis of metallic and metal oxide nanomaterial environmental emissions

Thabet Tolaymat[a] , Amro El Badawy[b], Ash Genaidy[b], Wael Abdelraheem[b,c], Reynold Sequeira[b]

[a]U.S. Environmental Protection Agency, Office of Research and Development, Cincinnati, OH, USA

[b]WorldTek Inc, Cincinnati, OH, USA

[c]Chemistry Department, Faculty of Science, Sohag University, Sohag, 82524, Egypt

The current study presents evidence on metallic and metal oxide engineered nanomaterial (ENM) emissions into the environment and an analytic perspective of the outcomes of evaluated studies with respect to different individual end points along the lifecycle trajectory. The key findings suggest that 1) the published literature on emissions of metallic ENMs is limited in both the number and information available on the characteristics of emitted ENMs; 2) the studies are classified as experimental and computational studies focused on predicting ENM emissions; 3) the majority of studies investigated ENM emissions during nanomaterial use and waste management, followed by raw material manufacturing, and finally, nano-enabled product manufacturing; 4) the studies primarily reported the concentration/ quantity of emitted ENMs, whereas the physicalechemical characteristics of emitted ENMs were rarely measured or reported; and 5) the published literature primarily focused on emissions of silver and titanium dioxide ENMs and lacked similar information on other surging metallic and metal oxide ENMs such as nano-zero valent iron (nZVI), aluminum (Al), and aluminum oxide (Al2O3) ENMs. The evidence suggests that emitted nanoparticles into the air cover a wide range of concentrations below and above the allowable occupational exposure limits. The concentrations of nanoparticles in water systems are considered in the toxic to very toxic range for a variety of biological species. Given the critical gaps in knowledge, one cannot read across different sources of emissions for metallic and metal oxide ENMs hampering efforts with respect to understanding realistic scenarios for transformations in the natural environment and biological media.

Journal of Cleaner Production, 143 (2017) 401–412

Physicochemical and photo-electrochemical characterization of novel N-doped nanocomposite ZrO_2/TiO_2 photoanode towards technology of dye-sensitized solar cells

Ibrahim M. A. Mohamed[a,d], Van-Duong Dao[b], Ahmed S.Yasin [a], Hamouda M. Mousa[a,e], Mohamed A. Yassin[a], Muhammad Yasir Khan[f], Ho-SukChoi[b], Nasser A.M. Barakat[a,c]

[a]*Bionanosystem Engineering Department, Chonbuk National University, Jeonju 561-756, Republic of Korea*
[b]*Department of Chemical Engineering & Applied Chemistry, Chungnam National University, 220 Gung-Dong, Yuseong-Gu, Daejeon 305-764, Republic of Korea*
[c]*Chemical Engineering Department, Faculty of Engineering, Minia University, El-Minia, Egypt*
[d]*Department of Chemistry, Faculty of Science, Sohag University, Sohag 82524, Egypt*
[e]*Department of Engineering Materials and Mechanical Design, Faculty of Engineering, South Valley University, Qena 83523, Egypt*
[f]*Department of Chemical Engineering, University of Karachi, Karachi, Pakistan*

This work introduces the synthesis of N-doped nanocomposite of ZrO_2/TiO_2nanofibers (NFs) by use of both electrospinning and hydrothermal methods. The physicochemical properties of the introduced TiO_2 NFs are investigated to describe the morphology, crystallinity and chemistry through FESEM, SEM-EDX, XRD, TEM and XPS. As the results, the investigated material can be described as $N@ZrO_2/TiO_2$NFs. The crystal structure of the prepared TiO_2 is only anatase structure. Then, the novel NFs are utilized to design novel photoanode and photo-electrochemical characterization such as current-potential response under light, incident photon-to-current efficiency (IPCE) and electrochemical impedance spectroscopy (EIS) of the dye-sensitized solar cell (DSC) are also investigated. The photovoltaic response showed that the efficiency of the DSCs employed $N@ZrO_2/TiO_2$ photoanode gave 4.95%, which was higher than those of DSCs designed with ZrO_2/TiO_2 NFs (4.51%) and $N@TiO_2$ NFs (4.41%) photoanodes. The high photo-response of DSC by use of $N@ZrO_2/TiO_2$ NFs can be attributed to enhanced electrical conductivity, which is studied via EIS, and presence of active sites of N. These active sites can easily absorb dye-molecules in the step of dye-loading in the fabrication of DSC.

Materials Characterization 127(2017), 357-364.

A regioselective and convenient one-pot multicomponent synthesis of 9-amino-3,5-diaryl-4,9-dihydro-5H-[1,2,4]triazolo[5,1-c] [1,2,4] triazepine-8-thiol

Moustafa, A. H., Amer, A. A.

Chemistry Department, Faculty of Science, Sohag University, Sohag, Egypt

An efficient and environment-friendly procedure for the synthesis of a new series of nitrogen bridge-head [1,2,4]triazolo[5,1-c] [1,2,4]triazepine derivatives through one-pot three-component reaction of polyfunctional triazole with aromatic aldehydes and acetophenone derivatives using alcoholic sodium hydroxide solution. The same new products were prepared in classical route through reaction of triazole with the corresponding chalcones under the same conditions.

Synthetic Communications, 47(11), 1102-1109, 2017

Fabrication of N-doped &SnO_2-incorporated activated carbon to enhance desalination and bio-decontamination performance for capacitive deionization

Ahmed S.Yasin[a], Jongku Jeong[b], Ibrahim M.A.Mohamed[a,c], Chan HeePark[a,b], Cheol Sang Kim[a,b]
[a]Bionanosystem Engineering Department, Chonbuk National University, Jeonju 561-756, Republic of Korea
[b]Division of Mechanical Design Engineering, Chonbuk National University, Jeonju, Jeonbuk 561-756, Republic of Korea
[c]Department of Chemistry, Faculty of Science, Sohag University, Sohag 82524, Egypt

Herein, nitrogen-doped tin oxide intercalated activated carbon nanocomposite (N-AC/SnO_2) were prepared using hydrothermal strategy and explored as an electrode for capacitive desalination and disinfection. Although tin oxide (SnO_2) has good characteristics, the nitrogen must be carefully considered for modifying the characteristics of the carbonaceous materials to improve the performance as an electrode in the CDI process. The characterization of the proposed materials which investigated by XRD, TEM, FE-SEM, XPS and FT-IR affirmed the formation of the nanocomposite. The electrosorption behavior investigated by electrochemical techniques demonstrates that, compared to the specific capacitance of the AC and AC/SnO_2 (207.46 F g^{-1} and 233.21 F g^{-1}), that of the N-AC/SnO_2 is higher at 408.8 F g^{-1}, and N-AC/SnO_2 exhibits better electrical conductivity. The CDI performance evaluated by batch mode experiments through an applied voltage of 1.2 V in a 50 mg L^{-1} NaCl aqueous solution shows that the N-AC/SnO_2 electrode introduces a higher electrosorptive capacity of 3.42 mg g^{-1}, an enhanced desalination efficiency of 61.13%, and good antibacterial performance. Overall, the present study demonstrates that N-AC/SnO_2 has considerable potential as an electrode material for CDI application.
Journal of Alloys and Compounds 729 (2017), 764-775.

ZrO_2 nanofibers/activated carbon composite as a novel and effective electrode material for the enhancement of capacitive deionization performance

Ahmed S.Yasin[a], M. Obaid[a,b], Ibrahim M.A.Mohamed[a,c], Ahmed Yousef[a], Nasser A M Barakat[a,b]
[a]Bionanosystem Engineering Department, Chonbuk National University, Jeonju 561-756, Republic of Korea
[b]Chemical Engineering Department, Faculty of Engineering, El-Minia University, El-Minia, Egypt
[c]Department of Chemistry, Faculty of Science, Sohag University, Sohag 82524, Egypt

Among the various forms of carbon materials, activated carbon still possesses the maximum attention as an optimum commercially available, cheap, and effective electrode material for the capacitive deionization desalination process. However, the well-known hydrophobicity and low specific capacitance limit its wide application. In this study, incorporation of zirconia nanofibers with activated carbon is reported as an effective and simple strategy to overcome the abovementioned problems. Typically, zirconia nanofibers, which were synthesized by the calcination of electrospun nanofiber mats, were added to the activated carbon to fabricate novel electrodes for the capacitive deionization units. In a single-mode cell, it was observed that the addition of the proposed metal oxide nanofibers distinctly enhanced the desalination process as the electrosorption capacity and the salt removal efficiency improved from 5.42 to 16.35 mg $g^{-1}$and from 16.37% to 53.26% for the pristine and composite electrodes, respectively. However, the inorganic nanofiber content should be optimized; a composite having 10 wt% zirconia nanofibers with respect to the activated carbon showed the best performance. This distinct enhancement in the performance is attributed to the improvement in the wettability and specific capacitance of the electrode. Numerically, the water contact angle and the specific capacitance of the pristine and composite electrodes were found to be 145° and 26.5°, and 875 and 225 F g^{-1}, respectively. Overall, the present study strongly draws attention towards zirconia nanostructures as effective, cheap, environmentally friendly, and biologically safe candidates to enhance the performance of capacitive deionization electrodes.
RSC Advances 7 (2017), 4616-4626.

Design of an efficient photoanode for dye-sensitized solar cells using electrospun one-dimensional GO/N-doped nanocomposite SnO_2/TiO_2

Ibrahim M.A. Mohamed[a,d], Van-Duong Dao[b], Ahmed S.Yasin [a], Nasser A.M. Barakat[a,c], Ho-Suk Choi[b]

[a] *Bionanosystem Engineering Department, Chonbuk National University, Jeonju 561-756, Republic of Korea*

[b] *Department of Chemical Engineering & Applied Chemistry, Chungnam National University, 220 Gung-Dong, Yuseong-Gu, Daejeon 305-764, Republic of Korea*

[c] *Chemical Engineering Department, Faculty of Engineering, Minia University, El-Minia, Egypt*

[d] *Chemistry Department, Faculty of Science, Sohag University, Sohag 82524, Egypt*

This study presents the combination of N, graphene oxide (GO) and SnO_2 as efficient dopants into TiO_2 nanofibers (NFs) photoanode substrate for highly efficient dye-sensitized solar cells (DSCs). The developed NFs are synthesized by electrospinning and hydrothermal processes and characterized by FESEM, TEM, XPS, FT-IR, Raman and EDX-studies. The formation of short NFs is confirmed through FESEM and TEM measurements. As the results, the major crystal structure of TiO_2 in the prepared NFs has anatase (85.23%) and rutile-structure (14.67%). XPS and EDX studies affirm that the material has Ti, O, Sn, N and C elements. In addition, FT-IR and Raman spectra give an indication about the GO-content. Typically, the DSC based on the novel NFs shows 6.18% efficiency. The J_{sc}, V_{oc}, FF and R_{ct} are estimated and found to be 10.32 mA cm^{-2}, 0.825 V, 0.73 and 21.66 Ω, respectively. The high-power efficiency is contributed by three reasons. The first one is the high dye-loading (2.16×10^{-7} mol cm^{-2}). The second reason is the enhanced charge transfer and decreasing of the electrons/holes recombination through formation of wide band-gap oxide (3.246 eV). Finally, the third one is GO-doping which may create new routes for the electron transfer in working electrode layer.

Applied Surface Science 400 (2017), 355-364.

Synthesis of Esters and Carbamothioates Contaminating Tramadol Moiety and Their HPLC Applications

A. Khodiary[1],*, E.A. Ahmed[1], Khaled M. Mohamed[2] and Shymaa A. Thabet[3]

1Chemistry Department, Faculty of Science, Sohage University, Sohage 82524, Egypt

2Assuit Chemical Laboratory, Medical legal Department, Ministry of Justice, Assuit, Egypt

3Central Research Laboratory, Faculty of Medicine, Sohage University, Sohage 82524, Egypt

In the present study, a variety of novel tramadol esters (2-6) were synthesized via the reaction of (±)-cis-2-[(dimethylamino)methyl]- 1-(3-methoxy-phenyl)cyclohexanol (tramadol) (1) with acid chlorides and triethylamine. Treatment of compound 1 with epichlorohydrin afforded corresponding ether derivative 7. The reaction of compound 1 with isothiocyanates gave the novel carbamothioate derivatives 8- 12. Tramadol derivatives were found more sensitive for detection with (HPLC-DAD) than tramadol itself.

Asian J. Chem. / 2017 / 2(1) / pp 23-28

Synthesis of novel ZrO_2&GO@TiO_2 nanocomposite as an efficient photoanode in dye-sensitized solar cells

Ibrahim M.A. Mohamed[a,d], Van-Duong Dao[b], Ahmed S.Yasin [a], Mohamed A Yassin[a], Nasser A.M. Barakat[a,c], Ho-Suk Choi[b]

[a] *Bionanosystem Engineering Department, Chonbuk National University, Jeonju 561-756, Republic of Korea*
[b] *Department of Chemical Engineering & Applied Chemistry, Chungnam National University, 220 Gung-Dong, Yuseong-Gu, Daejeon 305-764, Republic of Korea*
[c] *Chemical Engineering Department, Faculty of Engineering, Minia University, El-Minia, Egypt*
[d] *Chemistry Department, Faculty of Science, Sohag University, Sohag 82524, Egypt*

Due to the physicochemical and photo-electro properties, TiO_2 nanostructures still being the outstanding photoanode materials in the dye-sensitized solar cells (DSCs). However, it is well known that a low dye-loading and charge recombination constrain the limitation of large-scale application. This work introduces the synthesis of ZrO_2&GO@TiO_2 nanofibers (NFs) by facile two steps using electrospinning and hydrothermal treatment. Furthermore, the developed materials are applied as an efficient photoanode of DSCs. The synthesized NFs are described in terms of morphology, crystallography and chemistry via FESEM, TEM, XRD, Raman spectra and EDX analysis. As the results, the Ti, Zr, O and C elements are uniformly distributed in the synthesized sample. The percentages of the atomic elements are 10.77, 57.69, 1.45 and 30.09 for C, O, Zr and Ti, respectively. The synthesized composite shows only anatase with crystal size of 25.86 nm and cell volume of 142.39 $Å^3$. The developed material is employed as working electrode of DSCs. The J-V characteristic showed 5.09% efficiency for device using the synthesized material, which is higher than those of cells assembled with TiO_2 NFs and ZrO_2@TiO_2 NFs photoanodes. The obtained result is explained by enhanced dye-loading (1.055×10^{17} molecule/cm^2) and improved charge transfer resistance (R_{ct} = 9.18 Ω) of the photoanode substrate. Hence, the presented nanocomposite can be an efficient photoanode towards technology of DSC.

Superlattices and Microstructures 102 (2017), 235-245.

Hetaryl-1,5 Benzodiazepines-Part I: Synthesis of 3-pyrimidinyl- and Imidazolyl-1,5-benzodiazepines

Ahmed Khodairy,* Eman A. Ahmed, and Hossam Abdel Ghany
Chemistry Department, Faculty of Science, Sohag University, Sohag, Egypt

Nucleophilic substitution of 3-bromo-4-phenyl-1H-[1,5]benzodiazepin-2-one (1) with thiourea or guanidine in presence of potassium carbonate afforded 1,5-benzodiazepin-3-ylimidothiocarbamate 2 or 1,5-benzodiazepin-3-ylguanidine 3, respectively. Pyrimidylthiobenzodiazepines 5–13 were obtained via the reaction of compound 2 with malononitrile dimer, diethyl malonate, methylenemalononitriles, or a mixture of an aldehyde and β-keto esters or acetylacetone, catalyzed using ceric ammonium nitrate. Reaction of compound 2 or 3 with α-halo esters, nitriles, and/or ketones afforded imidazoles 14–20, respectively.

J. Heterocyclic Chem., 54, 242 (2017).

Assessment of the Secondary Metabolite Patulin and Lycium Barbarum Fruit on INS-1 Rat Pancreatic B-Cells

Madeha N.Al-Seeni[1], Ahmed R.Shatat[2] , Nagwa M. Elsawi[3] and Asma S.Abdo[3]

[1] *Biochemistry Department, Faculty of Science, King Abdel-Aziz University, Jaddah, Saudi Arabia.*

[2]*Chemistry department, faculty of science, Al –Azhar University, Assiut Branch, Egypt*

[3]*Chemistry Department, Faculty of Science, Sohag University, Sohag, Egypt.*

Patulin has been shown to have diabetogenic effects in mice. The effects on pancreatic β-cell viability and function of secondary metabolite patulin were investigated. Using forty adult albino male rats which divided into 4 groups. Control group was injected subcutaneously daily with distilled water for one week; group I was injected subcutaneously daily with Patulin (0.2 mg/kg/day) for two weeks. Group II was injected with the same toxin and dose for two weeks after that they were treated by Goji extract (2 ml/kg /day.) for two weeks. Group III was treated by Goji for two weeks after that they were injected with patulin for two weeks. Some biochemical parameters of blood samples for experimental rodents were evaluated. Patulin group shows significant increase in amylase and glucose levels. But level of C-peptide and Insulin decreased significantly in this group. However, there is no significant alteration in Lipase level between patulin group and control. Groups treated with goji extract in groups two and three (therapeutic and prophylactic) illustrated non significant alteration in biochemical parameters compared to control.

Agriculture and Food Sciences Research, 4 (1), 24-29, 2017, ISSN(E) 2411-6653/ISSN(P)2411-6653

Evaluation of Antidiabetic Activity of *Ipomoea Aquatica* Fractions in Streptozotocin Induced Diabetic in Male Rat Model

Nagwa El-Sawi[1,*], Mahmoud Hefny Gad[2], Madeha Nooh Al-Seeni[3], Sabry Younes[1], El-Mewafy El-Ghadban[2] and Soad Shaker Ali[3,4]

[1]*Department of Chemistry, Faculty of Science, Sohag University, Sohag, Egypt.*

[2]*Medicinal and Aromatic Plants Research Department, Horticulture Institute, Agriculture Research Center, Dokki, Giza, Egypt.*

[3]*Biochemistry Department, Faculty of Science, King Abdulaziz University, Jeddah, Saudi Arabia.*

[4]*Histology Department, Faculty of Medicine, King Abdoul Aziz University, Saudi Arabia*

Ipomoea aquatica (IA) is a common green leafy vegetable consumed in many parts of the world. The plant is considered as a good antidiabetic herbal plant. The present work was designed to investigate the oral hypoglycaemic activity of *Ipomea aquatica* fractions in streptozotocin induced diabetic male rats. The male rats with average weight 200-220 g were divided into four groups (n=6), control, diabetic (induced with a single dose of streptozotocin (50 mg/kg body weight), T-1 and T-2 as treated diabetic with the two fractions of *Ipomoea aquatica* (IA6-1 and IA9-2), respectively. Biochemical evaluation of blood glucose, serum insulin and C-peptide were carried out. Histological examination of islets of Langerhans was done for cellular population changes. The results revealed that the oral consumption of two fractions of *I. aquatica* for 15 days, effective significantly reduced the fasting blood sugar level of streptozotocin-induced diabetic rats ($p < 0.05$). The percent changes were a 51% and 31% decrease in the serum glucose concentration of the diabetic rats when treated with the plant fractions of IA6-1 and IA9-2, respectively. Most biochemical parameters tested returned to nearly normal levels. Histologically, islets area and normal cell population were preserved in treated animals with superior results in T-1 and T-2 groups. In conclusion, fractions IA6-1 and IA9-2 showed potential antidiabetic effects when given orally to diabetic rats. The mechanism of action requires further investigation using both molecular and immunohistochemical methods investigation of both insulin secreting cells and insulin receptors. Future clinical trials could be tried using volunteers to confirm the present results so could be marketed as a supplement for diabetic patients

Sohag J. Sci. 2, No. 1, 9-17 (2017) 9

Identification of some Bioactive Metabolites in a Fractionated Methanol Extract from Ipomoea aquatica (Aerial Parts) through TLC, HPLC, UPLC-ESI-QTOF-MS and LC-SPE-NMR Fingerprints Analyses

Mahmoud Hefny Gad,[a,b] Emmy Tuenter,[c] Nagwa El-Sawi,[d] Sabry Younes,[d] El-Mewafy El-Ghadban,[b] Kristiaan Demeyer,[e] Luc Pieters,[c] Yvan Vander Heyden[a]* and Debby Mangelings[a]

[a]*Department of Analytical Chemistry and Pharmaceutical Technology, Centre for Pharmaceutical Research, Vrije Universiteit Brussel (VUB), Laarbeeklaan 103, B-1090, Brussels, Belgium*

[b]*Medicinal and Aromatic Plants Research Department, Horticulture Institute, Agriculture Research Centre, Dokki, Giza, Egypt*

[c]*Natural Products & Food Research and Analysis (NatuRA), Department of Pharmaceutical Sciences, University of Antwerp, Universiteitsplein 1, B-2610, Antwerp, Belgium*

[d]*Department of Chemistry, Faculty of Science, Sohag University, Sohag, Egypt*

[e]*Department of Toxicology, Dermato-Cosmetology and Pharmacognosy, Centre for Pharmaceutical Research, Vrije Universiteit Brussel (VUB), Laarbeeklaan 103, B-1090, Brussels, Belgium*

The plant species Ipomoea aquatica contains various bioactive constituents, e.g. phenols and flavonoids, which have several medical uses. All previous studies were executed in Asia; however, no reports are available from Africa, and the secondary metabolites of this plant species from Africa are still unknown.

The present study aims finding suitable conditions to identify the bioactive compounds from different fractions.

Chromatographic fingerprint profiles of different fractions were developed using high-performance liquid chromatography (HPLC) and then these conditions were transferred to thin-layer chromatography (TLC). Subsequently, the chemical structure of some bioactive compounds was elucidated using ultra-performance liquid chromatography-quadrupole time of flight-tandem mass spectrometry (UPLC-QTOF-MS) and liquid chromatography-solid phase extraction-nuclear magnetic resonance (LC-SPE-NMR) spectroscopy.

Phytochem. Anal. 2017 P 1-11

Ugi Multicomponent Reaction Based Synthesis of Medium-Sized Rings

Abdelraheem, E. M. M.[ab], Madhavachary, R.[a], Rossetti, A.[a], Kurpiewska, K.[c], Kalinowska-Tluścik, J.[c], Shaabani, S.[a], Dömling, A.[a]

[a]*Department of Drug Design, University of Groningen, A. Deusinglaan 1, AV Groningen, Netherlands*

[b]*Chemistry Department, Faculty of Science, Sohag University, Sohag, Egypt*

[c]*Jagiellonian University, Faculty of Chemistry, Gronostajowa 2, Krakow, Poland*

An Ugi multicomponent reaction based two-step strategy was applied to generate medium-sized rings. In the first linear expansion phase, a series of diamines reacted with cyclic anhydrides to produce different lengths of terminal synthetic amino acids as the starting material for the second phase. The Ugi-4-center 3-component reaction was utilized to construct complex medium-sized rings (8-11) by the addition of isocyanides and oxo components. This method features mild conditions and a broad substrate scope.

Organic Letters Volume 19, Issue 22, 17 November 2017, Pages 6176-6179

Utility of bis(methylthio)methylene malononitrile as a synthon in the synthesis of new poly-functionalized cyanoiminopyrimidines

Moustafa, A.H., Amer, A.A.

Chemistry Department, Faculty of Science, Sohag University, Sohag 82524, Egypt

A new series of 4-(alkyl/arylamino)-6-amino-5-cyano-2-cyanoimino-1H-pyrimidine was obtained via one-pot three-component reaction of bis(methylthio)methylene malononitrile, primary amines, and cyanoguanidine using sodium ethoxide as basic catalyst. The same new products were prepared by classical route via reaction of (alkyl/arylamino)(methylthio)methylene malononitrile with cyanoguanidine in presence of sodium ethoxide. In absence of amines, bis(methylthio)methylene malononitrile reacts directly with cyanoguanidine in presence of sodium ethoxide to give 4-ethoxy-2-cyanoimino-1H-pyrimidine. On the other hand, multicomponents reaction of bis(methylthio)methylene malononitrile with cyanoguanidine and binucleophilic β-hydroxyamines and/or ortho-phenylenediamine gave perspective 4-methyl- and/or 5-methyl-1,3-oxazolidin-2-ylidenemalononitrile and 1,3-dihydro-2H-benzimidazol-2-ylidenemalononitrile, which are inactive compounds toward reaction with cyanoguanidine to give the expected 4-(alkyl/arylamino)-2-cyanoimino-1H-pyrimidines.

Monatshefte fur Chemie . 148(12), 2129-2134, 2017

Biochemical and Spectral Analysis of Roridin A Toxin and Copper (I) Nicotinate Complex as Antidote on Male Rat Liver

Nabawia M. Ismail[1], Hana M.Gashlan[2], Ahmed M. Ali[3] and Nagwa M. Elsawi[1,*]

[1]Chemistry Department, Faculty of Science, Sohag University, Sohag 82524, Egypt.

[2]Biochemistry Department, Faculty of Science, King Abdulaziz University, Jadda, kingdom of Saudi Arabia.

[3]Chemistry Department, Faculty of Science, Al –Azhar University, Assiut Branch, Egypt.

This work has been designed to evaluate the curative effect of copper (I) –nicotinate complex on the hepatotoxicity of Roridin A in male rats as well as the study of the spectral analysis of this complex. Healthy young male albino rats (n=40) were exposed to a single dose of Roridin A (60 µg/kg body weight) and scarified and another group was treated with the copper (I) –nicotinate complex.Such intoxication resulted in some biochemical parameters such as ALP, GGT, TAS, Ferritin and AFP. Finally, Copper (I)-Nicotinate complex reduced many undesired changes of liver tissue and this improvement was predicted since this complex has been confirmed previously as a therapeutic agent against induced mycotoxins as Roridin A.

J. Pharm. Appl. Chem., 3, No. 2, 1-11 (2017)

Microwave-Assisted, One-Pot Multicomponent Synthesis of Some New Cyanopyridines

Amer, A. A., Abdelhamid, A. A.

Chemistry Department, Faculty of Science, Sohag University, Sohag 82524, Egypt

An efficient and facile synthesis of cyanopyridines via a one-pot four-component reaction of aromatic aldehydes, acetophenones, malononitrile, or 2-aminoprop-1-ene-1,1,3-tricarbonitrile in presence of sodium alkoxide or ammonium acetate under both microwave and thermal reaction conditions was introduced.

Journal of Heterocyclic Chemistry 54(6), 3126-3132, 2017

Syntheses of Some New N-Linked Pyrimidine-2-amines with Pyrazinopyrimidines, Thienopyrimidines, and Benzazoles via Reactions of Various Nucleophiles with Cyanamides

Moustafa, A. H., Ahmed, W. W., Khodairy, A.

Chemistry Department, Faculty of Science, Sohag University, Sohag 82524, Egypt

New heterocycles containing 2-aminopyrimidine moiety linked with pyrazino[1,2-c]pyrimidines, thieno[2,3-d] pyrimidines, benzimidazoles, benzothiazoles, and benzoxazoles have been prepared by an efficient method starting from N-(pyrimidin-2-yl)cyanamides.

Journal of Heterocyclic Chemistry 54(6), 3490-3497, 2017

Synthesis of Novel Chromene, Pyridine, Pyrazole, Pyrimidine, and Imidazole Derivatives via One-pot Multicomponent Reaction

Khodairy, A., Ali, A. M., El-Wassimy, M. T.
Chemistry Department, Faculty of Science, Sohag University, Sohag 82524, Egypt

New series of chromenes 2–4, pyridines 5–8, and pyranopyrazoles 9a,b were synthesized via one-pot multicomponent reaction of 4-tosyloxybenzaldehyde (1) and malononitrile with phenols, amines or hydrazines, and ethyl acetoacetate, respectively. Compound 9a was reacted with acetic anhydride, formic acid, or formamide to afford N-acetyl derivative 10 and pyrazolopyranopyrimidines 11–13, respectively. Imidazole derivatives 14 and 15a–d were obtained by multicomponent reaction between compound 1 with ammonium acetate and benzil or aromatic amines in (1:2:1) or (1:1:1:1) ratio, respectively. The structures of new compounds were elucidated by elemental and spectral analyses.

Journal of Heterocyclic Chemistry, 54(6), 3342-3349, 2017

New route for the synthesis of new cyanoimino- and cyanoaminopyrimidines

Amer, A.A., Moustafa, A.H.
Chemistry Department, Faculty of Science, Sohag University, Sohag 82524, Egypt

A novel series of 4-aryl-2-cyanoimino-3,4-dihydro-1H-pyrimidines (aryl-CIDHPMs) was synthesized using a new method via the one-pot three-component reaction of cyanoguanidine with malononitrile and aromatic aldehydes using sodium methoxide as catalyst. These new aryl-CIDHPMs were also prepared by a classical route via reaction of cyanoguanidine with the corresponding arylidenemalononitriles under our conditions. In the same manner, the reaction of cyanoguanidine with cyclohexylidenemalononitrile and/or isatinylidenemalononitrile afforded new spiro-pyrimidines 9 and 10, respectively. A new series of polyfunctionalized 2-cyanoaminopyrimidines was obtained from the reaction of cyanoguanidine with cinnamaldehyde and/or ethoxyalkylenemalononitriles. Graphical Abstract: [Figure not available: see fulltext.].

Molecular Diversity 21(4), 875-880, 2017

Synthesis, in vitro Antibacterial and in vivo Anti-Inflammatory Activity of Some New Pyridines

Abd-El-Badih A. G. Ghattas[a]., Ahmed Khodairy[a]., Hassan M. Moustafa[a]., Bahgat R. M. Hussein[a]., Marwa M. Farghaly[b]., Moustafa O. Aboelez[c]

[a]Chemistry Department, Faculty of Science, Sohag University, Sohag, Egypt
Botany Department, Faculty of Science, Sohag University Sohag, Egypt
[c]Department of Pharmaceutical Medicinal Chemistry, Faculty of Pharmacy, Sohag University, Sohag, Egypt

Reaction of 4,6-diamino-3-cyano-2-methylthiopyridine (I) with chloroacetyl chloride or acetic acid afforded the corresponding 6-acetamide derivatives IIa and IIb, respectively. Chloroacetamide derivative IIa reacted with various thiols, secondary amines, potassium thiocyanate, compounds containing active methylene group, 1-anilino-2,2-dicyanoethenethiolate, and o-mercatocyanopyridines to give S-alkyl, N-alkyl, thiazole, pyrrole, thiophene, and thienopyridine derivatives, respectively. Antibacterial and anti-inflammatory activities of some new pyridine derivatives were studied.

Pharmaceutical Chemistry Journal, 51(8), 652-660, 2017

High Hydroxide Ion Conductivity with Enhanced Alkaline Stability of Partially Fluorinated and Quaternized Aromatic Copolymers as Anion Exchange Membranes

Mahmoud, A. M. A.[ac], Elsaghier, A. M. M.[c], Otsuji, K.[a], Miyatake, K.[ab]

[a]Clean Energy Research Center, University of Yamanashi, 4 Takeda, Kofu, Japan
[b]Fuel Cell Nanomaterials Center, University of Yamanashi, 4 Takeda, Kofu, Japan
[c]Chemistry Department, Faculty of Science, Sohag University, Sohag, Egypt

For enhancing hydroxide ion conductivity, alkaline stability, and fuel cell performance of quaternaized aromatic/perfluoroaklyl copolymer (QPAF) membranes, ammonium groups attached to the polymer backbone have been investigated. The ammonium groups included dimethylbutylamine (DMBA), dimethylhexylamine (DMHA), and 1,2-dimethylimidazole (DMIm) groups in comparison to the trimethylammonium (TMA) group. DMBA turned to be the optimum ammonium group for QPAF membranes in terms of its high hydroxide ion conductivity based on well-connected and larger phase-separated morphology than that of QPAF-TMA with similar ion exchange capacity (IEC) value. QPAF-DMBA (IEC = 1.33 mequiv g^{-1}) exhibited the highest hydroxide ion conductivity among the tested membranes up to 152 mS cm^{-1} in water at 80 °C, which was 1.6 times higher than that of QPAF-TMA (95 mS cm^{-1}). In addition, QPAF-DMBA exhibited reasonable alkaline stability in 1 M KOH at 60 °C for 1000 h. The remaining conductivity was 44 mS cm^{-1} (58%) for QPAF-DMBA, while that for QPAF-TMA was 1.0 mS cm^{-1} (1%). QPAF-DMBA (IEC = 1.09 mequiv g^{-1}) exhibited excellent stability in 1 M KOH at 80 °C without change in the ion conductivity (22 mS cm^{-1}) for 500 h. The post-test membranes exhibited a minor degradation in QPAF-DMBA as suggested by FT-IR spectra and DMA analyses. An H_2/O_2 fuel cell was operated with the QPAF-DMBA membrane to achieve the maximum power density of 167 mW cm^{-2} at the current density of 0.42 A cm^{-2}, which was higher than that (138 mW cm^{-2}) for QPAF-TMA membrane under the same operating conditions.

Macromolecules, 50(11), 4256-4266, 2017

Ring rearrangements and reactivity of 3-((4-oxo-4H-chromen-3-yl)methylene)-4-phenyl-1H-[1,5]benzodiazepin-2(3H)-one toward some nucleophiles

Salah, H.[a], Ahmed, E. A.[a], Hassan, M. M. [bc]

[a]Chemistry Department, Faculty of Science, Sohag University, Sohag, Egypt

[b]Chemistry Department, Faculty of Education, Ain Sham University, Cairo, Egypt

[c]Basic Science Department, Preparatory Year Deanship, Majmaah University, Majmaah, Saudi Arabia

Condensation of 4-phenyl-1H-[1,5]benzodiazepin-2(3H)-one (1) with 3-formylchromone (2) afforded a mixture of 3-(chromenylmethylene)[1,5]benzodiazepinone 3 and 14-chromenylbenzodiazepino[2,3:6,5]pyrano[2,3-b]benzodiazepine 4. Ring rearrangements of compound 3 with different nucleophilic reagents, such as potassium hydroxide and/or ammonium acetate led to rearrangement into pyranobenzodiazepine 5 and pyridobenzodiazepine 6, respectively. Treatment of compound 3 with hydrazine hydrate, hydroxylamine hydrochloride, malononitrile, cyanothioacetamide, 2-cyano-3,3-disufanylacrylonitrile, and/or 2-cyano-3-phenylamino-3-sufanylacrylonitrile, has been carried out at different conditions, leading to versatile heterocyclic substituted benzodiazepines at position 3, viz. pyrazole 8, isoxazole 9, pyridines 10 and 11, 1,3-dithiine 12, and 1,3-thiazine 13 derivatives.

Arabian Journal of Chemistry, 10(4), 548-555, 2017

New Heterocyclic Compounds Derived from 4,6-Diamino-3-cyano-2-methylthiopyridine and their Biological Activity

Ghattas, A. E.-B. A. G., Khodairy, A., Moustafa, H. M., Hussein, B. R. M.

Chemistry Department, Faculty of Science, Sohag University, Sohag, Egypt

Treatment of 4,6-diamino-3-cyano-2-methylthiopyridine (1) with aqueous KOH or hydrazine hydrate afforded the corresponding nicotinamide 2 and pyrazolo[3,4-b]pyridine 3, respectively. Reaction of compound 1 with bromine, sulfuryl chloride, formaldehyde, or aromatic diazonium salts gave 5-bromopyridine 4, 5-chloropyridine 5, dipyridylmethane 6, and azo dyes 7, 8, 9, 10, respectively. Compound 1 reacted with diketones to yield the corresponding butenylamino derivative 11 and amides 12, 13, 14, 15, respectively. Treatment of butanamide 13 with diazonium salts or a mixture of urea and aromatic aldehyde in the presence of drops of HCl as a catalyst yielded the corresponding arylhydrazones 16, 17, 18, 19, pyrimidines 20, 21, 22, 23, 24, and 1,8-naphthyridine 25, respectively. The potency of the results as anti-inflammatory and antifungal agents have been evaluated. The compounds have been characterized based on their spectral and elemental analysis.

Journal of Heterocyclic Chemistry, 54(2), 879-888, 2017

Hetaryl-1,5 Benzodiazepines-Part I: Synthesis of 3-pyrimidinyl- and Imidazolyl-1,5-benzodiazepines

Khodairy, A., Ahmed, E.A., Abdel Ghany, H.
Chemistry Department, Faculty of Science, Sohag University, Sohag, Egypt

Nucleophilic substitution of 3-bromo-4-phenyl-1H-[1,5]benzodiazepin-2-one (1) with thiourea or guanidine in presence of potassium carbonate afforded 1,5-benzodiazepin-3-ylimidothiocarbamate 2 or 1,5-benzodiazepin-3-ylguanidine 3, respectively. Pyrimidylthiobenzodiazepines 5, 6, 7, 8, 9, 10, 11, 12, 13 were obtained via the reaction of compound 2 with malononitrile dimer, diethyl malonate, methylenemalononitriles, or a mixture of an aldehyde and β-keto esters or acetylacetone, catalyzed using ceric ammonium nitrate. Reaction of compound 2 or 3 with α-halo esters, nitriles, and/or ketones afforded imidazoles 14, 15, 16, 17, 18, 19, 20, respectively.

Journal of Heterocyclic Chemistry, 54(1), 242-247, 2017

Synthesis, Characterization, Antimicrobial Evaluation and DFT Calculations of Fe(III), Ni(II) and Cu(II) Complexes of Tridentate ONO Donor Ligand

A. M. Abdel-Mawgoud, Mohamed Ismael, Aly Abdou
Chemistry Department, Faculty of Science, Sohag University, Sohag 82524, Egypt

A series of Fe(III), Ni(II) and Cu(II) complexes had been synthesized with molecular formula of [Fe(L)(H2 O)2Cl].2H2O, [Ni(L)(H2O)].2H2O and [Cu(L)(H2O)3].2H2O, where L is a Schiff base ligand was derived by condensation of anthranilic acid with 2-hydroxy-benzaldhyde. Structures of the obtained compounds had been characterized using elemental analyses, UV-Vis., FT-IR, magnetic moment and conductivity measurements. Results proposed octahedral geometry for both of Fe(III) and Cu(II) complexes while Ni(II) complex had a square planar geometry. Density Functional Theory (DFT) calculations were performed to confirm the 3D geometry of the compounds and estimate selected electronic parameters (e.g. chemical potential, hardness and electrophilicity index). Moreover free ligand and its metal complexes had been screened for in-vitro antibacterial (Escherichia coli (G-) and Bacillus cereus (G+)) and antifungal (aspergillus fumigatus) activities in terms of the minimum inhibitory concentration (MIC). Results indicated that biological activity increases with complexation.

Journal of Pharmaceutical and Applied Chemistry, 3(3), (2017), 259-266

An Efficient One-Pot Three-Component Synthesis of Some New Polyhydroquinolines via Enaminone Intermediates

Abdelhamid, A. A., Abd Allah, O. A., Tamam, A. H. A.
Chemistry Department, Faculty of Science, Sohag University, Sohag, Egypt

For a wide spectrum of pharmacological effects of polyhydroquinolines, this study introduces a developed safe, simple, higher yields and fast method for the synthesis of some new hexahydroquinoline derivatives using one-pot three-component cyclocondensation reaction, via the reaction of 1,3-cyclohexanedione with primary amine and arylidinemalononitrile or salicylaldehyde derivatives. The prepared compounds were reacted with different reagents as *N*,*N*-dimethylformamide dimethylacetal, acetic anhydride, sulphuric acid, and hydrazine hydrate forming several polycyclic hexahydroquinoline and acridine derivatives. All these new compounds have been characterized by spectral data and expected to be effective pharmaceutical drugs.

Journal of Heterocyclic Chemistry , 54(5), 2822-2829, 2017

One-Pot Multicomponent Synthesis of Novel 2-Tosyloxyphenylpyrans under Green and Conventional Condition with Anti-inflammatory Activity

Khodairy A., Ali A. M., Aboelez M. O., El-Wassimy M. T.
Chemistry Department, Faculty of Science, Sohag University, Sohag, Egypt

A mild, efficient, and environmentally green protocol for the synthesis of 2-tosyloxyphenylpyran derivatives 3, 4, 5, 6, 7, 8, 9, 10, 11 via reaction of 2-tosyloxybenzaldehyde (1) with malononitrile and some ketonic reagents in one-pot, three component reaction within few minutes under stirring in methanol in presence of ammonium hydroxide solution or ultrasonic irradiation. On the other hand, the same products 3, 4, 5, 6, 7, 8, 9, 10, 11 were obtained by traditional method, on treatment of 2-tosyloxybenzilidinemalononitrile (2) with the same ketonic reagents in refluxing ethanol in presence of TEA. 2-Tosyloxyphenylpyranopyrazoles 12 and 13 were obtained via treatment of compound 1 with malononitrile, hydrazine hydrate or phenyl hydrazine and ethyl acetoacetate, in one-pot, multicomponent reaction (MCRs). The structures of the new compounds were elucidated by elemental and spectral analyses. The newly synthesized compounds showed promising anti-inflammatory activity.

Journal of Heterocyclic Chemistry, 54(2), 1442-1449, 2017

Facile synthesis of GO@SnO_2/TiO_2 nanofibers and their behavior in photovoltaics

Ibrahim M.A. Mohamed[a,f], Van-Duong Dao[b], Ahmed S.Yasin[a], Ho-Suk Choi[b], Khalil Abdelrazek Khalil[c,d], Nasser A.M. Barakat[a,e]

[a]*Bionanosystem Engineering Department, Chonbuk National University, Jeonju 561-756, Republic of Korea*
[b]*Department of Chemical Engineering & Applied Chemistry, Chungnam National University, 220 Gung-Dong, Yuseong-Gu, Daejeon 305-764, Republic of Korea*
[c]*Mechanical Engineering Department, King Saud University, P.O. Box 800, Riyadh 11421, Saudi Arabia*
[d]*Materials Engineering and Design Department, Aswan University, Aswan, Egypt*
[e]*Chemical Engineering Department, Faculty of Engineering, Minia University, El-Minia, Egypt*
[f]*Chemistry Department, Faculty of Science, Sohag University, Sohag 82524, Egypt*

Chemical doping is a widely-used strategy to improve the performance of TiO_2 for the dye-sensitized solar cells (DSCs). However, the effect of two efficient dopants has been rarely investigated. We present the synthesis of GO@SnO_2/TiO_2 nanofibers (NFs) by a facile method using electrospinning and hydrothermal processes. The synthesized NFs are described in terms of morphology, crystallinity and chemistry through FESEM, TEM, HR-TEM, XRD, EDX, XPS, FT-IR and Raman spectra. As the results, the axial ratio and the average diameter of NFs decreased after the hydrothermal treatment and calcination process, respectively. The prepared Titania-based nanofibers have 81.82% anatase and 18.18% rutile-structure. The developed materials are applied as working electrodes of DSCs. The photovoltaic performances showed that the efficiency of the device employed GO@SnO_2/TiO_2 photoanode gave 5.41%, which was higher than those of cells fabricated with SnO_2/TiO_2 NFs (3.41%) and GO@TiO_2 NFs (4.52%) photoanodes. The photovoltaic parameters such as J_{sc}, V_{oc}, FF and R_{ct} are calculated and found to be 11.19 mA cm^{-2}, 0.72 V, 0.67 and 9.26 Ω, respectively. The high photovoltaic response of DSC based of GO@SnO_2/TiO_2 NFs may be attributed to the large surface area of the NFs, and the low electron recombination. Furthermore, the start-stop switches of the cell devices with the developed photoanode affirmed the stability and photovoltaic performance of the cell.

Journal of Colloid and Interface Science 490 (2017), 303-313.

Synthesis and Antimicrobial Screening of Fused Heterocyclic Pyridines

El-Remaily, M. A. A., Elhady, O. M., Abdel-Raheem, E. M. M.
Chemistry Department, Faculty of Science, Sohag University, Sohag, Egypt

In an attempt to find a new class of antimicrobial agents, a series of pyridoxazepine, pyridothiazepine, triazepine, naphthyridine, pyridopyrimidine, and other related products containing pyridine moiety were synthesized via the reaction of 2-amino-6-chloro-3,5-dicyanopyridine 1 with nucleophilic chemical reagents. These compounds were screened for cytotoxicity and their antimicrobial activity. Most of products showed inhibitory effect.

Journal of Heterocyclic Chemistry 54(2), 871-878, 2017

Iminophosphoranes in Heterocyclic Synthesis: A Facile Synthesis of Pyrido[4,3-D]Pyrimidine and Pyrido[4,3-D][1,3]Oxazine Derivatives via Intermolecular aza-Wittig Reactions

Omran O. A., Sayed S. M., Raslan M. A.
Chemistry Department, Faculty of Science, Sohag University, Sohag, Egypt

A novel series of pyrido[4,3-*d*]pyrimidine and pyrido[4,3-*d*][1,3]oxazine derivatives were synthesized via tandem aza-Wittig and annulation reactions with the corresponding iminophosphoranes, aromatic isocyanate, and amines. All newly synthesized compounds were elucidated by considering the data of both elemental and spectral analysis.

Journal of Heterocyclic Chemistry, 54(2), pp.1103-1108, 2017

Utility of CyanoaceticAcid Hydrazide in Organic Synthesis: Synthesis and Characterization of Some Novel Heterocycles bearing 1,3,4-Oxadiazole Moeity

Mounir A. A. Mohamed, Omar M. El-Hady, Ahmed M. El-Sayed
Chemistry Department, Faculty of Science,Sohag University, Sohag, Egypt

2,2-(1,3,4-oxadiazole-2,5-diyl)diacetonitrile 2 has been prepared expeditiously from 2-cyano-N'-(2cyanoacetyl)acetohydrazide1. Reaction of 2,2-(1,3,4-oxadiazole-2,5-diyl)diacetonitrile 2 with aromatic aldehydes under mild alkaline conditions afforded the corresponding condensation products 3a-d, which in turn allowed to react with hydrazine, phenylhydrazine or hydroxylamine to give pyrazole and iosxazole derivatives (4-6)a-d. Also compound 3a-d was reacted with acetylacetone or ethyl acetoacetate to give pyran derivatives (7,8)a-d. Condensation of compound 2 with cyclopentanone afforded compound 9 which was reacted with acetylacetone or ethyl acetoacetate to give the corresponding spiropyran derivatives 10 and 11 respectively. The one-pot reaction of compound 2 with carbon disulfide or phenylisocyanate and ethyl chloroacetate under phase transfer catalysis conditions afforded the corresponding thiophene derivatives 12 and 13 respectively. Finally, the reaction of compound 2 with ethylcyanoacetate was studied carefully under non-catalytic and catalytic conditions where compounds 14-16 were obtained respectively. The antimicrobial activity of the obtained compounds was examined. The obtained products were characterised by their elemental and spectral data

Journal of Pharmaceutical and Applied Chemistry, 3(2), 117-125

Two-StepSynthesis of Complex Artificial Macrocyclic Compounds

Rudrakshula Madhavachary[1], Eman M. M. Abdelraheem[1,2], Arianna Rossetti[1]

[1]Aleksandra Twarda-Clapa, Bogdan Musielak, Katarzyna Kurpiewska, Justyna Kalinowska-Tłuscik, TadA.Holak, and Alexander Dçmling

[2]Chemistry Department, Faculty of Science, Sohag University, Sohag, Egypt

The design and synthesis of head-to-tail linked artificial macrocycles using the Ugi-reaction has been developed. This synthetic approach of just two steps is unprecedented, short, efficient and works over a wide range of medium (8–11) and macrocyclic (≥12) loop sizes. The substrate scope and functional group tolerance is exceptional. Using this approach, we have synthesized 39 novel macrocycles by two or even one single synthetic operation. The properties of our macrocycles are discussed with respect to their potential to bind to biological targets that are not druggable by conventional, drug-like compounds. As an application of these artificial macrocycles we highlight potent p53–MDM2 antagonism.

Angewandte Chemie - International Edition, 56(36), 10725-10729,2017

Morpholinium hydrogen sulfate (MHS) ionic liquid as an efficient catalyst for the synthesis of bioactive multi-substituted imidazoles (MSI) under solvent-free conditions

Marzouk A. A., Abdelhamid A. A., Mohamed S. K., Simpson J.

Chemistry Department, Faculty of Science, Sohag University, Sohag, Egypt

Morpholinium hydrogen sulfate as an ionic liquid was employed as a catalyst for the synthesis of a biologically active series of multi-substituted imidazoles by a four-component reaction involving the combination of benzil with different aromatic aldehydes, ammonium acetate, and 1-Amino-2-propanol under solvent-free conditions. The key advantages of this method are shorter reaction times, very high yield, and ease of processing. Furthermore, the resulting products can be purified by a non-chromatographic method and the ionic liquid catalyst is reusable. All of these novel compounds have been fully characterized from spectral data. The X-ray crystal structures of two representative molecules are also detailed.

Zeitschrift fur Naturforschung - Section B Journal of Chemical Sciences, 72(1), 23-33, 2017

Synthesis, Characterization, DFT Calculations and Biological Studies of Mn(II), Fe(II), Co(II) and Cd(II) complexes based on a tetradentate ONNO donor Schiff base ligand

Laila H. Abdel-Rahman*, Nabawia M. Ismail, Mohamed Ismael, Ahmed M. Abu-Dief and Ebtehal Abdel-Hameed Ahmed

Chemistry Department, Faculty of Science, Sohag University, 82524 Sohag, Egypt

This study highlights synthesis and characterization of a tetradentate ONNO Schiff base ligand namely (1, 1`- (pyridine-2, 3-dimethyliminomethyl) naphthalene-2, 2`-diol) and hereafter denotes as "HNDAP" and selected metal complexes including Mn(II), Fe(II), Co(II) and Cd(II) as a central metal. HNDAP was synthesized from 1:2 molar ratio condensation of 2, 3-diaminopyridine and 2- hydroxy-1-naphthaldhyde, respectively. The stoichiometric ratios of the prepared complexes were estimated using complementary techniques such as; elemental analyses (-C, H, N), FT-IR, magnetic measurements and molar conductivity. Furthermore, their physicochemical studies were carried out using thermal TGA, DTA and kinetic–thermodynamic studies along with DFT calculations. The results of elemental analyses showed that these complexes are present in a 1:1 metal-to- ligand molar ratio. Moreover, the magnetic susceptibilities values at room temperature revealed that Mn(II), Fe(II) and Co(II) complexes are paramagnetic in nature and have an octahedral (O_h) geometry. In contrast, Cd(II) is diamagnetic and stabilizes in square planar sites. The molar conductivity measurements indicated that all complexes are nonelectrolytes in dimethyl formamide. Spectral data suggested that the ligand is as tetradentate and coordinated with Co(II) ion through two phenolic OH and two azomethine nitrogen. However, for Mn(II), Fe(II) and Cd(II) complexes, the coordination occurred through two phenolic oxygen and two azomethine nitrogen with deprotonation of OH groups. The proposed chemical structures have been validated by quantum mechanics calculations. Antimicrobial activities of both the HNDAP Schiff base ligand and its metal complexes were tested against strains of Gram (-ve) *E. coli* and Gram (+ve) *B. subtilis* and *S. aureus* bacteria and *C. albicans*, *A. flavus* and *T. rubrum* fungi . All the prepared compounds showed good results of inhibition against the selected pathogenic microorganisms. The investigated HNDAP Schiff base complexes showed higher activity and stability than their corresponding HNDAP Schiff base ligand and the highest activity observed for Cd(II) complex. Moreover, the prepared Schiff base ligand and its Mn(II) and Co(II) complexes have been evaluated for their anticancer activities against two cancer cell lines namely; colon carcinoma cells (HCT-116 cell line) and hepatocellular carcinoma (Hep-G2) cell lines The interaction of Mn(II) and Co(II) complexes with calf thymus DNA (CT-DNA) was studied by absorption spectroscopic technique and viscosity measurements. Both complexes showed a successful interaction with CT-DNA *via* intercalation mode.

Journal of Molecular Structure 1134 (2017) 851e862

Crystal structure of 1-[2-(4-chlorophenyl)-4,5-diphenyl-1H-imidazol-1-yl]propan-2-ol

Mohamed S. K., Marzouk A. A., Albayati M. R., Abdelhamid A. A., Simpson J.

Chemistry Department, Faculty of Science, Sohag University, Sohag, Egypt

The title compound, C24H21ClN2O, crystallizes with two unique molecules in the asymmetric unit. In each molecule, the central imidazole ring is substituted at the 2-, 4- and 5-positions by benzene rings. The 2-substituted ring carries a Cl atom at the 4-position. One of the imidazole N atoms in each molecule has a propan-2-ol substituent. In the crystal, a series of O - H···N, C - H···O and C - H···Cl hydrogen bonds, augmented by several C - H···π(ring) interactions, generate a three-dimensional network of molecules stacked along the a-axis direction.

Acta Crystallographica Section E: Crystallographic Communications, 73, 59-62, 2017

Design and Nonlinear Optical Properties (NLO) using DFT Approach of New Cr (III), VO(II), and Ni(II) Chelates Incorporating Tri-dentate Imine Ligand for DNA Interaction, Antimicrobial, Anticancer Activities and Molecular Docking Studies

Laila H. Abdel-Rahman[a], Ahmed M. Abu-Dief[a]*, H. Moustafa[b] and Azza A. Hassan Abdel-Mawgoud[a]

[a]*Chemistry Department, Faculty of Science, Sohag University-82524, Egypt*

[b]*Chemistry Department, Faculty of Science, Cairo University, 12613 Giza, Egypt*

In recent years, metals based antitumor complexes have played a vital role in chemotherapy. Therefore, in this study, some new imine Cr(III), VO(II) and Ni(II) complexes incorporating ESAP imine ligand (2- Ethoxy-6-((2-hydroxy-phenylimino)- methyl)-phenol were designed and synthesized. The investigated complexes were fully characterized by micro analysis, infrared, electronic spectra, thermal analysis (TGA), conductivity as well as magnetic susceptibility measurements. Moreover, the stability constants of the prepared complexes were determined spectrophotometrically. The results suggest that the titled ESAP imine ligand serves as tri-dentate moiety through deprotonated two phenolic oxygen and azomethene nitrogen atoms for coordination to Cr(III) in octahedral geometry, tetrahedral to Ni(II) and distorted square pyramidal to VO (II). The electronic structure and nonlinear optical parameters NLO of the newly synthesized complexes are investigated theoretically at the B3LYP/GEN level of theory. The studied complexes show promising optical properties. Indeed, the prepared compounds were evaluated for antimicrobial effect against some types of bacteria and fungi. The investigated complexes exhibit a stronger antimicrobial efficiency compared to its ligand. Moreover, the interaction of the complexes with CT-DNA was monitored using spectral studies, viscosity and gel electrophoreses measurements. Furthermore, the cytotoxic activity of the prepared imine complexes on human colon carcinoma cells, hepatic cellular carcinoma cells and breast carcinoma cells have shown promising results and enhancement of the anti-proliferative activity compared to its ligand. The molecular docking into TRK (PDB: 1t46) was done for the optimization of the investigated compounds as potential TRK inhibitors.

Arabian Journal of Chemistry (2017)

Biochemical and Spectral Analysis of Roridin A Toxin and Copper (I) Nicotinate Complex as Antidote on Male Rat Liver

Nabawia M. Ismail[1], Hana M.Gashlan[2], Ahmed M. Ali[3], Nagwa M. Elsawi[1]

[1]*Chemistry Department, Faculty of Science, Sohag University, Sohag 82524, Egypt*

[2]*Biochemistry Department, Faculty of Science, King Abdulaziz University, Jadda, kingdom of Saudi Arabia*

[3]*Chemistry Department, Faculty of Science, Al –Azhar University, Assiut Branch, Egypt*

This work has been designed to evaluate the curative effect of copper (I) –nicotinate complex on the hepatotoxicity of Roridin A in male rats as well as the study of the spectral analysis of this complex. Healthy young male albino rats (n=40) were exposed to a single dose of Roridin A (60 µg/kg body weight) and scarified and another group was treated with the copper (I) –nicotinate complex. Such intoxication resulted in some biochemical parameters such as ALP, GGT, TAS, Ferritin and AFP. Finally, Copper (I)-Nicotinate complex reduced many undesired changes of liver tissue and this improvement was predicted since this complex has been confirmed previously as a therapeutic agent against induced mycotoxins as Roridin A.

Journal of Pharmaceutical and Applied Chemistry, 3(2), 127-133

Alcohol Dehydrogenases Catalyze the Reduction of Thioesters

Sabry H. H. Younes[1,2], Yan Ni[1], Sandy Schmidt[1], Wolfgang Kroutil[3], Frank Hollmann[1]

[1]*Department of Biotechnology, Delft University of Technology Vander Maasweg 9, 2629 HZ Delft, Netherlands*

[2]*Department of Chemistry,Faculty of Sciences, Sohag University,Sohag 82524, Egypt*

[3]*Department of Chemistry,Organicand Bioorganic Chemistry University of Graz, 8010Graz, Austria*

Abstract:

Alcohol dehydrogenases are well-established catalysts for various reduction reactions. However, the reduction of carboxylic acid derivatives has not yet been reported with these enzymes. In this contribution, we demonstrated that carboxylic acid thioesters could be readily reduced by a range of alcohol dehydrogenases, albeit at significantly reduced rates relative to those observed for corresponding ketones. A molecular explanation, especially for the lower turnover rates for thioesters relative to those obtained for ketones, is presented, as is a preliminary substrate scope.

ChemCatChem 2017, 9, 1389.

Rapid chemoenzymatic route to glutamate transporter inhibitor L-TFB-TBOA and related amino acids

Haigen Fu[a], Sabry H. H. Younes[a], Mohammad Saifuddin[a], Pieter G. Tepper[a], Jielin Zhang[a], Erik Keller[b], André Heeres[b], Wiktor Szymanski[c] and Gerrit J. Poelarends[a]

[a]*Department of Chemical and Pharmaceutical Biology, Groningen Research Institute of Pharmacy, University of Groningen, Antonius Deusinglaan 1, 9713 AV Groningen, The Netherlands*

[b]*Syncom BV, Kadijk 3, 9747 AT Groningen, The Netherlands*

[c]*Department of Radiology, University of Groningen, University Medical Center Groningen, Hanzeplein 1, 9713 GZ Groningen, The Netherlands*

Abstract:

The complex amino acid (L-threo)-3-[3-[4-(trifluoromethyl)benzoylamino]benzyloxy]aspartate (L-TFB-TBOA) and its derivatives are privileged compounds for studying the roles of excitatory amino acid transporters (EAATs) in regulation of glutamatergic neurotransmission, animal behavior, and in the pathogenesis of neurological diseases. The wide-spread use of L-TFB-TBOA stems from its high potency of EAAT inhibition and the lack of off-target binding to glutamate receptors. However, one of the main challenges in the evaluation of L-TFB-TBOA and its derivatives is the laborious synthesis of these compounds in stereoisomerically pure form. Here, we report an efficient and step-economic chemoenzymatic route that gives access to enantio- and diastereopure L-TFB-TBOA and its derivatives at multigram scale.

Org. Biomol. Chem., 2017, 15, 2341-2344


Botany Department
قسم النبات

Botany


Botany Department
قسم النبات

Extracellular biosynthesis of silver nanoparticles using Rhizopus stolonifer

AbdelRahim K., Mahmoud S. Y. Ali, A.M. , Almaary, K. S., Mustafa, A. E.-Z. M. A, Husseiny, S. M.
Department of Botany and Microbiology, Sohag University, Sohag, Egypt

Synthesis of silver nanoparticles (AgNPs) has become a necessary field of applied science. Biological method for synthesis of AgNPs by Rhizopus stolonifer aqueous mycelial extract was used. The AgNPs were identified by UV–visible spectrometry, X-ray diffraction (XRD), transmission electron microscopy (TEM) and Fourier transform infrared spectrometry (FT-IR). The presence of surface plasmon band around 420 nm indicates AgNPs formation. The characteristic of the AgNPs within the face-centered cubic (fcc) structure are indicated by the peaks of the X-ray diffraction (XRD) pattern corresponding to (1 1 1), (2 0 0) and (2 2 0) planes. Spherical, mono-dispersed and stable AgNPs with diameter around 9.47 nm were prepared and affirmed by high-resolution transmission electron microscopy (HR-TEM). Fourier Transform Infrared (FTIR) shows peaks at 1426 and 1684 cm^{-1} that affirm the presence of coat covering protein the AgNPs which is known as capping proteins. Parameter optimization showed the smallest size of AgNPs (2.86 ± 0.3 nm) was obtained with 10^{-2} M $AgNO_3$ at 40 °C. The present study provides the proof that the molecules within aqueous mycelial extract of R. stolonifer facilitate synthesis of AgNPs and highlight on value-added from R. stolonifer for cost effectiveness. Also, eco-friendly medical and nanotechnology-based industries could also be provided. Size of prepared AgNPs could be controlled by temperature and $AgNO_3$concentration. Further studies are required to study effect of more parameters on size and morphology of AgNPs as this will help in the control of large scale production of biogenic AgNPs.
Saudi Journal of Biological Sciences (2017) 24, 208-216

Rise Potassium Content of the Medium Improved Survival, Multiplication, Growth and Scavenging System of in Vitro Grown Potato under Salt Stress

A. M. Hassanein and Jehan M. Salem
Department of Botany and Microbiology, Sohag University, Sohag, Egypt

IN VITRO grown potato cultivars shoots were used to understand ….. how polyvinyl pyrrolidone (PVP) and three levels of potassium interact with two levels of salinity to determine Na+ and K + contents, and antioxidant enzyme activities leading to control survival, multiplication and growth of cultured plant shoots. Explant survival and number of regenerants/explant decreased with increase of NaCl concentration but increased K+ content of the culture medium from 20 mM to 30 mM improved explants survival frequency and the growth parameters estimated under relatively high salt stress (80 mM NaCl) in both cultivars. Also, number of regenerants was influenced by K+ level where it was higher on medium containing 40 mM NaCl and 30 mM K + than other cultured on the same NaCl concentration with 20 mM K + . The positive effect of 30 mM K+ on the previous parameters was associated with increase shoot K+ content leading to decrease Na+ /K+ ratio and increase of some antioxidant enzymes (SOD, POX and CAT in Agria or SOD, POX and APX in Hermes) activity, especially under relatively high salt stress. PVP application increased K+ content and activities of some antioxidant enzymes (CAT and APX) but decreased Na+ /K+ ratio of shoots subjected to relatively high salt stress in Agria but under both salt stresses in Hermes. Consequently, sufficient potassium supply was necessary to conserve low Na+ /K+ ratio and efficient scavenging system by antioxidant agent (PVP) application or increase the endogenous antioxidant enzymes activities leading to minimize the negative effect of salt stress on in vitro grown potato.
Egypt. J. Bot., 57 (1), 259 - 275 (2017)

14 April, 2018

Shoot Regeneration and Isoenzyme Expression of Moringa oleifera L. under the influence of salt stress

A. M. Hassanein· J. M. Salem· F. A. Faheed· A. El-nagish
Department of Botany and Microbiology, Sohag University, Sohag, Egypt

Shoot regeneration and isoenzyme expression of Moringa oleifera L. under the influence of cytokinin type and different concentrations of NaCl were studied. Cotyledonary nodal segments obtained from in vitro grown seedlings (initial culture) and nodal segments obtained from their regenerants (first subculture) were subjected to shoot formation on MS medium supplemented with 0.56 mg/l BAP or KIN, for three weeks each. Generally, number of regenerated shoots was higher under the influence of BAP than that of KIN on cotyledonary nodal segments or during the two successive subcultures. On MS with BAP, high number of vigor shoots was associated with the formation of callus on the base of explants. During the initial culture, NaCl exerted negative effect on shoot formation and it increased with the increase of NaCl concentration. The presence of NaCl during the initial culture improved regeneration during the first subculture up to 4 gm/l NaCl and increased the expression of peroxidases, superoxide dismutases and esterases. On the other side, expression of glutamate oxaloactate transaminases was decreased. This indicated that M. oleifera shoots increased the expression of these enzymes to control the negative effect of NaCl on shoot regeneration and growth of regenerated shoots.

Phyton; annales rei botanicae April 2017

Response of duckweed to lead exposure: phytomining, bioindicators and bioremediation

A. K. Hegazy, M. H. Emam, L. Lovett-Doust, E. Azab, A. A. El-Khatib
Department of Botany and Microbiology, Sohag University, Sohag, Egypt

The ability of aquatic macrophytes to bioaccumulate toxic metals relative to the concentrations of these metals in wastewater has led to their use as phytoremediators. Lead (Pb) is among the most serious environmental contaminants. This study assesses the gibbous duckweed (Lemna gibba L.) as a bioaccumulator and bioindicator of Pb pollution. The plant recovery from a 12-d exposure period in terms of re-releases of Pb from its tissues, and recovery of pigmentation was monitored. Duckweed was exposed to Pb-contaminated water by adding PbCO3 at concentrations from 10 to 100 mg/L. At 2-d intervals, bioaccumulation, contaminant removal efficiency, pigment content, and bleaching were assessed. The efficiency of Pb removal after 12 d reached nearly 50% at the lowest Pb treatment (10 mg/L), but decreased at higher levels of Pb up to 100 mg/L. The highest bioconcentration factors (BCF) were achieved at low Pb treatment of 10 mg/L, which increased from nearly 200 mg/L after 2 d, to 943 mg/L after 12 d of exposure. Recovery from bleaching was around 50% for all photosynthetic pigments in plants exposed to 10–40 mg/L concentrations of Pb. The response of duckweed to Pb treatment and recovery from stress suggest its possible use as biosensor or biomonitor of Pb pollution, considering that active uptake, rather than low concentration gradient, is driving the absorption of Pb from the water medium. Keywords: Lemna gibba; Bioaccumulation; Removal efficiency; Photosynthetic pigments; Bleaching; Phytoremediation

Desalination and Water Treatment (2017) 1–8

Macrophytes-cyanobacteria allelopathic interactions and their implications for water resources management-A review

Zakaria A. Mohamed

Department of Botany & Microbiology, Faculty of Science, Sohag University, Sohag 82524, Egypt

Macrophytes and phytoplankton including cyanobacteria are main primary producers in aquatic environments.Macrophytes can maintain water quality by suppressing phytoplankton growth through a number of mechanisms: while e.g. the absorption of high amounts of nutrients and the provision of refuge from predation for herbivorous aquatic fauna are widely accepted macrophyte functions, the role of their release of allelopathic substances in suppressing phytoplankton is increasingly being studied. Some macrophyte species can support the growth of epiphytic cyanobacteria providing them an advantage over planktonic species in the competition for nutrients. On the other hand, some cyanobacteria dominate in eutrophic water bodies and produce cyanotoxins that exert allelopathic substances which may contribute to the decline of macrophytes. Macrophytes can interact with these cyanotoxins in different ways including bioaccumulation and biotransformation. This review focuses on such allelopathic interactions between macrophytes and toxic cyanobacteria. The article also suggests methods for researchers and water resources managers for the application of macrophytes to control harmful cyanobacterial blooms and as phytoremediators for toxin elimination from water bodies.

Limnologica 63:122-132 (2017)

Isolation, Optimization and Characterization of Cellulases and Hemicellulases from *Bacillus Cereus* LAZ 518 Isolated from Cow Dung Using Corn Cobs as Lignocellulosic Waste

M. A. Abu-Gharbia, N. M. El-Sawy, A. M. Nasr and L. A. Zedan

As a result of the magnitude of the problem of the accumulation of agricultural wastes and increase the environment and economic problems caused of it . It was necessary to find a scientific solution to face this problem and convert these wastes to high-value products , by using microbial organisms such as bacteria .Corn cobs have been chosen from shandawil research station in sohag governorate as an example of agriculture wastes and has been treated by physical and chemical methods to remove lignin and retain cellulose and hemicellulose free of any impurities. One hundred bacterial isolates, isolated from Water, Soil and cow dung in Sohag governorate, 6 isolates from cow dung were tested for their ability to produce extracellular Cellulases and hemicellulases, of all these 6 isolates isolate number (41 had the highest potential for celluolytic and hemicelluolytic activity was chosen. From various morphological, biochemical and 16S rRNA, the isolate was identified to be *Bacillus cereus* LAZ 518. Physiological studies were conducted to determine the optimum cultural conditions for maximum cellulases and hemicellulases production by *Bacillus Cereus* LAZ 518. The highest enzyme yield was obtained after 48 hours incubation at 50 °C and pH 7.0 when corn cobs was used as sole carbon source, respectively Carboxymethyl cellulose (CMC) was found to be a good inducer for cellulases and hemicellulases production . High level of enzyme production was obtained with the addition of yeast extract as a nitrogen source at concentration of 0.1 %. Tween-80 as an addition to medium inceases enzymes production. When examining the properties of cellulases and hemicellulases it was found that enzymes had a high degree of constancy at a temperature 70° C and pH 5 and improved performance when added with elements such as cobalt, calcium, sodium, potassium, and substances such as urea ,EDTA , β-mercaptoethanol , Tween-60 ,Tween- 80 and oxidizing agents such as hydrogen peroxide and sodium peroxide , it has been found that enzymes were strongly inhibited when added with mercury or high concentrations of oxidizing agents and surfactants.

J. Pharm. Appl. Chem., 3, No. 2, 1-11 (2017)

New saprobic marine fungi and a new combination

Abdel-Wahab M. A., Dayarathne M. C., Suetrong S., Guo S.-Y., Alias S. A., Bahkali A. H., Nagahama T., Elgorban A. M., Abdel-Aziz F. A., Hodhod M. S., Al-Hebshi M. O., Hyde K. D., Nor N. A. B. M., Ka-Lai Pang K. L. & E. B. Gareth Jones E. B. G.

Department of Botany and Microbiology, Faculty of Science, Sohag University, Egypt

This paper documents five new saprobic marine fungi occurring on various substrata in the marine environment. *Bacusphaeria nypae* gen. *et* sp. nov. was discovered on bases of fronds of *Nypa fruticans* in Malaysia and phylogenetically, it belongs to the Tirisporellaceae (Tirisporellales, Diaporthomycetidae, Sordariomycetes) based on 18S and 28S rDNA. *Cryptovalsa avicenniae*, *Ceriosporopsis minuta* and *Jattaea mucronata* also belong to the Sordariomycetes; *Cr. avicenniae* was saprobic on *Avicennia marina* collected in Saudi Arabia, *J. mucronata* on intertidal decaying bark of *Rhizophora mucronata* while *Ce. minuta* was found on driftwood collected on a sandy beach in Japan. Phylogeny based on 18S and 28S rDNA placed *Cr. avicenniae* with other *Cryptovalsa* species in the Diatrypaceae. *Jattaea mucronata* groups well in the Calosphaeriales and is closely related to *J. algeriensis* based on a phylogeny using ITS and 28S rRNA and *RPB2* genes. *Aegeanispora elanii* gen. *et* sp. nov. is an asexual fungus which produces pycnidia on decaying driftwood collected in the Aegean Sea. Combined 18S and 28S rDNA phylogenetic analyses suggest that it is a member of the Pleosporales, Dothideomycetes. *Ceriosporopsis minuta* resembles *C. capillacea* with its tubular, long polar appendages of ascospores but dimensions of ascomata and ascospores for the former species are considerably smaller. *Ceriosporopsis* is considered the best genus to accommodate *C. minuta* without support from sequence data. *Sammeyersia* is established as a new genus to accommodate *Lulworthia grandispora*, a species unrelated to *Lulworthia fucicola*, the type species. The diagnostic characteristic for the genus is a melanized region at the base of the neck of the ascomata.

Botanica Marina (2017) 60: 469-488

Genetic analysis of *Plectranthus* L. (Lamiaceae) in Saudi Arabia based on RAPD and ISSR markers.

Kadry Abdel Khalik and Gamal Hariedy.

Department of Botany and Microbiology, Sohag University, Sohag, Egypt

The genetic diversity and phylogenetic analyses of seven species of the genus Plectranthus (Lamiaceae) from Saudi Arabia were carried out by using the Inter Simple Sequence Repeats (ISSR), Randomly Amplified Polymorphic DNA (RAPD), and combined ISSR and RAPD markers. Ten RAPD primers and five ISSR primers generated 137 polymorphic amplified fragments, which pointed a relatively high level of genetic variation in Plectranthus. RAPD markers revealed a higher level of polymorphism (105 bands) than ISSR (32 bands). The clustering of genotypes within groups showed difference upon comparison of RAPD and ISSR derived dendrograms. We could identify four clades within Plectranthus, which are largely in support, with a bit contradiction, of traditional groupings. Taxonomic and phylogenetic implications are discussed in comparison with the available gross morphological, anatomical, and phytochemical data. The results of this study present useful data for assessing the taxonomy of Plectranthus both at subgeneric and sectional levels. Moreover, our results indicate some level of resemblance among the species of subgenus Germanea and support the monophyly of this subgenus. The most interesting outcome of this analysis was identifying P. arabicus with distinguishing characters and suggesting that it should be treated as a distinct subgenus. In the same vein, distinguishing differences between the closely related endemic species P. asirensis and P. hijazensis were also noted suggesting that they should be placed in different subgenus. Similarly, P. asirensis and P. cylindraceus should be placed under a monophyletic group and this shows some closeness with P. tenuiflorus.

Pakistan Journal of Botany 49 (3): 1073-1084.

Notes for genera: Ascomycota

Nalin N. Wijayawardene, Kevin D. Hyde, Kunhiraman C. Rajeshkumar, David L. Hawksworth, Hugo Madrid, Paul M. Kirk, Uwe Braun, Rajshree V. Singh, Pedro W. Crous, Martin Kukwa, Robert Lu¨cking, Cletus P. Kurtzman, Andrey Yurkov, Danny Haelewaters, Andre´ Aptroot, H. Thorsten Lumbsch, Einar Timdal, Damien Ertz, Javier Etayo, Alan J. L. Phillips, Johannes Z. Groenewald, Moslem Papizadeh, Laura Selbmann, Monika C. Dayarathne, Gothamie Weerakoon, E. B. Gareth Jones, Satinee Suetrong, Qing Tian, Rafael F. Castan˜eda-Ruiz, Ali H. Bahkali, Ka-Lai Pang, Kazuaki Tanaka, Dong Qin Dai, Jariya Sakayaroj. Martina Hujslova´, Lorenzo Lombard, Belle D. Shenoy, Ave Suija, Sajeewa S. N. Maharachchikumbura, Kasun M. Thambugala, Dhanushka N. Wanasinghe, Bharati O. Sharma, Subhash Gaikwad, Gargee Pandit, Laura Zucconi, Silvano Onofri, Eleonora Egidi, Huzefa A. Raja, Rampai Kodsueb, Marcela E. S. Ca´ceres, Sergio Pe´rez-Ortega, Patrı´cia O. Fiuza, Josiane Santana Monteiro, Larissa N. Vasilyeva, Roger G. Shivas, Maria Prieto, Mats Wedin, Ibai Olariaga, Adebola Azeez Lateef, Yamini Agrawal, Seyed Abolhassan Shahzadeh Fazeli, Mohammad Ali Amoozegar, Guo Zhu Zhao, Walter P. Pfliegler, Gunjan Sharma, Magdalena Oset, Mohamed A. Abdel-Wahab, Susumu Takamatsu, Konstanze Bensch, Nimali Indeewari de Silva, Andre´ De Kesel, Anuruddha Karunarathna, Saranyaphat Boonmee, Donald H. Pfister, Yong-Zhong Lu, Zong-Long Luo, Nattawut Boonyuen, Dinushani A. Daranagama, Indunil C. Senanayake, Subashini C. Jayasiri, Milan C. Samarakoon, Xiang-Yu Zeng, Mingkwan Doilom, Luis Quijada, Sillma Rampadarath, Gabriela Heredia, Asha J. Dissanayake, Ruvishika S. Jayawardana, Rekhani H. Perera, Li Zhou Tang, Chayanard Phukhamsakda, Margarita Herna´ndez-Restrepo, Xiaoya Ma, Saowaluck Tibpromma, Luis F. P. Gusmao, Darshani Weerahewa, Samantha C. Karunarathna

Department of Botany and Microbiology, Sohag University, Sohag, Egypt

Knowledge of the relationships and thus the classification of fungi, has developed rapidly with increasingly widespread use of molecular techniques, over the past 10–15 years, and continues to accelerate. Several genera have been found to be polyphyletic, and their generic concepts have subsequently been emended. New names have thus been introduced for species which are phylogenetically distinct from the type species of particular genera. The ending of the separate naming of morphs of the same species in 2011, has also caused changes in fungal generic names. In order to facilitate access to all important changes, it was desirable to compile these in a single document. The present article provides a list of generic names of Ascomycota (approximately 6500 accepted names published to the end of 2016), including those which are lichen-forming. Notes and summaries of the changes since the last edition of 'Ainsworth & Bisby's Dictionary of the Fungi' in 2008 are provided. The notes include the number of accepted species, classification, type species (with location of the type material), culture availability, life-styles, distribution, and selected publications that have appeared since 2008. This work is intended to provide the foundation for updating the ascomycete component of the ''Without prejudice list of generic names of Fungi'' published in 2013, which will be developed into a list of protected generic names. This will be subjected to the XIXth International Botanical Congress in Shenzhen in July 2017 agreeing to a modification in the rules relating to protected lists, and scrutiny by procedures determined by the Nomenclature Committee for Fungi (NCF). The previously invalidly published generic names Barriopsis, Collophora (as Collophorina), Cryomyces, Dematiopleospora, Heterospora (as Heterosporicola), Lithophila, Palmomyces (as Palmaria) and Saxomyces are validated, as are two previously invalid family names, Bartaliniaceae and Wiesneriomycetaceae. Four species of Lalaria, which were invalidly published are transferred to Taphrina and validated as new combinations. Catenomycopsis Tibell & Constant. is reduced under Chaenothecopsis Vain., while Dichomera Cooke is reduced under Botryosphaeria Ces. & De Not. (Art. 59).

Fungal Diversity (2017) 86: 1-594

Micromorphological studies on the genus *Lotus* L. (Fabaceae: Loteae) from Egypt

Momen Zareh, Ahmed Faried, Nashwa Farghaly

Department of Botany and Microbiology, Sohag University, Sohag, Egypt

Trichomes, epidermal cell features, and seed coat sculpturing of 12 *Lotus* taxa from Egypt were studied using scanning electron microscopy. In addition, statistical analysis for the taxa under investigation was carried out. The results revealed that trichomes have high taxonomic significances between studied taxa. Anticlinal and periclinal cell walls and epidermal cell shape for the stem, leaf, and calyx for each taxon were examined. Seed coat sculpturing exhibited 4 main different surface patterns ategories: rugose, reticulate, sulcate, and verrucate. These features can serve as good diagnostic characters at the species level of the genus *Lotus*.

Turkish Journal of Botany (2017) 41: 273-288

Natural products of *Nothophoma multilocularis* sp. nov. an endophyte of the medicinal plant *Rhazya stricta*

Mohamed A. Abdel-Wahab, Ali H. A. Bahkali, Abdallah M. El-Gorban and Mohamed S. Hodhod
Department of Botany and Microbiology, Sohag University, Sohag, Egypt

In the present study, we isolated endophytic fungi from the medicinal plant *Rhazya stricta* from Saudi Arabia. Twenty-eight fungal isolates representing five species were isolated from 21 leaves (10 young and 11 old) of *R. stricta*. These fungi include two species of *Alternaria*, *Aspergillus* sp., *Nothophoma* sp. and one species producing sterile mycelia. Based on morphology and phylogenetic analyses of LSU rDNA, we describe *Nothophoma* (E-2-5) as a new species to science. *Nothophoma multilocularis* is characterized by its large multiloculate pycnidia and its larger conidial dimensions than the six described *Nothophoma* species. A table (Table 3) comparing the morphology and the host of the seven *Nothophoma* species is provided, along with a key for their identification. The culture filtrates of the isolated endophytic fungi were extracted using ethyl acetate and were tested against pathogenic microbes. Fifty-five bioactive chemical compounds were identified from the crude extracts of *Nothophoma multilocularis* using GC-MS. Ten major bioactive compounds were recorded namely: Di-n-octyl phthalate representing 53.98 % of the crude extract, 2-Allyl-3,4-dimethoxybenzaldehyde (10.26 %), Maltol (9.45 %), Cetene (2.73 %), 1-Tetradecene (2.07 %), E-15-Heptadecenal (2.06 %), 2,5-Cyclohexadien-1-one (1.88 %), 1-Octadecene (1.36 %), Diethyldithiophosphinic acid (1.17 %) and Phenol, 2,4-di-t-butyl-6-nitrophenol (1.07 %). These compounds showed strong antimicrobial activity in combination.
Doi 10.5943/mycosphere/8/8/15

Floristic composition and vegetation: Environmental relationships of Wadi Fatimah, Mecca, Saudi Arabia

Kadry Abdel Khalik, Iman H. Al-Gohary, Yassin Al-Sodany
Department of Botany and Microbiology, Sohag University, Sohag, Egypt

The present study aimed to determine floristic composition, the structure of the vegetation, and species distribution at 16 sample plots in Wadi Fatimah, Mecca, Saudi Arabia, highlighting the ecological factors that affect species distribution. The study revealed 100 plant species belonging to 34 families. Fabaceae and Poaceae were the dominant families, and chamaephytes and therophytes were predominant life forms, which demonstrate a typical desert life-form spectrum. Altitude showed a highly significant association with species frequency distribution. The highest species richness value of 23 species per plot was recorded in the coastal plain (Vegetation groups II & III). The lowest species richness value of 9 species per plot was recorded in the littoral salt marsh (Vegetation group I). Chorological analysis exhibited the Saharao-Arabian–Sudano-Zambezian chorotypes, 47% of the studied species were bi-regional. Using TWINSPAN, DCA, and CCA multivariate analysis, four major vegetation groups were classified into three main ecosystems (I) *Halopeplis perfoliata, Suaeda fruticosa, Acacia tortilis*, and *Suaeda fruticosa*, representing the littoral salt marsh; (II) *Rhazya stricta* and *Haloxylon salicornicum*, characterized by the coastal plain; and (III) *Senna italica, Glinus lotoides*, and *Tribulus macropterus* were the leading groups in the inland mountainous country. The CCA ordination showed that the separation of Vegetation group III along the axis was affected by Mg, K, and P concentration, and VG IV was significantly associated with silt, clay, and fine sand content. Furthermore, the Vegetation group I was significantly correlated with Na and Ca concentration, and VG II group was significantly correlated with heavy metal concentrations of elements as Fe, Pb, Zn, Ni, and Cu.
Arid Land Research and Management 2017 31 (3): 316-334

HPLC Profile of Phenolic Constituents, Essential Oil Analysis and Antioxidant Activity of Six *Plectranthus* Species Growing in Saudi Arabia

Usama Shaheen, Kadry Abdel Khalik, Mohamed I. S. Abdelhady, Mohamed Aborehab
Department of Botany and Microbiology, Sohag University, Sohag, Egypt

Some plants used in Saudi folk medicine have little data about their phytochemical constituents. The HPLCPDA profile of phenolic constituents, GC-MS composition of essential oil and DPPH antioxidant capacity were performed for six Plectranthus species (P. arabicus, P. asirensis, P. pseudomarrubioides, P. barbatus, P. hijazensis and P. aegyptiacus) growing in Saudi Arabia. The essential oil content of the aerial parts of these species was varied from 0.1% to 0.3% v/w. Their volatile oils compose mainly of monoterpene hydrocarbons (18.79%, 8.52%, 39.14%, 71.27%, 0.97%, 26.77%), oxygenated monoterpenes (33.72%, 8.16%, 25,51%, 0.75%, 4.59%, 58.49%), sesquiterpene hydrocarbons (9.27%, 26.06%, 2.55%, 0%, 30.48%, 9.11%), and oxygenated sesquiterpenes (30.23%, 33.38%, 24.36%, 0%, 44.2%, 0%) in (P. arabicus, P. asirensis, P. pseudomarrubioides, P. barbatus, P. hijazensis and P. aegyptiacus) respectively. Thymol was the only phenolic component detected in P. aegyptiacus with high concentration 58.49%. The HPLC profiles of these plants were recorded and it imply for close similarity with minor differences between the six species of Plectranthus. Rosmarinic acid and gallic acid were detected in the studied species. All samples showed significant anti-free radical activity in comparison with trolox and ascorbic acid.
Journal of Chemical and Pharmaceutical Research (2017). 9(4): 1-20

Action of cadmium toxicity on growth, physiological activities and subcellular components of watercress (Eruca sativa L.) plant: The protective role of salicylic acid

Khalaf Ali Fayez
Department of Botany and Microbiology, Sohag University, Sohag, Egypt

Seed germination, seedling growth, leaf morphology, physiological alterations and cell ultrastructure of watercress (Eruca sativa L.) plant under cadmium (Cd) and salicylic acid (SA) treatments were studied. Cd concentrations (0.1 and 0.5 mM), decreased seed germination, shoot and root lengths, but with 1 mM Cd was inhibited. Cd-treated watercress displayed leaf chlorosis. Photosynthetic pigment contents of Cd-treated plants were declined with increasing Cd treatments. Malondialdehyde (MDA) and total phenolic contents increased while soluble proteins decreased in response to Cd treatments. Electron microscopic observations of Cd-treated plants revealed disorganization in the internal structure of chloroplasts and mitochondria. The lamellae and stroma thylakoids of chloroplasts were degenerated. An increase of plastoglobuli number within chloroplasts was observed in Cd-treated leaves. Addition of SA (50 and 100 µM) to 0.5 mM Cd improved seed germination and seedling shoot length but reduced root length of watercress compared to that only treated with Cd, however, SA was not able to alleviate seed germination at 1 mM Cd. Spraying of 50 and 100 µM SA three days before Cd-treated plants reduced chlorosis and increased pigment contents of leaves compared to that only treated with Cd. SA caused a decrease in MDA and soluble proteins contents, and increased total phenolic compounds of Cd treated plants. On the level of ultrastructure, SA-treated plants protected grana organization and reduced plastoglobuli number of chloroplast against Cd effect. The results correlated to oxidative stress, such as chlorosis, decreased photosynthetic pigment content, increased lipid peroxidation, and damage of cell organelles in response to Cd effect were resulted. SA pretreatment reduced the negative effect of Cd on plant parameters mentioned above associated with the decrease of oxidative stress.
Research Journal of Pharmaceutical, Biological and Chemical Sciences (2017) RJPBCS 8(2), 1853

Impact of Glyphosate Herbicide and Salicylic Acid on Seed Germination, Cell Structure and Physiological Activities of Faba Bean (*Vicia faba* L.) Plant

Khalaf Ali Fayez[1,2] and Esmat F. Ali[1,3]*

Department of Botany and Microbiology, Sohag University, Sohag, Egypt

The effects of salicylic acid (SA), glyphosate (Gly) and interaction of SA + Gly on seed germination and seedling growth, leaf morphology, cell ultrastructure and physiological alterations of *Vicia faba* plants were evaluated. SA (50 and 100 µM) reduced root seedling growth. Exposure to 250 and 500 µM Gly with or without SA caused an inhibition in seed germination and seedling growth of *V. faba* plants. Chlorosis, necrosis, welting, and growth reduction of *V. faba* was noticed in response to Gly and SA + Gly treatments. The photosynthetic pigment (Chlorophyll *a* (Chl *a*), Chlorophyll *b* (Chl *b*) and carotenoid (Car) contents of glyphosate and SA + Gly-treated plants were declined compared to the control. Electron microscopic observations of glyphosate-treated plants revealed disorganization in the internal structure of chloroplasts. Formation of vesicles within chloroplasts was observed in glyphosate and interaction of SA + Gly-treated plants. The lamellae and stroma thylakoids of chloroplasts were degenerated. Contents of soluble proteins and total phenolic compounds were decreased in glyphosate and SA + Gly-treated plants compared to the control. Peroxidase (POX) activity significantly increased with application of SA and glyphosate as well as with the interaction of SA + Gly compared to the control. Malondialdehyde (MDA) content in glyphosate and interaction of SA + Gly-treated plants increased compared to untreated one. The obtained results indicate that the root seedling growth of *V. faba* is sensitive to SA and Gly, while shoot was only sensitive to Gly herbicide treatments. The vegetative growth, cell organelles and physiological functions was negatively affected by Gly. Application doses of SA appear to be did not alleviate the toxicity of Gly herbicide on *V. faba*.

Annual Research & Review in Biology 17(4): 1-15, 2017; Article no. ARRB.36097

Toxicity of biosynthetic silver nanoparticles on the growth, cell ultrastructure and physiological activities of barley plant

K. A. Fayez• B. A. El-Deeb• N. Y. Mostafa

Department of Botany and Microbiology, Sohag University, Sohag, Egypt

Abstract Silver nanoparticles (AgNPs) were biosynthesized using the cell-free filtrate of bacterium Proteus mirabilis, reacted with 1 mM of AgNO3 solutions at 37 _C. The synthesis of AgNPs was monitored by UV–Vis spectroscopy and transmission electron microscopy (TEM) equipped with selected area electron diffraction (SAED). The results point to formation of spherical to cubical particles of AgNPs ranging in size from 5 to 35 nm with an average of 25 nm in diameter. The toxicity of Ag on barley (Hordeum vulgare L. cv. Gustoe) that was subjected to Ag? as AgNO3 and AgNPs was explored. The grain germination and seedling growth of barley decreased in the presence of 0.1 mM Ag? and was inhibited at 1 mM Ag?. In contrast, our results indicated that the AgNPs at low concentration (0.1 mM) could be useful for barley grain germination and seedling growth. However, the higher concentrations of AgNPs (0.5 and 1 mM) reduced grain germination and exhibited a stronger reduction in the root length. A decline in the photosynthetic pigments and disorganization of chloroplast grana thylakoids in Ag? And AgNPs-treated plants confirmed the leaf chlorosis. An increase of plastoglobuli within chloroplasts was observed in Ag? and AgNPs-treated leaves. Ag? caused dense aggregation of nuclear chromatin materials and degeneration of mitochondria. Ag? and AgNPs increased contents of malondialdehyde, soluble proteins, total phenolic compounds and activity of guaiacol peroxidase in barley leaves; these results point to activation of plant defence mechanisms against oxidative stress in barley.

Acta Physiol Plant (2017) 39:155

Exhalation Air Fungal Culture of Mechanically Ventilated Aspergillosis Suspected Patients in Concordance with Other Conventional Diagnostic Techniques

M Bassam Aboul-Nasr, Abdel-Nasser Zohri, Mohamed Adam and Enas Mahmoud Amer
Department of Botany and Microbiology, Sohag University, Sohag, Egypt

Aspergillosis remains one of the most challenging areas of illness. It has recently emerged as a world-wide health care problem, owing to extensive use of broad spectrum antibiotics, immunosuppressive agents and increasing population of terminally ill and debilitated patients. The ultimate aim of this investigation is to minimize morbidity and mortality of mechanically ventilated aspergillosis suspected patients, who have been notoriously difficult to be diagnosed and treated, by developing an accurate and easy diagnostic tool comparable to other conventional methods. Two hundred twenty seven suspected aspergillosis patients were screened for fungal infection using different conventional tools to evaluate different respiratory specimens sputum, bronchoalveolar lavage, plural fluid, blood, biopsy and ELISA technique for galactomannan and (1-3)-β-D-glucan antigens in serum and bronchoalveolar lavage. Four *Aspergillus* species (*A. niger*, *A. fumigatus*, *A. flavus* and *A. terreus*) were isolated and identified morphologically and genetically using the conventional diagnostic tools from suspected patients in all positive cultures. The results of the exhalation air of twenty three mechanically ventilated aspergillosis suspected patients came in accordance with those of the conventional methods used. Thus, exhalation air culture is an easily performed bedside tool for diagnosis of aspergillosis in ventilated patients.
Biology and Medicine (Aligarh) 2017, 9:6

Impact of Enzymes and Toxins Potentiality of Four Aspergillus Species to Cause Aspergillosis

Abdel-Nasser Zohri, M Bassam Aboul-Nasr, Mohamed Adam, Mohamed A Mustafa and Enas Mahmoud Amer
Department of Botany and Microbiology, Sohag University, Sohag, Egypt

Aspergillus species are the main causing agents of invasive apergillosis chest disease. Eighty isolates of *Aspergillus* species, *A. flavus* (20), *A. fumigatus* (15*), A. niger* (30) and *A. terreus* (15 isolates), previously isolated and identified from aspergillosis suspected patients at our lab in Assiut university hospitals, were assayed for their enzymes and toxins profile. The results revealed that, all of the tested isolates were able to utilize calf lung tissue and produce catalase and peroxidase enzymes. Meanwhile, 82.5-90% of the fungal isolates had the ability to produce protease, lipase, urease and phospholipase, whereas, 70% of isolates exhibited hemolytic activities. Thin layer chromatography (TLC) of the cleaned extracts of the tested isolates exhibited the ability of all *A. flavus* isolates assayed to produce aflatoxins B1 and G1, 53%, moreover, *A. fumigatus* isolates produced fumagillin and gliotoxin. On the other side, 43.3% and 23.3% of *A. niger* isolates produced ochratoxins and gliotoxin respectively. Virulence assay of 10 µl of gliotoxin standard and cleaned extracts of *A. fumigatus* toxic isolates showed necrotic area on Guinea Pigs lungs compared to the control. Thus, opportunistic fungi isolated from aspergillosis patients possess high enzymatic and toxic profile that might play an important role in their mycopathy.
Biology and Medicine (Aligarh) 2017, 9:5

Physico-chemical changes in karkade (Hibiscus sabdariffa L.) seedlings responding to salt stress

Galal A.

Department of Botany and Microbiology, Sohag University, Sohag, Egypt

Salinity is one of the major abiotic stress factors affecting series of morphological, physiological, metabolic and molecular changes in plant growth. The effect of different concentrations (0, 25, 50, 100 and 150 mM) of NaCl on the vegetative growth and some physiological parameters of karkade (Hibiscus sabdariffa var. sabdariffa) seedling were investigated. NaCl affected the germination rate, delayed emergence and retarded vegetative growth of seedlings. The length of seedling as well as the leaf area was significantly reduced. The fresh weight remained lower in NaCl treated seedlings compared to control. NaCl at 100 and 150 mM concentrations had significant effect on the dry matter contents of the treated seedlings. The chloroplast pigments in the treated seedlings were affected, suggesting that the NaCl had a significant effect on the chlorophyll and carotenoid biosynthesis. The results showed that the salt treatments induced an increase in proline concentration of the seedlings. The osmotic potential (ψs) of NaCl treated seedlings decreased with increasing NaCl concentrations. Salt treatments resulted in dramatic quantitative reduction in the total sterol percent compared with control ones. Salt stress resulted in increase and decrease of Na^+ and K^+ ions, respectively. NaCl salinity increased lipid peroxidation. SDS-PAGE was used to evaluate protein pattern after applying salt stress. High molecular weight proteins were intensified, while low molecular weight proteins were faint. NaCl at 100 and 150 mM concentration distinguished with new protein bands. Salt stress induced a new peroxidase bands and increased the band intensity, indicating the protective role of peroxidase enzyme.

Acta Biol Hung. 2017 68, 73-87

Synthesis, *in vitro* antibacterial and *in vivo* anti-inflammatory activity of some new pyridines

Abd-El-Badih A. G. Ghattas, Ahmed Khodairy, Hassan M. Moustafa, Bahgat R. M. Hussein, Marwa M. Farghaly, and Moustafa O. Aboelez

Department of Botany and Microbiology, Sohag University, Sohag, Egypt

Reaction of 4,6-diamino-3-cyano-2-methylthiopyridine (**I**) with chloroacetyl chloride or acetic acid afforded the corresponding 6-acetamide derivatives **IIa** and **IIb**, respectively. Chloroacetamide derivative **IIa** reacted with various thiols, secondary amines, potassium thiocyanate, compounds containing active methylene group, 1-anilino-2,2-dicyanoethenethiolate, and o-mercatocyanopyridines to give S-alkyl, N-alkyl, thiazole, pyrrole, thiophene, and thienopyridine derivatives, respectively. Antibacterial and anti-inflammatory activities of some new pyridine derivatives were studied.

Pharmaceutical Chemistry Journal, 51 (8), November, 2017 (Russian Original 51 (8), August, 2017)

Antioxidant and antimicrobial activities of the methanolic extracts of some edible seed spices

Deya Eldeen Mohammed Radwan, Ashraf Mohammed Mohammed Essa and Dia Mohammed Soltan
Department of Botany and Microbiology, Sohag University, Sohag, Egypt

This study was conducted to screen the antioxidant and antimicrobial activities of the methanolic extracts of ten types of edible seeds that are used commonly as food additives and beverages. Contents of flavonoids, polyphenols and ascorbate as well as total antioxidant activity of extracts were analyzed. At the same time, the antimicrobial activities were performed against different bacterial and fungal strains. Extracts of Cuminum cyminum and Pimpinella anisum showed the highest values of polyphenols while elevated levels of flavonoids and ascorbic acid were recorded in Linum usitatissimum, Piper nigrum, Pimpinella anisum and Portulaca oleraceae extracts. The tested extracts demonstrated a high capability to scavenge DPPH free radicals at levels above 89%. Furthermore, seed extracts of Piper nigrum, Brassica alba, recorded a remarkable antibacterial activities against wide range of bacterial strains. Simultaneously, the seed extracts of Coriandrum sativum, Cuminum cyminum, Piper nigrum and Nigella sativa recorded high potentiality to inhibit the growth of various fungal strains. It can be concluded that Cuminum cyminum, Linum usitatissimum, Piper nigrum, Pimpinella anisum, Coriandrum sativum and Nigella sativa seeds could have beneficial impacts on human health as a result of their high antioxidant and antimicrobial activities.
Journal of Environmental Studies 17:11-23

In vitro propagation, microtuberization, and molecular characterization of three potato cultivars

J. Salem and A. M. Hassanein
Department of Botany and Microbiology, Sohag University, Sohag, Egypt

Sprouts of potato tubers were excised from the three potato cultivars Agria, Hermes, and Spunta, sterilized and subjected to shoot formation and propagation on Murashige and Skoog (MS) medium supplemented with 1 mg dm^{-3} 6-benzylaminopurine (BAP) + 0.5 mg dm^{-3}gibberellic acid. Shoots were rooted on MS medium supplemented with 1 mg dm^{-3} indole-3-butyric acid. To increase shoot vigour prior tuber formation, shoots were subcultured on MS medium supplemented with 0.56 mg dm^{-3} BAP, 0.11 mg dm^{-3} 2,4-dichlorophenoxyacetic acid, and 0.96 mg dm^{-3} naphthaleneacetic acid. Under dark, microtuberization on MS media supplemented with 4 mg dm^{-3} of both BAP and kinetin was better than 4 mg dm^{-3} BAP alone, where they induced higher number of microtubers per shoot and/or the percentage of shoots that formed microtubers. The highest frequency of microtuber formation was achieved when sucrose at high concentration (8 %) was used as carbon source in culture media. Glucose ranked at the second position whereas fructose reduced the microtuber formation frequency when it was used alone or in combination with glucose. Under the applied culture conditions, cvs. Agria and Hermes showed better micropropagation and microtuberization in comparison to cv. Spunta. In addition, isozyme and RAPD techniques revealed that Agria and Hermes are closer to each other when compared with the third cultivar.
Biologia Plantarum (2017), 61 (3), 427-437

Differential responses of esterase isoenzyme of peanut to salinity and drought as influenced by salicylic acid

Dia M. Soltan and Jehan M. Salem
Department of Botany and Microbiology, Sohag University, Sohag, Egypt

The effect of salinity, drought and salicylic acid on growth and esterase expression of peanut plants were studied. Seeds of peanut were able to germinate even under relatively high concentration of NaCl (157.5 mM) or PEG (25%). In general, seedling growth was less tolerant to salt stress than vegetative growth stage of peanut plants grown in hydroponic culture containing NaCl, vice versa was detected when PEG was used. While the application of 0.1 mM salicylic acid (SA), inhibit peanut seed germination, it improved seedling and vegetative growth parameters under moderate concentration of NaCl (105 mM). Seedling and vegetative growth parameters were significantly reduced by increase the concentrations of PEG. Application of SA improved growth parameters of peanut plants subjected to 10% PEG. In hydroponic culture, peanut was more sensitive to PEG than NaCl where plants wilted in three days under relatively high PEG concentrations. Root of peanut seedlings increased the esterase expression under the influence of moderate salinity (105 mM) and drought (10% PEG) stresses through increase the number and staining intensity of isoenzyme forms. Increase the number of isoenzyme forms and/or staining intensity as an indicator of increased activity of the enzyme was detected when peanut plants were hydroponically grown in solution with relatively high NaCl or PEG. Application of SA increased the number and/or the staining intensity of isoenzyme forms during seedling or vegetative growth in hydroponic culture containing relatively high concentration of NaCl or PEG.

Journal of Environmental Studies [JES] 2017. 16: 9-20

Chemical Structure of Natural roducts and haracterization of Secretory issue of Sweet Basil (*Ocimumbasilicum L.*)Under Lead Stress

Naglaa Y. Abdallah, Amany M. Aboel kassem and Omer M. Elsheikh
Department of Botany and Microbiology, Sohag University, Sohag, Egypt

The present study was done to test the effect of Pb treatments on secretory tissue and the chemical structure of the essential oils of basil (Ocimumbasilicum L.). Lead treatments were as follow: 100, 250, 500 and 7500 ppm in addition to control. The experiment was done on Ocimumbasilicum L. in a greenhouse, arranged as a randomized complete block design with three replications for each treatment for 60 days.The morphological structure of the secretory tissue of basil leaves was investigated, using SEM (scanning electron microscope).The chemical composition of natural products of sweet basil exposed to lead treatments extracted by methanol and n-hexane, was analyzed by gas chromatography coupled with mass spectrometry (GC–MS). The Results revealed the presence of organic aldehyde, diterpenes, monoterpenes, and phenolic compounds in addition to unknown substances. Compounds in the hexane fraction included camphor, 1,8-Cineol, L-,alpha-Terpeniol, Eugenol, Methyl Eugenol, Beta Elemene, Pachoulene, gamma Cadinene, 9,12,15-octadecatrienoic acid,methyl ester, Delta Cadinene, Linolenic acid β- cadinene,stearic acid, and an unknown substances . Compounds in the methanol fraction included furfural, 1,8-Cineol, 4H-pyran-4-one,2,3-dihydro-3,5-dihydroxy-6-methyl, trans geraniol, β-Linalool,L-,alpha-Terpeniol, Alpha-Fenchyl acetate, Eugenol, Methyl Eugenol, 9,12,15-octadecatrienoic acid, methyl ester, gamma Cadinene, Linolenic acid, β-elemene, bicycle[3.1.1]hept-2-ene,2,6-dimethyl-6-[4-methyl-3-pentenyl]- and unknown substances. Results were concluded that Ocimumbasilicum is tolerant to lead treatments until 200 ppm, so it can be used as alternative crops for Pb enriched soils.

Journal of ecology of Health & Environment 5 (2), 57-64 (2017)

Identification and in vitro Susceptibility Pattern of Fungal Infection Isolated from Patients with Otomycosis

Abeer Sheneef, Hameda Hassan, Khaled A. Ali, Mahmoud Saad-Eldin, Amira Esmail
Department of Botany and Microbiology, Sohag University, Sohag, Egypt

Otomycosis is a superficial fungal infection affecting the pinna and the external auditory canal, It is common worldwide but more prevalent in tropical and subtropical countries. Objectives: The aim of this study was to determine the etiologic agents causing otomycosis in our hospital as well as their susceptibility to the commonly used antifungal agents. Methodology: This was a hospital based descriptive study conducted on 122 patients attending the outpatient clinic of ear, nose and throat (ENT) department of Sohag university hospital and fulfilling our inclusion and exclusion criteria during April 2016 to April 2017 . Ear discharge specimens were collected on sterile cotton swabs for direct microscopic examination and inoculation on Sabouraud′s Dextrose Agar. Identification of yeast species was done by Vitek-2 automated system, in vitro antifungal susceptibility testing was done using disc diffusion method against the commonly used antifungal drugs. Results: In this study 102/122(83.61%) of the collected samples were positive for fungal infection. The most common fungal pathogens isolated from patients with otomycosis were Aspergillus and candida species, Aspergillus niger was the predominant fungal isolate (51%). Determination of in vitro antifungal susceptibility pattern showed that the mould isolates had the highest sensitivity to Voriconazole (93.48%) followed by Turbinafine (75%), while the highest resistance was to Fluconazole (100%) followed by Amphotericin B (41.3%). For the yeast isolates, the highest sensitivity was to Nystatine (88.24%) followed by Amphotericin B (82.35%), while the highest resistance was to Turbinafine (100%) followed by Itraconazole (94.12%).
Egyptian Journal of Medical Microbiology Volume 26 / No.3 / July 2017 53-59

Pollen morphology and numerical analysis of *Tamarix* L. (Tamaricaceae) in Egypt and its systematic implication

Ahmed Elkordy and Ahmed Faried
Botany & Microbiology Department, Fac. of Science, Sohag University, 82524, Egypt

A palynological and multivariate study of six species of *Tamarix* L. distributed in Egypt was carried out. Pollen morphology was examined by Light Microscope (LM) and Scanning Electron Microscope (SEM). The systematic study of these species was conducted by means of numerical analysis using UPGMA clustering and PCO analysis based on 33 morphological characters, including life form, vegetative parts, fruits, floral characters, seeds and pollen grains. Pollen grains were found to be monads, radially symmetrical, isopolar, small-sized and homocolpate. *Tamarix nilotica* can be easily separated from other taxa by its subprolate pollen shape. Two major clades were identified by multivariate analysis of morphological characters; one of them included three species, namely *T. amplexicaulis*, *T. passerinoides* and *T. macrocarpa.* Our results indicate that there is a wide range of morphological similarity among the species of section Polyadenia. The other clade included *T. aphylla*, *T. tetragyna* and *T. nilotica* from section Tamarix and section *Oligadenia*.
Bangladesh J. Plant Taxon. 24(1): 91–105, 2017 (June)

Impact of some essential oils on the growth of toxigenic fungi and their toxin production

Zohri A. A., Saber S. M., Youssef M. S. and Marwa Abdel-Kareem, M
Department of Botany and Microbiology, Sohag University, Sohag, Egypt

The impact of twelve essential oils (ginger, black pepper, black cumin, turmeric, baladi mint, peppery mint, cumin, marjoram lupine, cinnamon, thyme and cloves) on the growth of 11 toxigenic fungi and their ability for producing toxins were examined. Thyme, clove, baladi mint, peppery mint and cumin completely inhibited the growth of all tested fungi at two tested concentrations (10 and 50 µl/ 20 ml medium). Marjoram essential oil completely inhibited the fungal growth at 50 µl. Cinnamon essential oil exhibited moderate inhibitory effect on the growth of all tested fungi at 50 µl. Ginger oil generally stimulated the growth of most the tested fungi. Black pepper, turmeric and lupine were recorded as low active oils. Whereas, Black cumin essential oil did not display any inhibitory effect on the growth of the toxigenic fungi at 50 µl. Thyme, clove and mint essential oils (50 µl/ 50 ml medium) completely inhibited toxin production by all the tested toxigenic fungi. Black pepper and ginger essential oils reduced mycotoxin formation.
Journal of Environmental Studies [JES] 2017, 17: 25-34

Impact of some essential oils on the growth of toxigenic fungi and their toxin production

Zohri A. A., Saber S.M., Youssef, M.S. and Marwa Abdel-Kareem M.
[1]*Botany & Microbiology Department, Faculty of Science, Assiut University, Egypt*
[2]*Botany Department, Faculty of Science, Sohag University, Egypt*

The impact of twelve essential oils (ginger, black pepper, black cumin, turmeric, baladi mint, peppery mint, cumin, marjoram lupine, cinnamon, thyme and cloves) on the growth of 11 toxigenic fungi and their ability for producing toxins were examined. Thyme, clove, baladi mint, peppery mint and cumin completely inhibited the growth of all tested fungi at two tested concentrations (10 and 50 µl/ 20 ml medium). Marjoram essential oil completely inhibited the fungal growth at 50 µl. Cinnamon essential oil exhibited moderate inhibitory effect on the growth of all tested fungi at 50 µl. Ginger oil generally stimulated the growth of most the tested fungi. Black pepper, turmeric and lupine were recorded as low active oils. Whereas, Black cumin essential oil did not display any inhibitory effect on the growth of the toxigenic fungi at 50 µl. Thyme, clove and mint essential oils (50 µl/ 50 ml medium) completely inhibited toxin production by all the tested toxigenic fungi. Black pepper and ginger essential oils reduced mycotoxin formation. Key words: toxigenic fungi, mycotoxins, essential oils.
Journal of Environmental Studies [JES] 2017, 17: 25-34

Inhibition of three toxigenic fungal strains and their toxins production using selenium nanoparticles

Marwa Mahmoud Abdel-Kareem[1], Abdel-Naser Ahmed Zohri[2]

[1]*Botany Department, Faculty of Science, Sohag University, EG-82524 Sohag, Egypt*

[2]*Botany & Microbiology Department, Faculty of Science, Assiut University, EG-71516 Assiut, Egypt*

Spoilage and poisoning of foods by microfungi are a major problem, especially in developing countries. While selenium nanoparticles (Se-NPs) have been used for a wide range of applications including antibacterial, antioxidant and anticancer applications, the effects of Se-NPs on fungal strains remain for the most part unknown to date. Our research is a pioneering attempt to evaluate the antifungal activity and antimycotoxin properties of Se-NPs (32 nm). Se-NPs at different concentrations were evaluated against the growth and mycotoxins production of three toxigenic fungal strains. The growth of *Aspergillus parasiticus, A. ochraceus* and *A. nidulans* was completely inhibited using 7000, 9000 and 3000 µg/ml of Se-NPs, respectively, while the complete inhibition in aflatoxins, ochratoxin A and sterigmatocystin production was reported by addition of 2000, 2000, and 800 µg/ml of Se-NPs, respectively. Results of this study show that Se-NPs were effective against the fungal strains tested and their toxin production. These results suggest that Se-NPs could be used as an effective microfungicide in agricultural and food safety applications against toxigenic microfungi

Czech mycology 69(2): 193-204, 2017

Responses of maize crop (Zea mays L.) to foilar spraying with humic acid at different nitrogen levels

E. I. Mohamed[1], Fayza A. Faheed[2] and Huda M. Mahmoud[1]

[1]Soil, Water and Environment Research Institute, Agriculture Research Center, Giza, Egypt.

[2]Botany Department, Faculty of Science, Sohag university, 82524 Sohag, Egypt.

Three field experiments in split-split plot design were carried out at Agriculture Research Center, Shandweel Research Station, Sohag Governorate, during the summer seasons 2010, 2011 and 2012 on clay loom soil to evaluate the effect of foliar spray of humic acid (4 cm^3/L) at 30 and 45 days from sowing, under three levels of nitrogen fertilizer (0, 90, and 120 kg N/fed.) on plant growth parameters, some biochemical and mineral contents (NPK) in leaves and grains of two maize hybrids (Single cross Pioneer 30K09 and Three way cross-310). Results showed that S.C.

Pioneer 30K09 hybrid surpassed T.W.C.-310 hybrid in the values of P_N, E and Gs as well as N and K-content in leaves and grains, while T.W.C.-310 hybrid surpassed S.C. Pioneer 30K09 hybrid in the values of crude protein content in grains, P-content in both leaves and grains also in N-content in grains, however there were no significant differences between the two maize hybrids in respect to chlorophyll, dry weight, leaf total carbohydrate and grain oil contents. There were gradual and significant increases in all parameters by increasing nitrogen fertilizer dose, the most effective dose of nitrogen fertilizer was 120 kg N/fed. for the most traits, while, application of 90 kg N/fed. led to significant and highest values of P_N, E and Gs, also, P and K-content in leaves and K-content in grains. Thus, it could be concluded that foliar spraying with humic acid combined with adding 90 kg N/fed. gave higher values of all criteria than those obtained by only the recommended dose (120 kg N/fed). Moreover, the two examined hybrids responded to spraying HA under 120 kg N/fed. comparing with their values at the recommended dose only.

Key words: Gas exchange, Humic acid, Nitrogen fertilizer

Journal of Environmental Studies [JES] 2017, 16: 55-74

Fungal diversity notes 603 - 708: taxonomic and phylogenetic notes on genera and species

Kevin D. Hyde, Chada Norphanphoun, Vanessa P. Abreu, Anna Bazzicalupo, K. W. Thilini Chethana, Marco Clericuzio, Monika C. Dayarathne, Asha J. Dissanayake, Anusha H. Ekanayaka, Mao-Qiang He, Sinang Hongsanan, Shi-Ke Huang, Subashini C. Jayasiri, Ruvishika S. Jayawardena, Anuruddha Karunarathna, Sirinapa Konta, Ivana Kusˇan, Hyun Lee, Junfu Li, Chuan-Gen Lin, Ning-Guo Liu, Yong-Zhong Lu, Zong-Long Luo, Ishara S. Manawasinghe, Ausana Mapook, Rekhani H. Perera, Rungtiwa Phookamsak, Chayanard Phukhamsakda, Igor Siedlecki, Adriene Mayra Soares, Danushka S. Tennakoon, Qing Tian, Saowaluck Tibpromma, Dhanushka N. Wanasinghe, Yuan-Pin Xiao, Jing Yang, Xiang-Yu Zeng, Faten A. Abdel-Aziz, Wen-Jing Li, Indunil C. Senanayake, Qiu-Ju Shang, Dinushani A. Daranagama, Nimali I. de Silva, Kasun M. Thambugala, Mohamed A. Abdel-Wahab, Ali H. Bahkali, Mary L. Berbee, Saranyaphat Boonmee, D. Jayarama Bhat, Timur S. Bulgakov, Bart Buyck, Erio Camporesi, Rafael F. Castan˜ eda-Ruiz, Putarak Chomnunti, Minkwan Doilom, Francesco Dovana,Tatiana B. Gibertoni, Margita Jadan, Rajesh Jeewon, E. B. Gareth Jones, Ji-Chuan Kang, Samantha C. Karunarathna, Young Woon Lim, Jian-Kui Liu, Zuo-Yi Liu, Helio Longoni Plautz Jr., Saisamorn Lumyong, Sajeewa S. N. Maharachchikumbura, Neven Matocˇec, Eric H. C. McKenzie, Armin Mesˇic´, Daniel Miller, Julia Pawłowska, Olinto L. Pereira, Itthayakorn Promputtha, Andrea I. Romero, Leif Ryvarden, Hong-Yan Su, Satinee Suetrong, Zdenko Tkalcˇec, Alfredo Vizzini, Ting-Chi Wen, Komsit Wisitrassameewong, Marta Wrzosek, Jian-Chu Xu, Qi Zhao, Rui-Lin Zhao, Peter E. Mortimer

Department of Botany and Microbiology, Sohag University, Sohag, Egypt

This is the sixth in a series of papers where we bring collaborating mycologists together to produce a set of notes of several taxa of fungi. In this study we introduce a new family Fuscostagonosporaceae in Dothideomycetes. We also introduce the new ascomycete genera *Acericola, Castellaniomyces, Dictyosporina* and *Longitudinalis* and new species *Acericola italica, Alternariaster trigonosporus, Amarenomyces dactylidis, Angustimassarina coryli, Astrocystis bambusicola, Castellaniomyces rosae, Chaetothyrina artocarpi, Chlamydotubeufia krabiensis, Colletotrichum lauri, Collodiscula chiangraiensis, Curvularia palmicola, Cytospora mali-sylvestris, Dictyocheirospora cheirospora, Dictyosporina ferruginea, Dothiora coronillae, Dothiora spartii, Dyfrolomyces phetchaburiensis, Epicoccum cedri, Epicoccum pruni, Fasciatispora calami, Fuscostagonospora cytisi, Grandibotrys hyalinus, Hermatomyces nabanheensis, Hongkongmyces thailandica, Hysterium rhizophorae, Jahnula guttulaspora, Kirschsteiniothelia rostrata, Koorchalomella salmonispora, Longitudinalis nabanheensis, Lophium zalerioides, Magnibotryascoma mali, Meliola clerodendri-infortunati, Microthyrium chinense, Neodidymelliopsis moricola, Neophaeocryptopus spartii, Nigrograna thymi, Ophiocordyceps cossidarum, Ophiocordyceps issidarum, Ophiosimulans plantaginis, Otidea pruinosa, Otidea stipitata, Paucispora kunmingense, Phaeoisaria microspora, Pleurothecium floriforme, Poaceascoma halophila, Periconia aquatica, Periconia submersa, Phaeosphaeria acaciae, Phaeopoacea muriformis, Pseudopithomyces kunmingnensis, Ramgea ozimecii, Sardiniella celtidis, Seimatosporium italicum, Setoseptoria scirpi, Torula gaodangensis* and *Vamsapriya breviconidiophora*. We also provide an amended account of Rhytidhysteron to include apothecial ascomata and a J? hymenium. The type species of *Ascotrichella hawksworthii* (Xylariales genera incertae sedis), *Biciliopsis leptogiicola* (Sordariomycetes genera incertae sedis), *Brooksia tropicalis* (Micropeltidaceae), *Bryochiton monascus* (Teratosphaeriaceae), *Bryomyces scapaniae* (Pseudoperisporiaceae), *Buelliella minimula* (Dothideomycetes genera incertae sedis), *Carinispora nypae* (Pseudoastrosphaeriellaceae), *Cocciscia hammeri* (Verrucariaceae), *Endoxylina astroidea* (Diatrypaceae), *Exserohilum turcicum* (Pleosporaceae), *Immotthia hypoxylon* (Roussoellaceae), *Licopolia franciscana* (Vizellaceae), *Murispora rubicunda* (Amniculicolaceae) and *Doratospora guianensis* (synonymized under *Rizalia guianensis*, Trichosphaeriaceae) were reexamined and descriptions, illustrations and discussion on their familial placement are given based on phylogeny and morphological data. New host records or new country reports are provided *for Chlamydotubeufia huaikangplaensis, Colletotrichum fioriniae, Diaporthe subclavata, Diatrypella vulgaris, Immersidiscosia eucalypti, Leptoxyphium glochidion, Stemphylium vesicarium, Tetraploa yakushimensis* and *Xepicula leucotricha*. *Diaporthe baccae* is synonymized under *Diaporthe rhusicola*. A reference specimen is provided for *Periconia minutissima*. Updated phylogenetic trees are provided for most families and genera. We introduce the new basidiomycete species *Agaricus purpurlesquameus, Agaricus rufusfibrillosus, Lactifluus holophyllus, Lactifluus luteolamellatus, Lactifluus pseudohygrophoroides, Russula benwooii, Russula hypofragilis, Russula obscurozelleri, Russula parapallens, Russula phoenicea, Russula pseudopelargonia, Russula pseudotsugarum, Russula rhodocephala, Russula salishensis, Steccherinum amapaense, Tephrocybella constrictospora, Tyromyces amazonicus* and *Tyromyces angulatus* and provide updated trees to the genera. We also introduce *Mortierella formicae* in Mortierellales, Mucoromycota and provide an updated phylogenetic tree.

Fungal Diversity (2017) 87:1-235.

Zoology

3-Glucocorticoid and cytokine crosstalk: Feedback, feedforward, and co-regulatory interactions determine repression or resistance

Newton R.[1], Shah S.[2], Altonsy M. O.[3,4], Gerber A. N.[5]

Inflammatory signals induce feedback and feedforward systems that provide temporal control. Although glucocorticoids can repress inflammatory gene expression, glucocorticoid receptor recruitment increases expression of negative feedback and feedforward regulators, including the phosphatase, DUSP1, the ubiquitin-modifying enzyme, TNFAIP3, or the mRNA-destabilizing protein, ZFP36. Moreover, glucocorticoid receptor cooperativity with factors, including nuclear factor-κB (NF-κB), may enhance regulator expression to promote repression. Conversely, MAPKs, which are inhibited by glucocorticoids, provide feedforward control to limit expression of the transcription factor IRF1, and the chemokine, CXCL10. We propose that modulation of feedback and feedforward control can determine repression or resistance of inflammatory gene expression toglucocorticoid.

J Biol Chem. 2017 Apr 28;292(17):7163-7172. doi: 10.1074/jbc.R117.777318. Epub 2017 Mar 10.

4-Long-acting β2-agonists promote glucocorticoid-mediated repression of NF-κB by enhancing expression of the feedback regulator TNFAIP3

Altonsy MO[1,2], Mostafa MM[1], Gerber AN[3,4], Newton R[5]

Glucocorticoids, or corticosteroids, are effective treatments for many chronic inflammatory diseases, and in mild/moderate asthma, long-acting β_2-adrenoceptor agonists (LABAs) enhance the efficacy of inhaled corticosteroids (ICSs) more than increasing the ICS dose. In human bronchial epithelial, BEAS-2B, cells, expression of TNFα-induced protein-3 (TNFAIP3), or A20, a dual-ubiquitin ligase that provides feedback inhibition of NF-κB, was induced by budesonide, an ICS, and formoterol, a LABA, and was further enhanced by budesonide-formoterol combination. The proinflammatory cytokine TNF induced TNFAIP3 and TNF expression. Whereas subsequent budesonide treatment enhanced TNF-induced TNFAIP3 and reduced TNF expression, formoterol amplified these differential effects. In primary human airway smooth muscle cells, TNFAIP3 expression was induced by TNF. This was largely unaffected by budesonide but was acutely enhanced by budesonide-formoterol combination. In BEAS-2B cells, TNF recruited RELA, the main NF-κB transactivating subunit, to a 3' region of the TNF gene. RELA binding was reduced by budesonide, was further reduced by formoterol cotreatment, and was associated with reduced RNA polymerase II recruitment to the TNF gene. This is consistent with reduced TNF expression. TNFAIP3 knockdown enhanced TNF expression in the presence of TNF, TNF plus budesonide, and TNF plus budesonide-formoterol combination and confirms feedback inhibition. A luciferase reporter containing the TNF 3' RELA binding region recapitulated TNF inducibility and was inhibited by an IκB kinase inhibitor and TNFAIP3 overexpression. Repression of reporter activity by budesonide was increased by formoterol and involved TNFAIP3. Thus LABAs may improve the anti-inflammatory properties of ICSs by augmenting TNFAIP3 expression to negatively regulate NF-κB.

Am J Physiol Lung Cell Mol Physiol. 2017 Mar 1;312(3):L358-L370

Distribution and Morphology of Defensive Acid-Secreting Glands in Nudipleura (Gastropoda: Heterobranchia), With an Emphasis on Pleurobranchomorpha

Heike Wägele[1], Kristina Knezevic[1] and Alaa Y. Moustafa[2]

[1]*Zoological Research Museum Alexander Koenig, Adenauerallee 160, 53113 Bonn, Germany*

[2]*Zoology Departments, Faculty of Science, Sohag University, Sohag 82524, Egypt*

Secretion of acidic substances with defence and repellent properties is known in several metazoan taxa, including Gastropoda. Here we investigate and compare defensive acid-secreting cell types of various genera within the heterobranch taxon Pleurobranchomorpha by analysing the sizes and distribution of the secretory epithelial cells and subepithelial glands of the epidermis. Additionally, we investigate the median buccal gland (MBG), which is only known from pleurobranchs and one nudibranch species, *Plocamopherus ceylonicus*. The present data indicate a high similarity among the epidermal acid glands (EAGs), which consist of highly elongate cells containing a large vacuole with nonstaining contents. When acid-gland cells are concentrated into larger subepidermal acid glands (SAGs), the cells are of cuboidal or globular form, again containing a large nonstaining vacuole. This is also the case for the internal MBGs, although here the epithelial cells are considerably larger. In the latter, overall cell size seems to be related to body size, because specimens of similar size possess acid cells of equal size, whereas larger specimens (e.g. adult *Bathyberthella*) exhibit much larger cells. In contrast to SAGs, in which cells are often fused, the cells in MBGs are always distinct and fusion was hardly observed. Preliminary results indicate a uniform distribution of EAGs all over the body, whereas SAGs (only present in *Berthellina* spp.) are more densely distributed along the lateral sides than along the mid-part of the notum. The evolution of acid-gland types within Pleurobranchomorpha is discussed. The MBG has probably evolved twice in Heterobranchia, once within the Pleurobranchomorpha and independently in *P. ceylonicus*, a member of the nudibranch Euctenidiacea.

Journal of Molluscan Studies (2017), Volume 83, Issue 4, Pages 422–433

Effects of seasonal acclimatization on action potentials and sarcolemmal K+ currents in roach (Rutilus rutilus) cardiac myocytes

Ahmed Badr[a,b*], Minna Hassinen[a], Mohamed F. El-Sayed[b], Matti Vornanen[a]

[a]Department of Environmental and Biological Sciences, University of Eastern Finland, Joensuu, Finland b Department of Zoology, Faculty of Science, Sohag University, Sohag, Egypt

Temperature sensitivity of electrical excitability is a potential limiting factor for high temperature tolerance of ectotherms. The present study examines whether heat resistance of electrical excitability of cardiac myocytes is modified by seasonal thermal acclimatization in roach (Rutilus rutilus), a eurythermal teleost species. To this end, temperature dependencies of ventricular action potentials (APs), and atrial and ventricular K^+ currents were measured from winter-acclimatized (WiR) and summer-acclimatized (SuR) roach. Under patch-clamp recording conditions, ventricular APs could be triggered over a wide range of temperatures (4–43 °C) with prominent changes in resting membrane potential (RMP), AP duration and amplitude. In general, APs of SuR were slightly more tolerant to high temperatures than those of WiR, e.g. the break point temperature (TBP) of RMP was 37.6 ± 0.4 °C in WiR and 41 ± 1 °C in SuR ($p < 0.05$). Of the two major cardiac K^+ currents, the inward rectifier K^+ current (IK1) was particularly heat resistant in both SuR (TBP 39.4 ± 0.4 °C) and WiR (TBP 40.0 ± 0.4 °C) ventricular myocytes. The delayed rectifier K^+ current (IKr) was not as heat resistant as IK1. Surprisingly, IKr of WiR tolerated heat better (TBP 31.9 ± 0.8 °C) than IKr of SuR (TBP 24.1 ± 0.5 °C) ($p < 0.05$). IKr (Erg2) channel transcripts of both atrial and ventricular myocytes were up-regulated in WiR. IK1 (Kir2) channel transcripts were not affected by seasonal acclimatization, although ventricular IK1 current was up-regulated in summer. Collectively, these findings show that thermal tolerance limits of K^+ currents in isolated myocytes between seasonally acclimatized roach are much less pronounced than the heat sensitivity of ECG variables in intact fish.

Comparative Biochemistry and Physiology, Part A 205 (2017) 15–27

Assessment of Biochemical and Histopathological Effects of Crude Venom of Cone Snail *Conus flavidus* on *albino* Mice

Mona F. Abou-Elezz[1], Alaa Y. Moustafa[2], Mohamed S. El-Naggar[1]
[1]Zoology Department, Faculty of Science, Suez Canal University, Ismaillia, Egypt
[2]Zoology Department, Faculty of Science, Sohag University, Sohag, Egypt

The genus *Conus* is equipped with a unique venomous mixture of conopeptides which secreted for predation and defense purposes. This work is aiming to explore and determine the effect of the crude venom of *Conus flavidus*, a worm hunting cone snail inhabiting the Red Sea, on the oxidant/ antioxidant system in mice using some oxidative stress biomarker assays. In addition to assess its histopathological effects on some treated organs. The LC50 were detected for the crude venom using the hemolytic assay (16.7 mg/ml) and male albino mice were injected intraperitoneally with ½ LC50 (8.3 mg/kg B.Wt). Biochemically, after 2, 4, 6, 12, 24 hours of injection the results revealed significant inhibition of superoxide dismutase (SOD) and catalase (CAT) activities in blood and liver in almost all time intervals comparing with control one. However, it showed elevation in lipid peroxide content (LPC), protein carbonyl content (PCC), nitric oxide level (NO) reduced glutathione content (GSH) and total antioxidant capacity (TAC) contents of both blood and liver in almost all time intervals. Histopathologicaly, liver and heart were dissected after 1, 3 and 7 days of injection. The treated liver showed vacuolar degeneration, karyolosis and pyknosis, mild blood sinusoidal congestion and centrilobular necrosis. The treated heart illustrated degenerated myofibrils, pyknosis, edema, blood vessel congestion, loss of striation normal construction and fascicular pattern in the myocardium. These results revealed that *C. flavidus* crude venom has distinct effects upon the oxidant/antioxidant cellular system and degenerative pathological effects in some tissues of treated animals, proving that this venom may contain bioactive peptides, which could be purified and used for further pharmacological and drug discovery investigations in the future.

International Journal of Ecotoxicology and Ecobiology (2017); 2(1): 33-44

Pathogenic bacteria carried by synanthropic filthy flies (*Musca* species) at farmed animals in Sohag Governorat, Egypt: 2-Percentage of bacterial infection in Musca species

Azza M. Khedre[1], Tarek G. Ismail[1], Amany A. Yousif[2], Gehad A. Hashem[2]
[1]*Zoology Department, Faculty of Science, Sohag University, Egypt*
[2]*Microbiology Department, Animal Health Research Institute, Sohag, Egypt*

Although flies are important vectors of bacterial pathogens, there is little information to assess the health risk of the presence of individual flies especially at animal barns in Sohag Governorate. This study determines the prevalence and the risk of bacterial pathogens associated with the body surfaces of individual wild flies at three different animal barns. A total of 148 caught flies (*Musca* spp.) were examined and identified into species level. Three fly species (*Musca domestica; M.tempestiva* and *M. sorbens)* were detected. Nearly all the collected flies (97.2%) were positive for carrying bacteria. Each positive fly harbored from 1 to 4 isolated bacterial species but most of the flies (61.5%) harbored two species of bacteria. According to the largest variety of bacterial species isolated from these flies, it can be concluded that *M. domestica* poses the highest risk to the animals and humans, as they are carrying more pathogenic bacteria capable of transmitting many animal diseases, in this particular area. This is followed by *M. tempestiva*; meanwhile *M. sorbens* poses the least risk.

Egyptian journal of zoology Dec. 2017. 68:23-36

Do the environment or the carcass affect the sarcosaprophagous community?

María Pérez-Marcos[1], María-Dolores García[1,2], María-Isabel Arnaldos[1,2], Elena LópezGallego[1], Azza Khedre[3], Aurelio Luna[2,4]

[1]Department of Zoology, Faculty of Biology, University of Murcia, 30100 Murcia, Spain
[2]External Service of Forensic Sciences and Techniques. University of Murcia. 30100 Murcia, Spain
[3]Department of Zoology, University of Sohag, Egypt
[4]Area of Legal Medicine. Faculty of Medicine. University of Murcia. 30100. Murcia, Spain

Studying the entomosarcosaprophagous community is useful in forensic practice to estimate postmortem interval both on the basis of larval development of the main species and considering the sarcosaprophagous community as a whole. Since such community is affected by different environmental variables, it is needed to be studied under different environmental conditions. For forensic purposes, the most important component of the community is the necrophagous, mainly Diptera, some of which are known to be the first arthropods to arrive at the corpse and show certain differences between urban and rural sites. Otherwise, and because experimental studies are usually conducted with biomodels other than human corpses, it is needed to verify whether the type of decomposing animal matter affects, or not, to decomposition process and related fauna. So, a seasonal study was conducted on sarcosaprophagous Diptera community in two different sites of Región de Murcia (SE Spain): a natural pinewood, where a piglet carcass was used, and a periurban site, where piglet and chicken carcasses were used. Three modified Schoenly traps were used as collecting device. Samples were taken daily for 15 days between autumn 2006 and summer 2007. To analyze possible differences regarding faunal composition among samples, a oneway PERMANOVA analysis was applied. Results show significant differences for the interaction locality-season but suggest that the community as a whole is similar in both localities despite environmental conditions. Results also show significant differences for the interaction baitseason, being families Calliphoridae, Muscidae, Fanniidae, Phoridae and Sarcophagidae the main groups responsible of such differences.

Legal Medicine 2017

Insulin-like 3 expression and fibrosis induction after intra-testicular injection of magnetic nanoparticles in rat testis and the ameliorative role of Echinacea purpurea extract

Aziz Awaad[1*], Mohamed A. Adly[1] & Doaa Hosny[1]

[1]Department of Zoology, Faculty of Science, Sohag University, Sohag, 82524, Egypt
E-mail: aziz1_awaad@yahoo.com; aawaad@science.sohag.edu.eg

The World Health Organization has approved magnetic nanoparticles (MNP) for use as a contrast agent for magnetic resonance imaging or tumor hyperthermia treatment. MNP are toxic over time after intra-testicular injection. A clear strategy to ameliorate the toxic side effects of MNP in normal tissues after medical application has not yet been developed. We used an extract of Echinacea purpurea EP) as a natural source of antioxidant and free radical scavenging product for detoxification of MNP in testicular tissues. MNP localization in the interstitial area of testicular tissue reduced the expression of insulin-like factor 3 (INSL3) proteins as well as serum testosterone levels. Further, MNP caused accumulation of both collagen and elastin in the interstitial area and increased the thickness of the tunica albuginea. Injection of MNP during administration of EP extract for short periods slightly reduced t he toxic side effects of MNP. After extended exposure to EP extract, INSL3 expression and testosterone returned to near control levels. Also, collagen and elastin accumulation caused by MNP was reduced after extended exposure to EP extract. We believe that the ameliorative effect of EP extract is due to its antioxidant properties.

Journal of Biotech Histochem., 29th Oct., 2017. Issue: Volume:

Scanning electron morphological studies of *Tribolium confusum* Jacquelin du Val (Coleopteran: Tenebrionidae)

Nasra M. H. Zohry
Department of Zoology, Faculty of Science, Sohag University, Egypt
E- mail: Nasramohamed917@gmail.com

The confused flour beetle *Tribolium confusum* is worldwide and most destructive pest of stored products and is cosmopolitan in distribution. It is the most common pest of wheat flour. This study describes and illustrates the larvae, pupae and adults of *Tribolium confusum* (Coleopteran: Tenebrionidae) using scanning electron microscopy. The first larval instars are 5-5.1mm long and 0.5-0.6mm wide, whereas, last larval instars are 5.75- 6.9 mm long and 0.75-0.95 wide. Adults of *T. Confusum* are reddish brown elongate beetles (4-4.5 mm in body length and from 1-1.2 mm in width). Electron micrographs revealed the structure of mouth parts of the larval, pupal and adult stages as well as the structure of thoracic and abdominal appendages. Results indicated that the setiferous sex patches which were reported in males can often be used for sexing specimens. A specific feature of 1st instar larvae of *Tribolium confusum* is the extreme shortened antenna with a reduced number of antennomeres and the presence of well developed and moderately long legs. SEM examination may help us also to discover, investigate and understand new morphological details as the pits with spine on the elytra and the spikes on the membrane wings which will facilitate the identification of this species and may help to clarify the functions of various body parts.
The Journal of Basic and Applied Zoology (2017) 78:6

Evaluation of Two Novel Feeding Protocols Utilizing Alive and Dried Chlorella *vulgaris* to Grow *Heterocypris salina* (Ostracoda: Crustacea)

Ebtesam A Yousef[1*] and Mahmoud H.Hegab[2]
[1]Department of Zoology, Faculty of Science, Sohag University, Egypt
[2]Freshwater and Lakes Division, National Institute of oceanography and Fisheries (NIOF), Egypt

Heterocypris salina is well-known for its high egg production and it can adapt to live in different environments. However, the data on *H. salina* culturing are still scarce, so it is necessary to study the best environmental conditions and food items to culture ostracod species. The current study was carried out to generate baseline information on the food and feeding protocols of *H. salina* by evaluating living and dried *Chlorella vulgaris* as a food source for this species .Gravid females of H.salina with the same length and age were separated to start the experiment, which divided into two treatments based on alive and dried *Chlorella vulgaris.* The current study concluded that, the alive and dried *C. vulgaris* is a suitable diet for *H. salina* because it led to enhance its growth rate, increasing its individual number and shortened the time to reach adulthood.
Journal of Zoological Research Volume 1, Issue 1, 2017, PP 10-15

Histological and histopathological studies on the protective role of Echinacea purpurea extract after intra-testicular injection of magnetic nanoparticles in male albino rats

Aziz Awaad*, Mohamed A. Adly & Doaa Hosny
Department of Zoology, Faculty of Science, Sohag University, Sohag, 82524, Egypt
E-mail: aziz1_awaad@yahoo.com; aawaad@science.sohag.edu.eg

Local intra-testicular injection for drug release is an important methodology for testicular diseases therapy. Magnetic nanoparticles (MNPs) are new nanomaterials which have several medical applications. This study aimed at investigating the time-dependent toxicity of MNPs after intratesticular injection, and the protective effect of Echinacea purpurea (EP) extract as antioxidant and immune cells activator. To investigate the protective role of EP extract against MNPs toxicity in testicular tissues, EP extract was simultaneously administrated with MNPs. The intra-testicular injection of MNPs caused spermatogenic apoptosis, cellular necrosis, and interstitial fibrosis. Also, MNPs were found freely in the interstitial area attached to fiber bundles and to lamina propria of the seminiferous tubules. Simultaneous EP extract administration with MNPs injection for 11 wk reduced MNPs toxicity, compared to MNPs only. Also, most MNPs were co-localized in some interstitial cells/macrophages after this EP extract simultaneous administration. In this regard, MNPs were found as groups aggregated in lysosomal vacuoles of macrophages after EP extract administration. In the case of MNPs only injection, MNPs were found freely outside interstitial cells, attached to fiber bundles and surrounding myoid cells of seminiferous tubules. To conclude the simultaneous administration of EP extract/MNPs injection changed both cellular and subcellular biodistribution of MNPs in the testicular tissues. Our present findings indicate a prominent protective role for EP extract as an antioxidant and immune activator against MNPs intra testicular injection-induced toxicity and may promise a new strategy for testicular disease therapies using nanomaterials.
Journal of Histotechnology, 2017; 40(4):100–114

Some biological aspects and population dynamics of the five-lined snapper, *Lutjanus quinquelineatus* (Family:Lutjanidae) from Red Sea off Hurghada, Egypt

Sahar F Mehanna, Taha S Baker, Faiza M Soliman and Hamdy A Soliman

Age and growth, reproductive strategy, mortality and yield per recruit analysis are essential to evaluate the fishery status of fish stocks. The fishery status of five-lined snapper *Lutjanus quinquelineatus* in Hurghada fishing area was assessed based on the monthly representative samples covered 12 months from January to December 2016. The von Bertalanffy equation for the growth in length was: Lt = 35.5 [1- e-0.35(t + 1.3)]. The total mortality coefficient 'Z', natural mortality coefficient 'M', and fishing mortality coefficient 'F' were estimated at 1.84, 0.69, and 1.15 year-1, respectively. The current exploitation rate 'E' was 0.62 year-1. The spawning season was found to extend from March to July, and the maximum absolute fecundity was estimated to be 389880 eggs. The yield and biomass per recruit were analysed using the Beverton and Holt's yield per recruit Model (1957). Results indicated that there is an opportunity to expand the fishery of *Lutjanus quinquelineatus* stock in Hurghada fishing area. But before any recommendation, the current status of different target species needs to be analysed as the fishery in Hurghada is multispecies.
International Journal of Fisheries and Aquatic Studies 2017; 5(5): 321-326

Protein, Electrophoresis Analysis and Heavy Metals in Muscles of Wild and Farmed *Oreochromis Niloticus*

Hamdy A. M. Soliman

Zoology Department, Faculty of Science, Sohag University, 8562 Sohag, Egypt

The present study aimed to assess the levels of some heavy metals (Cu, Fe, Pb, Zn and Cd) in muscles of wild and farmed *Oreochromis niloticus* as well as to evaluate the human hazard index associated with fish consumption. In addition, total protein, molecular weights and band counts of sarcoplasmic proteins were investigated with sodium dodecyl sulfate polyacrylamide gel electrophoresis (SDS-PAGE) method. The obtained results revealed that the accumulation of Cu has the highest value in farmed *Oreochromis niloticus* compared to wild *Oreochromis niloticus* while the highest Fe, Pb, Zn and Cd concentrations were recorded in wild *Oreochromis niloticus* compared to farmed *Oreochromis niloticus*. The calculated hazard index (HI) indicated that all metals had low HI except Pb and Cd levels in both wild and farmed fish were higher than their permissible limits for fish as a human food. There was no significant difference between them in total protein. Wild fish predominant farmed fish in the number of separated proteins. Wild fish muscle proteins were separated into 12 protein bands, whereas farmed fish muscle proteins were separated into 11 protein bands. Also, these bands were differed in quantitative parameters. Wild fish had unique bands (MW. 198.13, 97.92, 56.77 and 29.75) while farmed fish had unique bands (MW. 121.62, 79.05 and 26.16). The current data proposes that there are differences in electrophoretic pattern and heavy metals between wild and farmed *Oreochromis niloticus*.

Ass.Univ.Bull.Environ.Res.Vol.20 No.1 March 2017

Effects of seasonal acclimatization on thermal tolerance of inward currents in roach (Rutilus rutilus) cardiac myocytes

Ahmed Badr[1,2], Minna Hassinen[1], Mohamed F. El-Sayed[2], Matti Vornanen[1]

[1]*Department of Environmental and Biological Sciences, University of Eastern Finland, P.O. Box 111, 80101, Joensuu, Finland*

[2]*Department of Zoology, Faculty of Science, Sohag University, P.O. Box 82524, Sohag, Egypt*

To test the hypothesis of temperature-dependent deterioration of electrical excitability (TDEE) (Vornanen, J Exp Biol 219:1941-1952, 2016), the role of sodium (I Na) and calcium (I Ca) currents in heat tolerance of cardiac excitability was examined in a eurythermic fish, the roach (Rutilus rutilus). Densities of cardiac I Ca and I Na and their acute heat tolerance were measured in winter-acclimatized (WiR) and summer-acclimatized (SuR) fish maintained in the laboratory at 4 ± 1 and 18 ± 1 °C, respectively. A robust L-type Ca2+ current (I CaL), but no T-type Ca2+ current, was present in roach atrial and ventricular myocytes. Peak density of I CaL was smaller in atrial (-1.97 ± 0.14 and -1.75 ± 0.19 pA/pF for WiR and SuR, respectively) than ventricular myocytes (-4.00 ± 0.59 and -2.88 ± 0.47 pA/pF for WiR and SuR, respectively) ($p < 0.05$), but current density and heat tolerance of I CaL did not change between seasons in either cell type. In contrast to I Ca, marked differences appeared in I Na between WiR and SuR. I Na density was 38% higher in WiR than SuR atrial myocytes (-80.03 ± 5.92 vs. -49.77 ± 4.72 pA/pF; $p < 0.05$) and 48% higher in WiR than SuR ventricular myocytes (-39.25 ± 3.06 vs. -20.03 ± 1.79 pA/pF; $p < 0.05$). The winter increase in I Na density was associated with 55% (1.70 ± 0.27 vs. 0.77 ± 0.12) and 54% (1.08 ± 0.19 vs. 0.50 ± 0.10) up-regulation of the total Na+ channel (scn4 + scn5 + scn8) transcripts in atrium and ventricle, respectively ($p < 0.05$). Heat tolerance of atrial I Na was lower in WiR with a breakpoint temperature of 20.3 ± 1.2 °C than in SuR (23.8 ± 0.7 °C) ($p < 0.05$). The response of I Na to seasonal acclimatization conforms to the TDEE hypothesis. The lower heat tolerance of I Na in WiR is consistent with the lower heat tolerance of in vivo heart rate in WiR in comparison to SuR, but the match is not quantitatively perfect, suggesting that other factors in addition to I Na may be involved.

J Comp Physiol B. 2017 Sep 23. doi: 10.1007/s00360-017-1126-1

A New Aquatic Oribatid Mite, *Trimalaconothrus Crassipes* SP. N. (Family: Malaconothridae), Sohag, Egypt

Ramadan S. A., Ismail T. G. and Mustafa, A. N.

Zoology Department, Faculty of Science, Sohag University, Fax: +2 093 4601159, P.O.Box: 82524, Sohag

t_gad_2000@Sohag.edu.eg

Trimalaconothrus crassipes sp. n. was described for the first time from the roots of the floating aquatic plant, *Eichhornia crassipes*, River Nile, Girga, Sohag, Egypt. The present species has the characteristic features that are in accordance with those of family Malaconothridae and genus *Trimalaconothrus*. The present species has specific characters compared with characters of other species of the same genus. These characters are summarized as follows: six dorsal plates, fifteen pairs of notogastral setae, three pairs of granulated rounded organs, three pairs of exobothridial setae (ex1, ex2, ex3), epimeral setal formula (I- IV) is (3-2-2-2) and each coxal epimerae II is characterized by presence of two lateral processes.

Assiut Univ.J. Zoology, 46(2) 26-39

Immunohisto Chemical Expression Patterns of Glial Cell Line-Derived Neurotrophic Factor and its Cognate Receptor GFRα-1 in Lichen Planus

Mohamed A. Adly[1], Hanan A. Assaf[2], Mohammed Abu El-Hamd[2], Nagwa Sayed[3], Hemat Mostafa[2] and Mahmoud Rezk A. Hussein[3]

[1]*Department of Zoology, Faculty of Science, Sohag University, 82524, Sohag, Egypt*

[2]*Department of Dermatology, Venereology and Andrology, Faculty of Medicine, Sohag University, Egypt*

[3]*Department of Biochemistry and Molecular Biology, Faculty of Medicine, Sohag University, Egypt*

Abstract:

Background: Glial cell line-derived neurotrophic factor (GDNF), produced by basal cell keratinocytes, is a neurotrophic factor that plays diverse developmental roles and together with its cognate receptor (GFR Rα-1) are distal members of the transforming growth factor- β super family. To date, their expression pattern in lichen planus is still unknown. Objectives: To investigate the immunohis to chemical expression patterns of GDNF and its cognate receptor (GFRα-1) in lichen planus and compare the results with the normal skin from healthy controls.

Patients and Methods: Twenty patients with lichen planus were examined in addition to twenty age and sex matched healthy subjects (the control group). Punch biopsies from lesional and normal healthy skin were performed. Sections were examined using immunohis to chemical staining methods for GDNF and GFRα-1proteins expression patterns expression analysis.

Results: There was strong GDNF protein expression in the basal cell keratinocytes and moderate gene expression in the spinous layer and weak gene expression in the granular layer of the healthy skin. In contrast, in lichen planus, GDNF protein expression was absent in the basal cell keratinocytes and lower reaches of the spinous layer. Weak gene expression was noted in the upper reaches of the epidermis. In both healthy and lichen planus skins, the expression of GFRα-1in the adnesal structures showed no differences.

Conclusion: The altered GDNF protein expression may contribute to the pathogenesis of lichen planus.

Keywords: GDNF; GFRα-1; Immunohis to chemistry; Lichen planus

ABBR journal, 1, 2, 97-102 (2017)

Copper Oxide Nanoparticles and Copper Sulphate Act as Antigenotoxic Agents in Drosophila melanogaster

Mohamed Alaraby[1,2], Alba Hernandez[1,3] and Ricard Marcos[1,3*]

[1]Grup de Mutage`nesi, Departament de Gene`tica i de Microbiologia, Facultat de Biocie`ncies, Universitat Autonoma de Barcelona, Cerdanyola del Valle `s, Barcelona, Spain

[2]Zoology Department, Faculty of Sciences, Sohag University, Sohag, Egypt

[3]CIBER Epidemiologıa y Salud Publica, ISCIII, Madrid, Spain

The biological reactivity of metal and metal oxide nanomaterials is attributed to their redox properties, which would explain their pro- or anti-cancer properties depending on exposure circumstances. In this sense, copper oxide nanoparticles (CuONP) have been proposed as a potential anti-tumoral agent. The aim of this study was to assess if CuONP can exert antigenotoxic effects using Drosophila melanogaster as an in vivo model. Genotoxicity was induced by two well-known genotoxic compounds, namely potassium dichromate (PD) and ethyl methanesulfonate (EMS). The wing-spot assay and the comet assay were used as biomarkers of genotoxic effects. In addition, changes in the expression of Ogg1 and Sod genes were determined. The effects of CuONP cotreatment were compared with those induced by copper sulfate (CS), an agent releasing copper ions. Using the wing-spot assay, CuONP and CS were not able to reduce the genotoxic effects of EMS exposure, but had the ability to decrease the effects induced by PD, reducing the frequency of mutant twin-spots that arise from mitotic recombination. In addition, CuONP and CS were able to reduce the DNA damage induced by PD as determined by the comet assay. In general, similar qualitative antigenotoxic effects were obtained with both copper compounds. The antigenotoxic effects of environmentally relevant and non-toxic doses of CuONP and CS may be explained by their ability to partially restore the expression levels of the repair gene Ogg1 and the antioxidant gene Cu,ZnSod, both of which are inhibited by PD treatment. Environ. Mol. Mutagen. 58:46–55, 2017. VC 2017 Wiley Periodicals, Inc. Key words: drosophila; CuO nanoparticles; antigenotoxic; comet assay; wing-spots test INTRODUCTION Medical applications of nanoparticles (NP) are considered to be one of the most promising fields of nanotechnology. Currently, NP are used for drug delivery, gene therapy, and both diagnosis and treatment of cancer [Passeri et al., 2015]. These biomedical and cancerrelated applications of metal oxide NP are of particular interest to the scientific and medical communities [Rasmussen et al., 2010]. Of several metal oxide compounds with such potential applications, copper oxide NP (CuONP) have been found to possess anticancer properties, presumably by eradicating cancer cells through direct contact or initiation of oxidative stress [Piret et al., 2012; Moschini et al., 2013; Siddiqui et al., 2013]. It has been reported that CuONP selectively kill cancer cells in a dose-dependent manner without impacting normal cells [Shafagh et al., 2015], making them an attractive candidate for cancer therapy. Complexes containing copper, or other

Environmental and Molecular Mutagenesis 58:46-55 (2017)

The Ontogeny of Appendages and Carapace of *Neonesidea Schulzi* (Ostracoda: Bairdiidae) from the Red Sea Coast, Egypt

Ebtesam A. Yousef & Alaa Y. Moustafa

Department of Zoology, Faculty of Science, Sohag University, Sohag 82524, Egypt

The ostracod genus *Neonesidea* is broadly distributed in shallow marine waters. The ontogeny of the *N. schulzi* (Bairdiidae) is described in detail by studying the development of the appendages and variations in carapace form, size and structure. *Neonesidea schulzi* has eight post-embryonic instars, and a gap in its ontogenetic development during instar A-6, where no new *Anlage* is added. The *Anlagen* of the copulatory organs and the forked terminal claw of second antenna appear in the seventh (A-1) instar, and the first thoracic legs of podocopid ostracods are shown to descend from the thoracic region. For the first time in ostracods, observations of moulting from sixth and seventh instars are presented.

Journal of Invertebrates Reproduction and Development (2017), Volume 61 No 4. Pages 225-244

Geology

Coupling of field investigations and remote sensing data for karst hazards in Egypt: case study around the Sohag City

Ahmed M. Youssef[1,2], Abdel-Hamid El-Shater[1], Mohamed H. El-Khashab[1], Bosy A. El-Haddad[1]

[1]Geology Department, Faculty of Science, Sohag University, Sohag, Egypt

[2]Geological Hazards Department, Applied Geology Sector, Saudi Geological Survey, Jeddah, Kingdom of Saudi Arabia

Karst rocks cover a wide area of Egypt. These rocks include soluble sediments such as carbonate rock formations, evaporites, and sabkha deposits that are characterized by karstification features. Karst features could affect many current and developing projects (urban areas and infrastructure). The areas covered by the rocks susceptible to karstification need detailed studies to examine the presence of karst features and/or sinkholes. The current work provides a detailed evaluation of the karst and/or sinkhole hazards around the city of Sohag, Egypt. This research is rarely done in Egypt, using field investigation and remote sensing application to determine the main karstic rock formations and the distribution of the most problematic sinkhole areas. In this work, different types of the subsidence mechanisms were investigated. Our results indicated that field investigations help in finding different features related to karstification including small-scale versus large-scale features and empty caves versus filled caves. In addition, remote sensing techniques succeeded in predicting and locating the sinkhole areas, and those determinations were verified in the field. Finally, fundamental considerations are discussed to better evaluate and manage the hazard of karst and/or sinkholes.

Arabian Journal of Geosciences, 10 (11), (2017), art. no. 235.

Rainfall-induced landslide susceptibility assessment at the Chongren area (China) using frequency ratio, certainty factor, and index of entropy

Haoyuan Hong[a,b], Wei Chen[c], Chong Xu[a], Ahmed M. Youssef[d], Biswajeet Pradhan[e] and Dieu Tien Bui[f]

[a]Key Laboratory of Active Tectonics and Volcano, China Earthquake Administration, Institute of Geology, Beijing, P.R. China;

[b]Jiangxi Provincial Meteorological Observatory, Jiangxi Meteorological Bureau, Nanchang, China;

[c]School of Geology and Environment, Xi'an University of Science and Technology, Xi'an, China;

[d]Faculty of Science, Department of Geology, Sohag University, Sohag, Egypt;

[e]Faculty of Engineering, Department of Civil Engineering, University Putra Malaysia, Serdang, Malaysia;

[f]Geographic Information System Group, Department of Business Administration and Computer Science, Faculty of Art and Sciences, University College of Southeast Norway, Bo i Telemark, Norway

The main objective of the study was to evaluate and compare the overall performance of three methods, frequency ratio (FR), certainty factor (CF) and index of entropy (IOE), for rainfall-induced landslide susceptibility mapping at the Chongren area (China) using geographic information system and remote sensing. First, a landslide inventory map for the study area was constructed from field surveys and interpretations of aerial photographs. Second, 15 landslide-related factors such as elevation, slope, aspect, plan curvature, profile curvature, stream power index, sediment transport index, topographic wetness index, distance to faults, distance to rivers, distance to roads, landuse, NDVI, lithology and rainfall were prepared for the landslide susceptibility modelling. Using these data, three landslide susceptibility models were constructed using FR, CF and IOE. Finally, these models were validated and compared using known landslide locations and the receiver operating characteristics curve. The result shows that all the models perform well on both the training and validation data. The area under the curve showed that the goodness-of-fit with the training data is 79.12, 80.34 and 80.42% for FR, CF and IOE whereas the prediction power is 80.14, 81.58 and 81.73%, for FR, CF and IOE, respectively. The result of this study may be useful for local government management and land use planning.

Geocarto International, 32 (2), (2017), 139-154.

Karst induced geo-hazards in Egypt: Case study slope stability problems along some selected desert highways

Ahmed M. Youssef[1,2], Abdel-Hamid El-Shater[1], Mohamed H. El-Khashab[1], Bosy A. El-Haddad[1]

[1]*Geology Department, Faculty of Science, Sohag University, Sohag, Egypt*

[2]*Geological Hazards Department, Applied Geology Sector, Saudi Geological Survey, Jeddah, Kingdom of Saudi Arabia*

Karst environments are characterized by distinctive landforms related to dissolution characteristics. Karst terrains, frequently underlain by cavernous carbonate and/or evaporite rocks, may induce ground instability problems. Impacts and problems associated with karst are rapidly increasing as development expands upon the karst prone areas. This has led to an escalation of karst-related environmental and engineering problems such as landslides developed on rock cuts/slopes weakened by karstification features. In the current work, the effects of karstification and sinkholes on the stability of the rock cuts/slopes along some selected desert highways were evaluated. These highways represent the most used highways in Egypt, connecting most of the Governorates. They represent the backbone of Egyptian transportation and commercial traffic. Finally, the most optimum mitigation/remediation methods were summarized to decrease and minimize the consequences of slope instability.

GeoMEast conference "Sustainable Civil Infrastructures: Innovative Infrastructure Geotechnology", July 15-19, 2017, Sharm El- Sheikh, Egypt. J. Wasowski et al. (eds.), Engineering Geology and Geological Engineering for Sustainable Use of the Earth's Resources, Urbanization and Infrastructure Protection from Geohazards, Sustainable Civil Infrastructures, 149-164.

Suitability estimation for urban development using multi-hazard assessment map

George D.Bathrellos [a], Hariklia D. Skilodimou [a], Konstantinos Chousianitis [b], Ahmed M.Youssef [c], Biswajeet Pradhan [de]

[a]*Department of Geography and Climatology, Faculty of Geology and Geoenvironment, National and Kapodistrian University of Athens, University Campus, 15784, Zografou, Athens, Greece*

[b]*Institute of Geodynamics, National Observatory of Athens, Lofos Nymfon, 11810, Athens, Greece*

[c]*Geology Department, Faculty of Science, Sohag University, 82524, Sohag, Egypt*

[d]*Department of Civil Engineering, Geospatial Information Science Research Center (GISRC), Faculty of Engineering, University Putra Malaysia, 43400, UPM, Serdang, Malaysia*

[e]*Department of Energy and Mineral Resources Engineering, Choongmu-gwan, Sejong University, 209 Neungdong-ro Gwangjin-gu, Seoul, 05006, Republic of Korea*

Preparation of natural hazards maps are vital and essential for urban development. The main scope of this study is to synthesize natural hazard maps in a single multi-hazard map and thus to identify suitable areas for the urban development. The study area is the drainage basin of Xerias stream (Northeastern Peloponnesus, Greece) that has frequently suffered damages from landslides, floods and earthquakes. Landslide, flood and seismic hazard assessment maps were separately generated and further combined by applying the Analytical Hierarchy Process (AHP) and utilizing a Geographical Information System (GIS) to produce a multi-hazard map. This map represents the potential suitability map for urban development in the study area and was evaluated by means of uncertainty analysis. The outcome revealed that the most suitable areas are distributed in the southern part of the study area, where the landslide, flood and seismic hazards are at low and very low level. The uncertainty analysis shows small differences on the spatial distribution of the suitability zones. The produced suitability map for urban development proves a satisfactory agreement between the suitability zones and the landslide and flood phenomena that have affected the study area. Finally, 40% of the existing urban pattern boundaries and 60% of the current road network are located within the limits of low and very low suitability zones.

Science of the Total Environment, 575, (2017), 119-134.

Site investigation using engineering geology mapping and geological hazard evaluation: Case study of the New Hail Economic City, Hail Region, KSA

T. E. Al-Sehly[1], A. M. Youssef[1,2], A. A. Al-Otaibi[1], H. M. Al-Harbi[1]

[1]*Geological Hazards Department, Applied Geology Sector, Saudi Geological Survey, 54141, Jeddah 21514, KSA, Tel. +966-568448782*

[2]*Geology Department, Faculty of Science, Sohag University, Egypt*

The New Hail Economic City in the Kingdom of Saudi Arabia is one of the pioneer projects and represents a corner stone for the new development activities for Hail region. It is located to the north of the Hail city, covering an area of ~156 km^2. Fundamental facilities of this project will include infrastructure, residential, commercial, industrial, and a new international airport. The present study aims to establish a new approach of site investigation using engineering geologic mapping and geological hazard evaluation. To achieve this approach, physical and engineering characteristics of surface and subsurface soil and/or rocks of the study area were evaluated. Several data sources were used including: geologic and topographic maps, satellite images, previous data and reports, and detailed field and laboratory investigations of soil and rocks. Our finding indicated that the study area is characterized by soil layer which varies in thickness from 0 to 12 meter and rock outcrops. An engineering geology mapping of the new economic city was prepared using GIS environment. It classifies the area into six zones (4 for soils and 2 for rock outcrops) according to their physical and geotechnical properties. Three cross sections were prepared according to subsurface data showing the layers variations within the study area. Finally, the geological hazards causing negative impact on the area were identified. Various recommendations were proposed to help project decision makers to deal with the geological and geotechnical problems.

GeoMEast conference "Sustainable Civil Infrastructures: Innovative Infrastructure Geotechnology", July 15-19, 2017, Sharm El- Sheikh, Egypt. J. Wasowski et al. (eds.), Engineering Geology and Geological Engineering for Sustainable Use of the Earth's Resources, Urbanization and Infrastructure Protection from Geohazards, Sustainable Civil Infrastructures, 1-19.

Slope stability hazard assessment using 3D remote sensing and field sketching techniques along Sohag-Red Sea-Cairo highway, Egypt

Bosy A. El-Haddad[1], Ahmed M. Youssef [1,2], Abdel-Hamid El-Shater[1], Mohamed H. El-Khashab[1]

[1]*Geology Department, Faculty of Science, Sohag University, Sohag, Egypt*

[2]*Geological Hazards Department, Applied Geology Sector, Saudi Geological Survey, Jeddah, Kingdom of Saudi Arabia*

Coupling of 3D remote sensing images, Field sketching and field investigation represent interesting techniques to understand and evaluate the slope stability problems along rock cut slopes. These methods were applied along the highway section that connects the Sohag, Red Sea, and Cairo governorates on the eastern plateau, Egypt. It is one of the most used highways in Egypt during recent years and represents the backbone of Egyptian transportation and commercial traffic. This Highway passes through a difficult zone of rock cut slopes located 20 km north of Sohag city. Serious stability and rockfall and/or slides issues have been recognized along this section. The applied methods are considered to be good and are new techniques in understanding different types of slope stability hazards such as debris flows, rockfalls/sliding and determining the most relevant factors affecting slope stability problems. In addition, the potential instability zones were mapped. These techniques also could help in remediation/mitigation strategies.

4th World landslide forum, May 29 –June 2, 2017, Ljubljana, Slovenia. M. Mikoš et al. (eds.), Advancing Culture of Living with Landslides, 407-417.

Dynamic geotechnical properties evaluation of a candidate nuclear power plant site (NPP): P- and S-waves seismic refraction technique, North Western Coast, Egypt

A.M. Abudeif[a], A. E. Raef[b], A.A. Abdel Moneim [a], M.A. Mohammed[a], A.F. Farrag[c]

[a]*Geology Department, Faculty of Science, Sohag University, Sohag, Egypt*

[b]*Geology Department, Kansas State University, Manhattan, KS, USA*

[c]*Siting Department, Nuclear Power Plants Authority, Cairo, Egypt*

Determination of the dynamic geotechnical properties and V_s30 of soil and rocks from seismic wave velocities serves as essential inputs for a foundation design cognizant of seismic site response and rock strength. This study evaluates a site which was suggested for a Nuclear Power Plant (NPP) in El-Dabaa area, north western coast of Egypt. On the near subsurface geology is made up of a thick succession of limestone overlain by a thin layer of soft soil. Assessment of geotechnical materials and V_s30 of the near sub-surface lithological layers are required for design of the foundation of critical structures like turbo-generator and reactor buildings. Interpretation of ninety one shallow P-waves and S-waves seismic refraction profiles distributed within the study area in conjunction with data of 76 boreholes were undertaken to delineate the dynamic properties of shallow soil for construction NPP. The velocity of the P- and S-waves were acquired and interpreted using SeisImager Software Package, then the results were used to build a velocity-depth model to estimate the depth to the bedrock and the thicknesses of overburden layers. This model was verified using boreholes data dissected the seismic profiles to improve the final velocity depth model. The depth to bedrock was determined from both shallow seismic refraction profiles and boreholes. V_s30, elastic moduli and dynamic geotechnical parameters were calculated and the site was classified as a National Earthquake Hazard Reduction Program (NEHRP) class "B". The values of seismic velocities, the engineering consolidations, and the strength parameters showed that the bedrock in the study area is characterized by more competent rock quality.

Soil Dynamics and Earthquake Engineering, 99, (2017), 124-136.

Geology, structure, geochemistry and ASTER-based mapping of Neoproterozoic Gebel El-Delihimmi granites, Central Eastern Desert of Egypt

Asran Mohamed Asran[a], Ashraf Emam[b], Abdelhamid El-Fakharani[bc]

[a]*Department of Geology, Faculty of Science, Sohag University, Egypt*

[b]*Department of Geology, Faculty of Science, Aswan University, Egypt*

[c]*Department of Structural Geology and Remote Sensing, Faculty of Earth Sciences, King Abdulaziz University, Jeddah, Saudi Arabia*

The Gebel El-Delihimmi granite intrusion, located in the Central Eastern Desert of Egypt, cuts the core of a major anticlinal structure of calc-alkaline metavolcanics and ophiolitic mélange rocks. The intrusion is microscopically differentiated into granodiorite, monzogranite, syenogranite and alkali-feldspar granite. Decorrelation stretch and band-ratio techniques were applied to Advanced Spaceborne Thermal Emission and Reflection Radiometer data. Processing of ASTER-SWIR bands enabled discrimination of El-Delihimmi granite phases and generation of a detailed lithologic map of the study area. The structural and microfabric data suggest that the El-Delihimmi granite underwent at least two phases of deformations. The first was related to the Najd fault system during which the older granodiorite phase of the intrusion was affected by sinistral ductile shearing. During the second phase, monzogranite and syenogranite in the intrusion were affected by brittle E–W compressional deformation. Geochemical data reported here reveal that the granodiorite phase has K_2O/Na_2O ratio < 1 and represents an evolved calc-alkaline granite. The monzogranite, syenogranite and alkali-feldspar granite phases have K_2O/Na_2O ratio > 1. The granite phases are generally I-type, metaluminous to slightly peraluminous and are interpreted as formed above subducted slabs of oceanic lithosphere rather than in continental collision zones.

Lithos, 282-283, (2017), 358-372.

Historical Bricks Deterioration and Restoration from the Red Monastery, Sohag, Egypt: A Geochemical, Petrological and Statistical Approaches

Abd-Elkareem, E.[1], Ali, M.[2] & El-Sheikh, A.[2]
[1]Conservation dept., Faculty of Archaeology, South Valley Univ., Qena, Egypt.
[2]Geology dept., Faculty of Sciences, Sohag Univ., Sohag, Egypt.
E-mail: elashmawyabdelkareem@yahoo.com

The present study investigates for the first time the historical bricks of The Red Monastery (west Sohag, Egypt), built about fifth century AD, which showing several aspects of brick decay. Several techniques were employed (geochemical, petrographical, mineralogical and morphological) to determine their deterioration features and provenance of the raw material as well as shed lights on the firing techniques. In addition, integration of geochemical data with multivariate statistics (i.e. Cluster Analysis, Principal Component Analyses and Linear Discriminant Analyses) were used to provide insights into the nature and provenance of the raw material. Potential geological raw materials for bricks manufacturing, were taken from modern floodplain (Nile alluvium) and calcareous clay deposits from lowland desert near the monument site, and subjected to chemical analyses, to compare them with the chemical composition of the studied bricks. Results show that the starting raw materials for bricks were probably obtained by mixing Nile alluvium (quarried from the Nile River floodplain deposits) with the possible introduction of a calcium carbonate-rich flux component as a temper. This will provide guidelines for future conservation strategy for making new compatible and durable bricks and/or materials to be utilized for restoration, and contributes to the preservation of the historical masonry under study.
Egyptian Journal of Archaeological and Restoration Studies "EJARS", 2017,7 (2), 87-101

The Bivalve Fauna of the Eocene Succession of the Maghagha Area, East and West of the Nile Valley, Egypt

Elattaar, A. A. and Seddik, A. A.
Geology Department, Faculty of Science, Sohag University, Sohag, Egypt

Forty one bivalve species belonging to thirty one genera, twenty two families, sixteen superfamilies, six orders and three subclasses are identified from the Middle Eocene successions exposed in the Maghagha area, east and west of the Nile Valley. The bivalve fauna studied herein came from six sections, five of them are located on the eastern side of the Nile Valley (ElSheikh Fadl Butte, Gebel ElMehasham, South Gebel ElMehasham, Gebel ElMereir and Gebel Qarara sections), and the sixth section (Mingar Shinnara section) crops out in the western side. The studied succession consists of four formations, from base to top Muweilih, Midawara, Sath ElHadid, and ElGharaq, spanning the Middle Eocene (Lutetian and Bartonian), and Lower-Middle Mokattamian, levels MK3 to MK7. The highest species diversity is recorded in the Midawara Formation (33 species). Twenty-two bivalve species are endemic to Egypt and nineteen are common elsewhere in the world, in some regions of Europe, Africa and Asia. Two species are recorded for the first time from Egypt: *Perna* sp. and *Pycnodonte rarilamella* (Deshayes, 1861). All the bivalves identified in this work are systematically described and illustrated and their stratigraphical and paleobiogeographical distributionsare given.
Egyptian Journal of Geology, 61, (2017), 521-568

Study of Sea urchin Jacksonaster depressum (L. Agassiz, 1841) (Echinodermata, Echinoidea) from the Northern Bay of Safaga, Red Sea coast, Egypt, as an indicator of the change in the Red Sea Environment

Atef Abdelhamied Elattaar

Geology Department, Faculty of Science, Sohag University, Sohag, Egypt

One hundred and seventy seven living and dead complete tests of *Jacksonaster depressum* (L. Agassiz) were collected from different depths ranging between 10 and 52 meters depth from the Northern Bay of Safaga, Red Sea coast. Morphometric measurements were conducted on some specific characters of the skeletons in addition to use the scanning electron microscope in the study on spines, tubercles, ambulacral pores, and pedicellariae. The internal partitions, oral and aboral plate patterns, predation and failure growth of the test have been examined and reported. Five types of pedicellariae are recorded herein: ophicephalous, triphyllous, tridentate, and the two new types Pharaonic columns-like and cigar-like. Distribution of the complete living and dead tests related to water depths and both bottom and sedimentary facies of the study area are given. It is clear that the Red Sea environment, especially Safaga Bay, is more severe and of a lesser quality than that of the Pliocene Epoch and than the current seas especially that found in Mauritius, in which the species present.

Annals of the Geological Survey of Egypt, 34 no. ISSN 1110-0435, (2017)

Heavy metals seasonal variability and distribution in Lake Qaroun sediments, El-Fayoum, Egypt

Mostafa Redwan[a], Engy Elhaddad[b]

[a]*Geology Dept, Faculty of Science, Sohag University, 82524 Sohag, Egypt*

[b]*National Institute of Oceanography and Fisheries, Cairo, Egypt*

This study was carried out to investigate the seasonal variability and distribution of heavy metals "HMs" (Fe, Mn, Co, Cr, Cu, Ni, Pb, Zn and V) in the bottom sediments of Lake Qaroun, in Egypt. The samples were collected from 10 sites in summer and winter seasons in 2015. Total metals concentrations were measured using inductively coupled plasma spectrometer. Multivariate techniques were applied to analyse the distribution and potential source of heavy metals. The mean seasonal concentrations follow a descending order of Fe > Mn > V > Zn > Cr > Ni > Cu > Co > Pb. The mean concentrations of HMs in sediments during summer were higher than the concentrations during winter and above the average world shale values, except for Pb, suggesting potential adverse toxicity to aquatic organisms. All metals showed enrichment during summer and winter at sites S3 and S5 in the southeastern parts of the lake due to the heavy discharge of contaminants from El-Bats and El-Wadi drains. Principal component analysis results suggested two principal components controlling HMs variability in sediments, which accounted for 63.9% (factor 1: Co, Cr, Cu, Ni, Zn, Pb and V), 15.9% (factor 2: Mn and Fe) during summer, and 76.7% (factor 1: Fe, Co, Cr, Cu, Ni, Zn, Pb and V), 13.8% (factor 2: Mn) during winter of the total variance. Geo-accumulation index (I_{geo}) showed some pollution risk at the southeastern and southern parts (sites S3 and S5). Dilution during winter, concentration during summer, impact of non-point sources from different agricultural, industrial, municipal sewage and fish farms in the southern part of Lake Qaroun, adsorption and salt dissolution reactions and lithogenic sources are the main controlling factors for HMs in the study area. Monitoring of contaminant discharge at Lake Qaroun should be introduced for future remediation and management strategies.

Journal of African Earth Sciences, 134, (2017), 48-55.

Application of quantitative mineralogy on the neutralization–acid potential calculations within µm-scale stratified mine tailings

Mostafa Redwan[1], Dieter Rammlmair[2], Wilhelm Nikonow[2]

[1]Geology Department, Faculty of Science, Sohag University, Sohag, Egypt

[2]Bundesanstalt für Geowissenschaften und Rohstoffe (BGR)HannoverGermany

Estimation of the long-term environmental impact of mining wastes is of socio-economic interest. Bulk analytical approaches of the neutralizing (NP) and acid potentials (AP) provide in general worst-case scenarios for acid rock drainage (ARD) predictions and long-term evaluation. Taking individual graded layers with variable reactive mineral ratios into consideration, alternating zones, highly contrasting in their neutralizing and acid potential, can be identified and quantified using scanning electron microscope–mineral liberation analyzer (SEM–MLA) and µ-energy-dispersive X-ray fluorescence (EDXRF)–petrographic analyst (PA) for the first time. The bulk NP and AP values increased by a factor of 2.13 and 1.37, respectively, compared to the average values of the mineralogical NP/AP. At the contrasting boundaries, precipitation of pore-clogging secondary phases might be enhanced. This new information can be used as input parameters to model the future behavior of a non-homogeneous multiplied laminated body with reactive transport modeling.

Environmental Earth Sciences, 76 (1), (2017), art. no. 46.

Influence of Organo-Metal Interactions on Regeneration of Exhausted Clay Mineral Sorbents in Soil Columns Loaded with Heavy Metals

Yasser Refaey[ab], Boris Jansen[a], Pim DE Voogt[a], John Rparsons[a], Abdel-Hamid EL-Shater[b], Abdel-Aziz EL-Haddad[b], Karsten Kalbitz[ac]

[a]Institute for Biodiversity and Ecosystem Dynamics (IBED), University of Amsterdam, P.O. Box 94240, 1090GE Amsterdam (The Netherlands)

[b]Geology Department, Faculty of Science, Sohag University, P.O. Box 82524, Sohag (Egypt)

[c]Soil Resources and Land Use, Institute of Soil Science and Site Ecology, Faculty of Environmental Sciences, Technical University Dresden, 01737 Tharandt (Germany)

Natural clay minerals can play an important role in crude remediation of wastewater polluted with the heavy metals (HMs) Cu, Zn and Ni. The presence and timing of addition of natural dissolved organic matter (DOM) have a significant effect on the HM removal by clay mineral sorbents. However, the influence of the presence of DOM on the remediation of the used clay mineral sorbents once saturated with HMs is largely unknown. To resolve this, clay mineral-rich soil column of varying composition, loaded (i) with Cu, Zn and Ni only, (ii) first with DOM followed by Cu, Zn and Ni, or (iii) with DOM, Cu, Zn and Ni simultaneously, was used in a set of desorption experiments. The soil columns were leached with 0.001 mol L −1 CaCl 2 dissolved in water as control eluent and 0.001 mol L −1 CaCl 2 dissolved in DOM as treatment eluent. During the preceding loading phase of the sorbent, the timing of DOM addition (sequential or concurrent with HMs) was found to have a significant influence on the subsequent removal of the HMs. In particular when the column was loaded with DOM and HMs simultaneously, largely irreversible co-precipitation took place. Our results indicate that the regeneration potential of clay mineral sorbents in wastewater treatment will be significantly reduced when the treated water is rich in DOM. In contrast, in manured agricultural fields (where HMs enter together with DOM), HM mobility will be lower than expected from interaction dynamics of HMs and clay minerals.

Pedosphere, 27 (3), (2017), 579-587.

Effects of clay minerals, hydroxides, and timing of dissolved organic matter addition on the competitive sorption of copper, nickel, and zinc: A column experiment

Yasser Refaey[ab], Boris Jansen[a], John R. Parsons[a], Pimde Voogt[a], Simone Bagnis[ac], Adriaan Markus[ad], Abdel-Hamid El-Shater[b], Abdel-Aziz El-Haddad[b], Karsten Kalbitz[ae]

[a]Institute for Biodiversity and Ecosystem Dynamics (IBED), University of Amsterdam, P.O. Box 94240, 1090GE, Amsterdam, The Netherlands

[b]Geology Department, Faculty of Science, Sohag University, P.O. Box 82524, Sohag, Egypt

[c]Biogeochemistry Research Centre, Portland Square, Plymouth University, Drake Circus, Plymouth, Devon, PL4 8AA, United Kingdom

[d]Deltares, P.O. Box 177, 2600 MH, Delft, The Netherlands

[e]Soil Resources and Land Use, Institute of Soil Science and Site Ecology, Faculty of Environmental Sciences, Technical University Dresden, Pienner Strasse 19, 01737, Tharandt, Germany

Infiltration of heavy metal (HM) polluted wastewater can seriously compromise soil and groundwater quality. Interactions between mineral soil components (e.g. clay minerals) and dissolved organic matter (DOM) play a crucial role in determining HM mobility in soils. In this study, the influence of the timing of addition of DOM, i.e. concurrent with or prior to HMs, on HM mobility was explored in a set of continuous flow column experiments using well defined natural soil samples amended with goethite, birnessite and/or smectite. The soils were subjected to concurrent and sequential additions of solutions of DOM, and Cu, Ni and Zn. The resulting breakthrough curves were fitted with a modified dose-response model to obtain the adsorption capacity (q 0). Addition of DOM prior to HMs moderately enhanced q 0 of Cu (8–25%) compared to a control without DOM, except for the goethite amended soil that exhibited a 10% reduction due to the blocking of binding sites. Meanwhile, for both Zn and Ni sequential addition of DOM reduced q 0 by 1–36% for all tested soils due to preferential binding of Zn and Ni to mineral phases. In contrast, concurrent addition of DOM and HMs resulted in a strong increase of q 0 for all tested metals and all tested soil compositions compared to the control: 141–299% for Cu, 29–102% for Zn and 32–144% for Ni. Our study shows that when assessing the impact of soil pollution through HM containing wastewater it is crucial to take into account the presence of DOM.

Journal of Environmental Management, 187, (2017), 273-285.

Geomorphic and lithologic characteristics of wadi feiran basin, southern Sinai, Egypt, using remote sensing and field investigations

Ayman A Ahmed[1], Mohamed Abdelkareem[2], Asran M Asran[1], Tawfig M Mahran[1]

[1]Geology Department, Sohag University, Sohag, Egypt

[2]Geology Department, South Valley University, Qena, Egypt

Wadi Feiran is an important drainage basin in southern Sinai Peninsula covering an area of about 1785 km^2, its streams drain into the Gulf of Suez crossing variety of rocks and sedimentary units varied in age from Precambrian to Quaternary. Field investigations, geographic information systems (GIS) and remote sensing studies including Landsat-7 ETM+, Radarsat-1, and SRTM DEM were integrated to reveal its lithologic, geologic and geomorphic features. Besides the field investigations, rock units including basement and pre- and syn-rift sedimentary units were discriminated using band ratios and principal component analysis techniques (PCA). Such techniques revealed that the crystalline rocks covering W. Feiran are unaltered rocks lacking OH-bearing minerals. Radar data successfully displayed the structures and geomorphic features related to topography. Moreover, the techniques allowed the extraction of the dyke-like structures along faults and shear zones. This also characterized the topographic variations through analysis of the shaded terrain and the altitudinal profiles. The results of data integration, lineament analysis and lineament density maps revealed that the structural grain in the present study has four different trends: N20–45E, N30–45W, N–S and E–W. Based on analysis of radar data and geomorphic indices, W. Feiran is an asymmetrical basin, its left side occupies ~34% of the total area that leads to a supposedly massive tilt towards the south which caused the southwestward slope.

Journal of Earth System Science, 126 (6), (2017), art. no. 85.

The impact of eustasy, tectonics, and paleoclimate on the dolomitization of the syn-rift neogene carbonate platforms in the red sea coastal area, Egypt

Abdallah M. Hassan

Geology Department, Faculty of Science, Sohag University, Sohag, Egypt

A very significant quantity of dolomites and dolomitic limestones of variable origins occurs in the syn-rift Neogene carbonate platforms of the NW Red Sea coast and the Gulf of Suez. These are more common in the Um Diheisi Member of the Ranga Formation (early Miocene), the Um Mahara Formation (middle Miocene), the Um Gheig Formation (late Miocene), and the Dashet El Dabaa Member of the Shagra Formation (Pliocene). Based on their stratigraphic distribution, petrography, and cathodoluminescent characteristics, as supported by geochemical data, syn-rift irregular morphotectonic relief, and the eustasy, four distinct types of dolomites have been identified and were interpreted as follows: 1) Syndepositional stratiform dolomicrite of the Um Diheisi Member occurred in structurally half graben restricted basins favoring structural sites of cyclic peritidal dolomitization that developed in response to sea transgression and then short-term sea level fall of each cycle period. 2) Regional replacive dolomite of the Um Mahara Formation involved mixing meteoric, marine, and hypersaline waters associated with the highstand sea level and then the repeated emergence of the platform and the temporal drowning with restricted marine waters. 3) Mixed syndepositional, replacive, and void-filling cement dolomites of the Um Gheig Formation, which suggest three dolomitization events:- i- an early, penecontemporaneous dolomite associated with highstand phases; ii- diagenetic dolomites formed by mixing meteoric and hypersaline reflux waters during lowstands and falling sea level, and iii- the latest dolomitization phase that occurred as dolomite cement involving hydrothermal fluids during the exposure periods. 4) Replacive dolomite of the Dashet El Dabaa Member, which involved mixtures of hypersaline and marine waters. Paleoclimate played an important role in the dolomitization of the Neogene sediments. An arid climate prevailed during the dolomite of the Um Diheisi Member and the early dolomitization phases of the Um Gheig Formation. A humid climate predominated in the replacive dolomite of the Um Mahara Formation, in which the meteoric groundwater allowed the dissolution of precursor limestones and subsequent formation of extensive bodies of dolomites. Arid conditions also prevailed during the dolomitization of the Dashet El Dabaa Member, as evidenced by the lack of dissolution and the abundance of well-preserved unstable feldspars.

Turkish Journal of Earth Sciences, 26 (3), (2017), 249-276.

Miocene echinoids from the Sadat area, south Gebel Ataqa, NW Gulf of Suez, Egypt: systematics, palaeobiogeography

Atef A. Elattaar

Geology Department, Faculty of Science, Sohag University, Sohag, Egypt

The echinoid fauna from the Miocene sedimentary succession cropping out south Wadi Tweirig, and Wadi Hommath, south Gebel Ataqa, NW Gulf of Suez, has been examined with the aim to known their stratigraphic and paleogeographic distribution. The Miocene succession includes two formations: Sadat Formation, unconformably overlying the middle/upper Eocene rocks at the base and Hommath Formation at the top. Twenty-eight echinoid species (8 regular and 20 irregular) belonging to 18 genera, 13 families, and 7 orders have been identified, systematically described, and illustrated in this work. Eleven species are recorded for the first time from Egypt: ten of these came from the Hommath Formation (*Schizechinus* cf. *serresii* Desor (1856), *Schizechinus pentagonus* Kier 1972, *Clypeaster* cf. *martini* des Moulins 1837, *Scutella checchiae occidentalis* Desio 1934, *Scutella melitensis* Airaghi 1902, *Echinodiscus desori* Duncan and Sladen 1883, *Echinolampas* cf. *zeitensis* Fourtau 1920, *Schizaster lovisatoi* Cotteau 1895, *Agassizia (Agassizia) powersi* Kier 1972, and *Hemipatagus ocellatus* Defrance (1827)), and one from the Sadat Formation (*Clypeaster campanulatus* Schlotheim (1820)). The identified fauna shows a strong affinity with the Mediterranean bioprovince.

Arabian Journal of Geosciences, 10 (11), (2017), art. no. 250.

Mineral composition and geochemistry of the Upper Cretaceous siliciclastics (Nubia Group), Aswan District, south Egypt: Implications for provenance and weathering

Abdallah M. Hassan

Geology Department, Faculty of Science, Sohag University, Sohag, Egypt

The Upper-Cretaceous clastic succession (Nubia Group) in the area northeast of Aswan includes three rock units, from base upwards: Abu Aggag Formation (Turonian), Timsah Formation (Coniacian -Santonian) and Um Barmil Formation (Santonian – Campanian). Quartz and clay minerals are the predominant phases throughout the whole succession while feldspars are very rare. Kaolinite is overwhelming among the clay minerals, in addition to less important amounts of illite and illite/smectite. The ultrastable heavy minerals are the prevailing non- opaque phases and they significantly change in relative abundance upsection. SiO_2, Al_2O_3 and Fe_2O_3 are the dominant chemical components. The statistical examination had revealed that the chemical constituents are loaded on three main geochemical trends; the siliceous, the argillaceous and the ferruginous. The enrichment factor shows that the geochemical behavior of the major and trace elements is uniform throughout the sandstones and mudstones of the Abu Aggag Formation. A significant geochemical contrast is documented between the sandstones and mudstones of both the Timsah and the Um Barmil formations. The provenance – critical elemental ratios Ti/Nb and Ti/Y are nearly constant throughout the sandstones and mudstones of the Abu Aggag Formation, and they fall within the range of granitic-granodioritic composition. The Timsah sandstones have Ti/Nb and Ti/Y ratios that are consistent with those of the Abu Aggag rocks, suggesting a similar provenance. These elemental ratios are extremely higher in the Timsah mudstones, reflecting a great influx of mafic material. The Um Barmil sandstones exhibit exceedingly dispersed values of Ti/Nb and Ti/Y, reflecting their derivation from large catchment's areas of different rock types with the eroded products being mixed in various relative proportions. The Ti/Nb and Ti/Y of the Um Barmil mudstones are closely akin to those of the Timsah mudstones suggesting analogous source. The chemical index of alteration (CIA) and the A-CN-K relation, together with the mineral composition, indicate that the siliciclastic rocks throughout the whole succession were derived mainly from deeply weathered detritus under steady-state weathering conditions. Recycling is limited in the Abu Aggag Formation and increases upwards to be more common in the Um Barmil rocks.

Journal of African Earth Sciences, 135, (2017), 82-95

Engineering properties of concrete made with crushed aggregates of diorite, Jeddah, Saudi Arabia

El-Sayed Sedek Abu Seif[1,2] and Abdullah R. Sonbul[1]

[1]Faculty of Earth Sciences, King Abdulaziz University, Jeddah, Saudi Arabia
[2]Geology Department, Faculty of Science, Sohag University, P.O. Box 82524, Sohag, Egypt

The aggregate characteristics play an effective role in both fresh and hardened concrete properties. The western parts of Saudi Arabia characterized by rareness of natural aggregates resources so that the Precambrian rocks of the Arabian Shield considered as very important source of crushed aggregates. The studied Precambrian diorite is a hard and dense coarse-grained plutonic igneous rock that represents a local source of crushed aggregates of concrete, mortar and pavement materials. It composes mainly of plagioclase feldspar (andesine), biotite, hornblende and pyroxene. Sometimes, diorite contains small amounts of quartz. The studied samples were plotted in the field of diorite and quartz diorite of discrimination diagram. Its absorption values indicated that the studied crushed diorite aggregates have standard limits for aggregates absorption in the specified standards. The studied crushed aggregates are consisting mainly of equidimensional or cubical grains, that means these crushed grains are enough resist shear strength. The studied crushed aggregates have standard limits for aggregates absorption. The Los Angles abrasion values indicate relatively high resistance to wear. The compressive strength values of the studied concrete mix were ranging from 34.43 MPa to 38.32 MPa and having a strong direct proportional relationship with very angular grains content of coarse aggregates (R 2 value = 0.96).

Acta Montanistica Slovaca, 22 (3), (2017), 225-237.

Geotechnical hazardous effects of municipal wastewater on plasticity and swelling potentiality of clayey soils in Upper Egypt

El-Sayed Sedek Abu Seif[1,2]

[1]*Faculty of Earth Sciences, King Abdulaziz University, Jeddah, Saudi Arabia*

[2]*Geology Department, Faculty of Science, Sohag University, P.O. Box 82524, Sohag, Egypt*

In Upper Egypt, the settled areas were constructed on the flood plain clayey soils which situated on both sides of River Nile course. These clayey sediments are consisting of silts, clays and sands with average values of 47.4, 40.3 and 12.3% respectively and classified as inorganic clays (CL). The clay mineral composition of these inorganic clayey soils constitutes of montmorillonite, kaolinite, illite–montmorillonite mixed layer and minor percents of chlorite and illite. These populated old cities were extended during last three decades in the same time the sewage networks are not found in new extended areas. So that, the private sector was forced to storage wastewater in so called wastewater-tanks below or near the houses. These tanks sometimes filled completely or broken then the wastewater which rich in organic matter will saturate the clayey soils. The wastewater had been caused an increasing in original plasticity and swelling potentiality of these clayey soils. So that, serious damages such as wall cracks and foundation tilting were observed.

Seif Geo-Engineering (2017), 8:1

Palynofacies analysis and palaeoenvironmental reconstruction of the Upper Cretaceous sequence drilled by the Salam-60 well, Shushan Basin: Implications on the regional depositional environments and hydrocarbon exploration potential of north-western Egypt

Magdy S. Mahmoud[a], Amr S. Deaf[a], Mohamed A. Tamam[b], Miran M. Khalaf[b]

[a]*Geology Department, Faculty of Science, Assiut University, Assiut, Egypt*

[b]*Geology Department, Faculty of Science, Sohag University, Sohag, Egypt*

A palynofacies analysis was carried out on thirty ditch-cuttings from the Upper Cretaceous sequences drilled by the Salam-60 well in the Shushan Basin, north-western Egypt. Quantitative vertical distributions of palynomorphs and particulate organic matter exhibit two palynofacies (PF) types. PF-1 suggests deposition of the clastic-carbonate section of upper Bahariya and the lowermost "G" Member of Abu Roash in a brackish, proximal inner shelf environment of prevailing reducing (suboxic-anoxic) conditions that witnessed occasional local oxic-dysoxic conditions. A slight shift from a proximal to a distal inner shelf environment that witnessed notable fluctuations resulted in deposition of the mainly carbonate section of the uppermost "G" and "F" to "C" members, during a late Cenomanian-Turonian marine transgression, under the same suboxic-anoxic conditions. This relative sea level rise was mostly connected to the global late Cenomanian marine transgression. PF-2 represents the rest of the carbonate section ("B" and "A" members) of Abu Roash and Khoman formations, which was deposited in middle shelf environments of prominent suboxic-anoxic conditions during a major regional marine transgression that was mostly connected to the global Turonian-Maastrichtian eustatic sea level rise. Nevertheless, minor fluctuations in the local Turonian sea level may have occurred. Regional comparison indicates Bahariya and the "G" Member of Abu Roash formations have similar marginal to inner shelf depositional settings across most of the northern Western Desert. Except at western Matruh Basin, where they have a deeper open marine, middle shelf setting. The "F" to "C" members have an outer inner shelf setting in the coastal basins (Shushan and Matruh basins) and a deeper, inner middle shelf setting at the central basinal area (Abu Gharadig Basin). This interbasinal difference in their depositional settings is mostly related to the late Cretaceous tectonic differentiation of Abu Gharadig Basin. The "B" and "A" members of Abu Roash and Khoman formations were deposited in central Abu Gharadig and at southern Matruh basins in deeper, outer shelf and upper to middle slope settings in comparison to their suggested inner middle and outer middle shelf settings in Shushan Basin. This was due to the progressive late Cretaceous tectonic development of Abu Gharadig and Matruh basins. Local pteridophytes on wet lowlands and conifers on elevated hinterlands were growing near Salam-60 under a regional warm and relatively dry palaeoclimate.

Revue de Micropaleontologie, 60 (4), (2017), 449-467.

Comparison of four kernel functions used in support vector machines for landslide susceptibility mapping: A case study at Suichuan area (China)

Haoyuan Hong[a,b], Biswajeet Pradhan[c,d], Dieu Tien Bui[e], Chong Xu[a], Ahmed M. Youssef[f] and Wei Chen[g]

[a]Key Laboratory of Active Tectonics and Volcano, Institute of Geology, China Earthquake Administration, Beijing,P.R. China; [b]Jiangxi Provincial Meteorological Observatory, Jiangxi Meteorological Bureau, Nanchang, China; [c]Department of Civil Engineering, Geospatial Information Science Research Center (GISRC), Faculty of Engineering,University Putra Malaysia, Selangor Darul Ehsan, Malaysia; [d]Department of Energy and Mineral Resources, Engineering, Choongmu-gwan, Sejong University, Seoul, Republic of Korea; [e]Geographic Information System group, Department of Business Administration and Computer Science, University College of Southeast Norway, Bø i Telemark, Norway; [f]Department of Geology, Faculty of Science, Sohag University, Sohag, Egypt; [g]College of Geology& Environment, Xi'an University of Science and Technology, Xi'an, China

Suichuan is a mountainous area at the Jiangxi province in Central China, where rainfall-induced landslides occur frequently. The purpose of this study is to assess landslide susceptibility of this region using support vector machine (SVM) with four kernel functions: polynomial (PL), radial basis function (RBF), sigmoid (SIG), and linear (LN). A total of 178 landslides were used to accomplish this approach, of which, 125 (70%) landslides were randomly selected for training the landslide susceptibility models, whereas the remaining 53 (30%) were used for the model validation. Fifteen landslide conditioning factors were considered including slope-angle, altitude, slope-aspect, topographic wetness index (TWI), sediment transport index (STI), stream power index (SPI), plan curvature, profile curvature, distance to rivers, distance to faults, distance to roads, precipitation, landuse, normalized difference vegetation index (NDVI), and lithology. Using the training dataset, nine landslide susceptibility models for the Suichuan area were constructed with the four kernel functions. To evaluate the performance of these models, the receiver-operating characteristic curve (ROC) and area under the curve (AUC) were used. Using the training dataset, AUC values for the SVM-PL models with six degrees PL function (1–6) are 0.715, 0.801, 0.856, 0.891, 0.919, 0.953, respectively, and for the SVM-RBF model, the SVM-SIG model, and the SVM-LN model are 0.716, 0.741, and 0.740, respectively. Using the validation dataset, AUC values for the SVM-PL models with six degrees PL function (1–6) are 0.738, 0.730, 0.683, 0.648, 0.608, and 0.598, respectively, and for the SVM-RBF model, the SVM-SIG model, and the SVM-LN model are 0.716, 0.741, and 0.740, respectively. Our results suggested that the SVM-RBF model is the most suitable for landslide susceptibility assessment for the study area.

Geomatics, Natural Hazards and Risk, 8 (2), (2017), 544-569.

Damage Blocks Granite of Philip Arrhidaeus Compartment and its Source and Treatment, Karnak, Egypt

Abd-Elkareem, E.[1], Asran, M.[2] & El Shater, A.[2]

[1]Conservation dept., Faculty of Archaeology, South Valley Univ., Qena, Egypt.
[2]Geology dept., Faculty of Sciences, Sohag Univ., Sohag, Egypt.
E-mail: elashmawyabdelkareem@yahoo.com

The compartment of Philip Arrhidaeus is one of the most significant Roman landmarks in Karnak Temple. It is exposed to various damage factors. For example, ground water is rising in the study area, causing serious damage to granite used in the compartment Granite was variously used in Ancient Egypt, both in statues and obelisks. Samples were collected to study their mineral and chemical composition using polarized microscopy, X-ray diffraction, X-ray fluorescence, and scanning electron microscope. Finally, results showed the source of granite, mechanical damage, and the proposed treatment.

Egyptian Journal of Archaeological and Restoration Studies "EJARS", 2017,7 (2), 111-121

GIS-based multi-criteria earthquake hazards evaluation using analytic hierarchy process for a nuclear power plant site, west Alexandria, Egypt

A. M. Abudeif[1], A. A. Abdelmoneim[1], A. F. Farrag[2]

[1]*Geology Department, Faculty of Science, Sohag University, Sohag, Egypt*

[2]*Siting Department, Nuclear Power Plants Authority, Cairo, Egypt*

Nuclear power plants are designed to prevent the hazardous effects of the earthquakes and any external events to keep the safety of the plant. Ninety-one shallow seismic refraction profiles were performed to determine shear wave velocity of the engineering layers at the site of El Dabaa area that is situated to the northern coastline of Egypt for seismic hazard microzonation evaluation according to hazard index values. A microzonation is a procedure of delineating an area into individual zones having different ranks of numerous seismic hazards. This will aid in classifying areas of high seismic risk which is vigorous for industrial design of nuclear structures. The site response analysis requires the characterization of subsurface materials considering local subsurface profiles of the site. Site classification of the area under investigation was undertaken using P- and S-waves and available borehole data. The studied nuclear power plant site has been characterized as per NEHRP site classification using an average velocity of transverse wave (V_s 30) of depth 30 m which acquired from seismic survey. This site was categorized into two site classes: the major one is "site class B," and the minor one is "site class A." The attenuation coefficient, the damping ratio and the liquefaction potential are geotechnical parameters which were derived from P- and S-waves, and have their major effects on the seismic hazard contribution. 1D ground response analysis was carried out in the places of seismic profiles inside the site for estimating the amount of ground quaking using peak ground acceleration (PGA), site amplification, predominant frequency and spectral accelerations on the surface of ground by the DEEPSOIL software package. Seven factors (criteria) deliberated to assess the earthquake hazard index map are: (1) the peak ground acceleration at the bedrock, (2) the amplification of the site, (3) the liquefaction potential, (4) the main frequency of the earthquake signal, (5) the average V_s of the first 30 m from the ground surface, (6) the depth to the groundwater and (7) the depth to the bedrock. These features were exemplified in normalized maps after uniting them to 0–1 scores according to some criteria by the minimum and maximum values as linear scaling points. Multi-criteria evaluation is an application of multi-criteria decision analysis theory that used for developing a seismic hazard index map for a nuclear power plant site at El Dabaa area in ArcGIS 10.1 software. Two models of decision making were used in this work for seismic hazard microzonation. The analytic hierarchy process model was applied to conduct the relative weights of the criteria by pairwise comparison using Expert Choice Software. An earthquake hazard index map was combined using Weighted Linear Combination model of the raster weighted overlay tool of ArcGIS 10.1. The results indicated that most of the study site of the nuclear power plant is a region of low to moderate hazard; its values are ranging between 0.2 and 0.4.

Environmental Earth Sciences, 76 (23), (2017),796.